Strathclyde Institute of Pharmacy and Biological Sciences

An investigation of nitric oxide synthase in neuronal function and in phencyclidine models of relevance to schizophrenia

Graham Lee

A thesis presented in fulfilment of the requirements for the degree of Doctor of Philosophy

2014

This thesis is the result of the author's original research. It has been composed by the author and has not been previously submitted for examination which has led to the award of a degree.

Signed: 

Date: 2014-04-22

Abstract

Schizophrenia is a complex and debilitating psychiatric disorder. Dysfunction of the NMDA subtype of glutamate receptors is implicated in deficits found in schizophrenia, and some of these deficits may be reproduced in rodents using the NMDA receptor antagonist, phencyclidine (PCP). Nitric oxide synthase (NOS) is the synthesising enzyme of the gaseous neuromodulator, nitric oxide. The neuronal isoform of NOS (nNOS) is functionally associated with NMDA receptors. The role of NOS in schizophrenia is not fully understood. The primary aim of this thesis is to investigate NOS signalling in cultured neurones and in rodent PCP models of relevance to schizophrenia.

Using diaminofluorescein microscopy of primary neuronal cultures, it is shown that non-selective inhibition of NOS using L-NAME, and selective inhibition of nNOS using L-NPA reversed glutamate-stimulated nitric oxide generation in hippocampal and cerebellar neurones, but inhibition of endothelial NOS using L-NIO did not. Novel compounds that modulate the NOS cofactor, tetrahydrobiopterin, altered nitric oxide generation in cerebellar neurones.

NOS activity was increased in the hippocampus, and decreased in the reticular thalamus in mice administered acute PCP (5 $mg.kg^{-1}$, i.p.), as determined by NADPH-diaphorase activity. NOS activity normalised in these areas with subchronic PCP (5 $mg.kg^{-1}$ twice daily for 5 days), and NOS activity was decreased in the prefrontal cortex. Decreased activity of thioredoxin reductase was found in the hippocampus and thalamus with acute PCP, but was unchanged with subchronic PCP. Pretreatment with L-NAME (40 $mg.kg^{-1}$) and L-NIO (20 $mg.kg^{-1}$) improved hyperlocomotion and

deficits in prepulse inhibition observed with PCP, but L-NPA (20 $mg.kg^{-1}$) did not.

In conclusion, the results presented in this thesis give evidence for a role of NOS in deficits observed in rodent PCP models of relevance to schizophrenia. Selective inhibition of NOS isoforms is a potential therapeutic strategy to improve deficits associated with NMDA receptor dysfunction found in schizophrenia.

Acknowledgments

I would like to thank my supervisors, Professors Judy Pratt, Brian Morris, and Colin Suckling, for the opportunity to do this project. Their guidance and support throughout my PhD study has been invaluable. Judy, your encouragement has kept me going, thank you. Brian, for every experimental storm in a teacup that I came to you with you had a solution. I will hope and strive to develop such a scientific acumen. Colin, I'll admit that I felt trepidation about using your BH_4 compounds (timing, dosing, etc., etc.), but they worked out brilliantly. Thank you for your advice and encouragement during the project.

I would also like to thank past and present PsyRING members that have helped me during my time in the group: Allan McVie, Prof. Bob Hunter, Dr. Catherine Winchester, Dr. David Mark Thomson and Dr. Neil Dawson. I lack the space here to give thanks individually and sufficiently. My work and abilities have benefitted so much from their advice and training.

My thanks go to the Neuroscience Group at University of Strathclyde for the stimulation of ideas and discussion during meetings and for feedback on my work. Special thanks go to Dr. Ben Pickard for the generous gift of SH-SY5Y cells.

Many thanks go to those that helped me as I was developing assays to work with my cultures: Prof. Imre Vida, Dr. Sam Booker and Prof. Rodger Wadsworth for advice and suggestions for my assay development; Dr. Stuart Cobb for allowing me to use his microscope, Dr. Paul Turko for helping me with the pilot experiment for DAF until the wee small hours on a Saturday, and Dr. Francis Burton for helping me in my attempts to automate image analysis.

My friends and comrades: Alex & Kristy, Faye, Rhiannon, Sam, Belle & Jase, Jake, Paul, Tamara, thank you for your companionship, for putting up with me when I'm being grumpy and wittering-on about 'nitric-bloody-oxide', and for putting me up when I've had one-too-many shandys at the Three Judges. My time in Glasgow has been so much richer for knowing you.

My wonderful partner, Maria, who has supported me during those flashes of inspiration and of despair; who has inspired me to be a better scientist: thank you.

Finally, I would like to thank my family: Cheryl, Stephen, and Mum, who have always been there for me.

Abbreviations

5-HT	5-hydroxytryptamine
7-NI	7-nitroindazole
ACh	Acetylcholine
ADDP	6-actyl-7,7-dimethyl-5,6,7,8-tetrahydropterin
ADMA	Asymmetrical dimethylarginine
AMC	7-amino-4-methylcoumarin
AMPA	2-amino-3-(5-methyl-3-oxo-1,2-oxazol-4-yl)propanoic acid
ANOVA	Analysis of variance
AU	Arbitrary units
AVVL	Anteroventeral venterolateral thalamus
BH_4	Tetrahydrobioterin
CA(1-3)	Cornu Ammonis
cAMP	Cyclic adenosine monophosphate
CAPON	Carboxyl-terminal PDZ ligand of nNOS
CBF	Cerebral blood flow
CGC	Cerebellar granule cell
cGMP	Cyclic guanosine monophosphate
CNQX	6-cyano-7-nitroquinoxaline-2,3-dione
CREB	cAMP response element-binding protein
DA	Dopamine
DAF-2DA	Diaminofluorescein diacetate
DAHP	2,4-Diamino-6-hydroxypyrimidine
DAT	Dopamine uptake transporter
dB	Decibels
DG	Dentate gyrus
DMEM	Dulbecco's modified Eagle's medium
DMSO	Dimethyl sulfoxide
eNOS	Endothelial NOS
FAD	Flavin adenine dinucleotide
FBS	Foetal bovine serum
FMN	Flavin mononucleotide
GABA	γ-aminobutyric acid
GTP	Guanosine triphosphate
GTPCH	GTP cyclohydrolase I
i.p.	Intraperitoneal
iNOS	Inducible NOS
KO	Knock-out
LMA	Locomotor activity
L-NAME	N^{ω}-nitro-L-arginine methyl ester

L-NIO	*N*$^{\omega}$-(1-iminoethyl)-L-ornithine
L-NNA	*N*$^{\omega}$-nitro-L-arginine
L-NPA	*N*$^{\omega}$-propyl-L-arginine
mAChR	Muscarinic acetylcholine receptor
MAO	Monoamine oxidase
mGluR	Metabotropic glutamate receptor
MK-801	(+)-5-methyl-10,11-dihydro-5H-dibenzo [a,d] cyclohepten-5,10-imine
mRNA	Messenger RNA
MWM	Morris water maze
NAc	Nucleus accumbens
nAChR	Nicotinic acetylcholine receptor
NADPH	β-nicotinamide adenine dinucleotide phosphate
NBT	Nitroblue tetrazolium
NMDA	N-methyl-D-aspartate
nNOS	Neuronal NOS
NO	Nitric oxide
NOS	Nitric oxide synthase
NOS1AP	nNOS adaptor protein
NOX	NADPH-oxidase
NO_x	Nitrite and nitrate
OD	Optical density
ODQ	(1,2,4)oxadiazolo(4,3-a)quinoxalin-1-one
PBS	Phosphate-buffered saline
PCP	Phencyclidine
PDZ	PSD-95/Discs large/zona occludens-1
PFC	Prefrontal cortex
PKG	Protein kinase G
PMS	Phenazine methosulfate
PPI	Prepulse inhibition
PrL	Prelimbic region of the prefrontal cortex
PSD-95	Post-synaptic density 95
PV	Parvalbumin
RAM	Radial-arm maze
RFI	Relative fluorescence intensity
RNA	Ribonucleic acid
ROD	Relative optical density
ROI	Region of interest
RSp	Retrosplenial cortex
SEM	Standard error of the mean
sGC	Soluble guanylate cyclase
SIN-1	3-morpholinosydnonimine hydrochloride
SNAP	*S*-nitroso-N-acetylpenicillamine

SNP	Single nucleotide polymorphism
ST	Stria terminalis
Trx	Thioredoxin
TrxR	Thioredoxin reductase
Veh	Vehicle
VTA	Ventral tegmental area
WSG1023	2,6,7,7-tetramethyl-7,8-dihydro-1-thia-3,3a,5,8,9-pentaazacyclopenta[*b*]naphthalen-4-one
WSG2001	2-amino-4-oxo-4,7-dihydro-3H-pyrrolo[2,3-*d*]pyrimidine-6-carboxylic acid ethyl ester
XTT	2,3-Bis(2-methoxy-4-nitro-5-sulfophenyl)-2H-tetrazolium-5-carboxanilideinner salt

Table of Contents

1 INTRODUCTION 1

1.1 SCHIZOPHRENIA 1

1.1.1 Background 1
1.1.2 Symptomatology and treatment 2
1.1.3 Pathophysiology 3

1.2 AETIOLOGY 5

1.2.1 Genetic and environmental risk factors 5
1.2.2 The Dopamine Hypothesis of Schizophrenia 7
1.2.3 The Glutamate Hypothesis of Schizophrenia 7
1.2.4 Oxidative stress and schizophrenia 10

1.3 ANIMAL MODELS OF RELEVANCE TO SCHIZOPHRENIA 11

1.3.1 Pharmacological models 11
1.3.2 Developmental models 16
1.3.3 Genetic models 17

1.4 NITRIC OXIDE IN THE BRAIN 18

1.4.1 Nitric generation and signalling 18
1.4.2 Modulation of neural transmission 21
1.4.3 Modulation of cerebral blood flow and neurovascular coupling 25
1.4.4 Nitrosative and oxidative stress 25

1.5 NITRIC OXIDE AND SCHIZOPHRENIA 26

1.5.1 Evidence from clinical trials 26
1.5.2 Genetic evidence 27
1.5.3 Biochemical evidence 29
1.5.4 Evidence from animal models of relevance to schizophrenia 31

1.6 HYPOTHESIS AND AIMS 38

1.6.1 General hypotheses 38
1.6.2 Thesis aims 38

2 MATERIALS AND METHODS 40

2.1 ANIMALS 40

2.2 REAGENTS 40
2.2.1 Routinely-used reagents 40
2.2.2 Novel NOS-modulating compounds 41
2.3 *IN VIVO* DRUG TREATMENTS AND EXPERIMENTAL DESIGN 41
2.3.1 Acute PCP experiments 42
2.3.2 Subchronic PCP experiments 43
2.3.3 Acute PCP with NOS drug pretreatment experiments 44
2.4 CELL CULTURE 45
2.4.1 Cell lines 45
2.4.2 Primary neuronal cultures 46
2.5 NADPH-DIAPHORASE ACTIVITY 47
2.5.1 Histochemistry 47
2.5.2 Brain tissue homogenates 49
2.5.3 NADPH-diaphorase activity in cultured cells 50
2.6 DETERMINATION OF NITRIC OXIDE GENERATION 51
2.6.1 Diaminofluorescein-2-diacetate microplate fluorometry 51
2.6.2 Diaminofluorescein-2-diacetate live-cell microscopy 51
2.6.3 Griess assay for assessment of nitrite concentration 54
2.7 THIOREDOXIN REDUCTASE ACTIVITY 55
2.8 CASPASE ACTIVITIES 56
2.9 BEHAVIOUR 58
2.9.1 Open field apparatus 58
2.9.2 Locomotor activity 58
2.9.3 Prepulse inhibition apparatus 58
2.9.4 Prepulse inhibition of acoustic startle 58
2.10 DATA AND STATISTICAL ANALYSES 59
2.10.1 NADPH-diaphorase kinetics analysis 60
2.10.2 Image analysis of NADPH-diaphorase staining 60
2.10.3 Fluorescence image analysis 61
2.10.4 Analysis of behavioural parameters 61
3 EVALUATION OF CELL CULTURE ASSAYS FOR MODELLING NEURONAL NOS ACTIVITY 62

3.1 INTRODUCTION 62

3.2 AIMS 65

3.3 EVALUATING THE SUITABILITY OF PLATE-BASED ASSAYS TO DETERMINE NOS ACTIVITY IN NEURONAL CELLS 67

3.3.1 Neuroblastoma cells 67

3.3.2 Primary neuronal cultures 71

3.4 MULTIPLE SIGNALLING PATHWAYS CONTRIBUTE TO NEURONAL NOS ACTIVITY *IN VITRO*.....73

3.4.1 Cerebellar granule cells.....73

3.4.2 Hippocampal Cells 78

3.5 DISCUSSION 81

3.5.1 The use of plate-based assays to determine nitric oxide synthase activity in neuronal cells.....81

3.5.2 Evaluating glutamate-mediated nNOS activity in cerebellar and hippocampal neurones 82

4 SPATIAL AND TEMPORAL DIFFERENCES IN NOS AND THIOREDOXIN REDUCTASE ACTIVITIES FOLLOWING PHENCYCLIDINE TREATMENTS.....87

4.1 INTRODUCTION 87

4.2 HYPOTHESES AND AIMS 88

4.3 REGIONAL NADPH-DIAPHORASE ACTIVITY 89

4.3.1 Histochemical assessment of NOS activity.....91

4.3.2 NADPH-diaphorase activity in brain region homogenates 100

4.4 TISSUE NITRITE CONCENTRATIONS 105

4.5 THIOREDOXIN REDUCTASE AND CASPASE ACTIVITIES 107

4.6 LOCOMOTOR ACTIVITY AND PREPULSE INHIBITION 115

4.6.1 Prepulse inhibition and startle reactivity with acute PCP.....115

4.6.2 Prepulse inhibition and startle reactivity with subchronic PCP.....117

4.6.3 Locomotor activity.....119

4.6.4 Locomotor activity with acute PCP.....119

4.6.5 Locomotor activity with subchronic PCP 122

4.7 DISCUSSION 129

4.7.1 NADPH-diaphorase staining is influenced by NOS inhibition..... 131

4.7.2 The influence of acute and subchronic PCP on NOS activity in the mouse brain..... 132

4.7.3 The implications of acute and subchronic PCP on redox state and apoptosis in the mouse brain..... 138

4.7.4 Behavioural deficits propagated by PCP..... 141

4.8 CONCLUSIONS.....145

5 THE INFLUENCE OF NITRIC OXIDE SYNTHASE ISOFORMS ON THE NEUROCHEMICAL AND BEHAVIOURAL EFFECTS OF ACUTE PCP.....147

5.1 INTRODUCTION.....147

5.2 HYPOTHESIS AND AIMS.....148

5.3 BEHAVIOURAL DEFICITS INDUCED BY PCP AND THE INFLUENCE OF NOS-MODULATING DRUGS 149

5.3.1 Prepulse inhibition..... 151

5.3.2 Locomotor activity..... 156

5.4 NADPH-DIAPHORASE ACTIVITY IN THE HIPPOCAMPUS AND RETICULAR THALAMUS.....161

5.5 DISCUSSION.....168

5.5.1 Reversal of behavioural deficits with NOS inhibitors..... 168

5.5.2 Histochemical findings..... 172

5.6 CONCLUSIONS.....174

6 TETRAHYDROBIOPTERIN AS A TARGET FOR THE MODULATION OF NITRIC OXIDE SIGNALLING.....176

6.1 INTRODUCTION.....176

6.2 HYPOTHESES AND AIM.....177

6.3 SELECTIVE MODULATION OF TETRAHYDROBIOPTERIN.....179

6.3.1 Activation of NOS using a BH_4 analogue..... 179

6.3.2 The influence of putative NOS inhibitors in neuronal nitric oxide signalling..... 182

6.4 DISCUSSION.....185

7 GENERAL DISCUSSION.....189

7.1 KEY FINDINGS 189

7.2 TECHNICAL CONSIDERATIONS AND FUTURE DIRECTIONS 191

7.2.1 On the suitability of methods for determining nitric oxide synthase activity 191

7.2.2 Neurochemical and behavioural changes with acute and subchronic PCP 195

7.2.3 Selective NOS isoform inhibition 196

7.2.4 Targeting tetrahydrobiopterin as a means to modulate NOS activity 199

7.3 CONCLUDING REMARKS 200

8 REFERENCES 201

List of Figures

Figure 1.1. NMDA receptor hypofunction can lead to increased glutamate efflux: relevance to the Glutamate Hypothesis of Schizophrenia. 9

Figure 1.2. Nitric oxide synthase. 23

Figure 1.3. Endogenous inhibitors of nNOS. 24

Figure 3.1. A microplate-based assay for NADPH-diaphorase activity is unsuitable to determine drug effects in neuroblastoma cells. 69

Figure 3.2. A microplate-based assay for nitric oxide generation in NG-108-15 cells using DAF-2DA. 70

Figure 3.3. NMDA stimulates nitric oxide generation in cortical neurones. 72

Figure 3.4. Thioredoxin reductase is insensitive to altered nitric oxide in cerebellar neurones. 75

Figure 3.5. Neuronal and non-selective NOS inhibition reverses glutamate-stimulated nitric oxide generation in cerebellar neurones. 76

Figure 3.6. Glutamate-stimulated nitric oxide generation is mediated by multiple receptor interactions in cerebellar neurones. 77

Figure 3.7. Glutamate-stimulated nitric oxide generation is reversed by nNOS inhibition in hippocampal neurones. 79

Figure 3.8. Nitric oxide generation in hippocampal neurones is mediated by multiple receptor interactions. 80

Figure 4.1. Experimental schemata for drug administrations, behavioural and neurochemical assays. 90

Figure 4.2. NADPH-diaphorase stained of neurones in the prefrontal cortex of the mouse...... 93

Figure 4.3. NADPH-diaphorase activity is attenuated by NOS inhibitors in the rat striatum. 94

Figure 4.4. Altered NADPH-diaphorase activity discreet brain regions of mice administered acute PCP...... 97

Figure 4.5. Increased NADPH-diaphorase activity in Brain Region Homogenates of acute PCP-treated Mice. 102

Figure 4.6. NADPH-diaphorase activity in brain region homogenates following subchronic PCP administration in mice. 103

Figure 4.7. Acute PCP does not influence nitrite concentrations in mouse brain regions......106

Figure 4.8. Thioredoxin reductase activity is decreased in hippocampi and thalami of mice treated with acute PCP......108

Figure 4.9. Thioredoxin reductase activity in brain regions of mice treated with subchronic PCP or vehicle. 109

Figure 4.10. Caspase 3 activity is decreased in the hippocampus with subchronic PCP, but not acute PCP administration in mice. ..114

Figure 4.11. Prepulse inhibition and startle reactivity in mice administered acute PCP. 116

Figure 4.12. PPI deficits do not persist in mice with subchronic PCP administration. 118

Figure 4.13. The influence of acute PCP administration on locomotor activity in mice......121

Figure 4.14. Mouse Locomotion During Repeated Administrations of PCP. 125

Figure 4.15. Time-dependent changes on locomotor activity with subchronic PCP in mice. 128

Figure 5.1. Experimental schemata for drug administrations, behavioural assays and histological sampling......150

Figure 5.2. Influence of NOS-modulating drugs on prepulse inhibition deficits induced by PCP. 153

Figure 5.3. Mouse startle responses are altered with NOS inhibition with and without PCP......155

Figure 5.4. PCP-induced hyperlocomotion is reversed with NOS inhibition. 159

Figure 5.5. PCP alters locomotor activities: minimal influence of NOS inhibitiors......160

Figure 5.6. NADPH-diaphorase staining in the mouse hippocampus. 162

Figure 5.7. L-NAME attenuates PCP-induced increase in CA3 NADPH-diaphorase activity......165

Figure 5.8. NADPH-diaphorase activity is unchanged in the reticular thalamus following antagonism of NMDA receptors and NOS. 167

Figure 6.1. Chemical structures of NOS-modulating drugs. 178

Figure 6.2. Neuronal nitric oxide production is stimulated with a BH_4 analogue while thioredoxin reductase activity is unaffected. 181

Figure 6.3. Neuronal TrxR and NOS activities are altered with GTP cyclohydrolase inhibition. 184

List of Tables

Table 1 Rodent models of relevance to schizophrenia...... 15

Table 2.1 Compound incubation times for live-cell imaging 53

Table 2.2 Caspase-selective compounds..... 57

Table 3.1. Selective and non-selective inhibitors of nitric oxide synthase. 66

Table 4.1. NADPH-diaphorase activity in neurones of brain regions of acute PCP treated mice...... 98

Table 4.2. NADPH-diaphorase activity in blood vessels of brain regions of acute PCP treated mice. 99

Table 4.3. NADPH-diaphorase activity following subchronic PCP administrations......104

Table 4.4. Caspase activities in brain regions of mice administered acute PCP. 112

Table 4.5 Caspase activities in brain regions of mice administered subchronic PCP. 113

Table 4.6 Main neurochemical findings with acute and subchronic PCP. 130

Table 5.1. Neuronal NADPH-diaphorase staining intensity in the hippocampus and thalamus. 163

Table 5.2. Blood vessel NADPH-diaphorase staining intensity in the hippocampus and thalamus 164

1 Introduction

The focus of this thesis is on the potential role of nitric oxide (NO) signalling in animal models of relevance to schizophrenia. In this chapter, I will review current knowledge of schizophrenia, with particular focus on glutamate dysfunction, and the potential role of NO in this disorder.

1.1 Schizophrenia

1.1.1 Background

Schizophrenia is a complex and debilitating psychiatric disorder that affects approximately 1% of the global population. There is an estimated 5 million people with a diagnosis of schizophrenia and associated psychotic disorders in Europe, alone (Wittchen *et al.*, 2011). Symptoms usually develop during adolescence to early adulthood and may persist throughout life. Schizophrenia comprises a diverse spectrum of symptoms that is outlined in the next section, and it is by the presence of these symptoms that schizophrenia is diagnosed. The identification of this collection of common symptoms coincident in people was originally termed "Dementia Praecox" (premature loss of mind), notably used by Kraepelin (1893), and relabelled as "Schizophrenia" (split mind) by Bleuler in 1908. The latter label has persisted in the western world to date. In Japan, the syndrome was re-termed; from "Seishin Bunretsu Byo" (mind-split disease), to "Togo Shitcho Sho" (integration disorder). This has had a positive impact on diminishing the inappropriate stigma attached to the disorder (Sato, 2006), and is certainly a more appropriate term for the disorder.

A recent study by the Schizophrenia Commission (2012) found that schizophrenia has a total societal cost of an estimated £11.8 billion per year

in England alone. This cost is comprised of many factors, including treatments and therapies, hospitalisation, social welfare support, and loss of earnings from employment. This reflects the fact that the disorder is not treated well; by current antipsychotic drugs (reviewed by: Miyamoto et al., 2012), and by limited access to other treatments that may be beneficial such as cognitive-behavioural therapy (The Schizophrenia Commission, 2012).

1.1.2 Symptomatology and treatment

Positive symptoms are a collection of affective disorders that are commonly found in schizophrenia, and include sensory hallucinations, delusions and thought disorder. A dysfunctional dopaminergic mesolimbic system is likely to cause positive symptoms. These distortions of reality are both distressing and disruptive, and although well treated by antipsychotic treatments, may be exacerbated by common factors such as substance abuse and poor drug compliance. Negative symptoms are affective impairments that include avolition, anhedonia, social withdrawal, and flattened affect. Cognitive deficits are often attributed to dysfunction of the prefrontal cortex (PFC), and these include; executive function, attention, learning and memory, and social cognition. Cognitive deficits generally precede the onset of psychosis, and persist throughout. Negative symptoms and cognitive deficits generally persist throughout the course of the illness. The severity of cognitive deficits is a good predictor of functional outcome of a patient. The incidence and severity of these symptoms are highly heterogeneous, though are the means by which that disorder is diagnosed (reviewed by: Tandon et al., 2009).

Current antipsychotic drug treatments for schizophrenia include typical antipsychotics, such as haloperidol, and atypical antipsychotics, such as clozapine. Typical antipsychotic drugs antagonise dopamine receptors and are generally effective to alleviate positive symptoms in patients. Their

potency is proportional to their affinity for dopamine D_2 receptors. Typical antipsychotics are less effective in treating negative symptoms and cognitive deficits, and may produce unwanted effects such as extrapyramidal side effects (EPS), hyperprolactinaemia and tardive dyskinesia. Atypical antipsychotics have a marginally improved therapeutic profile and fewer EPS, often attributed to their action at other targets such as greater affinity at D_4 than D_2 receptors, 5-HT_{2A} receptor antagonism and others. There are, however, unwanted effects associated with atypical antipsychotics, such as agranulocytosis (clozapine) and weight-gain (olanzapine) (reviewed by: Miyamoto et al., 2012). There is a great need to develop new drugs that treat negative symptoms and cognitive deficits, with minimal unwanted effects, and ultimately, improve the quality of life for people with schizophrenia.

1.1.3 Pathophysiology

There are small differences in overall gross brain anatomy found in schizophrenia compared to the healthy brain. One of the most marked, and reproducible of these is an increased ventricular volume (~126%, overall). Brain volume is generally somewhat smaller (~98%), with no apparent difference in grey and white matter ratio. Brain structure volumes appear to be different in a regionally-specific fashion: frontal lobes, amygdalae, thalami, and temporal structures are generally smaller; and striatal structures are generally larger (meta-analysis by: Wright *et al.*, 2000).

Abnormalities in the density, morphology and behaviour of γ-amino butyric acid (GABA) synthesising interneurones have been found in schizophrenia. A loss of parvalbumin (PV), and somatostatin -expressing interneurones has been noted in the hippocampus of people with schizophrenia (Konradi *et al.*, 2011). A loss of PV interneurones has also been found in the PFC and

thalamus (Lewis *et al.*, 2005). GABAergic interneurone dysfunction may result in many of the synaptic, circuit and brain network aberrations found in schizophrenia (reviewed by: Jones, 2010; Nakazawa et al., 2011; Seshadri et al., 2013).

Several aberrations in sensory-evoked electrophysiological responses are common in people with schizophrenia. These include altered P300 event phase, mismatch negativity, and others (Javitt *et al.*, 2008). The asynchrony of evoked γ rhythms is associated with psychotic and cognitive symptoms in schizophrenia (Uhlhaas and Singer, 2010), and these rhythms are attributed to the dysfunction of PV-interneurone oscillatory behaviour (Sohal *et al.*, 2009). Sensorimotor gating, as determined by prepulse inhibition (PPI), is also commonly deficient in schizophrenia (reviewed by: Keshavan et al., 2008). Non-sensory-evoked patterned behaviour may also be dysfunctional in schizophrenia too; such as in the case of aberrant θ rhythms and their possible disruptive influence during sleep (reviewed by: Jones, 2010). Together, these physiological signs represent a dysfunction in the processing and integration of information, and these are thought to contribute to the cognitive impairments commonly found in people with schizophrenia (reviewed by: Keshavan et al., 2008).

Alterations in the brain at the network level have been associated with symptoms found in schizophrenia, particularly cognitive deficits. Network analyses of structural and functional aberrations between regions in the brain have led to the term, 'dysconnectivity' (reviewed by: Pettersson-Yeo et al., 2011). Dysconnectivity in and between the PFC and thalamus have been shown to have an important role in cognitive deficits in rodent models (Dawson et al., 2011; Parnaudeau et al., 2013) and in people with schizophrenia (Pinault, 2011; Dauvermann et al., 2013).

1.2 Aetiology

1.2.1 Genetic and environmental risk factors

There is a large (~80%) contribution of genetic risk factors to the development of schizophrenia (reviewed by: Tandon et al., 2008). The genetic architecture of schizophrenia is complex and it is probable that a combination of genetic variants contribute to the risk of developing schizophrenia. These include single nucleotide polymorphisms (SNPs) that have a small effect, as well as rare coding variants that have a high penetrance (reviewed by: Harrison and Weinberger, 2005). Some examples of these genetic risk factors are summarised below.

A translocation between chromosomes 1 and 11 was first identified in a large Scottish family with a high prevalence of psychiatric diagnoses. Approximately half of the family members (16 of 34) that possessed the translocation were also diagnosed with mental illnesses, including, schizophrenia, bipolar disorder and major depression (St Clair *et al.*, 1990). This locus was named *DISC1* (*Disrupted-in-schizophrenia-1*). The DISC1 protein is thought to influence radial migration during development, and to influence phosphodiesterase (PDE4) signalling (reviewed by: Porteous et al., 2011), and altered function of DISC1 may impact on glutamatergic signalling (reviewed by: Seshadri et al., 2013).

The genes, *ERBB4* and *NRG1*, encode proteins that are thought to interact with NMDA receptor signalling, especially during development. SNPs in these genes are highly implicated in schizophrenia, and their interaction has been associated with PFC-mediated deficits (Nicodemus *et al.*, 2010).

A polymorphism in the gene that encodes catechol-*O*-methyl transferase (COMT), (val-158-met) *COMT*, is highly associated with schizophrenia and, unlike many implicated genes, has a known function. COMT metabolises catecholamines such as dopamine and noradrenaline. The polymorphism of *COMT* may contribute to increased mesolimbic dopamine, and decreased cortical dopamine concentrations. *COMT* is located within the 22q11.2 locus where deletions cause velocardiofacial syndrome, a condition that is associated with a 30 % risk of schizophrenia (reviewed by: Harrison and Weinberger, 2005).

Genetic risk factors are shared between many neurodevelopmental psychiatric disorders (Smoller *et al.*, 2013), and it may be the interactions of these that brings about the deficits that are unique to schizophrenia (Nicodemus *et al.*, 2010). The functional outcome of what these genetic risk factors may confer is still being studied, as outlined in Section 1.3.3. There is, for example, emerging evidence of possible altered calcium regulation and signalling (reviewed by: Giegling et al., 2010), such as that by L-type calcium channels (Smoller *et al.*, 2013) that may be accounted for by genetic variation.

Substance abuse, and particularly that of cannabis, is prevalent in people with schizophrenia and commonly exacerbates symptoms (reviewed by: Tandon et al., 2009). Substance abuse is thought to contribute as an environmental risk towards developing the disorder. Other environmental risk factors include perinatal infection, pregnancy and birth complications, and adverse life events (reviewed by: McDonald and Murray, 2000).

Multiple risk factors converge to bring about the biological and psychological deficits previously mentioned. Outlined below are hypotheses that attribute

dysfunction in brain systems to be fundamentally causal of the symptoms and deficits found in schizophrenia.

1.2.2 The Dopamine Hypothesis of Schizophrenia

It is the mechanism of action of typical antipsychotic drugs that implicates dopaminergic dysfunction in the production of positive symptoms. The primary evidence for increased dopamine transmission comes from the efficacy of D_2 antagonist antipsychotic drugs to improve positive symptoms (reviewed by: Miyamoto et al., 2012). A recent meta-analysis found that elevated presynaptic dopamine synthesis, and not receptor availability, in the striatum is a common finding in patients with schizophrenia (Howes *et al.*, 2012). Potentiation of synaptic dopamine levels, by drugs such as amphetamine, exacerbates positive symptoms in patients with schizophrenia (reviewed by: Janowsky and Risch, 1979), and may replicate these behaviours in animal models (Sams-Dodd, 1998a). Cognitive deficits and negative symptoms are however less influenced by current antipsychotic drugs (reviewed by: Miyamoto et al., 2012), suggestive of other causative factors.

1.2.3 The Glutamate Hypothesis of Schizophrenia

Antagonists of the glutamate *N*-methyl-*D*-aspartate (NMDA) receptor, such as phencyclidine (PCP), and ketamine, are well regarded as eliciting a comprehensive spectrum of symptoms and deficits in healthy humans and exacerbating symptoms in people with schizophrenia (Luby et al., 1959; Lahti et al., 2001). These, unlike DA agonists, reproduce PFC-associated negative symptoms and cognitive deficits, and are commonly utilised to model schizophrenia (reviewed by: Jentsch and Roth, 1999). These give an

indication of a possible glutamate dysfunction in schizophrenia, likely mediated via NMDA receptors.

Decreased glutamate concentrations in the PFC of people with schizophrenia are frequently found in imaging studies; results of hippocampal and thalamic glutamate concentrations are inconclusive in these (Marsman *et al.*, 2013). Decreased glutamate is also found in the PFC and hippocampus in the brain, *post mortem* (Tsai *et al.*, 1995). Increased glutamate levels in the anterior cingulate cortex, and not that of dopamine, may also account for poor response to antipsychotic treatment (Demjaha *et al.*, 2013). NMDA receptor dysfunction may also give rise to altered neurotransmitter systems, such as with dopamine (Jentsch *et al.*, 1998b) and γ-amino butyric acid (GABA) (Xue *et al.*, 2011).

GABAergic interneurones are rich in NMDA receptors, and the loss or dysfunction of these cells (Section 1.1.3.) may account for aberrant glutamate signalling. Altered expression of glutamic acid decarboxylase (GAD) enzymes, which catalyse glutamate to give GABA, has been found to be decreased in schizophrenia (Lewis *et al.*, 2005). A loss of GABAergic tone may lead to increased glutamate signalling, as illustrated by **Figure 1.1**. This is found in rodents with NMDA receptor inhibition (Adams and Moghaddam, 2001) and with selective knockout of the GluN1 subunit of NMDA receptors at GABAergic interneurones during postnatal development (Belforte *et al.*, 2010).

Much of the evidence in support of the Glutamate Hypothesis is derived from animal models of NMDA receptor hypofunction, and these will be outlined in Section 1.3.1.

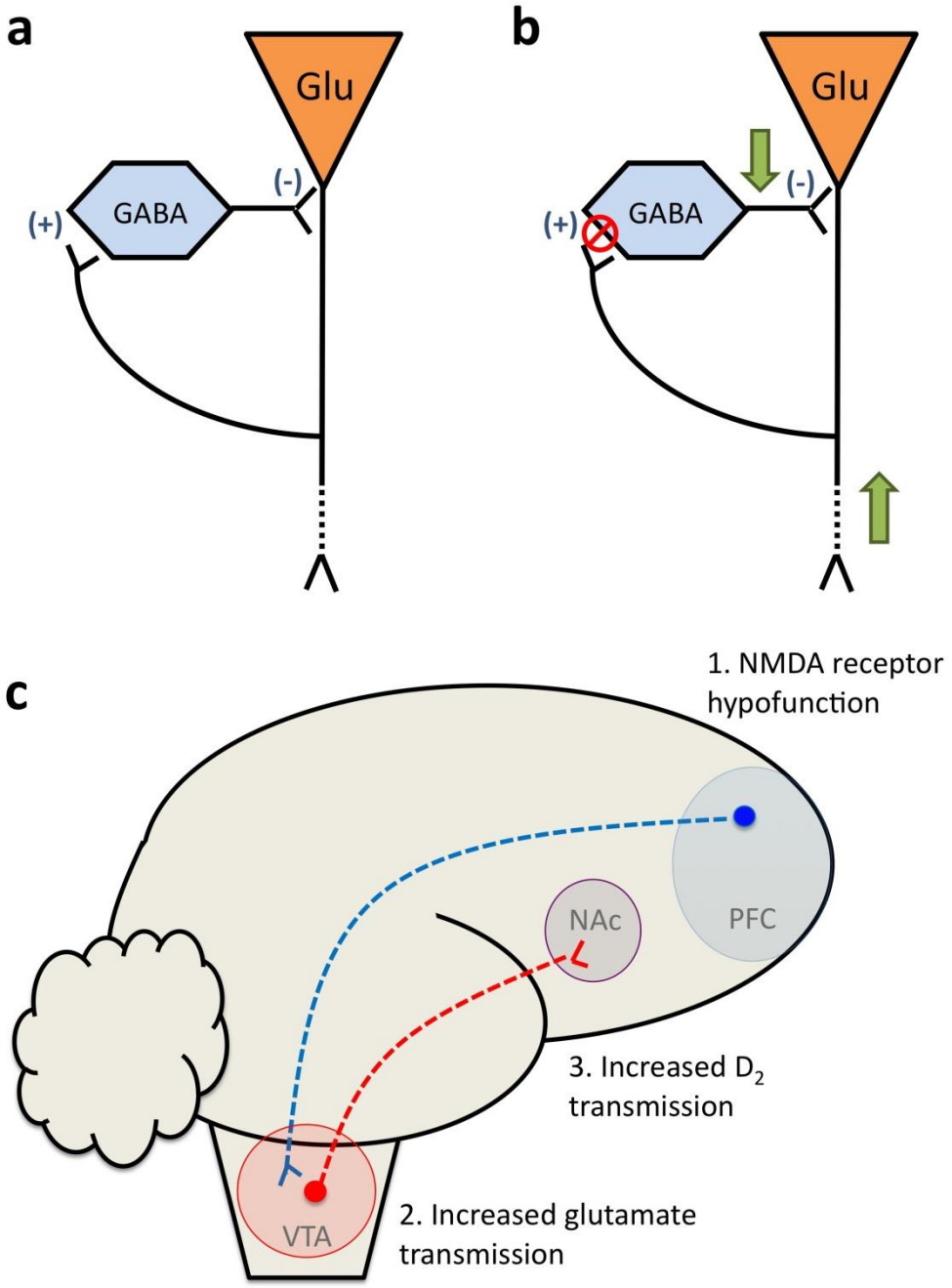

Figure 1.1. NMDA receptor hypofunction can lead to increased glutamate efflux: relevance to the Glutamate Hypothesis of Schizophrenia. (**a**) NMDA receptors at GABAergic interneurones (GABA) are stimulated (**+**) by glutamate that is released from innervating recurrent collateral branches of glutamatergic pyramidal cells (Glu). Tonic release of GABA suppresses (**-**) excess pyramidal cell activity. (**b**) NMDA receptor hypofunction gives rise to a loss of GABAergic tone, and a consequent increase in glutamate release. (**c**) GABAergic disinhibition may give rise to brain network dysfunction, such as that implicated in the Glutamate Hypothesis of Schizophrenia: (1.) NMDA receptor hypofunction in the prefrontal cortex (PFC) leads to (2.) increased glutamate release from PFC projection neurones in the ventral tegmental area (VTA), and subsequently, (3.) enhanced transmission at dopaminergic D_2 receptors in the nucleus accumbens (NAc).

1.2.4 Oxidative stress and schizophrenia

Evidence for increased oxidative stress in the brain has been found in people with schizophrenia (reviewed by: Bitanihirwe and Woo, 2011). For example, alterations in mitochondrial respiration (Prabakaran *et al.*, 2004), immune function (reviewed by: Bernstein et al., 2009; Ezeoke et al., in press), and nitric oxide signalling (Section 1.5.) have been implicated in the disorder. The potential roles of NADPH-oxidases (NOX) and the thioredoxin – thioredoxin reductase (Trx/TrxR) system are outlined here.

There is compelling evidence that the dysfunction and loss of PV interneurones seen in schizophrenia (Section 1.1.3.) may be mediated by oxidative stress (reviewed by: Behrens and Sejnowski, 2009; Nakazawa et al., 2011). NOX are a superoxide generating family of enzymes, and the NOX2 subtype is expressed in neurones. The Behrens group have found that altered NOX2 activity contributes to the loss of PV interneurones following NMDA receptor antagonist exposure in the mouse PFC (Behrens *et al.*, 2007), and appears to be mediated by interleukin 6 (Behrens *et al.*, 2008). Superoxide dismustase (SOD) catalyses the conversion of superoxide to oxygen and hydrogen peroxide, and this enzyme is also found to be elevated in people with schizophrenia (Wu *et al.*, 2012). This increased SOD activity may be reversed by antipsychotic drugs (Zhang *et al.*, 2012b), but their influence on NOX2 has yet to be determined.

The Trx/TrxR system is important for the maintenance of cellular redox state. Trx/TrxR are antioxidant, and may alter protein function by the regulation of thiol denitrosylation (reviewed by: Sengupta and Holmgren, 2012). These are also important in apoptosis, and are involved in the induction of caspases (reviewed by: Shahani and Sawa, 2011). Trx has been found to be increased in unmedicated, first-episode patients with schizophrenia, but not with those

with established schizophrenia (Zhang *et al.*, 2009a), and may be associated with impairments in attention (Zhang *et al.*, 2012a). The Trx/TrxR system is important in cellular stress, and is a key mediator of a nitric oxide signalling mechanism (Benhar *et al.*, 2010). The role of this system in schizophrenia is yet to be fully elucidated.

1.3 Animal models of relevance to schizophrenia

Animal models have provided a wealth of information that has contributed to our understanding of schizophrenia. Outlined here are examples of rodent models with relevance to schizophrenia, with a particular focus on NMDA receptor antagonist models which have relevance to this thesis. **Table 1** summarises and allows comparison of the deficits that may be modelled with these rodent models.

1.3.1 Pharmacological models

Potentiation of dopaminergic transmission using amphetamine may elicit behaviours in rodents that are relevant to positive symptoms of schizophrenia, and some deficits related to negative symptoms and cognition (Sams-Dodd, 1995; Featherstone et al., 2008). Continuous amphetamine administration dose-dependently induces hyperlocomotion in rats, but does not influence social withdrawal (Sams-Dodd, 1998a). Sensitisation to amphetamine by repeated exposures elicits a long-lasting (60 days withdrawal) deficit in sensorimotor gating and latent inhibition, whereas that with PCP does not (Tenn *et al.*, 2005). Deficits in attention (Martinez and Sarter, 2008) and cognitive flexibility are found too with amphetamine sensitisation, but there are no deficits in spatial or working memory in rats with this treatment (Featherstone *et al.*, 2008). Increased dopamine release is seen in the PFC and nucleus accumbens (reviewed by: Featherstone et al.,

2007). While antagonism of D2 receptors in the mesolimbic dopamine system alleviates psychotic symptoms (Section 1.1.2.), the use of animal models with amphetamine has identified D1 receptors in the PFC as a potential therapeutic target that may improve cognitive deficits (Fletcher et al., 2005; Fletcher et al., 2007; Bay-Richter et al., 2013). Together, potentiation of dopamine via amphetamine is a useful means to produce deficits relevant to positive symptoms and some cognitive domains, but does not give as complete a range of deficits as the other models outlined in this section.

NMDA receptor antagonists elicit a broader range of deficits in rodents that are relevant to schizophrenia than dopaminergic drugs do (reviewed by Jentsch and Roth, 1999). Changes seen with acute NMDA receptor antagonism include hyperlocomotion, deficits in sensorimotor gating, cognitive flexibility (Egerton *et al.*, 2005), and disrupted thalamocortical connectivity (Dawson *et al.*, 2011). Cognitive deficits are produced by acute PCP and by repeated administrations; the latter are likely to be more translationally relevant to schizophrenia (Egerton et al., 2008; Thomson et al., 2011). NMDA receptor antagonists produce deficits in working memory too, though perhaps not in the same way as seen in schizophrenia (Smith *et al.*, 2011). Decreased social behaviours are seen with subchronic administrations of PCP (Sams-Dodd, 1995; Wass et al., 2009). Deficits in sensorimotor gating, as determined by prepulse inhibition of a startling stimulus, persist in rats with repeated administrations of PCP, but do not following drug withdrawal (Egerton *et al.*, 2008).

An increase in PFC glutamate, 5HT and dopamine are observed with acute PCP in rats (Adams and Moghaddam, 2001), and this is thought to arise from the attenuation of GABAergic tone via NMDA receptor blockade (Section 1.2.3.), the latter two possibly mediated by GABAergic disinhibition and

subsequent stimulation of non-NMDA receptors (Moghaddam *et al.*, 1997). Acute NMDA receptor antagonism in the PFC by PCP also appears to elicit hyperlocomotion and stimulate dopamine release in the nucleus accumbens (Jentsch *et al.*, 1998b). Conversely, subchronic PCP appears to elicit a hypodopaminergic state in the rat PFC, dopamine levels in the nucleus accumbens are normalised, and rats are more sensitive to amphetamine-stimulated hyperlocomotion (Jentsch *et al.*, 1998a) and PFC dopamine release (Balla *et al.*, 2003).

Loss of cortical and hippocampal PV interneurones is found with subchronic ketamine (Keilhoff et al., 2004; Behrens et al., 2007), PCP (Cochran *et al.*, 2003) and with MK801 (Braun *et al.*, 2007). Though, this finding is not reproduced by all (Benneyworth et al., 2011; Featherstone et al., 2012). Interestingly, a delayed effect of decreased PV expression is seen in the reticular thalamus following acute PCP (Cochran *et al.*, 2002), and both this region and the PFC are affected with repeated administrations (Cochran *et al.*, 2003), implicating temporally-specific changes in PV expression. Administrations of PCP in neonatal mice also elicits a loss of PV interneurones in the cortex, hippocampus and nucleus accumbens, that is found in adulthood (Nakatani-Pawlak *et al.*, 2009).

NMDA receptor antagonist models are a popular choice for researchers, and especially for evaluating potential drug treatments. As outlined above, these models have good face validity, though there is some variation in the behavioural responses of rodents with different NMDA receptor antagonists (Anastasio et al., 2009; Smith et al., 2011). There is a replication of the relative efficacy of antipsychotic drugs in the alleviation of behavioural deficits related to those seen in schizophrenia (Ogren and Goldstein, 1994; Sams-Dodd, 1996; Thomson et al., 2011). However, the predictive validity of

these models has come in to question (reviewed by: Large, 2007; Pratt et al., 2012).

Table 1 Rodent models of relevance to schizophrenia.

	Intervention	PPI	LMA	Spatial memory	Working memory	Attention	Anhedonia	Sociability	PV loss / dysfunction	Mesolimbic DA	References
Pharmacological	Acute amphetamine	X	↑	X	X	↓	X	X	ND	↑	(Sams-Dodd, 1995; Jentsch et al., 1998b; Sams-Dodd, 1998a; Cochran et al., 2003; Tenn et al., 2005; Featherstone et al., 2007; Egerton et al., 2008; Martinez and Sarter, 2008; Jones et al., 2011; Thomson et al., 2011)
	Repeated amphetamine	↓	↑	X	X	↓	↑	X	X	↑	
	Acute NMDAR antagonism	↓	↑	X	X	X	X	X	X	↑	
	Repeated NMDAR antagonism	X	↑	↓	↓	↓	X	↓	**Y**	↑	
Developmental	Poly(I:C)	↓	↓	X	↓	↓	↑	↓	**Y**	ND	(Fone and Porkess, 2008; Lodge and Grace, 2009; Tseng et al., 2009; Jones et al., 2011; Meyer, 2013)
	MAM	↓	↑	↓	↓	↓	X	↓	**Y**	↑	
	NVHL	↓	↑	↓	↓	↓	↑	↓	**Y**	X	
	Post-weaning social isolation	↓	↑	X	ND	X	↓	↑	**Y**	↑	
Genetic	*Disc1*	↓	X	↓	↓	ND	Variable	Variable	**Y**	ND	(Jaaro-Peled, 2009; Papaleo et al., 2012; Pratt et al., 2012)
	Nrg1/Erbb4	↓	↑	↓	↓	ND	ND	ND	**Y**	ND	
	Comt	X	X	↓	↑	↓	ND	X	ND	ND	

The behavioural, anatomical and neurochemical changes of relevance to schizophrenia reported in popular animal models. Table legend: **X**, no change from controls detected; **Y**, deficit is present; ↑, increased from controls; ↓, decreased or deficient from controls, **ND**, not determined / reported; **Variable**, variable outcomes between different mouse background strains. Abbreviations: DA, dopamine; LMA, locomotor activity; MAM, methylazoxymethanol acetate; NMDAR, *N*-methyl-D-aspartate receptor; NVHL, neonatal ventral hippocampus lesion; Poly(I:C), polyriboinosinic-polyribocytidilic acid; PPI, prepulse inhibition; PV, parvalbumin.

1.3.2 Developmental models

Several rodent models have been developed that feature an intervention during neural development. Briefly described here are some of these models that improve upon the construct validity of pharmacological models by the very nature of schizophrenia being a neurodevelopmental disorder.

Maternal administration of polyriboinosinic-polyribocytidilic acid, or poly(I:C), mimics viral infection and brings about deficits in offspring around late adolescence to early adulthood, reproducing the illness onset period commonly seen in schizophrenia (reviewed by: Meyer, 2013)

Administration of methylazoxymethanol acetate (MAM) on embryonic day 17 disrupts brain development and elicits an array of behavioural deficits in adulthood, such as impaired sensorimotor gating and working memory. There are also gross neuroanatomical changes, such as decreased volumes of cortical and temporal structures (reviewed by: Lodge and Grace, 2009), that may reflect some of those seen in schizophrenia (Section 1.1.3). The 'MAM Model' is the current rodent model of choice for pharmaceutical companies for evaluating potential therapeutic agents for schizophrenia.

Neonatal ventral hippocampus lesion (NVHL) produces behavioural abnormalities of relevance in the adult rodent, such as deficits in sensorimotor gating and cognitive flexibility, and abnormal sociability. Unlike many developmental models, enlarged ventricles are found in the adult rats as is found in people with schizophrenia (Section 1.1.3). NHVL rodents lack hyperdopaminergia in the nucleus accumbens (reviewed by: Tseng et al., 2009), as found with other models and in schizophrenia (Section 1.2.2). These models also lack a decreased expression of cortical PV interneurones

and GAD, though there appears to be interneurone dysfunction in the PFC (Tseng *et al.*, 2008).

Post-weaning social isolation of rodents produces many behavioural deficits that are translationally relevant to schizophrenia, such as sensorimotor gating deficits, anhedonia, and deficits in cognitive flexibility (reviewed by: Fone and Porkess, 2008). These models reinforce how early life social interactions are critical for cognitive function (Nelson *et al.*, 2007), and there are long-lasting neurochemical and anatomical changes present too. Adult isolates display increased dopamine in the nucleus accumbens, decreased dopamine and glutamate in the PFC, and a reduced PFC volume (reviewed by: Jones et al., 2011). Socially isolated rats also show a decrease in PV interneurones that is mediated by NOX (Schiavone *et al.*, 2009).

1.3.3 Genetic models

Genetically-modified mice are used to explore the implications of genetic risk factors on deficits that have relevance to schizophrenia. The behavioural consequences of genetic modification of *Disc1*, *Erbb4*, and *Grin2*, for example, in mice have produced some deficits of relevance, as (reviewed by: Pratt et al., 2012). These models give an indication of the influence of a single gene may have on brain function. So far, genetic models do not produce as comprehensive a model (i.e. face validity) as those previously mentioned, but enable the development of models of gene-gene, gene-environment, etc., -interactions to provide a model with a much better construct validity than previously available.

1.4 Nitric oxide in the brain

Nitric oxide is a small gaseous messenger that can freely diffuse across membranes. NO has a half-life of about four seconds and spreads in a spherical manner that may influence targets within a diameter of about 300 μm from its source (reviewed by: Garthwaite and Boulton, 1995). Due to this, NO signalling may act in a paracrine or autocrine manner. The synthesis and actions of NO will be outlined with particular emphasis on nitrergic influence on neurotransmission in the brain.

1.4.1 Nitric generation and signalling

Nitric oxide is produced by the enzyme, nitric oxide synthase (NOS), and may be localised in various cell types. There are three major isoforms of NOS that have been identified; neuronal NOS (Type I, or nNOS), inducible NOS (Type II, or iNOS), and endothelial NOS (Type III, or eNOS). Neuronal and endothelial isoforms are not constitutively active and are calcium-dependent; whereas, iNOS is calcium-independent and constitutively active when present. As illustrated by Figure 1.2, NOS is active as a homodimer and the binding of L-arginine (henceforth referred to as arginine) and calcium-bound calmodulin drives the production of citrulline (L-/D- isomer not determined) and nitric oxide from the constitutive isoforms of NOS. Arginine is the substrate that drives NOS activity and its structural analogue, asymmetric dimethyarginine (ADMA), competes with the substrate and inhibits nitric oxide generation (Vallance *et al.*, 1992), as illustrated by Figure 1.3a. All isoforms are expressed in the human brain, though it is thought that nNOS accounts for about 95% of the NO production in the brain (Kirchner *et al.*, 2004). nNOS is expressed in about 1% of all neurones, and is distributed throughout the brain, including; the cerebellum, cerebral cortex, hippocampus, hypothalamus, medulla, midbrain, and striatum (Egberongbe

et al., 1994; Blum-Degen et al., 1999). nNOS is expressed in the CNS in a range of neurones that have diverse morphologies and may be co-expressed with a range of neurotransmitters and neuropeptides (González-Albo et al., 2001; Jinno and Kosaka, 2002; Benavides-Piccione and DeFelipe, 2003)

There are several cofactors required for nNOS activity, these are; Ca^{2+}-bound calmodulin, nicotinamide adenine dinucleotide phosphate (NADPH), flavin adenine dinucleotide (FAD), flavin mononucleotide (FMN), haem, thiol, and tetrahydrobiopterin (BH_4). The roles these cofactors in NOS function are Reviewed byAlderton, Cooper and Knowles (2001). Of particular relevance to the work in Chapter 6 is the role of BH_4 in NO generation. BH_4 has been shown to promote NOS dimerisation, and thus facilitate activity (Reif *et al.*, 1999), and has also been shown to prevent the more detrimental properties of NOS activities by the suppression of superoxide (Kotsonis *et al.*, 2000). BH_4 is also an essential cofactor for other enzymes, such as tyrosine hydroxylase (reviewed by: Ichinose et al., 2008), and is therefore an interesting target that not only may influence nitric oxide generation and be neuroprotective, but may also have an impact on monoamine synthesis that may be relevant to schizophrenia (Richardson et al., 2007; Choi and Tarazi, 2010).

There is a close functional relationship between NMDA-R and nNOS and it is by this connection that NO acts as a second messenger of NMDA-R signalling (Kano et al., 1998; Buchholzer and Klein, 2002). This is achieved via linkage of postsynaptic density-95 (PSD-95) proteins at PSD-95/Discs large/zona occludens-1 (PDZ) domains of cytoplasmic nNOS and NMDA-R (Brenman et al., 1996; Sattler et al., 1999). As illustrated by Figure 1.2., These interactions tether nNOS close to the Ca^{2+} channel of the NMDA-R so that the NOS has foremost access to the influx of Ca^{2+} ions for its activity (Garthwaite et al., 1988; Ishii et al., 2006). CAPON (carboxyl-terminal PDZ

ligand of neuronal nitric oxide synthase), also known as nNOS adaptor protein (NOS1AP), competes with PSD-95 at nNOS PDZ domains (Jaffrey *et al.*, 1998). Figure 1.3b illustrates how CAPON may dislocate nNOS and PSD-95 thereby disrupting the functional link with NMDA-R and nNOS.

Splice variants of nNOS exist too, including nNOSβ, nNOSγ, nNOSμ, and nNOS-2 (reviewed by: Alderton et al., 2001). nNOSβ and nNOSγ are the only variants shown to be enzymatically functional in the brain (Brenman *et al.*, 1997), but lack a PDZ domain (Brenman *et al.*, 1996) and therefore do not possess the same PSD-95 – NMDA receptor interactions as the full length isoform (designated nNOSα, in this context). The gamma variant has been shown to have minimal function (~3%) compared to nNOSβ (~80%) and nNOSα (Eliasson *et al.*, 1997). The functional role of these variants is yet to be elucidated.

Nitric oxide has multiple influences in the brain. The stimulation of soluble guanylate cyclase (sGC) drives the catalysis of guanosine triphosphate (GTP) to cyclic guanosine 3',5'-monophosphate (cGMP). Nitric oxide-stimulated cGMP may activate protein kinase G (PKG) which mediates the relaxation of vascular smooth muscle, as outlined in Section 1.4.3., and also actions on other protein kinases and phosphodiesterases (reviewed by: Kleppisch and Feil, 2009). Nitric oxide may also modify protein function by the nitrosation of free thiols (*S*-nitrosylation). There is a diverse list of influenced proteins and the impact that *S*-nitrosylation (reviewed by: Seth and Stamler, 2011), and denitrosylation (reviewed by: Benhar et al., 2009) has on their functions. The roles of these in the context of brain function are outlined below.

1.4.2 Modulation of neural transmission

Nitric oxide-stimulated PKG may have a role in the modulation of long-term potentiation (Lu *et al.*, 1999) and long-term depression (Stricker and Manahan-Vaughan, 2009), and nitric oxide may also act independently of sGC - cGMP signalling, such as with the induction of immediate early genes (Morris, 1995). These implicate a role for nitric oxide in synaptic plasticity, and thus learning and memory (reviewed by: Prast and Philippu, 2001; Hopper and Garthwaite, 2006). Nitric oxide may also serve as a feedback inhibitor of NMDA receptors (Lipton et al., 1993; Choi et al., 2000), and of its synthesising enzyme (Qu *et al.*, 2012) by *S*-nitrosylation.

While some may argue that nitric oxide may not nitrosylate free thiols of proteins at physiological concentrations (Hopper *et al.*, 2004), one must question what concentrations endogenous nitric oxide may achieve. There is a wide and varied range of concentrations that have been reported, most from electrochemistry infer a nanomolar range, as Reviewed by(Hall and Garthwaite, 2009), and some propose a picomolar range, albeit by less direct measures (Wood *et al.*, 2011).

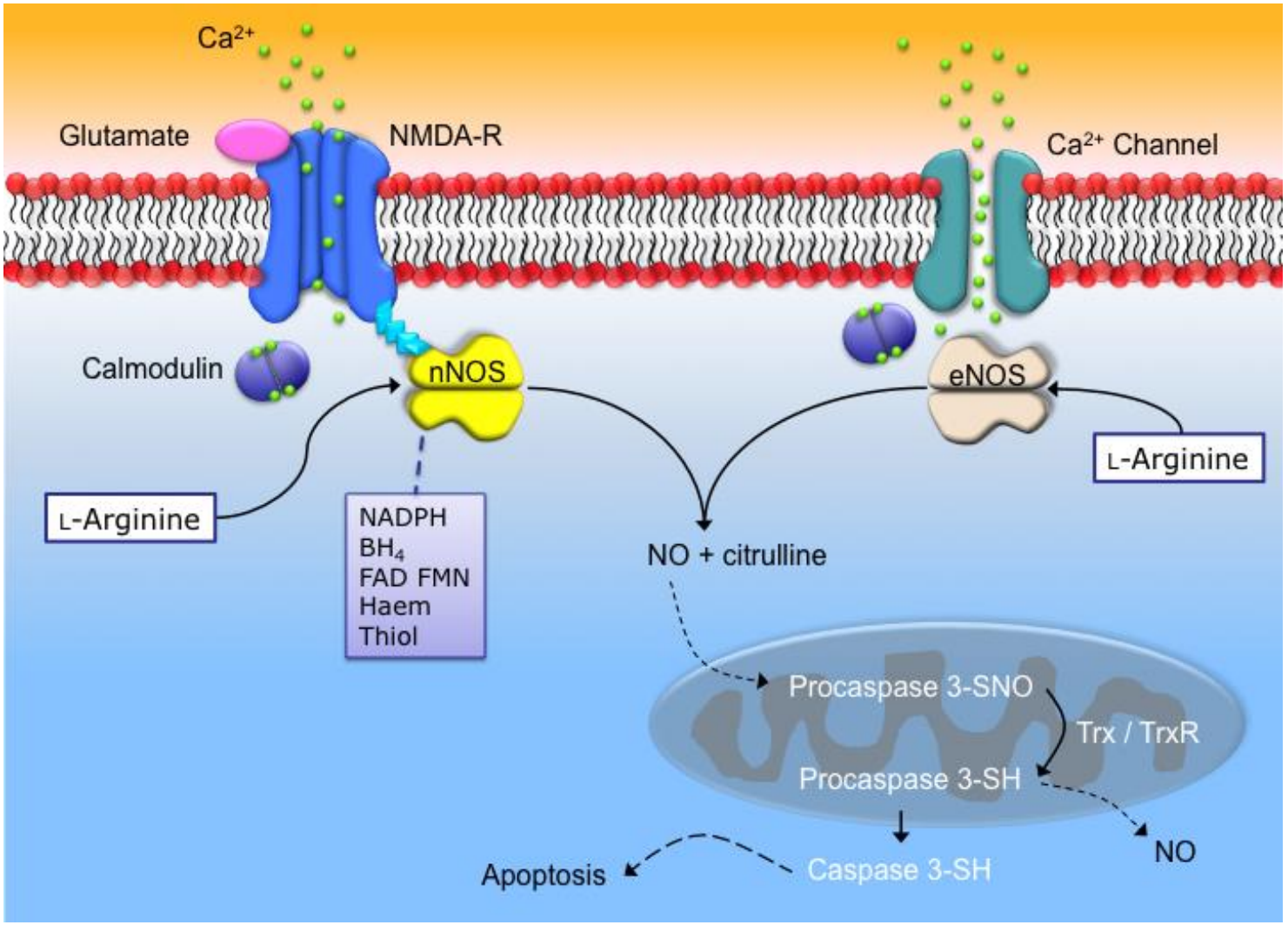
Ca2+
Glutamate
NMDA-R
Ca2+ Channel
Calmodulin
nNOS
eNOS
L-Arginine
L-Arginine
NADPH
BH4
FAD FMN
Haem
Thiol
NO + citrulline
Procaspase 3-SNO
Trx / TrxR
Procaspase 3-SH
NO
Apoptosis
Caspase 3-SH

Figure 1.2. Nitric oxide synthase. The constitutive isoforms of NOS, neuronal (nNOS) and endothelial (eNOS), require calcium (Ca^{2+}) -bound calmodulin and several cofactors to drive the catalysis of arginine to nitric oxide (NO) and citrulline. In neurones, nNOS is physically and functionally tethered to the NMDA subtype of glutamate receptor (NMDA-R) that provides the calcium source for nNOS activity upon NMDA receptor activation. In endothelial cells, eNOS is activated by Ca^{2+} from muscarinic acetylcholine receptors and other Ca^{2+} channels, and from intracellular stores in the endoplasmic reticulum. Nitric oxide has multiple cellular targets and effects. For example, the *S*-nitrosylation of free thiols on procaspase 3 stabilises this enzyme. The liberation of NO (denitrosylation) by the thioredoxin / thioredoxin reductase system (Trx/TrxR) promotes the activation of procaspase 3 to form active caspase 3 which may then initiate a apoptotic cascade.

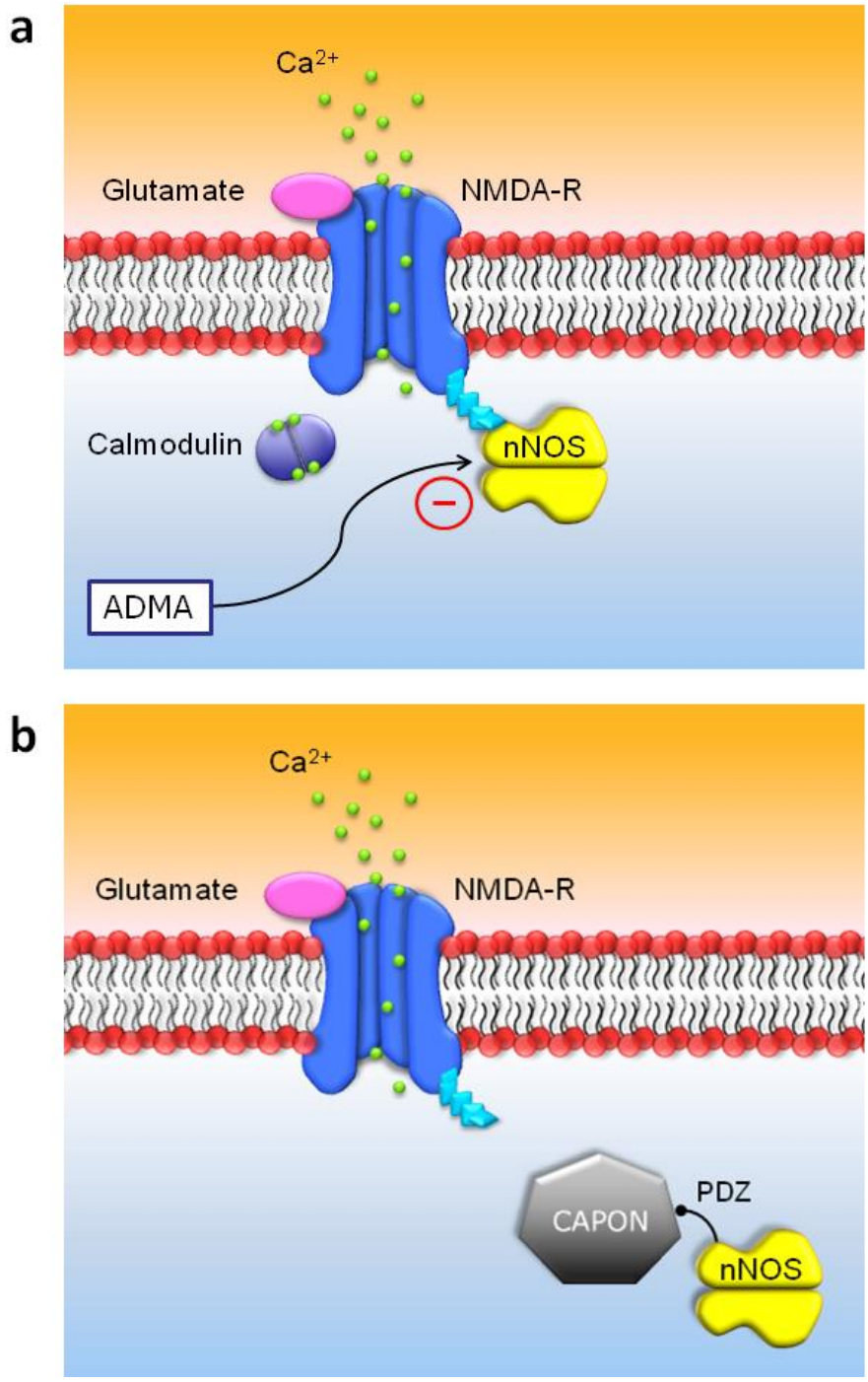

Figure 1.3. Endogenous inhibitors of nNOS. (a) Asymmetric dimethylarginine (ADMA) is an endogenous arginine analogue that competes with the arginine substrate to inhibit NOS activity. (b) nNOS and NMDA receptors are linked via PSD-95 proteins. The PSD-95/discs large/zona occludens-1 (PDZ) domain of nNOS interacts with PSD-95 that enables NMDA receptor activation, and subsequent calcium influx, to activate nNOS. This interaction may be competed for by CAPON (carboxy-terminal PDZ ligand of nNOS), which sequesters nNOS and thereby disrupts the generation of nitric oxide (NO) as a function of NMDA receptor activity..

1.4.3 Modulation of cerebral blood flow and neurovascular coupling

Nitric oxide mediates the relaxation in smooth muscle of blood vessels thus decreasing blood pressure and increasing blood flow. In the brain, this forms the basis of functional hyperaemia, where increased metabolic demands of an active brain region requires increased nutrient and waste flow. This neurovascular coupling forms a fundamental interaction between the functions of neurones and glia with the local vasculature. Cerebral blood flow correlates with neuronal activity in proximity (Mullinger *et al.*, 2013) and appears to be mediated by NOS activity ubiquitously (Macrae *et al.*, 1993). NOS in neurones, not just blood vessels, may regulate local blood flow (reviewed by: Duchemin et al., 2012). Similarly, nitric oxide derived from blood vessels may regulate neuronal transmission (Garthwaite *et al.*, 2006).

1.4.4 Nitrosative and oxidative stress

Nitric oxide is implicated in both cellular stress and death, and also as a protective agent. Of relevance to brain function, this is mostly studied in the context of stroke and neurodegenerative diseases such as Alzheimer's and Parkinson's disease (reviewed by: Chabrier et al., 1999; Terpolilli et al., 2012). Nitric oxide interacts with superoxide (O_2^-) to form peroxynitrite ($ONOO^-$). Peroxynitrite is a highly reactive nitrating molecule that leads to cellular stress and necrotic death, whereas high concentrations of nitric oxide appear to induce caspases (Meij et al., 2004; Fatokun et al., 2008). Therefore the activities of NOS and superoxide-generating enzymes such as NOX, together, are important for normal functioning of cells and must be regulated. For example, nitric oxide may also inhibit superoxide production via NADPH oxidase (Selemidis *et al.*, 2007) thus reducing the production of peroxynitrite.

Nitric oxide may also mediate cellular stress and death via *S*-nitrosylation and denitrosylation. *S*-nitrosylation may also contribute to the neuroprotective properties of nitrergic neurones (Andoh *et al.*, 2003). The caspase-mediated apoptotic cascade is induced by process of denitrosylation of procaspase 3 (Tenneti et al., 1997; Benhar et al., 2008). Nitric oxide may also induce apoptosis signal-regulating kinase-1 (ASK1) via *S*-nitrosylation (Liu *et al.*, 2013). The actions of nitric oxide on caspase 3 and ASK1 may also involve the Trx/TrxR system (outlined in Section 1.2.4.) (reviewed by: Sengupta and Holmgren, 2012). The activities of Trx and TrxR are protective against oxidative and nitrosative stress (Andoh et al., 2002; Andoh et al., 2003), and are important in the regulation of nitric oxide signalling (reviewed by: Wu et al., 2011).

1.5 Nitric oxide and schizophrenia

Increasingly compelling evidence is emerging that suggest a role of NO in schizophrenia (reviewed by: Bernstein et al., 2005; O'Donovan et al., 2008). Presented here is some of this evidence, and how the potential for NO as a therapeutic target for the disorder has been revealed in animal models of relevance to schizophrenia.

1.5.1 Evidence from clinical trials

A recent clinical study found that positive and negative symptoms were improved in patients with schizophrenia following systemic administration of the nitric oxide donor, sodium nitroprusside, and that this effect remained 4 weeks after administration (Hallak *et al.*, 2013). This has yet to be replicated. A trial using single doses of sildefinil, a PDE5 inhibitor, revealed no improvement in symptoms over placebo treatment (Goff *et al.*, 2008). Potentiation of nitric oxide-mediated cGMP activity via PDE5 inhibition has

been shown to improve cognitive deficits in rodents (Rodefer *et al.*, 2012), but this appears not to be the case in the human. Acute and chronic administration of the antibiotic, minocycline has been shown to improve positive, negative and cognitive symptoms in patients with schizophrenia when used as an adjuvant with antipsychotic drugs (Miyaoka et al., 2008; Levkovitz et al., 2010). This was replicated in a long-term, multi-centre study by Chaudhry and colleagues (2012). These effects of minocycline are often attributed to the inhibition of NOS, but this has yet to be shown directly, and minocycline has multiple effects (such as inactivating microglia and its antioxidant properties) that may contribute to its action (reviewed by: Chaves et al., 2009).

1.5.2 Genetic evidence

Schizophrenia is a neurodevelopmental disorder and has a strong genetic component (Tandon *et al.*, 2008). Many genes are now implicated in schizophrenia (Harrison and Weinberger, 2005; Owen, 2012), from studies focussing on single genes to meta-analyses of large cohort-genome-wide association studies (GWAS). The challenge now is to study the functional impact that altered genes have. Evidence of alterations in the nNOS-encoding gene (*NOS1*) in people with schizophrenia, and the potential functional impact of these alterations, is presented below.

A GWAS of data obtained from people with schizophrenia identified a single nucleotide polymorphism (SNP) of *NOS1* as being potentially associated with the disorder (O'Donovan *et al.*, 2008). The rs6490121 risk allele has since been associated with reduced grey matter density (Rose *et al.*, 2012) and deficits in sensory processing (O'Donoghue *et al.*, 2011), verbal intelligence and working memory (Donohoe *et al.*, 2009). Other GWAS however, found

no significant association of this rs6490121 with the disorder (Okumura et al., 2009; Riley et al., 2009).

Smaller-scale genetic studies too have identified *NOS1* as a potential susceptibility factor for schizophrenia. For example, Baba, and colleagues (2004) showed a significant increase in nNOS mRNA expression (but not of sGC) in the PFC of schizophrenic patients compared with controls. This finding was replicated by Silberberg and colleagues (2010), and went on to suggest that alternate transcripts of *NOS1* may be upregulated in the PFC. SNPs in the *NOS1* gene have been found in close association in people with schizophrenia in Asian populations (Shinkai et al., 2002; Tang et al., 2008) and in a study of Ashkenazi Jewish families (Fallin *et al.*, 2005).

Polymorphisms of regulatory, but not coding regions of *NOS1* have also been associated with altered PFC function in schizophrenic patients (Reif *et al.*, 2006). These polymorphisms were more frequent in the *NOS1* reductase domain, while the oxygenase domain was highly conserved, and this may translate to altered cofactor binding and redox function of nNOS (Alderton *et al.*, 2001). The same group have shown that this *NOS1* SNP is associated with a deficit in working memory performance (Reif *et al.*, 2011). A variable number tandem repeat (VNTR) polymorphism of the promoter region of *NOS1* has also been identified that may be associated with working memory performance in people with schizophrenia (Kopf *et al.*, 2011). Genetic associations regarding the nNOS-sequestering protein, CAPON, have also been identified in schizophrenic patients. An increased expression of a short form of CAPON mRNA in the dorsolateral PFC has been reported (Xu *et al.*, 2005). A range of SNPs within the *CAPON* gene, and not *NOS1*, was found to be associated with people with schizophrenia in a study by Nicodemus and colleagues (2010). SNPs in the *CAPON* have also found to be more frequent in people with schizophrenia in South American family trios, and particularly

associated with negative symptoms (Kremeyer *et al.*, 2009). However, a different collection of SNPs were found to be associated with psychiatric syndromes, but not in schizophrenic patients within a French population (Delorme *et al.*, 2010). Alterations in *NOS1* may give rise to altered nNOS function, and the disruption of nNOS and NMDA-R by increased CAPON expression may confer decreased NO generation.

Overall, the genetic evidence for an association between NOS and schizophrenia is not conclusive. GWAS have identified many SNPs as potential risk factors in amongst the several thousands of SNPs in the human genome (Owen *et al.*, 2010). That *NOS1* has been identified at all in these risk alleles (O'Donovan *et al.*, 2008) is promising; SNPs generally have a small contribution to disease risk and must meet very strict statistical criteria (Owen, 2012). Polymorphisms of *NOS1* and of *CAPON* have also been associated with cognitive deficits in people with schizophrenia obtained from neuroimaging and electrophysiological techniques (Donohoe et al., 2009; Kremeyer et al., 2009; Reif et al., 2011), indicating that, while these polymorphisms have a small contribution overall, may still be penetrant in certain symptoms. To date, no study has investigated the role of epigenetic influences or that of *NOS1* in people at risk of developing schizophrenia. Until then, these findings remain as phenomena in people with established schizophrenia with the possible time-dependent changes of this unclear.

1.5.3 Biochemical evidence

Many regions in the *post mortem* brains of people with schizophrenia have been identified to have altered morphologies, distributions and densities of NOS-containing neurones (Bernstein *et al.*, 2005). A decreased density, and possible altered morphology of nitrergic interneurones in the putamen has been reported (Lauer et al., 2005; Fritzen et al., 2007). Increased nitric oxide

metabolites have also been found in the striatum (Yao *et al.*, 2004). Together, these may influence dopaminergic (Salum *et al.*, 2008), and cholinergic transmission (Buchholzer and Klein, 2002) in the striatum. Decreased NOS activity, but not expression, has been shown in the PFC of people with schizophrenia (Xing *et al.*, 2002). NOS-expressing neurones have been shown to be differentially localised in the PFC, hippocampus and temporal lobe in the brains of patients with schizophrenia compared to controls (Akbarian et al., 1993b; Akbarian et al., 1993a). This may be due to altered migration or pruning of nitrergic neurones during development.

Determining NOS activity is also possible in the live human, albeit using less direct measures in blood plasma or serum. Using plasma nitrate and nitrite (NO_x) concentrations as a marker of NO metabolism, Das and colleagues (1996) reported decreased concentrations of NO_x and increased ADMA, the endogenous NOS inhibitor, in drug-naïve patients with schizophrenia, compared to controls. In some of the samples, antipsychotic drug treatment apparently reversed NO_x and ADMA to levels similar to controls. Similarly, Lee and Kim (2008) found decreased NO metabolites in patients with schizophrenia. A six-week follow-up revealed a normalisation of NO_x in patients whose symptoms improved with risperidone treatment. Increased NO_x concentrations were also found in patients with chronic schizophrenia that were treated with antipsychotic drugs, indicating hypernitrergic activity (Yilmaz *et al.*, 2007). In contrast, increased NO_x was found in drug-naïve and in chronic patients with schizophrenia, and this increase was reversed with antipsychotic drug treatment (Zhang *et al.*, 2012b). A meta-analysis of data related to NO_x in people with schizophrenia determined that, as outlined here, results are variable, and best explained by antipsychotic treatment (Maia-de-Oliveira *et al.*, 2012).

Chittiprol and colleagues (2009) have reported increased biopterin (indicative of BH_4) plasma concentrations in antipsychotic-naïve patients with schizophrenia compared to controls. Following 3-months treatment with antipsychotic drugs, plasma biopterin levels were found to be decreased in these patients. Decreased biopterin has also been found in people with established schizophrenia with long-term antipsychotic drug treatment (Richardson *et al.*, 2007).

These studies give evidence of altered morphologies, distributions and densities of nitrergic neurones (Akbarian et al., 1993b; Akbarian et al., 1993a; Fritzen et al., 2007), but report conflicting evidence on the levels of NO metabolites (Das et al., 1996; Yilmaz et al., 2007; Zhang et al., 2012b) and biopterin (Richardson et al., 2007; Chittiprol et al., 2009) observed in patients with schizophrenia. It is likely that illness duration and type of medication are the source of this variation (Maia-de-Oliveira *et al.*, 2012). Studies of NO_x lack regionally-specific detail that *post mortem* data possess, but can provide details of changes over time, especially at critical periods such as before and after drug treatment, and with illness onset. Until technologies develop to allow more direct and relevant measurements to be taken in the live human, it is data from animal models with translational relevance to schizophrenia (Section 1.3.) that provide the details necessary to elucidate the role of nitric oxide signalling in schizophrenia.

1.5.4 Evidence from animal models of relevance to schizophrenia

As discussed in Section 1.3.1., NMDA receptor antagonists produce a convincing model of deficits in animals that are relevant to schizophrenia, including PFC-associated cognitive deficits (reviewed by: Jentsch and Roth, 1999; Pratt et al., 2008; Jones et al., 2011). Given the close association of

NMDA receptors and nNOS function (Section 1.4.), it is possible that nitric oxide signalling is altered with NMDA receptor dysfunction. Outlined below are examples where NOS inhibitors have been shown to reverse behavioural deficits elicited by NMDA receptor antagonists, such as phencyclidine (PCP), ketamine and MK-801. Examples of changes in genetically-modified rodents of relevance are also given.

Johansson and colleagues (1997) showed that pre-treatment with the non-selective NOS inhibitor, nitro-L-arginine methyl esther (L-NAME), reversed hyperlocomotion and a prepulse inhibition (PPI) deficit induced by acute PCP treatment. NOS inhibition may also reverse acute PCP-induced deficits in learning and memory (Wass *et al.*, 2006), cognitive flexibility (Wass *et al.*, 2008), and social interaction (Wass *et al.*, 2009). The NOS inhibitor, 7-nitroindazole (7-NI) is somewhat more selective for the neuronal isoform of NOS than L-NAME (discussed by: Alderton *et al.*, 2001). 7-NI too, may reverse behavioural deficits elicited by NMDA receptor antagonism (Deutsch et al., 1996; Wiley, 1998).

Interruption of sGC appears to mitigate the NMDA receptor antagonist-induced deficits in PPI and spatial working memory, but not that of hyperlocomotion (Yamada et al., 1996; Fejgin et al., 2008), suggestive that nitric oxide affects multiple targets to influence the effects of NMDA receptor blockade. The latter may be influenced by a direct modulation of neurotransmission by nitric oxide (Meffert *et al.*, 1994), perhaps mediated by *S*-nitrosylation (Choi et al., 2000; Lu et al., 2009). This mechanism is also implicated in the modulation of synaptic plasticity (Morris, 1995; Huang et al., 2005; Selvakumar et al., 2009). A role for sGC in synaptic plasticity has also been described (Lu et al., 1999; Kleppisch and Feil, 2009; Sammut et al., 2010), and this may impact on cognitive function (Komsuoglu-Celikyurt *et al.*, 2011). The reversal of NMDA-receptor antagonist-mediated behavioural

deficits by methylene blue is often attributed to the inhibition of sGC (Deutsch *et al.*, 1996), including that of hyperlocomotion (Klamer et al., 2004a). Methylene blue is now generally accepted to not be selective for NOS or sGC, and the effects mentioned above may be explained by its influence on mitochondrial respiration or other non-selective interactions (Rojas *et al.*, 2012). The potential role of sGC as a function of NOS activity in these deficits also gives evidence that the effects are likely mediated by nitric oxide rather than peroxynitrite. Indeed, NMDA receptor antagonists appear not to alter peroxynitrite formation (Genius *et al.*, 2013). A nitric oxide/sGC/cGMP-mediated pathway appears to account for some of the deficits elicited by NMDA receptor antagonism but not all. Selective modulation of sGC may be beneficial for specifically targeting those deficits from a therapeutic standpoint, but perhaps serves better to explain the pathways that may contribute to them.

Cardiovascular effects of NOS inhibition both in the brain (Macrae *et al.*, 1993) and systemically (Rees *et al.*, 1990) are a potential unwanted effect in this context. Therefore, selective inhibition of nNOS may mitigate these cardiovascular effects, and potentially elucidate the role of this NOS isoform downstream from NMDA receptor dysfunction. Johansson and colleagues (1999) found that both L-NAME and a nNOS-selective inhibitor (AR-R 17477) reversed PPI and locomotor deficits elicited by PCP in rats. However, L-NAME also increased blood pressure and decreased heart rate, whereas AR-R 17477 did not. Selective inhibition of nNOS with *N*$^{\infty}$-propyl-L-arginine also may block PCP-induced PPI deficits and hyperlocomotion (Klamer et al., 2004b). Because NOS-modulating drugs may have cardiovascular influence, consideration should be given to these when assessing drugs effects *in vivo*. The influence of NOS inhibition in the context of PPI and locomotor activity has been attributed to altered monoamine transmission in the brain (Issy et al., 2010; Salum et al., 2011), and probably involves other neural

interactions (Getting et al., 1996; Geyer et al., 2001; Del Bel et al., 2005). Therefore, cardiovascular effects may not influence responses measured in this context, but ought to be a consideration as to the therapeutic potential of NOS-modulating drugs and selective inhibition of nNOS appears to be a means to avoid these unwanted effects.

In contrast to these findings, some reports indicate that non-selective (Echeverry et al., 2007; Georgiadou and Pitsikas, 2011) and selective nNOS inhibition (Komsuoglu-Celikyurt et al., 2011; Utkan et al., 2012) alone induces deficits in rodents. This is reinforced in studies of genetic knockout of the nNOS encoding gene (*Nos1*$^{-/-}$) which also appears to produce deficits in locomotion, social interactions, learning and memory (Kirchner et al., 2004; Tanda et al., 2009; Zoubovsky et al., 2011) in adult rodents. The inverse has also been shown for the former two behaviours, though there does appear to be a common learning and memory deficit in *Nos1*$^{-/-}$ rodents (Wultsch *et al.*, 2007), possibly due to altered dopamine and glutamate neurotransmission (Kano et al., 1998; Tanda et al., 2009). Deficits in long-term potentiation have been reported in eNOS knockout mice too; both eNOS and nNOS appear to have different roles in their influence on synaptic plasticity (Hopper and Garthwaite, 2006). PCP administered to *Nos1*$^{-/-}$ mice appears to bring about prepulse facilitation (Klamer *et al.*, 2005a), although the wildtype mouse used in this study lacked a PPI response to PCP perhaps indicating that this mouse strain was inappropriate. nNOS knockout mice may be revealing a compensatory role, albeit exaggerated, of splice variants of nNOS (Putzke *et al.*, 2000), likely that of nNOSβ (Eliasson *et al.*, 1997) if this is the case.

It is counterintuitive that inhibition of NOS may reverse the influence of NMDA receptor antagonism because here, the primary source of calcium for NOS activity is blocked. By this simple association, a hyponitrergic state

would be expected. Blockade of NMDA receptor mediated calcium influx by MK-801 has been found to attenuate nitric oxide generation in the hippocampus, and NO^x in the hippocampus and cerebellum are stimulated with NMDA and AMPA receptor agonism (Bhardwaj et al., 1997a; Yamada and Nabeshima, 1997). PCP has also been shown to inhibit nitric oxide generation overall in the rodent brain (Desaiah *et al.*, 1999). However, the findings from some groups are that NOS activity is increased in the PFC with acute PCP (Fejgin et al., 2008; Pålsson et al., 2010; Finnerty et al., 2013). Decreased citrulline concentrations have been found in the rat PFC with subchronic administration of PCP in a metabolomic study (Xiao *et al.*, 2011). Increased NO^x has been shown in the hippocampus and striatum with acute ketamine in a dose-dependent manner (Wu *et al.*, 2000). Increased nitrite has been found in the hippocampus following a large (100 $mg.kg^{-1}$), single dose of ketamine, but not in the cortex or striatum, whereas, a decreased expression of nNOS in the cortex was found following chronic ketamine (100 $mg.kg^{-1}$ for 10 days), but with no change in nitrite (Chatterjee *et al.*, 2012). Increased expression of NOS in the hippocampus has also been shown with subchronic ketamine (Keilhoff *et al.*, 2004), although the activity of NOS with this administration course has yet to be elucidated. Together these indicate that NOS activity is differentially modulated by NMDA receptor antagonists, and in specific brain regions; MK-801 appears to block nitric oxide generation overall, acute PCP appears to block NOS in the brain overall but stimulates nitric oxide generation in the PFC, NOS activity may be decreased with subchronic PCP, and hippocampal NOS may be stimulated with acute ketamine at high doses (50-100 $mg.kg^{-1}$) while repeated administrations of this has varying effects.

NOS antagonists appear to be less effective in the improvement of behavioural deficits evoked by amphetamine (Johansson, 1998), and there is conflicting evidence in the reversal of PPI deficits elicited by this and by more

direct dopamine receptor agonists (Salum et al., 2006; Salum et al., 2011). Selective inhibition of nNOS also appears to not influence amphetamine-induced PPI deficits (Johansson *et al.*, 1999). While evidence suggests that nitric oxide may facilitate dopamine transmission (West and Galloway, 1997; Segieth et al., 2000), the evidence presented here suggests that NOS inhibition is not efficacious in modulating behaviours elicited by potentiated dopamine transmission.

Black and colleagues (1999) showed that disruption of NOS during development in the rat has significant impact on behaviours in adulthood. Inhibition of NOS using nitro-L-arginine (L-NNA) in neonate rats gave rise to hypersensitivity to PCP, PPI deficits and increased locomotor activity. A later study saw a social interaction deficit in neonatally L-NNA-treated adult rats that was reversed by atypical antipsychotic drugs, but not by haloperidol (Black *et al.*, 2002). It is possible that this developmental model may explain the changes in nitrergic neuronal distribution, such as those observed by Akbarian and colleagues (1993b; 1993a). Unfortunately, this cannot be confirmed due to a lack of histological data from this model (Black et al., 1999; Black et al., 2002). Neonatal L-NNA treatment also produces altered dopamine receptor binding in the striatum and a hypersensitivity to amphetamine-induced hyperlocomotion (Morales-Medina *et al.*, 2008). The locomotor and social deficits are replicated with neonatal administration of L-NPA, suggestive that nNOS is involved in the development of these deficits in adulthood (Dec *et al.*, 2013).

Neonatal ventral hippocampus lesion in the rat produces a convincing model of deficits with relevance to schizophrenia (Section 0.). Increased NO^x has been found in the striatum and the prefrontal and occipital cortices of these rats, and NO^x generation appears to be sensitive to clozapine and haloperidol in a regionally-specific manner (Negrete-Díaz et al., 2010; Bringas et al.,

2011). These findings are suggestive of a dopaminergic modulation of nitric oxide generation (Morris et al., 1997; Hoque et al., 2010) downstream from ventral hippocampus lesion, and may arise from an influence of dysfunctional nitric oxide signalling on cellular functioning (Stojkovic et al., 1998; Martínez-Ruiz et al., 2011) and circuit behaviour (Shlosberg et al., 2012; Tricoire and Vitalis, 2012; Bartus et al., 2013). It would be interesting to see if similar changes occur in other developmental animal models with relevance to schizophrenia, such as with post-weaning social isolation, gestational MAM administration or maternal poly(I:C) (reviewed by: Jones et al., 2011; Pratt et al., 2012), but for now these remain to be elucidated.

The evidence for a role of nitric oxide in animal models with relevance to schizophrenia is compelling. Perhaps the most convincing of these is the potential of NOS inhibitor drugs to reverse some of the behavioural deficits elicited by NMDA receptor antagonists that have translational relevance to schizophrenia (Wass et al., 2006; Wass et al., 2009). A role of sGC/cGMP signalling downstream from NOS activation, and not that of peroxynitrite (Genius *et al.*, 2013), appears to be involved in some of these deficits (Fejgin *et al.*, 2008). nNOS-selective inhibitors also appear to be effective in reversing some, but not all, behavioural deficits induced by PCP (Johansson et al., 1999; Klamer et al., 2004b). However, a direct comparison has yet to be made of the role of eNOS and nNOS in these models. The biochemical evidence of altered NOS activity in NMDA receptor antagonist models varies with both the drug used (Bhardwaj et al., 1997a; Fejgin et al., 2008) and administration course (Chatterjee *et al.*, 2012). Other variables that may explain the different results are the site of sampling (Pålsson *et al.*, 2010) - suggestive of a possible regional specificity, dose of drug (Wu *et al.*, 2000), and the use of direct (Finnerty *et al.*, 2013) or indirect (Chatterjee *et al.*, 2012) measures of nitric oxide generation. Finally, evidence is emerging that altered NOS during development may have a role in deficits in the adult

rodent (Black et al., 2002; Bringas et al., 2011), and that this may confer dysfunctional systems in the brain as found in schizophrenia (Bitanihirwe and Woo, 2011; Seshadri et al., 2013).

There is a lack of data of NOS activity in brain regions using a systems approach, and no data on the state of cerebral vasculature in animal models of relevance to schizophrenia. There is a key role of the Trx/TrxR system in nitric oxide signalling, and especially that in caspase activation. So far, no study has investigated this in animal models of relevance to schizophrenia. There has also been no direct comparison between nNOS and eNOS on behaviours and neurochemistry.

1.6 Hypothesis and aims

1.6.1 General hypotheses

NOS activity is dysfunctional in schizophrenia and this will be reflected in translational animal models via NMDA receptor blockade using PCP. NO may contribute to schizophrenic-like deficits downstream from altered NMDA receptor function and drug modulation of NOS will reverse these deficits in animal models.

1.6.2 Thesis aims

The aims for this project are to evaluate NADPH-diaphorase and diaminofluorescein assays as a means to determine NOS activity in cultured cells to study nitric oxide signalling *in vitro*. NADPH-diaphorase and thioredoxin reductase activities will be assessed to determine the influence of PCP treatment on nitric oxide signalling in translationally-relevant brain

regions of mice. Non-selective and selective NOS inhibitors will be evaluated in their ability to reverse neurochemical and behavioural deficits elicited by PCP.

Specific aims:

1. Develop *in vitro* assays of NOS activity in neuronal cells to characterise the role of NMDA receptors in NOS activity and for the evaluation of novel drugs.

2. Characterise NOS related activity in brain areas that may be important in schizophrenia in NMDA receptor antagonist models relevant to schizophrenia.

3. Evaluate and characterise the role of NOS isoforms in schizophrenia relevant behaviours in NMDA receptor antagonist models relevant to schizophrenia.

4. Evaluate the efficacy of novel drugs that modulate tetrahydrobiopterin to influence nitric oxide signalling in neuronal cells.

2 Materials and Methods

2.1 Animals

All *in vivo* experiments were carried out in male C57BL6J mice (Harlan, UK), aged 6 - 14 weeks, group housed in solid-bottom plastic cages (43 x 22 x 16 cm). Mice were kept in a temperature (21˚C) and humidity (45-65%) regulated room with a 12 hour dark/light cycle (7am lights on). Animals were given access to environmental enrichments (plastic shelters), food and water, *ad libitum*. Bedding and sawdust was changed once per week. All *in vivo* experiments were carried out under the UK Animal (Scientific Procedures) Act, 1986.

2.2 Reagents

All reagents were sourced from Sigma-Aldrich (Dorset, UK) unless otherwise stated. Experimental protocols were done at ambient light levels and temperatures unless otherwise stated.

2.2.1 Routinely-used reagents

Distilled water (dH_2O), and double-distilled water (ddH_2O) were used in all solutions, unless otherwise indicated. 10X phosphate buffered saline (PBS), was made with 1.3M NaCl, 30mM $NaH_2PO_4.2H_2O$, 70mM Na_2HPO_4, pH 7.4. PBS was diluted to 1X using ddH_20 for use, unless otherwise indicated. Dimethyl sulfoxide (DMSO) and ethanol (EtOH) were used as solvents, as required. All other reagents are described in the text as they were used.

2.2.2 Novel NOS-modulating compounds

The novel compounds outlined below are putative NOS-modulating compounds that were synthesised and supplied by C.J. Suckling's group (University of Strathclyde). The efficacy of these compounds to modulate NOS activity will be assessed in neuronal cultures. 6-actyl-7,7-dimethyl-5,6,7,8-tetrahydropterin (ADDP) is a tetrahydrobiopterin (BH_4) analogue that has been shown to promote NOS activity in macrophages and endothelial cells (Suckling et al., 2008; Kunuthur et al., 2011). 2-Amino-4-oxo-4,7-dihydro-3H-pyrrolo[2,3-*d*]pyrimidine-6-carboxylic acid ethyl ester (WSG2001) inhibits the synthesis of guanosine triphosphate cyclohydrolase I (Gibson *et al.*, 2004). 2,6,7,7-Tetramethyl-7,8-dihydro-1-thia-3,3a,5,8,9-pentaazacyclopenta[*b*]naphthalen-4-one (WSG1023) is a novel, putative NOS inhibitor of unknown mechanism. These compounds were dissolved in DMSO, and stock solutions were stored at -20°C, to be used within 4 days. The structures of these compounds are given in Chapter 6.

2.3 *In vivo* drug treatments and experimental design

Drugs given *in vivo* were prepared thus: 0.9% w/v NaCl solution (vehicle), 2.5 $mg.ml^{-1}$ phencyclidine (PCP; Tocris, R&D Systems, U.K.), 20 $mg.ml^{-1}$ nitro-L-arginine methylester (L-NAME; Calbiochem, Merck, UK), 10 $mg.ml^{-1}$ N^5-(1-iminoethyl)-L-ornithine dihydrochloride (L-NIO; Tocris), 10 $mg.ml^{-1}$ N^{ω}-propyl-L-arginine hydrochloride (L-NPA; Tocris).

All drugs were dissolved in 0.9% saline vehicle, and given at 2ml / kg body weight. The same saline vehicle was used throughout for control drug treatments. Solutions were buffered to approximately pH 7.4, as required. All drugs were administered to animals intraperitoneally (i.p.). Body weight was measured on the morning of experimentation to calculate the amount of

drug to be administered. Weights were regularly monitored and drug amounts were adjusted accordingly in subchronic dosing protocols. Mean mouse body weights were not significantly different between experimental groups, as tested by two-sample t-test or one-way analysis of variance (ANOVA), as appropriate. Mean age of experimental groups was also tested in this manner, where appropriate, and were not significantly different.

Mice were euthanised by cervical dislocation 30 mins following injection of PCP, unless otherwise stated, and brains were immediately removed and frozen in -80°C isopentane, then stored in a -80°C freezer for up to 12 weeks. One adult male Sprague Dawley rat was euthanised by cervical dislocation. The brain was immediately removed and frozen in -80°C isopentane, then stored in a -80°C freezer for 4 weeks for use with NADPH-diaphorase histochemistry (Section 2.5.1).

2.3.1 Acute PCP experiments

Acute PCP was administered to mice to assess the influence of NMDA receptor antagonism on neurochemical and behavioural measures outlined below. These data are presented in Chapter 4.

Adult, male C57BL6J mice were administered either 5 $mg.kg^{-1}$ PCP or saline vehicle alone. NADPH-diaphorase activity in histochemical sections (Section 2.5.1) was assessed using 12 mice (9 weeks old; 23.9 ± 0.284 g) that were administered either PCP (n = 6) or saline vehicle (n = 6). These mice had previously undergone behavioural testing as saline-treated control groups as part of another project. For determination of NADPH-diaphorase activity in brain region homogenates (Section 2.5.2), 12 mice (11.8 ± 0.3 weeks old; 26.1 ± 0.5 g) were administered either 5 $mg.kg^{-1}$ PCP (n = 6) or saline

vehicle (n = 6). These mice had previously undergone behavioural testing as saline-treated control groups and were food restricted during this time as part of another project.

Brain region thioredoxin reductase (TrxR) activity and nitrite concentration (Sections 2.7 and 2.6.3, respectively) was done using 13 mice (6 weeks old; 20.8 ± 0.41 g) that were administered either 5 $mg.kg^{-1}$ PCP (n = 7) or saline vehicle (n = 6). For determination of locomotor activity, caspase activities and nitrite concentration (Sections 2.9.2, 2.7 and 2.6.3, respectively), 16 mice (10 weeks old; 27.1 ± 0.35 g) were administered either 5 $mg.kg^{-1}$ PCP (n = 8) or saline vehicle (n = 8). Prepulse inhibition of acoustic startle (Section 2.9.4) was assessed in 24 mice (9 weeks old; 20.9 ± 0.56 g) that were administered either 5 $mg.kg^{-1}$ PCP (n = 12) or saline vehicle (n = 12).

2.3.2 Subchronic PCP experiments

Subchronic PCP was administered to mice to assess the influence of NMDA receptor antagonism on neurochemical and behavioural measures outlined below. These data are presented in Chapter 4.

Adult, male C57BL6J mice were administered 5 $mg.kg^{-1}$ PCP or saline vehicle twice daily, with a 6 hour inter-drug interval, for 5 days. Body weight and general condition was monitored every 2-3 days during the experiment. Mice were euthanised by cervical dislocation on the 8^{th} experimental day, 72 hours following their final injection, i.e. following a 2 day wash-out period.

For determination of NADPH-diaphorase activity in brain region homogenates (Section 2.5.2), 18 mice (11.3 ± 0.57 weeks old) were administered drugs as

above. Initial mean mouse weight was 25.4 ± 0.77 g. Drug groups in this study were saline vehicle twice daily (n = 6), PCP twice daily (n = 6), and PCP (am) and vehicle (pm) injections daily (n = 6). Mean body weight on the final day of experimentation (day 8) was 25.5 ± 0.68 g.

For behavioural testing, 15 mice (11 weeks old) were administered drugs as above. Drug groups in this study were saline vehicle (n = 7) or PCP (n = 8) twice daily. Initially, mice were habituated to open field arenas as detailed in Section 2.9.2, returned to home cages and administered PCP or vehicle. Mice were then replaced into the open field box for testing. The second dose was given as above. These procedures were repeated for the following 4 days. On day 8, mice were tested in the open field for 1 hour and then returned to home cages for 3 hours. Prepulse inhibition of acoustic startle was then assessed as per Section 2.9.4, and were euthanised by cervical dislocation immediately afterwards. These brains were used to determine brain region thioredoxin reductase and caspases activities, as described in Sections 2.7 and 2.8, respectively. Initial mean mouse weight was 27.4 ± 0.44 g, and on the final day of experimentation (day 8) was 27.8 ± 0.48 g. One mouse was removed from study on day 3 of experimentation due to an injured eye and decrease in body weight (-3 g from initially recorded weight).

2.3.3 Acute PCP with NOS drug pretreatment experiments

The NOS antagonists outlined below were administered to mice to assess the influence of NOS inhibition on neurochemical and behavioural outcomes with PCP. These data are presented in Chapter 5.

Adult, male C57BL6J mice were administered 40 mg.kg^{-1} L-NAME, 20 mg.kg^{-1} L-NIO, 20 mg.kg^{-1} L-NPA, or saline vehicle alone. After 15 mins, 5 mg.kg^{-1}

PCP or saline vehicle was administered. To assess prepulse inhibition of acoustic startle (Section 2.9.4), 94 mice (8.2 ± 0.15 weeks old; 23.7 ± 0.27 g) were administered drugs, as described above. Drug groups were: vehicle + vehicle (n = 12), vehicle + PCP (n = 12), L-NAME + vehicle (n = 11), L-NAME + PCP (n = 12), L-NIO + vehicle (n = 11), L-NIO + PCP (n = 12), L-NPA + vehicle (n= 12), and L-NPA + PCP (n = 12).

Locomotor activity (Section 2.9.2) was determined in 48 mice (8 weeks old; 23.5 ± 0.28 g) that were administered drugs as above. Drug groups were the same as above (n = 6 per group). Mice were euthanised by cervical dislocation 90 mins following PCP administration, and brains were used for NADPH-diaphorase histochemistry, as described in Section 2.5.1.

2.4 Cell culture

All tissue culture media and supplements were obtained from Gibco (Life Technologies, UK), unless otherwise stated. Aseptic technique and sterile equipment was used throughout.

2.4.1 Cell lines

Mouse neuroblastoma x rat glioma 108-15 (NG108-15) cells (ATCC, Harwell) were maintained in Dulbecco's modified Eagle's medium (DMEM) supplemented with 10% (v/v) foetal bovine serum (FBS), 100 units/ml penicillin and 0.1 mg/ml streptomycin and 2 mM Glutamax I. For differentiation, cells were seeded into 12 well or 96 well culture plates in DMEM supplemented with 1.5% dimethyl sulfoxide (DMSO)/ 0.5% (v/v) FBS, 100 units/ml penicillin and 0.1 mg/ml streptomycin and 2 mM Glutamax I. Cultured cells were maintained in a humidified atmosphere of 95% air and 5% CO_2 at 37°C.

Human neuroblastoma cells (SH-SY5Y; ATCC, Harwell) were maintained in a 1:1 solution of Dulbecco's modified Eagle's medium (DMEM) and Ham's F-12 nutrient mixture. This was supplemented with 15mM 4-(2-hydroxyethyl)-1-piperazineethanesulfonic acid (HEPES), 10% FBS, 100 units/ml penicillin and 0.1 mg/ml streptomycin and Glutamax I. For differentiation, cells were seeded into 6-, 12- or 96- well flat bottom microtitre plates in DMEM/F-12 supplemented with 1.5% dimethyl sulfoxide (DMSO)/ 0.5% FBS, 100 units/ml penicillin and 0.1 mg/ml streptomycin and 2 mM Glutamax I. Cultured cells were maintained in a humidified atmosphere of 95% air and 5% CO^2 at 37°C. Approximately 50% of medium was replaced with fresh medium, composition as appropriate, every 3-4 days. Optimem I lacking phenol red was used for determining nitric oxide generation using DAF-2DA plate fluorometery (Section 2.6.1).

2.4.2 Primary neuronal cultures

Sprague Dawley neonate pups (postnatal day 1 – 3) were euthanised with a lethal dose of pentobarbital (Euthatal, 100 µl per pup). Aseptic technique was used throughout. Dissection was done using surgical instruments on a surface sterilised with 70% ethanol. Hippocampi (and surrounding cortical tissue), cortices or cerebella were dissected, as appropriate. All subsequent procedures were done in a laminar-flow cabinet (Holten LaminAir, Model: HLB 2448 BS) with surfaces sterilised using 70% ethanol. Dissected tissue was cut in to small blocks in ice-cold Hank's balanced salt solution (HBSS) using a sterile scalpel blade and transferred to a 0.67% trypsin solution containing EDTA. Tissue suspensions were incubated at 37°C for 5 mins to dissolve the extracellular matrix. The trypsin solution was removed and replaced with DMEM supplemented with 2 mM Glutamax I, 100 units/ml penicillin and 0.1 mg/ml streptomycin, and 10% (v/v) FBS. The tissue was then triturated using a Pasteur pipette to further dissociate the cells in the medium. Cells were then seeded into 6-, 12- or 96- well flat bottom

microtitre plates pre-coated with poly-D-lysine (4 µg/ml) and laminin (6 µg/ml). The following day, approximately 60% of the medium was replaced with Neurobasal medium with 2 mM Glutamax, 100 units/ml penicillin, 0.1 mg/ml streptomycin, and 1X B27 supplement, to inhibit non-neuronal cell proliferation. A 25 mM KCl supplement was added for cerebellar granule cell (CGC) cultures. Cultured cells were maintained in a humidified atmosphere of 95% air and 5% CO_2 at 37°C. Cells were used for experimentation on *in vitro* day 8-11, unless otherwise stated. Approximately 50% of the culture medium was replaced with fresh supplemented medium every 3-4 days, as appropriate. Neurobasal lacking phenol red was used in Griess assays (Section 2.6.3) to determine nitrite concentration in culture medium samples, and in DAF-2DA plate fluorometery (Section 2.6.1).

2.5 NADPH-diaphorase activity

2.5.1 Histochemistry

NADPH-diaphorase histochemistry was used to assess the activity state of NOS in mouse brain regions. Brains stored at -80°C were acclimatised to -20°C overnight and then transferred to a cryostat chamber (Leica, model: C1870) that was maintained between -22 and -20°C. 20 µm brain sections containing prefrontal cortex (PFC), striatum and retrosplenial cortex (RSp) were cut by reference to a mouse brain atlas (Paxinos and Franklin, 2001).

Replicate sections were taken consecutively from each mouse brain. Sections containing PFC were taken from (approximately) 2.1 mm rostral to bregma, striatal slices were taken from 1.18 mm rostral to bregma, and sections containing RSp and hippocampus were taken from 1.34 mm caudal to bregma, in a rostro-caudal fashion. Sections were mounted on gelatine-coated slides and then fixed in 4% formalin for 20 mins followed by three

washes in 0.1 M PBS and one wash in PBS containing 0.25% Triton X-100 for 5 mins each at room temperature. The slides were then incubated in PBS containing Triton X-100 (0.25% v/v), nitroblue tetrazolium (NBT, 0.1 $mg.ml^{-1}$) and β-nicotinamide adenine dinucleotide phosphate reduced tetrasodium salt (NADPH; 0.2 $mg.ml^{-1}$) on a rotary shaker for 5 mins at 25°C then 2 hrs at 37°C (adapted from: Morris *et al.*, 1997). Negative controls were done in replicate sections incubated as above without NADPH. Slides were rinsed in 1X PBS then dehydrated in increasing concentrations of ethanol (70%, 95% and 100%) for 5 mins each. Sections were cleared using Histo-Clear (National Diagnostics, Fisher Scientific, U.K.), then coverslips were hard-mounted using Histo-Mount (National Diagnostics). Prior to staining, fixed sections were stored in PBS in a 4°C refrigerator overnight and up to 16 days. All solutions were prepared in a low-light room and reactions were performed in the dark.

Histochemical sections of rat striata were taken and processed as above, with the following changes: sections were incubated with vehicle (ddH_2O), 100 µM *N*ω-nitro-L-arginine (L-NNA; Calbiochem, Merck, UK; 20 mins), or 1 mM L-NAME (20 mins) before fixation. Replicate sections were incubated with these drugs after fixation during the NADPH-diaphorase reaction (2 hours).

Brain section images were captured using an Olympus BH-2 microscope with a mounted Sony video camera (Model XC-77CE) that was interfaced with Image software (v.5.2, NIH, Maryland, USA) for Macintosh, or MCID imaging software (v.5; InterFocus Imaging Ltd, Cambridge, UK) for PC. Microscope lamp intensity was unchanged throughout to provide consistent illumination for comparable optical density measurements.

2.5.2 Brain tissue homogenates

NADPH-diaphorase activity in dissected tissue homogenates was used to assess the activity state of NOS in mouse brain regions. Brains stored at -80°C were transferred to a -20°C freezer and left to acclimatise overnight. The frontal cortices, striata, hippocampi, thalami, and cerebella were dissected on a chilled tile. Dissected regions were washed with 1X PBS and fixed in 1 ml 4% formalin for 18-21 hrs at 4°C. Samples were then washed in 1X PBS for 1 hr and washed again overnight at 4°C. Brain regions were homogenised manually using a homogenisation rod in 1 ml ice-cold 0.1X PBS, 0.25% Triton X-100. Samples were centrifuged at 15000 g for 10 mins at 4°C using a Sigma 2K15 benchtop centrifuge. Supernatants were collected and stored at -20°C for up to 20 days. 10-30 µl of each sample was added to a reaction solution, comprising: 1xPBS, 0.2 $mg.ml^{-1}$ NADPH, 100 µM 2,3-bis(2-methoxy-4-nitro-5-sulfophenyl)-2H-tetrazolium-5-carboxanilide inner salt (XTT), and 50 nM phenazine methosulphate (PMS) to a final volume of 100 µl in a 96-well microtitre plate. Negative control reactions were also done of diaphorase activity in the absence of tissue sample, and in replicate sample reactions without NADPH. Reactions were done in triplicate. The accumulation of formazan was measured at 450 nm at 5 min intervals for an hour at 37°C, using a Thermo Multiskan Spectrum multiwell spectrophotometer.

The total protein content of samples was determined by comparing the absorbance (630 nm) of samples against a standard curve generated by known concentrations of bovine serum albumin using Bio-Rad protein assay dye reagent based on the reaction of the negative residues of proteins with coomassie blue (adapted from: Bradford, 1976). Technical replicates of NADPH-diaphorase and protein assays were done, and the results per sample were averaged.

2.5.3 NADPH-diaphorase activity in cultured cells

NADPH-diaphorase activity in cultured cells was to assess the activity state of NOS in neuronal cell cultures. Cells were treated with vehicle (ddH_2O, 1% DMSO), 100 µM L-NAME (45 mins), or 100 µM N-methyl-D-aspartate (NMDA; 30 mins).

Cells were fixed for 30 mins using 4% formalin on ice, then washed in 1xPBS for a further 30 mins. A reaction solution was added, comprising, 1xPBS, 0.2 $mg.ml^{-1}$ NADPH, 150 µM 2,3-bis(2-methoxy-4-nitro-5-sulfophenyl)-2H-tetrazolium-5-carboxanilideinner salt (XTT), and 50 nM phenazine methosulfate (PMS) to make up a volume of 100µl per well. The microtitre plate was then immediately transferred to a multiwell spectrophotometer (Thermo Multiskan Spectrum). Optical density was measured at 450 nm every 5 mins over an hour, and incubated at 37°C throughout. All procedures were done in the microtitre plate that cells were cultured in. Due to the light-sensitivity of XTT, reaction solutions were prepared in the dark.

For NADPH-diaphorase cytochemistry, cells cultured on laminin/poly-d-lysine –coated coverslips were treated with drugs and processed for time-lapse imaging, as described in Section 2.6.2. Fixed cells were stored in 1X PBS at 4°C for up to 2 weeks. Cells were then processed as with NADPH-diaphorase histochemistry (Section 2.5.1), with the following changes: cells were incubated in NADPH-diaphorase reaction solution for 3 hours, and some cells were counterstained with 0.2% neutral red solution for 5 mins, prior to ethanol dehydration.

2.6 Determination of nitric oxide generation

2.6.1 Diaminofluorescein-2-diacetate microplate fluorometry

The pharmacological modulation of NO generation in NG108-15 cells and primary cortical neurones was determined using the NO-selective fluorescent probe, 4,5-diaminofluoresein diacetate (DAF-2DA; Merck Chemicals, UK). Cell culture medium was replaced with appropriate media lacking phenol red and further incubated for 1-2 hours before experimentation. Cells were treated with vehicle (dH_2O, 1% v/v DMSO), 100-500 µM L-NAME (45 mins), 100 µM NMDA (30 mins), or 4mM DAHP (24 hours). 50-500 µM *S*-nitroso-*N*-acetylpenicillamine (SNAP; Enzo, UK) was added immediately before measurement.

10 µM DAF-2DA was added to wells and immediately transferred to a fluorescent plate reader (Thermo Labsystems, Fluoroskan Ascent FL). The accumulation of fluorescent DAF-2 triazole (DAF-2T) was measured every 5 mins over an hour at an excitation wavelength of 485 nm (Ex_{485}), and emission wavelength of 538 nm (Em_{538}), incubated at 30°C. All work was done in a dark room when working with DAF-2DA prior to transfer to the plate reader. Background fluorescence of DAF-2DA in culture medium (plus vehicle) with no cells present was subtracted from cellular assay values.

2.6.2 Diaminofluorescein-2-diacetate live-cell microscopy

CGCs or hippocampal neurones were cultured on 12 or 24 -well microplates containing poly-D-lysine and laminin -coated coverslips, as described in Section 2.4.2. CGCs were imaged at 10-14 days *in vitro* (DIV), hippocampal cells were imaged at 8-11 DIV. Coverslips were transferred to 35mm petri dishes containing 2ml Hibernate-A Low Fluorescence medium (BrainBits, UK) to maintain healthy cells at ambient CO_2 and temperature while imaging.

Compounds were added to cells for the times indicated in Table 2.1, and 1 μM DAF-2DA was added 30 mins prior to imaging.

Images of DAF-2T fluorescence within cells was captured using Winfluor software (v3.4, University of Strathclyde). Cells were illuminated using an Optoflash light source (Cairn Research, UK) at 470 nm, 1.54 A. Cells were visualised using a Nikon Eclipse E600FN microscope via a 20x (NA = 0.5w) immersible differential interference contrast objective lens (Nikon), and digitised using a Hamamatsu Orca-R^2 digital CCD camera (model C10600) connected to a PC. Bright-field images of the field of view (FoV) were taken to aid the identification of cells for image analysis.

Table 2.1 Compound incubation times for live-cell imaging

Compound	Dose (μM)	Incubation Time
L-arginine	50	30 min
Glutamate	100	30 min
CNQX	10	35 min
MK-801	10	35 min
A23187	1	0 min
Nifedipine	10	35 min
L-NAME	300	2 hr
L-NIO	150	2 hr
L-NPA	150	2 hr
DAHP	4000	24 hr
ADDP	30	1 hr
WSG2001	30	24 hr
WSG1023	30	24 hr

Vehicle treatment was given appropriate to the time-point and composition for comparison to the compounds applied to cells. Abbreviations: CNQX, 6-cyano-7-nitroquinoxaline-2,3-dione; MK-801, (+)-5-methyl-10,11-dihydro-5H-dibenzo [a,d] cyclohepten-5,10-imine; L-NAME, N^{ω}-nitro-L-arginine methyl ester; L-NIO, N^{ω}-(1-iminoethyl)-L-ornithine; L-NPA, N^{ω}-propyl-L-arginine; DAHP, 2,6-diamino-4-pyrimidinol. ADDP and WSG compounds are described in the text.

2.6.3 Griess assay for assessment of nitrite concentration

The concentration of the nitric oxide metabolite, nitrite, was determined using the Griess diazotisation reaction with primary cortical neurones and dissected brain tissue. Brain regions were dissected as described in section 2.4.2. Cells were lysed or tissue samples were homogenised in ice-cold lysis buffer, comprising: dH_2O, 20 mM HEPES and 5 mM $MgCl_2$, pH 7.6. Samples were then centrifuged at 13,000 g for 10 mins at 4°C. The supernatants were eluted and transferred to fresh sample tubes.

Cultured cortical neurones were incubated in 6-well microtitre plates for 4-6 days in Neurobasal (-)phenol red (Section 2.4.2). Culture medium volume was reduced to 1.5 ml from 3 ml 24 hours prior to experimentation to increase nitrite concentration per sample. Cells were treated with vehicle (dH_2O, 1% v/v DMSO), 100 µM L-NAME (45 mins), or 100 µM NMDA (30 mins). Medium was eluted and transferred to sample tubes. Cells were washed with 1X PBS, and lysed in 20 µl ice-cold lysis buffer. Cell lysates and media samples were centrifuged at 15,000 g for 10 mins at 4°C, supernatants were then transferred to fresh sample tubes.

Reactions were done in 96-well microtitre plates and were protected from light throughout. Cell lysate or tissue homogenate samples were diluted in lysis buffer as appropriate. 50 µl of sample was added to 25 µl 10 $mg.ml^{-1}$ sulphanilamide in 60% (v/v) acetic acid for 10 mins. 25 µl 2 $mg.ml^{-1}$ *N*-(1-naphthyl)-ethylenediamine dihydrochloride was added to wells for 15 mins and then reaction plates were immediately transferred to a multiwell spectrophotometer (Thermo Multiskan Spectrum). The formation of azo dye product by samples was determined by measuring optical density of reactions at 540 nm. The concentration of nitrite present in a sample was

determined by comparing the optical density of azo dye product against a standard curve generated by known concentrations of $NaNO_2$ dissolved in lysis buffer or culture medium, as appropriate. Reactions were done in triplicate and averaged.

2.7 Thioredoxin reductase activity

Brain region homogenate samples were prepared as described in Section 2.6.3. Samples were added to 5 mM 5,5'-dithiobis(2-nitrobenzoate) (DTNB; Enzo and Sigma-Aldrich), 0.3 mM NADPH in an assay buffer (100 mM potassium phosphate, 1 mM EDTA, pH 7.4). The microtitre plate was then immediately transferred to a multiwell spectrophotometer (Thermo Multiskan Spectrum) and was incubated at 37°C throughout. The accumulation of 5-thio-2-nitrobenzoate (TNB) was determined by measuring optical density at 412 nm every 2 mins for 30 mins. Reactions were done in duplicate or triplicate and averaged. The rate of TNB accumulation was calculated per reaction by subtracting the OD measured at 0 or 2 mins (kept consistent per experiment) from that at 30 mins, and dividing by the number of minutes assayed. TrxR-specific activity was assessed by subtracting the rates of duplicate samples incubated with 10 µM myricetin to inhibit TrxR activity (Lu et al., 2006). Values were corrected to total protein content of each sample, determined by coomassie blue reactivity, as described in Section 2.5.2.

TrxR activity was determined in cells cultured in 96-well plates as described above with the following changes: Following drug incubation, medium was removed, cells were washed with 1X PBS, and lysed in 20 µl ice-cold lysis buffer. Reaction solution was added to these in the culture plate (+/- myricetin) and assayed as above. Reactions were done in quadruplicate to octuplet and averaged.

2.8 Caspase activities

Brain regions were dissected as described in section 2.4.2, washed in 1X PBS and then homogenised in lysis buffer comprising: 25 mM HEPES, 5 mM $MgCl_2$, pH 7.6. Brain regions were manually homogenised using a homogenisation rod and trituration using a surgical needle and centrifuged at 15,000 g for 10 mins at 4°C. Supernatants were transferred to fresh sample tubes and stored for up to 8 weeks at -20°C.

2-10 µl of sample was diluted in lysis buffer to 25 µl and added to 20 µM fluorogenic synthetic caspase substrate (see Table 2.2. for substrate specificities), 25 mM HEPES and 0.5 mM ethylenediaminetetraacetic acid (EDTA), pH 7.6, to give a final volume of 100 µl. The fluorescence of cleavage product, 7-amino-4-methylcoumarin (AMC; Ex_{340} nm, Em_{450} nm), was measured every 2 mins for 30 mins at 37°C. The rate of caspase activity was determined by comparing the accumulation of AMC against a standard curve generated by known concentrations of unconjugated AMC. Caspase 3-specific activity was assessed by subtracting the rates of parallel reactions (i.e. replicate samples) incubated with the selective caspase 3 inhibitor, Ac-DMQD-CHO (50 µM). Fluorogenic substrates, unconjugated AMC, and caspase 3 inhibitor were obtained from Enzo Life Sciences (Exeter, UK).

Table 2.2 Caspase-selective compounds

Caspase Substrate / Inhibitor	Caspase Specificity	Sequence
Ac-DEVD-AMC	Caspase 3	Acetyl-Asp-Glu-Val-Asp-AMC
Ac-IETD-AMC	Caspase 8	Acetyl-Ile-Glu-Thr-Asp-AMC
Ac-LEHD-AMC	Caspase 9	Acetyl-Leu-Glu-His-Asp-AMC
Ac-DMQD-CHO	Caspase 3	Acetyl-Asp-Met-Gln-Asp-CHO

Abbreviations: 7-amino-4-methylcoumarin (AMC), aldehyde group (CHO)

2.9 Behaviour

2.9.1 Open field apparatus

Four, infrared (IR) translucent open-top cubes measuring 40 cm^3 were situated atop an IR light box. Locomotor activity (LMA) within each arena was recorded by an overhead IR-sensitive CCD camera that was connected to a computer in an adjacent room. LMA was tracked using Ethovision XT (Noldus Information Technology, The Netherlands) video tracking software.

2.9.2 Locomotor activity

Locomotor activity was done in a room with low lighting (55 lux). Mice were placed in an open field box for 1 hour to habituate to the environment and then returned to their home cage. Drug treatments were administered as specified in Section 2.3. Mice were placed back in to the corresponding open field box immediately following the final injection and observed for an hour. Each arena was thoroughly cleaned between subjects to prevent conspecific odour influence on behaviour. Groups were equally distributed between arena locations within the testing room to prevent external cue bias.

2.9.3 Prepulse inhibition apparatus

Four acoustically-attenuated cubicles (MED Associates, USA) containing a cylindrical (inner diameter = 4.4 cm, length = 9.5 cm) acrylic mouse holder with a mounted piezoelectric transducer, and acoustic speakers for background noise and for stimulus generation.

2.9.4 Prepulse inhibition of acoustic startle

5 $mg.kg^{-1}$ PCP or saline vehicle was administered i.p. 15 mins prior to assaying prepulse inhibition (PPI) of acoustic startle response (ASR), as described in Section 2.3.1. PPI was assayed 72 hours following final drug injection in mice that were administered subchronic drug treatments, as

described in Section 2.3.2. NOS drugs or vehicle were given to mice for 30 mins, and 5 $mg.kg^{-1}$ PCP or saline vehicle was given for 15 mins prior to PPI measurement, as described in Section 2.3.3.

Mice were restrained in mouse holders and placed in cubicles. Mice were habituated to background noise (continuous white noise, 65 dB RMS) for 5 mins prior to testing sequence; background noise was present throughout the protocol. The startle stimulus was a 120 dB pulse (40 ms) that was presented alone or preceded by a less intense prepulse (4, 8 and 16 dB above background noise, 100 ms interval and 20 ms duration). Prepulse and startling stimulus pairs were presented 10 times in a pseudorandom order, but for startle-alone stimuli which were presented at the beginning (6 times), middle (12 times) and end (6 times) of the protocol.

2.10 Data and statistical analyses

Data values are presented as mean ± standard error mean (SEM) as absolute values, or standardised to control groups (i.e. as percent of control group mean). Values stated for n, were taken as the source of the greatest variance. For experiments using cell lines, the greatest variance is considered between populations of cells, i.e. between wells containing cells cultured in a microtitre plate. For *in vivo*, *ex vivo* and primary cell culture experiments, the greatest variance is considered between individual animals, unless otherwise stated. All other experimental and technical replicates were averaged (mean).

Data not normally distributed were corrected by BoxCox or Johnson Transformation. Statistical differences between groups were tested using two-sample t-tests, or Analysis of Variance (ANOVA) with Tukey's *post hoc*

tests, where appropriate. One-way t-tests were used when comparing results (corrected to percentage of control) against a control set to 100 %. Mann-Whitney or Kruskal-Wallis with Dunn's multiple comparisons tests were used where data could not be transformed to Gaussian distribution. Differences were considered significant at $p < .05$. Linear regressions were done using GraphPad Prism (v.3), all other statistical analyses were performed using Minitab (v.15).

2.10.1 NADPH-diaphorase kinetics analysis

NADPH-diaphorase activity in cell cultures and brain region homogenates was measured over the course of an hour. The linear phase of formazan accumulation was analysed by linear regression to give the rate of NADPH-diaphorase activity per sample. The time interval that produced the most linear reactions (as established by the coefficient of determination by linear regression) per reaction plate was selected. The rate of buffer activity (i.e. without sample/cells present) was subtracted from sample data to give a specific rate of activity (OD_{450} / min). Sample data were then corrected by protein content as determined by Bradford Protein Assay, to give OD_{450} / min / µg total protein.

2.10.2 Image analysis of NADPH-diaphorase staining

Histochemical images (Section 2.5.1), were manually processed using FIJI software (FIJI Is Just ImageJ, v.1.47; Schindelin *et al.*, 2012). Flat-field correction was applied to all images. The outlines of cells or blood vessels were traced and the optical density was measured. Stained neurones were selected for measurement as per the cellular patterns of staining similar to findings characterised in the rat (Hope and Vincent, 1989; Morris et al., 1997) and human (Akbarian et al., 1993b). A total of 4 brain sections containing each region of interest (ROI) per brain were analysed. For each ROI, the optical density of staining in neurones and blood vessels were

sampled. Background OD was subtracted from each value obtained from the corresponding field-of-view to give relative optical density (ROD).

2.10.3 Fluorescence image analysis

Fluorescence images (Section 2.6.2) were manually analysed using FIJI software. Flat-field correction was applied to all fluorescent images. The outline of cells was traced and the optical density was measured. The background fluorescence was subtracted per frame.

2.10.4 Analysis of behavioural parameters

Startle responses are the mean responses to startling stimuli alone, and are expressed in arbitrary units (AU). PPI is expressed as the prepulse response as a percentage of the startle response (of the first stimulus) in mice.

Locomotor activity of mice was recorded and analysed using Ethovision XT video tracking software. The centre of mass of mice was tracked within open field boxes. The following parameters were analysed for locomotor activity: distance moved (cm), number of rotations (where one rotation is >50°), and duration (mins) spent in the inner 20 cm^2 of open field boxes. Data are presented as average values per 10 min time interval, as the mean rate of locomotor response (i.e. $cm.min^{-1}$ and $rotations.min^{-1}$), or as the percentage of total time spent in the arena.

3 Evaluation of Cell Culture Assays for Modelling Neuronal NOS Activity

3.1 Introduction

The measurement of nitric oxide is challenging due to its transience (Wang *et al.*, 2006), multiple effects (Morris, 1995; Prast and Philippu, 2001; Garthwaite, 2005), and low physiological concentration (Hall and Garthwaite, 2009). This challenge is magnified when studying nitric oxide in the brain due to the relative low incidence of nitrergic neurones in rodents (Kharazia et al., 1994; Gotti et al., 2005) and in humans (Egberongbe *et al.*, 1994). Technologies are emerging that may allow more specific determination of nitric oxide generation, such as amperometric voltammetry (Finnerty *et al.*, 2012), and fluorescence bioimaging (Kojima *et al.*, 1998). However, more established methods include quantifying indirect measures such as cGMP accumulation (Bartus et al., 2013; Pigott et al., 2013), radio-labelled arginine to citrulline conversion rate (Kiedrowski et al., 1992; Bhardwaj et al., 1997a), and nitrate / nitrite concentrations (Fang and Silverman, 2009).

The purpose of this study is to identify a suitable microplate-based assay for NOS activity in cultured neurones. The use of cell cultures is desirable because of the flexibility available to manipulate the timing and magnitude of drug administrations, and in various combinations, that would not be appropriate to do *in vivo*. Many of the reports concerning NOS activity in neuronal cultures feature cells, many non-neuronal, that are genetically-modified to express, or to enhance expression of nNOS (Ishii et al., 2006; Fang and Silverman, 2009; Brzozowski et al., 2011). For maximum translation to neuronal cells, it is important to perform investigations in cell types that display neuronal phenotypes and exhibit physiologically-relevant concentrations of the target in question. For this study, assays will be initially assessed using mouse neuroblastoma x rat glioma hybrid (NG-108-15) cells

and SH-SY5Y human neuroblastoma cells because of their neuronal phenotypic characteristics (reviewed by: Xie et al., 2010; Nomura et al., 2013) and expression of NOS (Grant et al., 2002; Müller et al., 2010). Based on these results, the assay that is found to be suitable will then be used with primary neuronal cultures to study glutamate-mediated nitric oxide signalling *in vitro* further.

NADPH-diaphorase staining is a robust and reliable means to identify nitric oxide synthase (NOS) in aldehyde-fixed biological samples (Bredt et al., 1991; Hope et al., 1991). However, little has been reported using the NADPH-diaphorase assay as a means to determine NOS activity in cultured cells. The usefulness of NADPH-diaphorase staining to reflect both the presence and the activity of NOS in cultured neurones and in histochemical sections has been shown previously (Morris *et al.*, 1997). A novel method utilising a water-soluble tetrazolium salt for NADPH-diaphorase was used here, as described in Chapter 2.5, to determine the kinetic activity of NOS in cultured neurones. In Chapters 4 and 5, histochemical and kinetic NADPH-diaphorase reactions will be shown to be a useful measure of NOS activity in tissue samples. The suitability of this assay will be assessed for use in neuronal cell lines and primary neuronal cultures in this chapter.

Diaminofluorescein-2-diacetate (DAF-2DA) fluorescence imaging is an emerging technique that enables a more direct measure of nitric oxide *in vitro*. The DAF-2DA is cell-permeable and non-reactive. Following hydrolysation by intracellular esterases, DAF-2 may not cross membranes and is reactive to an oxidation product of nitric oxide. The resultant sum fluorescence of the triazole (DAF-2T) in a cell, therefore, is representative of the concentration of nitric oxide within a cell for the time that the probe has been present. Diaminofluoresceins have been shown to be sensitive to changes in endogenous nitric oxide production (Kojima et al., 1998; Brown et

al., 1999; Leikert et al., 2001), and sensitive even to detect nitrosyl groups liberated from proteins (King *et al.*, 2005). However, there are few studies that utilise diaminofluoresceins to investigate nitric oxide signalling in primary neuronal cultures. The ability of this probe to detect altered nitric oxide concentrations in response to pharmacological challenge will be assessed for use in neuroblastoma and primary neuronal cultures in this chapter. DAF-2DA will also be used to assess nitric oxide generation at the cellular level using fluorescence imaging. The modulation of nitric oxide generation in neurones by the NOS inhibitors described in **Table 3.1** will be assessed. These drugs will be evaluated *in vivo* in Chapter 5. This technique will also be used to assess influence of glutamate receptor antagonists on neuronal nitric oxide generation in this chapter, and be used to study novel compounds that modulate NOS activity in Chapter 6.

The thioredoxin / thioredoxin reductase (TrxR) complex is essential for the maintenance for cellular redox state and modulates protein function via the transnitrosylation of thiol groups (Wu *et al.*, 2011). Nitric oxide signalling in the brain is not only implicated in the modulation of neuronal function, neurotransmission (Prast and Philippu, 2001), and cerebral blood flow (Macrae *et al.*, 1993), but also has implications on neuronal survival (Benhar *et al.*, 2009). The influence of altered nitric oxide, including that by NOS inhibitors, on TrxR activity in cultured cells will be assessed.

3.2 Aims

The overall aim of this work is to evaluate the use of cultured cells, and the suitability of the methods used, as an *in vitro* model of NOS activity.

The specific aims of this work are:

1. To determine the suitability of assays for NOS activity developed for use with cultured cells.

2. To use these assays to determine the pharmacological sensitivity of neuroblastoma cells to NMDA receptor activation and NOS inhibition.

3. To investigate nitric oxide signalling in primary cerebellar and hippocampal neurones.

Table 3.1. Selective and non-selective inhibitors of nitric oxide synthase.

	IC_{50} (μM)		
NOS Drug	nNOS	iNOS	eNOS
N^{ω}-nitro-L-arginine methyl ester (L-NAME) (a)	0.5	10	0.6
N^{ω}-(1-iminoethyl)-L-ornithine (L-NIO) (b)	10	7.7	5.8
N^{ω}-propyl-L-arginine (L-NPA) (c)	0.057	180	8.5

IC_{50} values representing the selectivity of inhibitors obtained from purified nitric oxide synthase (NOS) isoform enzyme activities. (a) **(Johansson et al., 1999)**; (b) **(Moore et al., 1996)**; (c) **(Zhang et al., 1997)**.

3.3 Evaluating the suitability of plate-based assays to determine NOS activity in neuronal cells

3.3.1 Neuroblastoma cells

NADPH-diaphorase activity in NG-108-15 cells was significantly decreased with 45 mins incubation with L-NAME (p = .003) compared to vehicle treatment. However, NADPH-diaphorase activity was unaltered by 10 mins incubation with 100 µM NMDA, as shown in Figure 3.1a. Figure 3.1b shows how NADPH-diaphorase activity in SH-SY5Y cells was unaltered by NMDA or L-NAME compared to vehicle treatment.

The rate of DAF-2T accumulation was significantly increased in the presence of NG-108-15 cells with the nitric oxide donor, *S*-nitroso N-acetylpenicillamine (SNAP) at 125 µM (p = .027), 250 µM (p < .001), and 500 µM (p < .001), compared to cell-free reactions, as shown in Figure 3.2a&b. There was also a trend towards significant increase in DAF-2T fluorescence with 62.5 µM SNAP in NG-108-15 cells (p = .061) compared to without cells, as determined by two-way ANOVA with Tukey's multiple comparisons. Figure 3.2c shows how DAF-2T accumulation rate in NG-108-15 cells was significantly decreased by L-NAME at 250 µM (p = .037), and 500 µM p = .002) compared to vehicle treatment. There was also a trend towards a significant decrease with 100 µM L-NAME (p = .051), as determined by two-way ANOVA with Tukey's multiple comparisons. Depletion of the BH_4 cofactor essential for NOS activity by 24 hour incubation with the GTP cyclohydrolase inhibitor, 2,4-diamino-6-hydroxypyrimidine (DAHP; 8 mM), highly and significantly decreased DAF-2T accumulation (p < .001).

Together, these results suggest that NADPH-diaphorase activity is sensitive to NOS inhibition in NG-108-15 cells, but not in SH-SY5Y cells. NADPH-

diaphorase activity was not stimulated by NMDA in either cell line. A microplate-based assay to determine DAF-2T accumulation rate is suitable for use in cultured cells because of a good specificity of signal and the sensitivity to NOS inhibition.

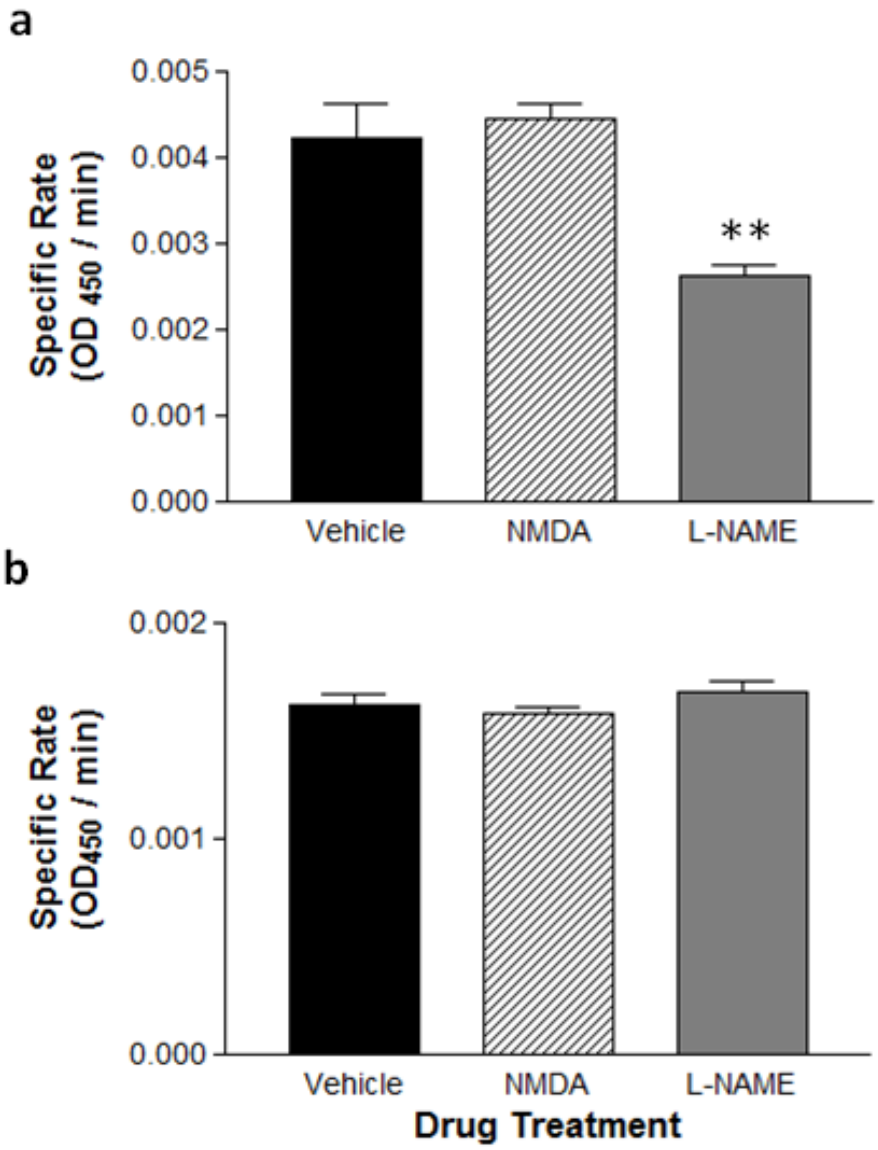

Figure 3.1. A microplate-based assay for NADPH-diaphorase activity is unsuitable to determine drug effects in neuroblastoma cells. NADPH-diaphorase activity was determined in neuroblastoma cells cultured in 96-well microplates and incubated with 100 µM NMDA for 10 mins or 100 µM L-NAME for 45 mins. (**a**) The specific rate of NADPH-diaphorase activity in NG-108-15 cells was significantly decreased with L-NAME (2.6 x 10-3 ± 1.2 x 10-4 OD_{450} / min, median = 2.5 x 10-3 OD_{450} / min, p = .003, n = 8) compared to vehicle treatment (4.2 x 10-3 ± 4.0 x 10-4 OD_{450} / min, median = 3.9 x 10-3 OD_{450} / min, n = 30). This activity did not alter with NMDA (4.4 x 10-3 ± 1.6 x 10-4 OD_{450} / min, median = 4.3 x 10-3 OD_{450} / min, n = 16). (**b**) The specific rate of NADPH-diaphorase activity in SH-SY5Y cells was unaltered by NMDA (1.6 x 10-3 ± 2.9 x 10-5 OD_{450} / min, median = 1.6 x 10-3 OD_{450} / min, n = 12) or L-NAME (1.7 x 10-3 ± 5.1 x 10-5 OD_{450} / min, median = 1.7 x 10-3 OD_{450} / min, n = 12), compared to vehicle treatment (1.6 x 10-3 ± 5.1 x 10-5 OD_{450} / min, median = 1.6 x 10-3 OD_{450} / min, n = 20). Data are presented as mean ± SEM, and were analysed by Kruskal-Wallis tests with Dunn's multiple comparisons. **, $p < .01$ vs. vehicle (Dunn's test).

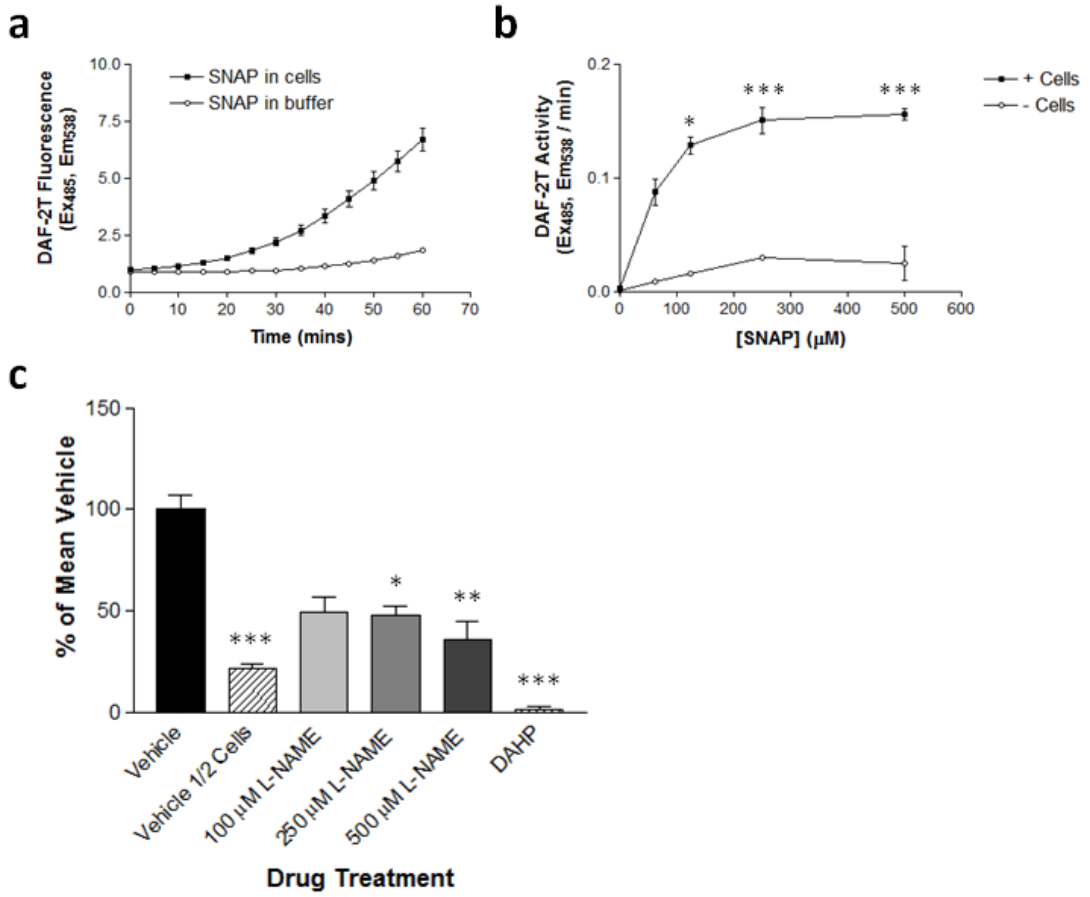

Figure 3.2. A microplate-based assay for nitric oxide generation in NG-108-15 cells using DAF-2DA. 10 µM DAF-2DA was added to NG-108-15 cells cultured in a 96-well microtitre plate and the rate of DAF-2T accumulation was determined in the presence of drugs and in the absence of cells. (**a**) Representative progress curves of DAF-2T fluorescence plus 250 µM S-nitroso N-acetylpenicillamine (SNAP) in the presence and absence of cultured NG-108-15 cells (n = 8 / group). (**b**) The overall rate of DAF-2T accumulation with a range of concentrations of SNAP was significantly higher in the presence of cells than without ($F_{1,47}$ = 71.8, p < .001), and was highly significantly influenced by SNAP concentration ($F_{4,47}$ = 21.3, p < .001). These factors significantly interact ($F_{4,47}$ = 3.5, p = .016) to influence DAF-2T accumulation rate. (**c**) There was a highly significant overall effect of inhibition on DAF-2T accumulation in NG-108-15 cell ($F_{5,71}$ = 35.2, p < .001). There was a trend towards a significant decrease in DAF-2T accumulation in NG-108-15 cells treated for 45 mins with 100 µM nitro-L-arginine methyl ester (L-NAME; 49.6 ± 6.8 % of mean vehicle, p = .051, n = 4), and significantly so with 250 µM (47.4 ± 5.2 % of mean vehicle, p = .037, n = 4), and 500 µM (35.7 ± 8.8 % of mean vehicle, p = .002, n = 4) compared to vehicle treatment. DAF-2T accumulation was highly significantly diminished with 24 hour treatment with 8 mM 2,4-diamino-6-hydroxypyrimidine (DAHP; 2.0 ± 1.0 % of mean vehicle, p < .001, n = 8). The rate of DAF-2T accumulation was significantly decreased in NG-108-15 cells that were cultured at half density (21.2 ± 2.6 % of mean vehicle, p < .001 , n = 26) of that of the other experimental groups. Data are presented as mean ± SEM, and were analysed using one-way or two-way ANOVA, as appropriate, with Tukey's multiple comparisons tests. *, p < .05; **, p < .01; ***, p < .001 compared to rate in the absence of cells for (**b**), and compared to mean vehicle treatment for (**c**) (Tukey's test).

3.3.2 Primary neuronal cultures

DAF-2DA was incubated with primary rat cortical neurones, and the rate of DAF2T accumulation was determined with various drug treatments. Figure 3.3a shows how nitric oxide accumulation in cultured cortical neurones, as determined by DAF-2T fluorescence intensity, was significantly increased with NMDA treatment (0.36 ± 0.09 Ex_{486}, Em_{538} / min, p = .039, n = 8), but not by L-NAME (0.13 ± 0.01 Ex_{486}, Em_{538} / min, n = 8), compared to vehicle treatment (0.14 ± 0.04 Ex_{486}, Em_{538} / min, n = 8), as determined by one-way ANOVA with Tukey's multiple comparisons. Vehicle treated neurones that were cultured at a half density to those in the experimental groups produced a near-half rate of DAF-2T accumulation (0.07 ± 0.01 Ex_{486}, Em_{538} / min, n.s., n = 4; data not shown).

Cortical neurone NADPH-diaphorase activity was unaltered by 200 µM NMDA (17.7 ± 2.79 x 10^{-4} OD_{450} / min, n = 7), or 100 µM L-NAME (20.8 ± 0.8 x 10^{-4} OD_{450} / min, n = 7), compared to vehicle treatment (19.0 ± 2.8 x 10^{-4} OD_{450} / min, n = 7), as shown in Figure 3.3b. Vehicle treated neurones that were cultured at a half density to those in the experimental groups produced a diminished NADPH-diaphorase rate of activity (13.2 ± 6.5 x 10^{-4} OD_{450} / min, n = 3), and no NADPH-diaphorase activity was detected in cells in the absence of NADPH (data not shown). Figure 3.3c shows how culture medium nitrite concentration, too, was unaltered by NMDA (9.6 ± 0.97 nM, n = 8), or L-NAME (9.3 ± 1.48 nM, n = 8) compared to vehicle treatment (11.6 ± 0.75 nM, n = 16). Addition of 250 µM SNAP produced a highly significant increase in medium nitrite content (27.9 ± 2.5 nM, p < .001, n = 8; data not shown) compared to vehicle. Data were analysed using one-way ANOVA tests with Tukey's multiple comparisons.

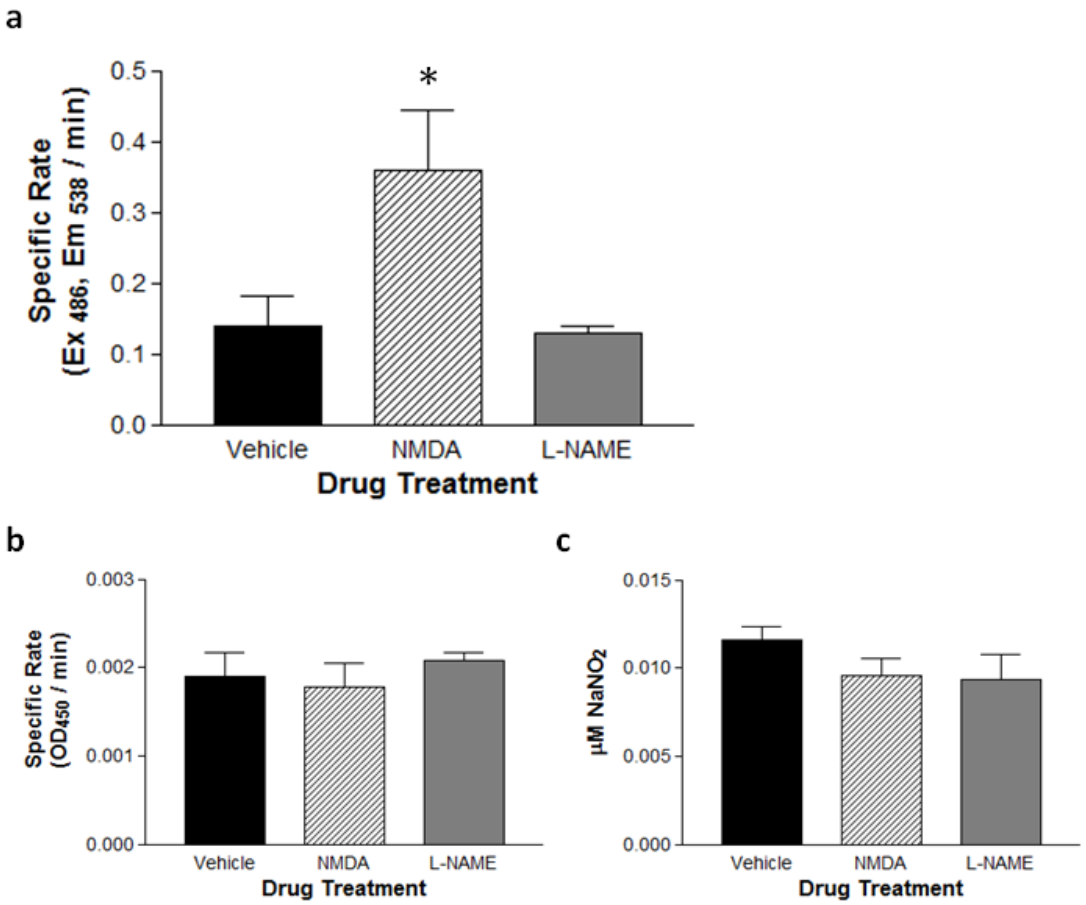

Figure 3.3. NMDA stimulates nitric oxide generation in cortical neurones. Primary cortical neuronal cultures were incubated with 10 µM DAF-2DA, 100 µM L-NAME or vehicle for 24 hours, and 200 µM NMDA for 20 mins. (**a**) Nitric oxide accumulation, as determined by DAF-2T fluorescence intensity, was significantly increased with NMDA treatment (0.36 ± 0.09 Ex486, Em538 / min, p = .039, n = 8), but not by L-NAME (0.13 ± 0.01 Ex486, Em538 / min, n = 8), compared to vehicle treatment (0.14. ± 0.04 Ex486, Em538 / min, n = 8). (**b**) Nitric oxide synthase activity, as determined by the rate of NADPH-diaphorase activity, was unchanged with drug treatment. (**c**) Nitrite concentration, as determined by Griess assay, was also unaltered with drug treatments. Data are presented as mean ± SEM, and were analysed by one-way ANOVA tests with Tukey's multiple comparisons. *, p < .05 vs. vehicle (Tukey's test).

3.4 Multiple signalling pathways contribute to neuronal NOS activity *in vitro*

3.4.1 Cerebellar granule cells

The activity of thioredoxin reductase (TrxR) was determined in cerebellar granule cells (CGCs). Figure 3.4a shows how TrxR activity was unchanged by 100 μM glutamate, the nitric oxide donor *S*-nitroso N-acetylpenicillamine (SNAP) at 100 μM or 300 μM, or by 100 μM of the peroxynitrite donor, 3-morpholinosydnonimine hydrochloride (SIN-1). Figure 3.4b shows how TrxR activity was unchanged with non-selective NOS inhibition by L-NAME at 100 μM or 300 μM. Two hour treatment with 150 μM L-NIO or 150 μM L-NPA similarly did not alter TrxR activity, as determined by one-sample t-tests.

The intracellular nitric oxide –sensitive fluorescent probe, DAF-2DA was used to determine nitric oxide generation in CGCs to determine the efficacy of non-selective and selective NOS inhibitors in the inhibition of nitric oxide generation. Figure 3.5 shows how DAF-2T intensity of vehicle-treated CGCs was significantly decreased with 300 μM L-NAME (p = .04), but not by 150 μM L-NIO, or 150 μM L-NPA. Glutamate significantly increased nitric oxide generation (p = .04), and this was partially reversed by pretreatment with L-NAME (p = .01) and by L-NPA (p = .008), but not by L-NIO, as revealed by two-sample t-tests.

The contributions of glutamate receptors, and L-type calcium channels to glutamate-stimulated nitric oxide generation were explored using MK801, CNQX and nifedipine in CGCs, as shown in Figure 3.6. There was a significant increase in DAF-2T intensity with 30 mins incubation with 100 μM glutamate (p = .04) compared to vehicle alone, as determined by one sample t-test. Glutamate-stimulated DAF-2T intensity was reversed with pretreatment with the L-type calcium channel blocker, nifedipine (30 μM; p = .02), and there

was a trend towards this with the AMPA/kainate receptor antagonist, CNQX (10 μM; p = .053), but not by blockade of NMDA receptors with 10 μM MK801 (p = .064), as revealed by two-sample t-tests.

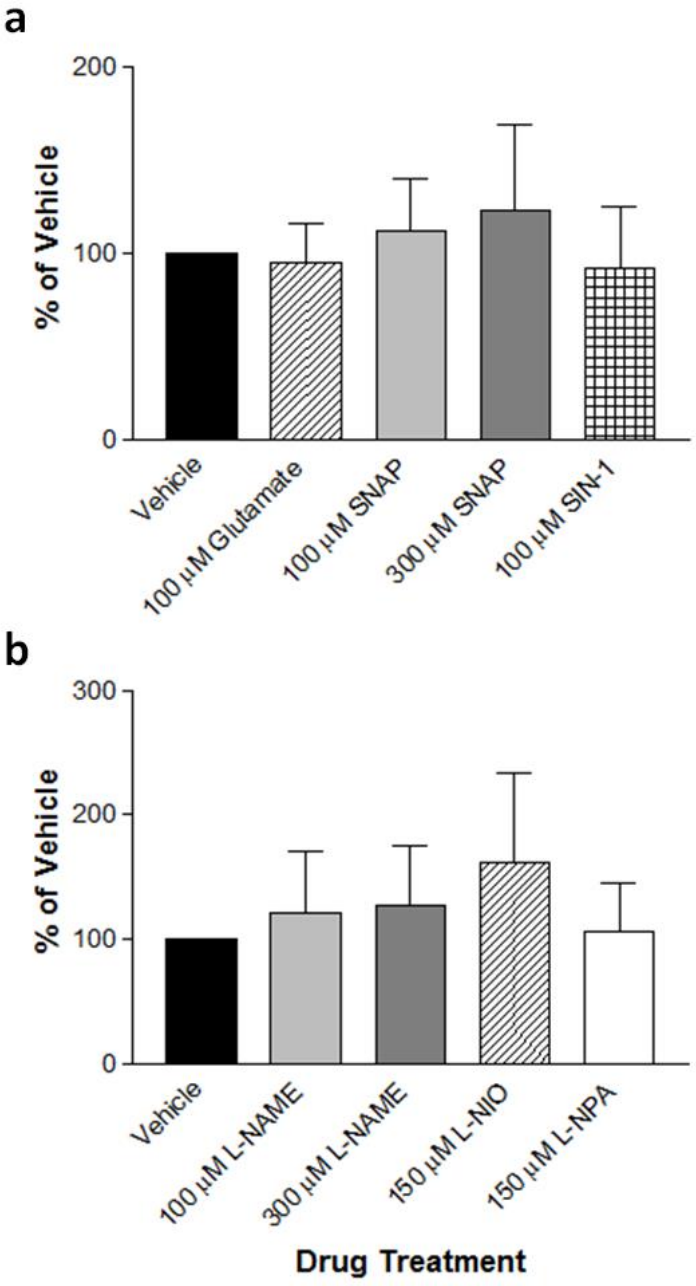

Figure 3.4. Thioredoxin reductase is insensitive to altered nitric oxide in cerebellar neurones. (**a**) Cultured cerebellar granule cells (CGCs) were incubated with glutamate (94.6 ± 21.1 % of vehicle, n = 8) for 90 mins, or the nitric oxide donors SNAP (100 µM: 111.7 ± 27.5 % of vehicle, n = 8; 300 µM: 122.3 ± 46.2 % of vehicle, n = 4) and SIN-1 (100 µM; 91.9 ± 32.6 % of vehicle, n = 4) for 2 hours. No significant differences in thioredoxin reductase (TrxR) activity were detected between these treatment groups. (**b**) CGCs were treated with the nitric oxide synthase inhibitors, L-NAME (100 µM: 120.5 ± 49.9 % of vehicle, n = 5; 300 µM: 127.1 ± 47.6 % of vehicle, n = 3), L-NIO (150 µM: 161.8 ± 71.6 % of vehicle, n = 3), or L-NPA (150 µM: 105.3 ± 39.6 % of vehicle, n = 3) for 2 hours. No changes in TrxR activity was detected using one-sample t-tests. Data are presented as mean percent of vehicle ± SEM.

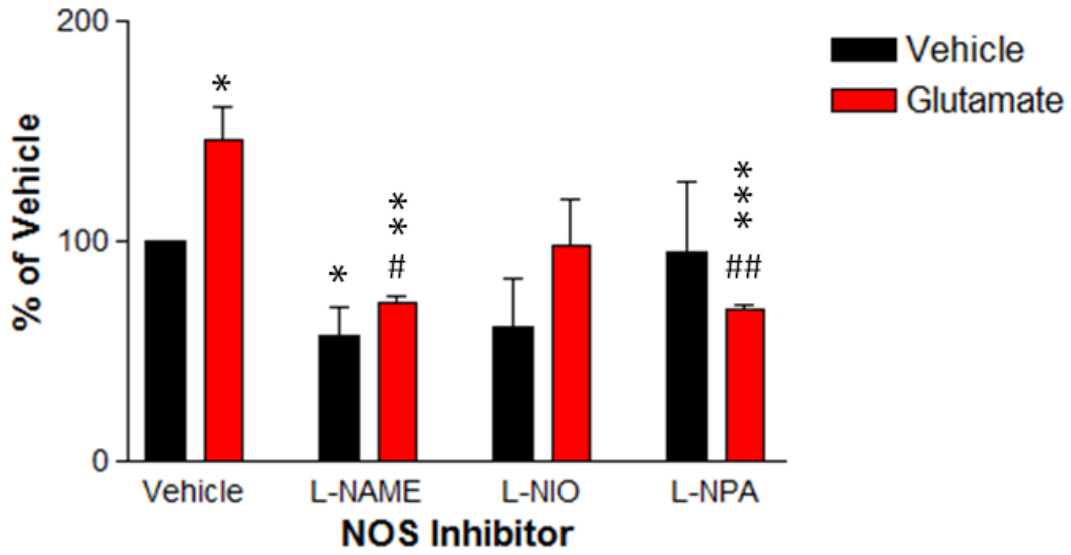

Figure 3.5. Neuronal and non-selective NOS inhibition reverses glutamate-stimulated nitric oxide generation in cerebellar neurones. Primary cerebellar granule cell cultures were incubated with the nitric oxide synthase (NOS) inhibitors, L-NAME, L-NIO or L-NPA for 2 hours and a fluorescent probe that is sensitive to intracellular nitric oxide (DAF-2DA) for 30 mins. 300 µM L-NAME significantly decreased DAF-2T intensity from that with vehicle treatment (56.9 ± 12.8 % of vehicle, p = .04, n = 4). Glutamate significantly increased nitric oxide generation (145.5 ± 15.5 % of vehicle, p = .04, n = 5), and this was significantly decreased with L-NAME (71.6 ± 3.4 % of vehicle, p = .01, n = 4) and by 150 µM L-NPA (68.3 ± 1.9 % of vehicle, p = .008, n = 4), but not by 150 µM L-NIO (97.9 ± 21.1 % of vehicle, n = 4). Data are presented as mean percent of vehicle ± SEM, and were analysed using one- and two- sample t-tests, as appropriate. *, p < .05; **, p < .01; ***, p < .001 vs. vehicle control; #, p < .05, ## p < .01 vs. glutamate only.

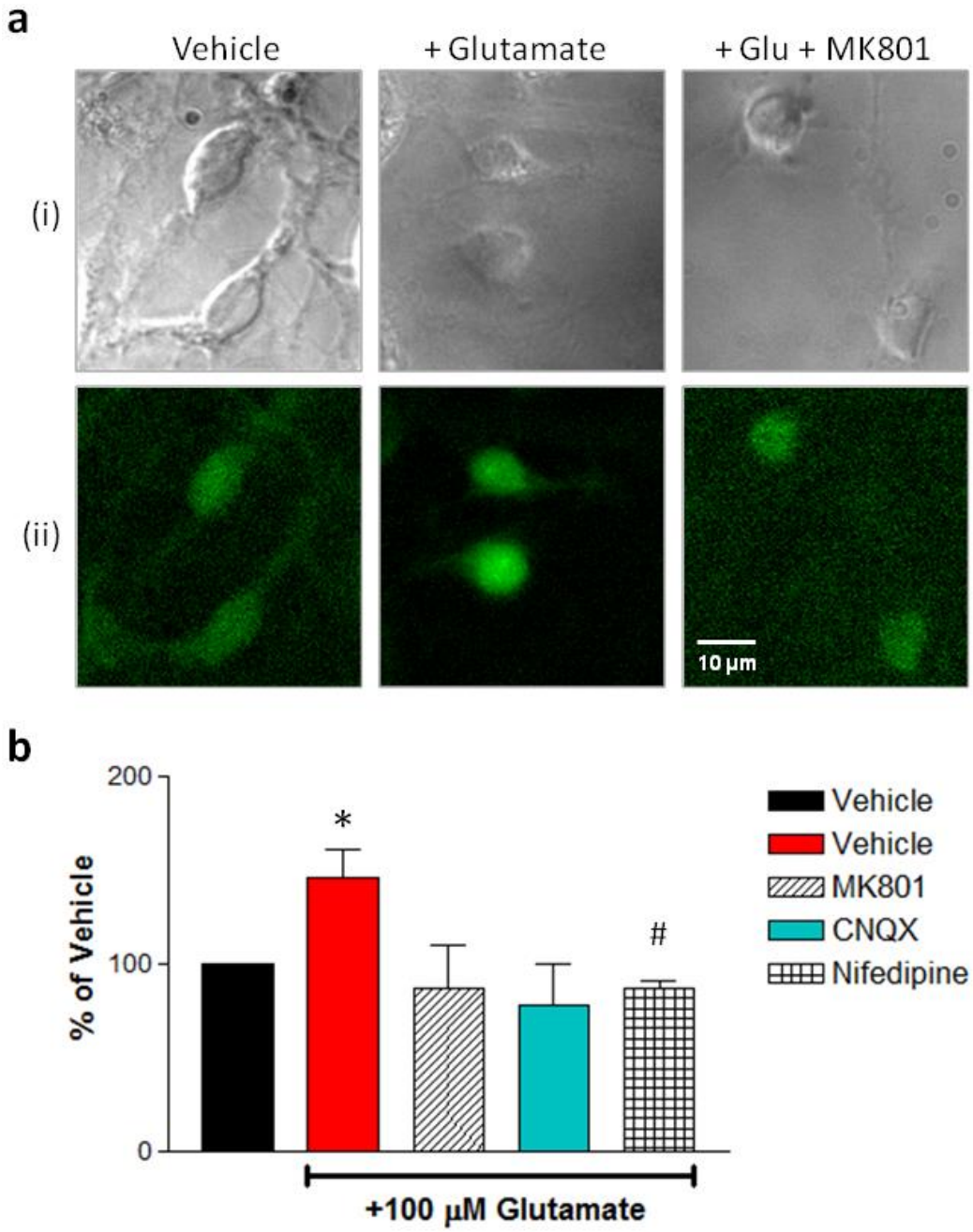

Figure 3.6. Glutamate-stimulated nitric oxide generation is mediated by multiple receptor interactions in cerebellar neurones. Primary cerebellar granule cell (CGC) cultures DAF-2DA for 30 mins. (**a**) Illustrative bright field (**i**) and DAF-2T fluorescence (**ii**) micrographs of CGCs following incubation with vehicle only (left), glutamate (centre), and MK801 and glutamate (right). (**b**) There was a significant increase in DAF-2T intensity with 30 mins incubation with 100 µM glutamate (145.5 ± 15.5 % of vehicle, p = .04, n = 5). Glutamate-stimulated DAF-2T intensity was reversed by 30 µM nifedipine (86.6 ± 4.3 % of vehicle, p = .02, n = 3), and there was a trend towards this with 10 µM CNQX (77.5 ± 22.1 % of vehicle, p = .053, n = 4), but by 10 µM MK801 (87.0 ± 22.8 % of vehicle, n = 4). Data are presented as mean percent of vehicle ± SEM, and were analysed using one- and two-sample t-tests, as appropriate. *, p < .05 vs. vehicle; # p < .05 vs. glutamate alone. Scale bar applies to all micrographs.

3.4.2 Hippocampal Cells

The fluorescence intensity of DAF-2T was imaged in primary rat hippocampal neurones. Figure 3.7b shows how DAF-2T fluorescence intensity was significantly increased following 30 mins incubation with 100 μM glutamate (p = .03). There was a significant decrease with 150 μM L-NPA (p = .005) from that of the vehicle control, and L-NPA also reversed the glutamate-stimulated increase in DAF-2T signal (p = .023), as illustrated in Figure 3.7a. 300 μM L-NAME also partially reversed the increase in DAF-2T accumulation with glutamate alone (p = .047), and there was a trend towards this with 150 μM L-NIO (p = .066). Non-receptor-mediated stimulation of NOS using 1 μM A23187 was significantly decreased with pretreatment with L-NPA (p = .006), but not by L-NAME or L-NIO, as revealed using two-sample t-tests.

The contributions of NMDA and non-NMDA receptors, and L-type calcium channels to glutamate-stimulated nitric oxide generation in hippocampal neurones was explored using MK801, CNQX and nifedipine, respectively. Figure 3.8 shows how DAF-2T fluorescence intensity in hippocampal neurones incubated with glutamate (p = .03) was reversed by combined treatment with 30 μM nifedipine, 10 μM MK801 and 10 μM CNQX (p = .03), but not individually. There was a trend towards a significant decrease from glutamate alone DAF-2T intensity with cotreatment with MK801 and nifedipine (p = .067), as revealed using two-way t-tests.

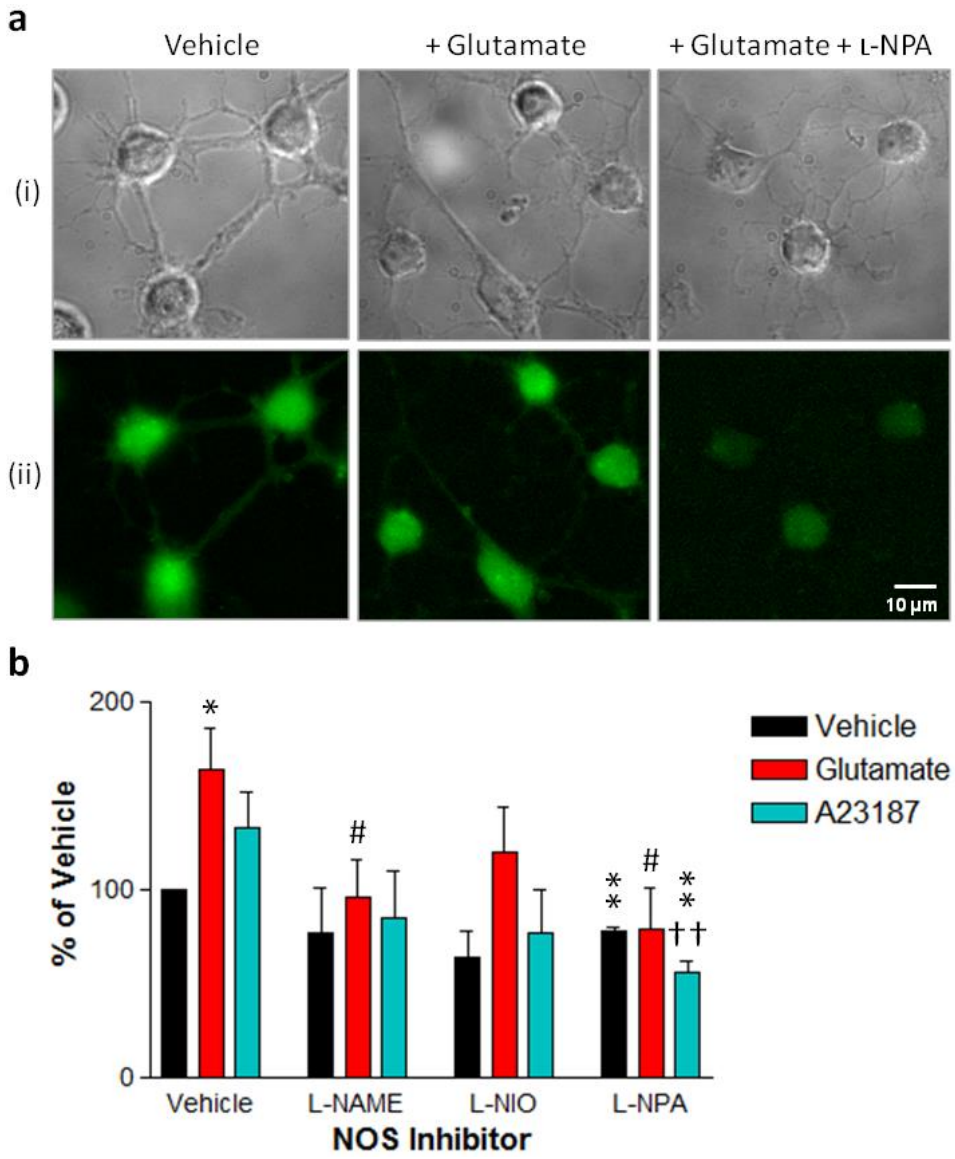

Figure 3.7. Glutamate-stimulated nitric oxide generation is reversed by nNOS inhibition in hippocampal neurones. Primary hippocampal cell cultures were incubated with the nitric oxide synthase (NOS) inhibitors, L-NAME, L-NIO or L-NPA for 2 hours and a fluorescent probe that is sensitive to intracellular nitric oxide (DAF-2DA) for 30 mins. (**a**) Illustrative bright field (**i**) and DAF-2T fluorescence (**ii**) micrographs of hippocampal cells following incubation with vehicle only (left), glutamate (centre), and L-NPA and glutamate (right). (**b**) The fluorescence intensity of DAF-2T was significantly increased in cells with 30 mins incubation with 100 µM glutamate (163.3 ± 22.6 % of vehicle, p = .03, n = 8), and significantly decreased with 150 µM L-NPA (78.1 ± 1.5 % of vehicle, p = .005, n = 3). Glutamate stimulation of DAF-2T signal was reversed by 300 µM L-NAME (96.0 ± 19.9, % of vehicle, p = .047, n = 6), and L-NPA (79.0 ± 21.6 % of vehicle, p = .023, n = 5), but not by 150 µM L-NIO (120.0 ± 23.9 % of vehicle, p = .066, n = 8). Stimulation of NOS using the calcium ionophore, A23187 (1 µM, 2 mins; 132.9 ± 18.9 % of vehicle, n = 7), was partially reversed with pretreatment with L-NPA (56.0 ± 5.7 % of vehicle, p = .006, n = 4). Data are presented as mean percent of vehicle ± SEM, and were analysed using one- and two-sample t-tests, as appropriate. *, p < .05; **, p < .01 vs. vehicle control; #, p < .05, vs. glutamate only; ††, p < .01 vs. A23187 only. Scale bar applies to all micrographs.

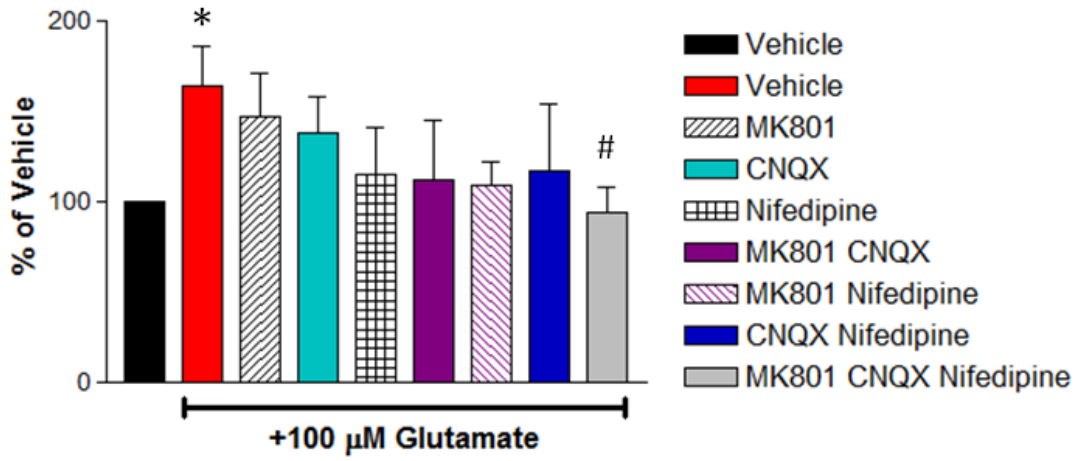

Figure 3.8. Nitric oxide generation in hippocampal neurones is mediated by multiple receptor interactions. DAF-2T fluorescence intensity was significantly increased following 30 mins incubation with 100 µM glutamate (163.3 ± 22.6 % of vehicle, p = .03, n = 8). Glutamate-stimulated nitric oxide generation in hippocampal cell cultures was reversed by 35 min incubation with 30 µM nifedipine + 10 µM MK801 + 10 µM CNQX (93.7 ± 13.5 % of vehicle, p = .03, n = 4), and trended towards this with cotreatment of MK801 + nifedipine (108.8 ± 13.2 % of vehicle, p = .067, n = 4). Data are presented as mean percent of vehicle ± SEM, and were analysed using one- and two- sample t-tests, as appropriate. *, p < .05 vs. vehicle control; #, p < .05 vs. glutamate only.

3.5 Discussion

3.5.1 The use of plate-based assays to determine nitric oxide synthase activity in neuronal cells

NADPH-diaphorase activity was inhibited by L-NAME in NG-108-15, but not SH-SY5Y cells, as shown in Figure 3.1. Both cell lines have been shown to express nNOS (Grant et al., 2002; Müller et al., 2010), but no evidence exists yet that these are functional. NG-108-15 cells appear to possess functional NMDA receptors (Ohkuma *et al.*, 1994), but NADPH-diaphorase activity did not respond to NMDA treatment (Figure 3.1a), suggestive that if NMDA receptors and NOS are indeed expressed together, they are not functionally linked as expected. SH-SY5Y cells also did not respond to NMDA (Figure 3.1b). These cells appear to have incomplete and/or non-functional NMDA receptors (Kulikov et al., 2007; Sun et al., 2010), and were therefore unsuitable as a model to study glutamate-mediated NOS activity.

Expanding on the positive response of NG-108-15 cells to NOS inhibition, these cells were then used to validate the use of the intracellular nitric oxide probe, DAF-2DA. Figure 3.2 shows how intracellular DAF-2T accumulation far outweighs that of the non-specific (DAF-2) fluorescence of the probe, bearing in mind that DAF-2 maximally fluoresces at the same wavelength at DAF-2T (Ye *et al.*, 2004). Non-specific fluorescence from cell-free media was subsequently subtracted from DAF-2T values to give specific accumulation rates. NG-108-15 cell nitric oxide generation, as assessed by specific DAF-2T fluorescence, was inhibited to ~50% with 250 and 500 μM L-NAME (Figure 3.2c), and was near-completely abolished in the absence of tetrahydrobiopterin cofactor (i.e. with DAHP inhibition of GTP cyclohydrolase I). Therefore, NG-108-15 neuroblastoma cells are compatible with this assay for monitoring NOS activity, but not suitable for monitoring glutamate effects.

Figure 3.3 confirms that DAF-2DA is sufficient to detect NMDA receptor-mediated nitric oxide release, as shown in primary cortical neurone cultures, while NADPH-diaphorase activity and nitrite concentration in media are not. Unlike NG-108-15 cells, cortical neurones did not respond to NOS inhibition by L-NAME. The likely reason for this is that nitrergic neurones constitute a small proportion (approximately 1%) of cortical cells (Kharazia et al., 1994; Gotti et al., 2005), and that the inhibition of such a small population of cells is below the detection threshold of DAF-2T. It would have been useful to see whether L-NAME could reverse the NMDA-mediated stimulation of nitric oxide generation. For the purpose of evaluating NOS inhibitor activity (as in Chapter 3.4) and to be relevant to later Chapters, the assay would need the potential to detect diminished nitric oxide generation by NOS inhibition in neurones that possess a functional NMDA receptor-NOS relationship. For this purpose, microplate-based assays for NOS activity in cultured neurones were not pursued further.

3.5.2 Evaluating glutamate-mediated nNOS activity in cerebellar and hippocampal neurones

CGCs are rich in nNOS and are numerous within the cerebellum (Blottner et al., 1995; Gotti et al., 2005), making them an excellent source for nitrergic neurones with which to culture. There is a rich and diverse population of neuronal cells in the hippocampus, and much of the patterned behaviours of circuits in this region are mediated by GABAergic interneurones (Lapray *et al.*, 2012). NOS expression is largely found in somatostatin (SOM) and calretinin (CR) –expressing interneruones (Tricoire and Vitalis, 2012). Glutamate-mediated nitric oxide generation in CGCs and hippocampal neurones was inhibited by non-selective NOS, and selective nNOS inhibition, by L-NAME and L-NPA, respectively. Nitric oxide generation in these cells was also inhibited by glutamate receptor and L-type channel antagonists

Together, these suggest that nNOS is the major isoform of NOS active in these regions, and that multiple receptors are involved in its activity.

DAF-2DA concentration was reduced from the reported optimum, 10 μM, (Kojima *et al.*, 1998) to 1 μM in order to minimise non-specific fluorescence (Rodriguez *et al.*, 2005) and possible toxicity (Shlosberg *et al.*, 2012). This concentration was shown to be effective in these experiments, as illustrated by Figure 3.6a and Figure 3.7a.

Glutamate-stimulated nitric oxide release in CGCs was partially reversed by non-selective and nNOS inhibition by L-NAME and L-NPA, respectively, as shown in Figure 3.5. This activity was not significantly inhibited by L-NIO. Together, these suggest that nNOS, but not eNOS, accounts for the glutamate-mediated nitric oxide release in CGCs. However, the data in the presence of L-NIO were not significantly different from those with L-NPA. Therefore, conclusions must be tentative, and further studies would be needed to confirm the lack of effect of L-NIO. Figure 3.6b shows how pretreatment with nifedipine reversed the glutamate-stimulated nitric oxide generation in CGCs. A caveat to this is that due to time constraints, the effect of the antagonists alone was not tested, and they could be suppressing basal nitric oxide generation rather than reversing the effect of glutamate. However, this implies that L-type calcium channels contribute to nNOS activity. With further replicates, it is likely that MK801 or CNQX would also reverse the glutamate-stimulated increase in nitric oxide generation; the lack of a significant difference likely due to too few replicates and variance in these groups. NMDA and non-NMDA receptors may contribute to nNOS activity; the latter likely being calcium-permeable AMPA receptors (Bhardwaj et al., 1997a; Frade et al., 2009). Evidence has been shown for glutamate-stimulated nitric oxide release that may also be mediated by metabotropic glutamate receptors, and that these differential receptor interactions may be

anatomically distinct in the cerebellum (Okada *et al.*, 2004). Non-NMDA receptor mediated nitric oxide release in the cerebellar neurones may be insensitive to NOS inhibition (Yamada and Nabeshima, 1997).

Nitric oxide generation has been shown to be mediated by NMDA receptor-independent glutamate transmission in the cerebellum (Yamada and Nabeshima, 1997). The data presented in Figure 3.6 oppose the hypothesis that this is mediated by NMDA receptors alone. Indeed, these data implicate non-NMDA receptors (i.e. AMPA and kainate receptors) and voltage-gated calcium channels also contribute to glutamate-stimulated nitric oxide generation. GluA2-lacking AMPA receptors, which are calcium-permeable, have been shown to be present and functional in cultured CGCs (Incontro *et al.*, 2011). Here, DAF-2T intensity displayed sensitivity to nifedipine with glutamate stimulation. This suggests that NOS in the cerebellum may be activated by L-type channels, as well as glutamate receptors. An interesting finding from Incontro and colleagues (2011) is that GluA subunit expression is enhanced with L-type channel blockade, and is sensitive to KCl concentration. The CGCs used in this study were maintained in a depolarising mileu (25 mM KCl), and hippocampal cells were not. An interesting experiment would be to alter conditions (such as altering KCl concentrations or by prolonged incubation with nifedipine) to see if AMPA receptor subunit compositions alter with these conditions, and whether NOS sensitivity changes as a result of this.

Hippocampal cell nitric oxide generation stimulated by glutamate also showed sensitivity to L-type channel, NMDA and non-NMDA receptor inhibition, as shown in Figure 3.8, but unlike that in CGCs, nifedipine was not effective alone with glutamate. This may be suggestive of multiple redundancies to maintain functional NOS signalling in the absence of a single glutamate receptor interaction. L-type and P/Q-type calcium channels have

previously been shown to contribute to NOS activity in the cortex (Oka *et al.*, 2003). The implication of both NMDA receptor and non-NMDA receptor – mediated NOS activation also suggests that there are mechanisms for rapid and protracted induction interactions with NOS. NMDA and AMPA receptors (Bhardwaj et al., 1997a) and metabotropic glutamate receptors (Bhardwaj et al., 1997b) have been shown to contribute to glutamate-stimulated nitric oxide release in the hippocampus, and GluA2-lacking AMPA receptors may provide an additional source of calcium for NOS in neurones here (Szabo *et al.*, 2012). An avenue for further study would be to use more selective inhibitors, such as 1-naphthyl acetyl spermine (NASPM) to evaluate any sensitivity of NOS to calcium-permeable AMPA receptors that may be present.

Glutamate-stimulated nitric oxide generation in hippocampal neurones and CGCs was blocked by selective nNOS inhibition with L-NPA, whereas, L-NIO failed to block nitric oxide generation. Expression of eNOS has been shown in the hippocampus (Dinerman *et al.*, 1994), though the activities of this isoform may be below a detectable threshold, such as shown in Figure 3.7b. Changes in thioredoxin reductase activity were not detected in CGCs by altering nitric oxide concentrations with nitric oxide donors or NOS inhibitors. This may be because of a lack of sensitivity of the assay, or perhaps due to insufficient sample. Nitric oxide generation stimulated by glutamate was blocked by the L-type calcium channel antagonist, nifedipine in CGCs, and by MK801, CNQX and nifedipine in combination in hippocampal neurones. Together, there appears to be differential contributions of glutamate receptors and voltage-gated channels in the cerebellum (Figure 3.6b) and hippocampus (Figure 3.8) in the modulation of nNOS activity.

Taken together, these data validate the use of DAF-2T imaging in primary neuronal cultures as a means to study nNOS activity as a function of

glutamate signalling, and this will be used to evaluate novel compounds that modulate NOS activity in Chapter 6. The neuronal isoform of NOS appears to contribute the majority of nitric oxide generation in hippocampal neurones and CGCs. nNOS in the hippocampus and cerebellum appears to have more complex interactions with receptors and channels than previously thought, and may have implications for differential responses between these regions *in vivo*.

4 Spatial and Temporal Differences in NOS and Thioredoxin Reductase Activities Following Phencyclidine Treatments

4.1 Introduction

Many signalling pathways related to glutamate signalling have been implicated in deficits as found in schizophrenia (reviewed by: Jentsch and Roth, 1999; Javitt et al., 2012). Here, we use phencyclidine (PCP), an antagonist of the NMDA class of glutamate receptor, to block the flux of ions through the NMDA receptor channel. Because of the physical and functional association of nNOS with NMDA receptors, via PSD-95 protein interactions, NMDA receptor mediated calcium influx serves as the primary source of nNOS activity (Sattler *et al.*, 1999). This has lead to the suggestion that dysfunctional NOS signalling may be implicated in schizophrenia (reviewed by: Bernstein et al., 2005).

The thioredoxin (Trx) / thioredoxin reductase (TrxR) system is the primary mediator of protein denitrosylation, and its activities are essential for the maintenance of cellular redox state (Wu *et al.*, 2011). For example, the denitrosation of procaspase 3 by Trx / TrxR initiates an apoptotic cascade mediated by caspase 3 (Benhar *et al.*, 2008). This forms a basis for a role of nitric oxide signalling in programmed cell death. Dysfunctional Trx/TrxR signalling has been implicated in deficits found schizophrenia (Zhang *et al.*, 2012a). Dysfunction and loss of parvalbumin-expressing GABAergic interneurones has been strongly implicated in the altered circuit and network synchrony found in schizophrenia (reviewed by: Jones, 2010), and caspase-mediated apoptosis may be involved in this cellular loss (Wang *et al.*, 2008a).

Many symptomatic deficits that are common in people with schizophrenia (reviewed by: Tandon et al., 2009) may be replicated in rodents by NMDA receptor antagonists (reviewed by: Jentsch and Roth, 1999; Pratt et al., 2012). Aberrant locomotion and prepulse inhibition (PPI) are two behavioural measures that are commonly used in animal models that are translationally relevant to schizophrenia (Amann *et al.*, 2010), and are used here to reveal the behavioural outcomes in mice with the acute and subchronic PCP treatment.

4.2 Hypotheses and aims

It is hypothesised that PCP will block the calcium source for NOS function and will therefore inhibit its activity, with the most pronounced effects predicted to be in brain regions associated with schizophrenia.

We propose that altered NOS signalling will confer a disruption in TrxR activity and therefore caspase 3 activity in these regions. Subchronic PCP administration will exacerbate the neurochemical effects seen with acute administration. Acute PCP will elicit a deficit in prepulse inhibition and increase locomotor activity in mice, and these deficits will persist with subchronic PCP administration.

The aims of the work in this chapter were to investigate the influence of PCP on the activity of NOS in the mouse brain. Brain regions were selected because of the density of NOS expression in these regions in c57bl6 mice (Hara et al., 1996; Gotti et al., 2005), and their implication in schizophrenia (Bernstein *et al.*, 2005). Acute and subchronic administrations of PCP in the mouse will be compared and contrasted to assess whether acute and persistent NMDA receptor antagonism produces a differential effect in these brain regions. The activities of TrxR and caspases will also be evaluated

because of the implications of altered nitric oxide signalling upon these enzymes, in the context of maintenance of cellular redox state and in apoptosis. The behavioural effects of these drug treatments on PPI and locomotor activity are also assessed in parallel experiments.

4.3 Methods

Detailed methods are given in Chapter 2. Drug administrations are outlined in Section 2.3, behavioural procedures are given in Section 2.9, and details of neurochemical assays are given in Sections 2.5-2.8. Schemata for *in vivo*, and subsequent *ex vivo* experiments are given in **Figure 4.1**.

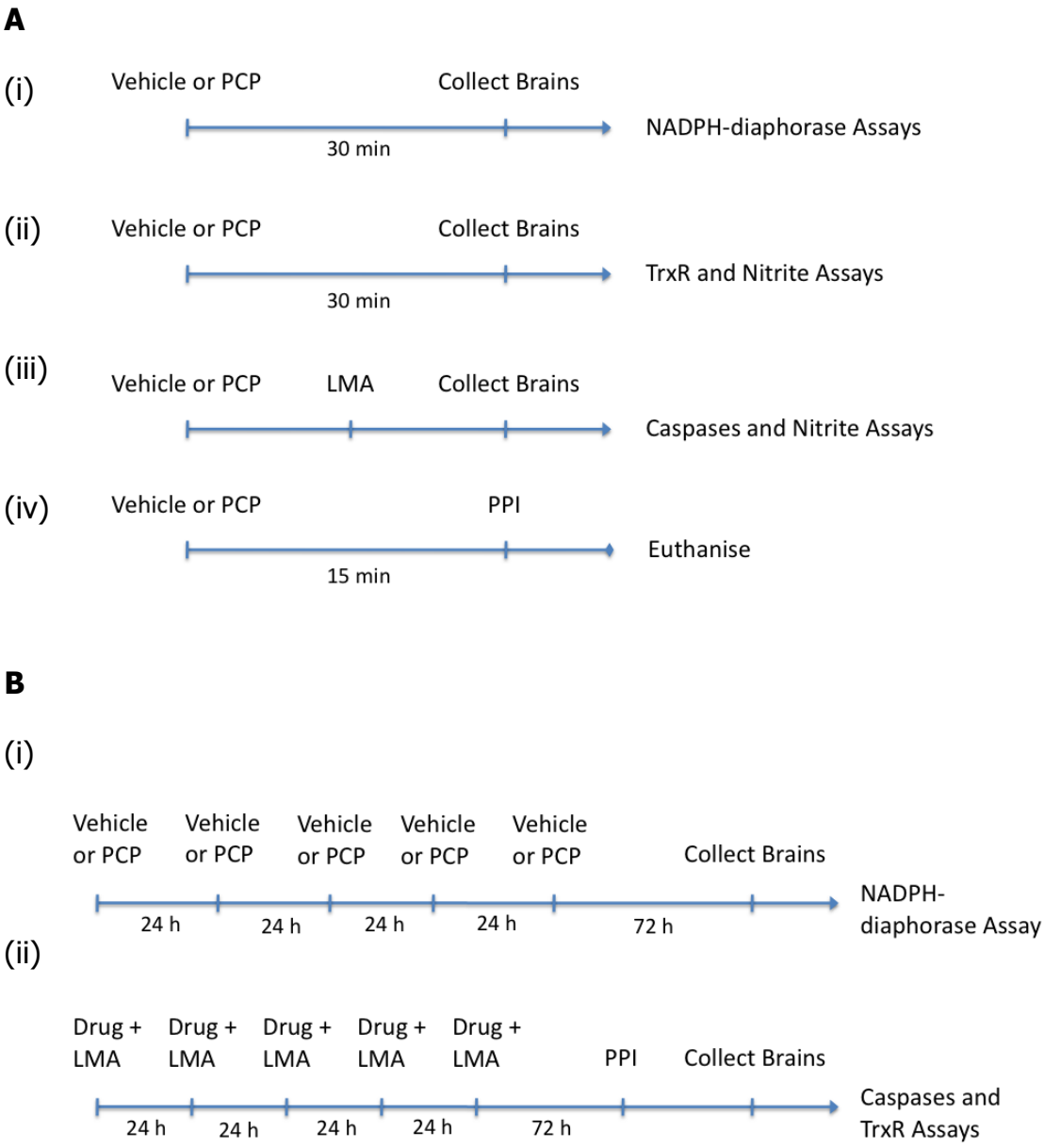

Figure 4.1. Experimental schemata for drug administrations, behavioural and neurochemical assays. Schemata are given for experiments featuring (A i-iv) acute and (B i-ii) subchronic drug administrations.

4.4 Regional NADPH-diaphorase activity

4.4.1 Histochemical assessment of NOS activity

Sections of mouse brain were stained using NADPH-diaphorase histochemistry. The blue formazan product was more densely localised in the somata and proximal parts of processes of discrete populations of neurones, as demonstrated by **Figure 4.2**.

The relative optical density (ROD) of NADPH-diaphorase staining was assessed in replicate sections of the striatum of the rat brain that were incubated with vehicle (PBS), or the NOS inhibitors, *N*ω-nitro-L-arginine (L-NNA; 100 μM) or *N*ω-nitro-L-arginine methyl ester (L-NAME; 1 mM) for 20 mins before or after fixation. **Figure 4.3a** illustrates how NADPH-diaphorase staining intensity was decreased by NOS inhibition prior to fixation in the striata of the rat brain. Tissue was sectioned and then incubated in buffer containing inhibitors for 20 mins, and then tissue was fixed. There was a highly significant overall influence of inhibition ($F_{(2,2)} = 27.2$, $p < .001$), and in staining between neurones and blood vessels ($F_{(1,2)} = 96.0$, $p < .001$). There was also a significant interaction between these factors ($F_{(2,2)} = 4.6$, $p = .04$), as determined by repeated measures ANOVA. Multiple comparisons by Tukey's *post hoc* tests revealed that there was an overall significant decrease in staining in neurones and blood vessels when incubated prior to fixation with L-NNA ($p = .0006$) and with L-NAME ($p = .0001$). Incubation with 100 μM L-NNA significantly decreased staining in both neurones ($p = .01$) and in blood vessels ($p = .01$). Whereas, 1 mM L-NAME significantly decreased staining in neurones ($p = .001$), but not in blood vessels.

Replicate sections of rat striatum were incubated with inhibitors for 20 mins following fixation. There was an overall significant effect of NOS inhibition (*F*

$_{(2,2)}$ = 15.9, p = .001), and between blood vessels and neurones ($F_{(1,2)}$ = 156.7, p < .001), as revealed by repeated measures ANOVA. **Figure 4.3b** shows how overall NADPH-diaphorase staining was significantly decreased in both neurones and blood vessels when incubated with L-NNA (p = .02) and with L-NAME (p = .0006) after fixation, as revealed by Tukey's multiple comparisons. Incubation with 1 mM L-NAME significantly decreased staining in neurones (p = .01), and in blood vessels (p = .04). 100 µM L-NNA did not significantly decrease staining in neurones or blood vessels (both, p > .05). No NADPH-diaphorase staining was present in replicate sections when NADPH was omitted from reactions (data not shown).

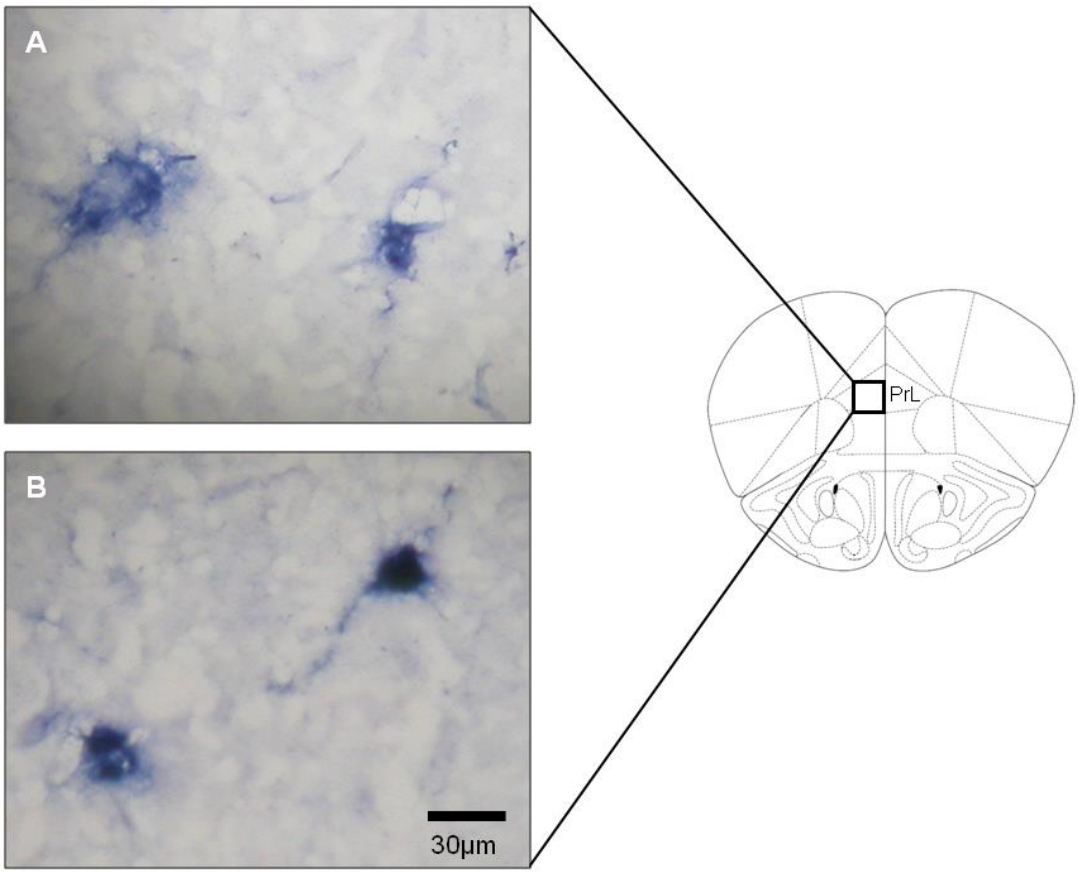

Figure 4.2. NADPH-diaphorase stained of neurones in the prefrontal cortex of the mouse. Illustrative photomicrographs of neurones stained using NADPH-diaphorase histochemistry in the prelimbic (PrL) region of the prefrontal cortex of mice. Neurones were generally less intensely stained in vehicle-treated mice (**A**) than those in PCP-treated mice (**B**). Lens aperture was altered during image acquisition for optimal photograph quality. Scale bar applies to both images. Diagram of coronal cross-section of mouse brain adapted from: (Paxinos and Franklin, 2001).

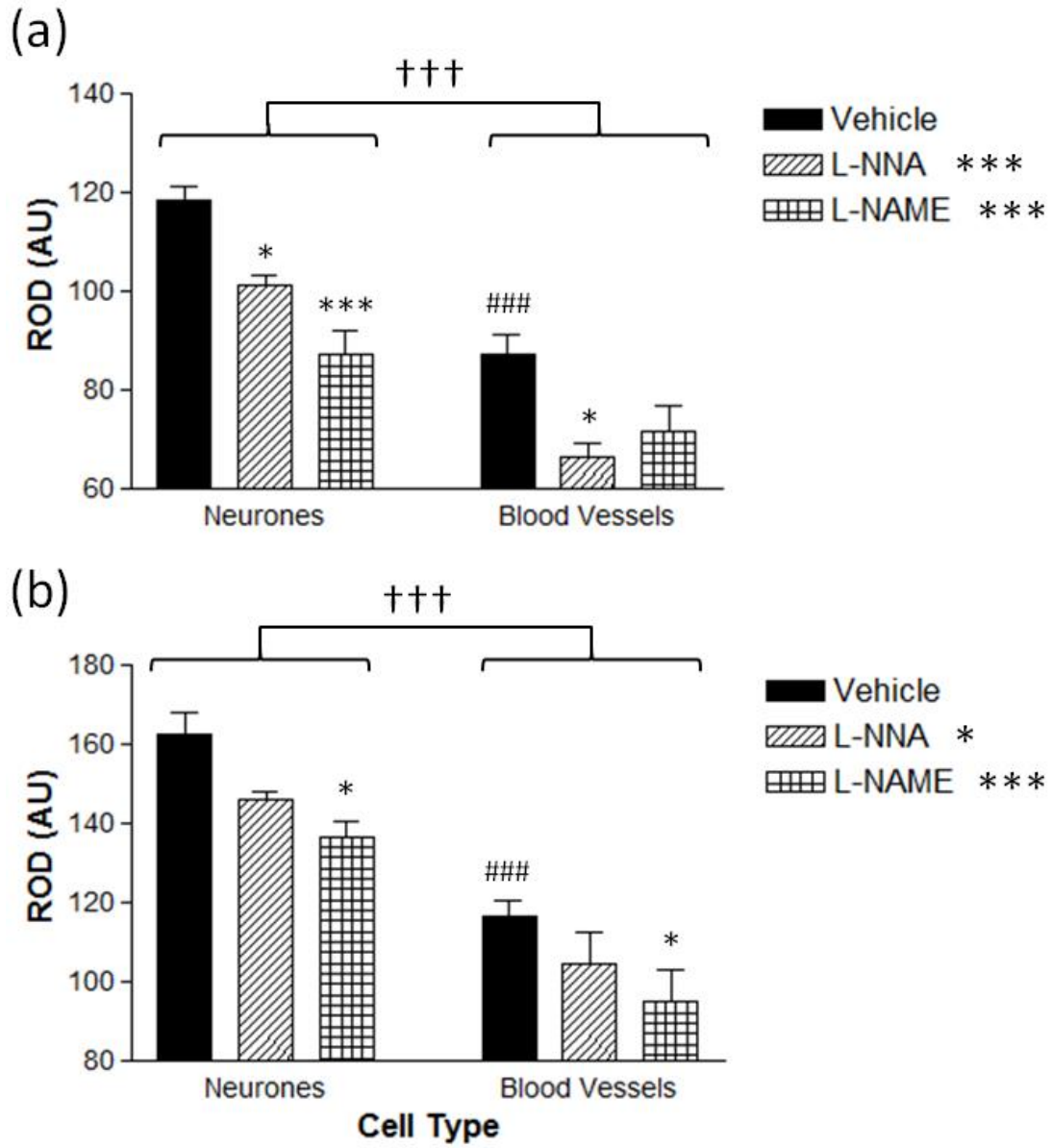

Figure 4.3. NADPH-diaphorase activity is attenuated by NOS inhibitors in the rat striatum. Replicate sections of rat striatum were incubated with 100 µM L-NNA, 1 mM L-NAME, or vehicle (**a**) before or (**b**) after fixation. NADPH-diaphorase staining intensity was significantly diminished in blood vessels compared to neurones in both conditions (both, $p < .001$), including the vehicle treated groups (both, $p < .001$). (**a**) There was an overall significant decrease in staining in both cell types (i.e. neurones and blood vessels) with L-NNA ($p = .0006$) and with L-NAME ($p = .0001$). Staining in blood vessels with L-NAME trended towards a significant decrease (71.4 ± 5.4 ROD units, $p = .068$, n = 3), and was significantly decreased with L-NNA (66.1 ± 2.9 ROD units, $p = .01$, n = 3), compared to vehicle treatment (87.1 ± 3.8 ROD units, n = 3). Inhibition by L-NAME was highly significant (86.9 ± 5.1 ROD units, $p = .0007$, n = 3) and by L-NNA (101.1 ± 2.2 ROD units, $p = .04$, n = 3) compared to vehicle treatment (118.5 ± 2.7 ROD units, n = 3), in neurones. The intensity of staining was highly significantly lower in blood vessels ($p = .0007$) compared to neurones with vehicle treatment, and staining was significantly lower ($p < .001$) in blood

vessels compared to neurones across all treatment groups. (**b**) In sections incubated with NOS inhibitors following fixation, staining across all treatments was significantly decreased in blood vessels compared to neurones ($p < .001$), and was highly, and significantly lower in vehicle-treated blood vessels (116.2 ± 4.1 ROD units, $p = .0002$, n = 3) than in vehicle-treated neurones (162.1 ± 5.9 ROD units, n = 3). There was an overall significant decrease in staining in both objects with L-NNA ($p = .02$) and with L-NAME ($p < .001$). L-NNA treatment did not significantly decrease staining in blood vessels (104.3 ± 8.1 ROD units, n = 3) and neurones (145.6 ± 2.0 ROD units, n = 3), but L-NAME treatment significantly decreased staining in blood vessels (94.6 ± 8.2 ROD units, $p = .04$, n = 3) and in neurones (136.5 ± 3.9 ROD units, $p = .01$, n = 3). Data are presented as mean % of vehicle ± SEM, and were analysed by repeated measures ANOVAs with Tukey's multiple comparisons. †††, $p < .001$; *, $p < .05$; ***, $p < .001$; compared to vehicle treatment in that cell type; ###, $p < .001$ compared to vehicle treatment in neurones.

Figure 4.4i illustrates the influence that acute PCP had on NADPH-diaphorase staining in different brain regions. A significant decrease in staining intensity was observed in the reticular thalamus (p = .036), but not in the other regions analysed. These data are summarised in **Table 4.1**. Blood vessel ROD was measured in each field of view (where present) in vehicle- and PCP- treated mouse brains. **Figure 4.4ii** shows how NADPH-diaphorase staining of blood vessels in brain regions of the mouse brain is highly variable between PCP and vehicle treatment groups. The ROD of vessels was unchanged in PCP-treated mice compared to vehicle-treated mice, as determined by Mann-Whitney tests. These data are summarised in **Table 4.2**. No NADPH-diaphorase staining was present in replicate sections when NADPH was omitted from reactions (data not shown).

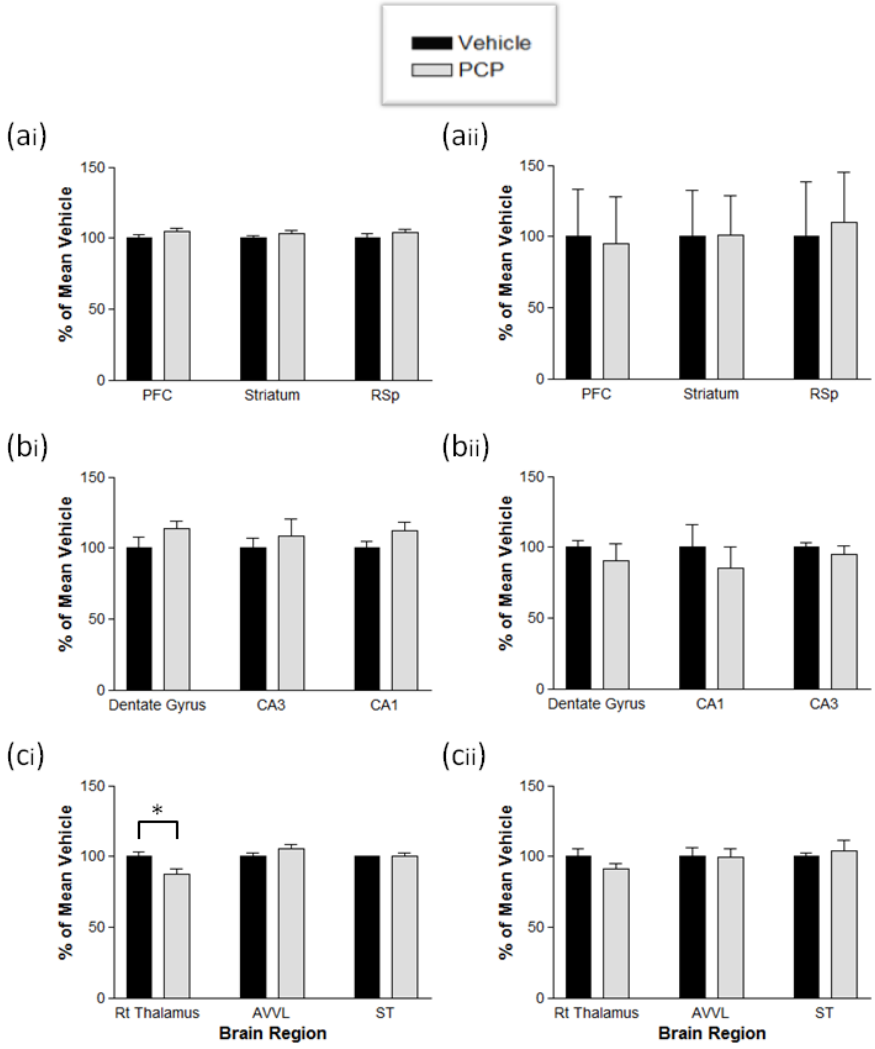

Figure 4.4. Altered NADPH-diaphorase activity discreet brain regions of mice administered acute PCP. NADPH-diaporase activity was determined in cells (**a-c$_{i}$**) and blood vessels (**a-c$_{ii}$**) in histochemical brain sections of mice treated with 5 mg.kg-1 PCP (n = 6) or saline vehicle (n = 5 for hippocampus, n = 6 for all other regions). (**a$_{i}$**) A significant overall effect of PCP on NADPH-diaphorase ROD was detected across the PFC, striatum and retrosplenial cortex (repeated measures ANOVA; $F_{(1,10)} = 10.7$, $p = .004$). Post hoc multiple comparisons revealed no significant differences between drug groups between these brain regions. (**b$_{i}$**) A trend towards a significant effect of PCP treatment in hippocampal regions ($F_{(1,9)} = 3.94$, $p = .063$) was revealed by repeated measures ANOVA, when compared to the vehicle group. (**c$_{i}$**) A significant interaction between the thalamic regions and drug treatment ($F_{(2,10)} = 5.8$, $p = .01$) was revealed by analysis via repeated measures ANOVA. Analysis of thalamic regions individually revealed a significant decrease (two-sample t-test; 87.2 ± 3.8% of mean vehicle group, $p = .036$) in cellular ROD in the reticular thalami (Rt) of PCP-treated mice when compared to the vehicle group. (**$_{ii}$**) Blood vessel NADPH-diaphorase staining was unchanged with PCP treatment. Data are presented as percent of mean vehicle ± SEM, and were analysed by repeated measures ANOVA with Tukey's multiple comparisons and two-way t-tests. *, $p < .05$ (t-test). Abbreviations: prefrontal cortex (PFC), retrosplenial cortex (RSp), anteroventeral, venterolateral (AVVL) thalamus, stria terminalis (ST).

Table 4.1. NADPH-diaphorase activity in neurones of brain regions of acute PCP treated mice.

		Vehicle			PCP				Tukey	t-test
Brain Region		**ROD**	**SEM**	***n***	**ROD**	**SEM**	***n***	**% Change**	***p* value**	***p* value**
	PFC	148.7	2.2	6	155.4	2.7	6	6.7	.305	.083
	Striatum	143.9	0.9	6	149.8	3.0	6	5.9	.436	.120
	RSp	142.5	3.5	6	147.6	3.3	6	5.1	.588	.317
Hippocampus	**DG**	85.4	6.9	5	96.9	5.0	6	11.5	.782	.220
	CA1	94.7	4.2	5	106.2	5.7	6	11.5	.783	.147
	CA3	91.1	6.6	5	98.6	11.0	6	7.5	.955	.591
Thalamus	**Rt**	84.9	3.0	6	74.0	3.2	6	-10.9	.064	**.036**
	AVVL	125.2	3.3	6	132.3	3.2	6	7.1	.996	.155
	Stria Terminalis	185.5	0.6	6	186.1	4.5	6	0.6	.630	.894

Summary of mean relative optical density (ROD) measurements of neurones in brain regions of mice administered acute PCP (5 $mg.kg^{-1}$) or saline vehicle. Regional differences between PCP and vehicle groups were analysed together by repeated measures ANOVA with Tukey's multiple comparisons and individually by two-way t-tests; the resultant *p* values are stated. Significance is accepted when $p < .05$. Abbreviations: PFC, prefrontal cortex; RSp, retrosplenial cortex; DG, dentate gyrus; CAx, cornu ammonis; Rt, reticular thalamus; AVVL, anteroventral-venterolateral thalamus.

Table 4.2. NADPH-diaphorase activity in blood vessels of brain regions of acute PCP treated mice.

		Vehicle			PCP				Tukey	t-test
Brain Region		**ROD**	**SEM**	***n***	**ROD**	**SEM**	***n***	**% Change**	***p* value**	***p* value**
	PFC	72.5	2.5	6	67.7	2.3	6	-4.8	.931	.191
	Striatum	67.7	4.1	6	68.9	4.7	6	1.2	.999	.860
	RSp	61.0	5.4	6	68.5	5.6	6	7.5	.694	.361
Hippocampus	**DG**	57.9	2.6	4	50.0	6.2	6	-7.9	.773	.289
	CA1	60.9	12.0	4	59.0	8.8	6	-1.9	.989	.907
	CA3	46.4	1.4	5	44.1	2.7	6	-2.3	.998	.472
Thalamus	**Rt**	62.4	3.6	6	56.8	2.5	6	-5.6	.827	.243
	AVVL	68.0	4.3	6	67.5	4.5	6	-0.5	.999	.934
	Stria Terminalis	45.0	1.2	6	46.7	3.5	6	1.7	.999	.656

Summary of mean relative optical density (ROD) measurements of blood vessels in brain regions of mice administered acute PCP (5 $mg.kg^{-1}$) or saline vehicle. Regional differences between PCP and vehicle groups were analysed together by repeated measures ANOVA with Tukey's multiple comparisons and individually by two-way t-tests; the resultant *p* values are stated. Significance is accepted when $p < .05$. Abbreviations: PFC, prefrontal cortex; RSp, retrosplenial cortex; DG, dentate gyrus; CAx, cornu ammonis; Rt, reticular thalamus; AVVL, anteroventral-venterolateral thalamus.

4.4.2 NADPH-diaphorase activity in brain region homogenates

Extracts of fixed brain region homogenates produced a steady rate of formazan product in the presence of XTT over the course of an hour. Reactions without tissue present (Buffer only) were taken as non-specific activity and these values were subtracted from sample rates to give specific activities. No NADPH-diaphorase activity was observed in reactions where NADPH cofactor was omitted (data not shown). **Figure 4.5** shows how acute PCP treatment did not affect NADPH-diaphorase activities in. There was a trend towards an significant effect of PCP treatment ($F_{(1,10)} = 3.8$, $p = .063$) overall in the brain, as analysed by repeated measures ANOVA, but *post hoc* tests using Tukey's multiple comparisons detected no significant differences between drug groups in brain regions. Analysis of brain regions individually using two-sample t-tests revealed a significant increase ($p = .01$) in NADPH-diaphorase activity in the hippocampi of PCP-treated mice compared to the vehicle group.

NADPH-diaphorase activity was determined in brain regions of mice following subchronic administrations of PCP or saline vehicle. Mice were administered twice daily injections of saline vehicle (Veh/Veh, n = 6), 5 $mg.kg^{-1}$ PCP (PCP/PCP, n = 6), or PCP (morning) and vehicle (evening; PCP/Veh, n = 6), for 5 days. The rate of NADPH-diaphorase activity was significantly influenced by an overall effect of drug treatments ($F_{2,15} = 3.7$, $p = .03$), and was significantly different between regions ($F_{4,15} = 5.7$, $p = .001$), as analysed by repeated measures ANOVA. No significant differences were detected between drug groups per brain region in *post hoc* analyses by Tukey's multiple comparisons. Analysis of brain regions individually using one-way ANOVAs revealed a significant overall effect of drug treatment in the PFC ($F_{(2,17)} = 4.8$, $p = .02$). **Figure 4.6** shows a decrease in NADPH-

diaphorase activity was observed in the prefrontal cortex (PFC) that was significant in mice treated with PCP/PCP (p = .03), and trended towards significance in the PCP/Veh group (p = .067), compared to Veh/Veh, as determined by Tukey's multiple comparisons tests. These data are summarised in **Table 4.3**.

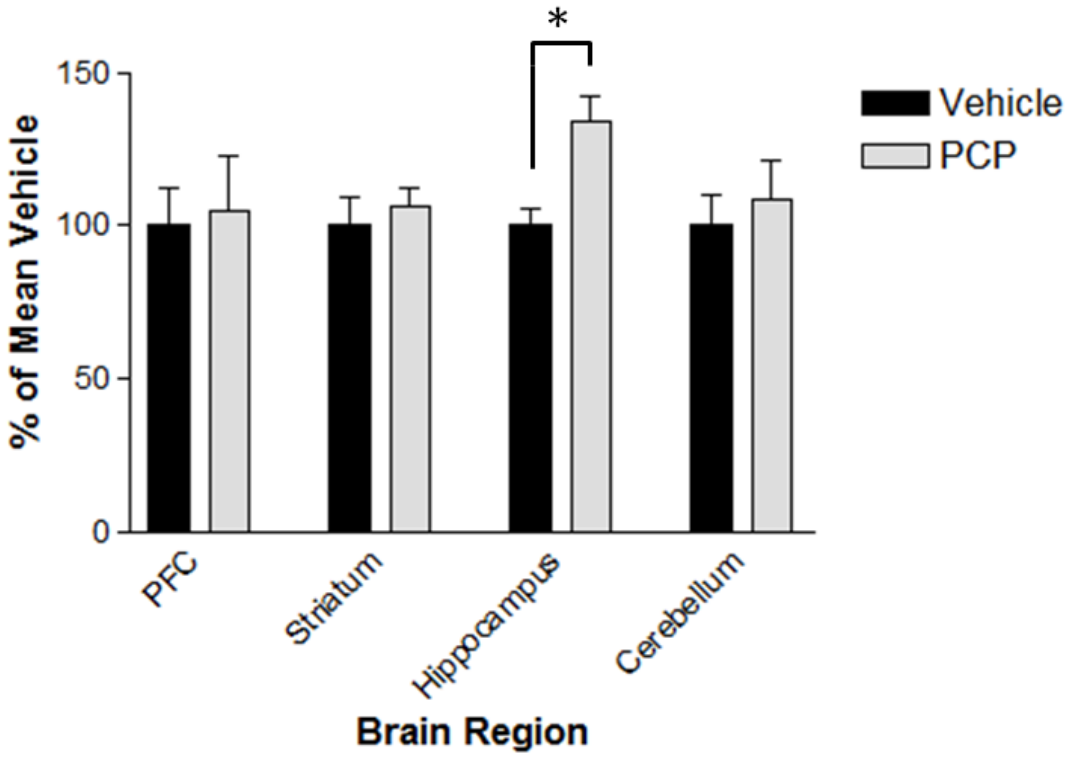

Figure 4.5. Increased NADPH-diaphorase activity in Brain Region Homogenates of acute PCP-treated Mice. A significant increase in NADPH-diaphorase specific activity (OD_{450} / min) was observed in the homogenates of the hippocampi (133.9 ± 8.5% of vehicle group, $p = 0.01$) of mice acutely treated with PCP (5 $mg.kg^{-1}$) compared to vehicle-treated mice. No change was detected with PCP treatment in the prefrontal cortex (PFC; 104.7 ± 17.8%, n.s., n = 6), striatum (106.3 ± 6.1%, n.s., n = 6), or cerebellum (108.2 ± 12.9%, n.s., n = 6) compared with vehicle treatment. No NADPH-diaphorase activity was observed when NADPH cofactor was omitted (data not shown). All groups are n = 6, except the vehicle treated PFC group which is n = 5. Data are presented as % of mean vehicle ± SEM. *, $p < .05$ (two-sample t-test).

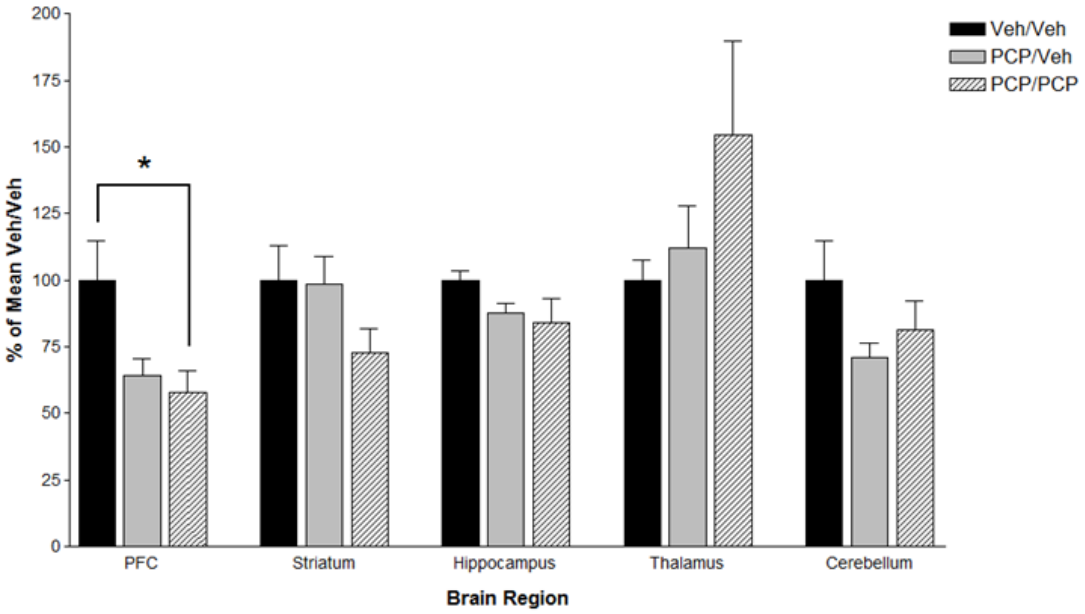

Figure 4.6. NADPH-diaphorase activity in brain region homogenates following subchronic PCP administration in mice. Mice were administered twice daily injections of saline vehicle (Veh/Veh), 5 mg.kg^{-1} PCP (PCP/PCP), or single doses of PCP (morning) and vehicle (evening; PCP/Veh), for 5 days. A significant decrease in NADPH-diaphorase activity was observed in the prefrontal cortex (PFC) of mice treated with PCP/PCP (p = .03) compared to Veh/Veh. Activity was increased in the thalami of mice treated with PCP/PCP, but did not meet significance (154.6 ± 35.3% of Veh/Veh). Data are presented as percent (± SEM) of mean Veh/Veh response per region. Data were analysed per region using one-way ANOVA with Tukey's multiple comparisons tests; *, $p < .05$ (Tukey test).

Table 4.3. NADPH-diaphorase activity following subchronic PCP administrations.

	Veh/Veh			PCP/Veh			Tukey	PCP/PCP			Tukey
	Mean %	**SEM**	***n***	**Mean %**	**SEM**	***n***	***p* value**	**Mean %**	**SEM**	***n***	***p* value**
PFC	100	14.6	6	64.2	6.4	6	.067	57.8	8.2	6	**.029**
Striatum	100	12.7	6	98.6	10.4	6	.995	72.6	9.2	6	.210
Hippocampus	100	3.3	6	87.5	3.9	6	.325	84.0	8.9	6	.170
Thalamus	100	7.7	6	111.9	15.9	6	.988	154.6	35.3	6	.632
Cerebellum	100	15.0	6	71.1	5.4	6	.192	81.2	10.9	6	.476

Data are expressed as percent of mean Veh/Veh NADPH-diaphorase activity ± SEM, and were analysed by region using one-way ANOVA tests with Tukey's multiple comparisons. The comparisons shown are from these *post hoc* tests versus the Veh/Veh group per region. Abbreviation: PFC, prefrontal cortex

4.5 Tissue nitrite concentrations

Nitrite concentrations were determined in brain regions of mice administered acute 5 mg.kg^{-1} PCP (n = 15) or saline vehicle (n = 14). There was a highly significant difference in nitrite content between brain regions ($F_{(4,25)}$ = 33.8, p < .001), but no significant influence of drug treatment (p > .05), as illustrated by **Figure 4.7**. No significant differences were detected between drug treatments per brain region in *post hoc* tests using Tukey's multiple comparisons. Analysis of brain regions individually by two-sample t-tests also revealed no significant differences between drug groups, however an increase in hippocampal nitrite in the PCP group approached significance (p = .077) when compared to the vehicle group. Nitrite concentrations were not determined in brain regions of mice with subchronic PCP administration, as the assay appears insensitive to detect changes in NOS activity compared to NADPH-diaphorase activity in tissue homogenates that was used in section 4.4.2.

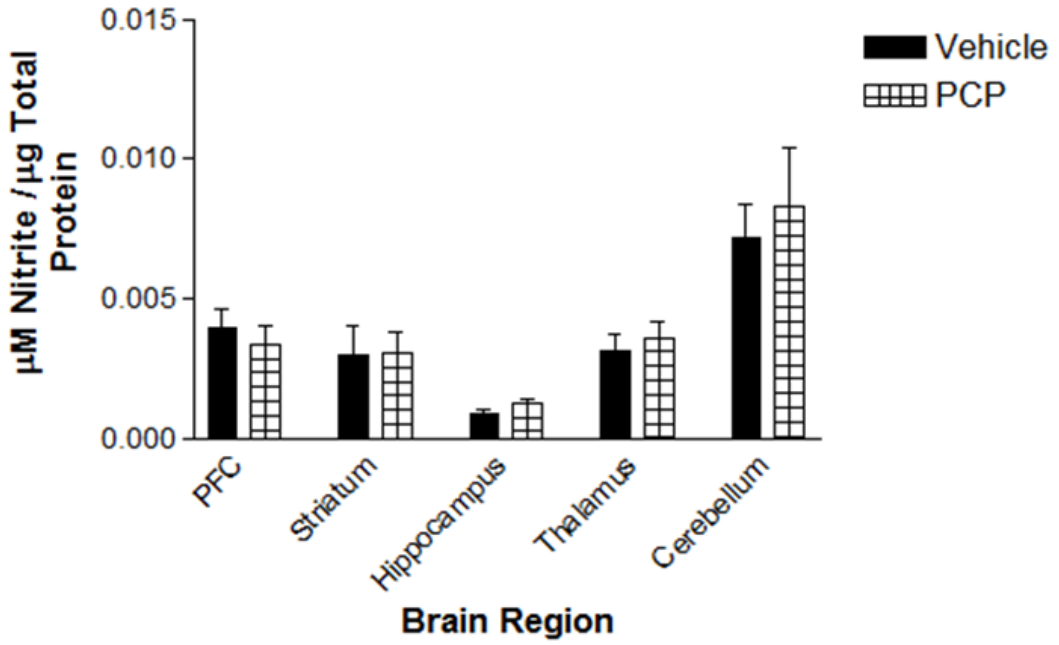

Figure 4.7. Acute PCP does not influence nitrite concentrations in mouse brain regions. The concentration of nitrite was determined in brain regions of mice administered saline vehicle (n = 14) or acute 5 mg.kg^{-1} PCP (n = 15). There was a trend towards a significant increase in hippocampal nitrite in the acute PCP group (1.27 ± 0.16 µM / mg total protein, p = .077) when compared to the vehicle group (0.91 ± 0.11 µM / mg total protein). Data are presented as mean ± SEM, and were analysed by repeated measures ANOVA with Tukey's multiple comparisons tests. Abbreviation: PFC, prefrontal cortex

4.6 Thioredoxin reductase and caspase activities

A significant overall effect of acute PCP treatment on the activity of TrxR was detected ($F_{(1,11)} = 4.8$, $p = .03$), as analysed by repeated measures ANOVA. No significant differences between drug groups were detected between brain regions using Tukey's multiple comparisons. **Figure 4.8** shows the significant decrease in thioredoxin reductase specific activity in homogenates of hippocampi ($p = .03$) and thalami ($p = .02$) of mice following acute PCP treatment, as analysed by two-sample t-tests.

TrxR activity was also assessed after subchronic PCP treatment. TrxR activity varied significantly according to brain region ($F_{(4,12)} = 10.9$, $p < .001$), when analysed by repeated measures ANOVA, but no effect of subchronic drug treatment was detected using Tukey's multiple comparisons, or by analysis of brain regions individually using two-sample t-tests. The largest change was observed in the PFC, with a 29% (70.7 ± 15.2% of mean vehicle group) decrease in TrxR activity with PCP/PCP treatment compared to Veh/Veh treatment. This change was not significantly different, perhaps due to the high variability in these groups, as illustrated by **Figure 4.9**.

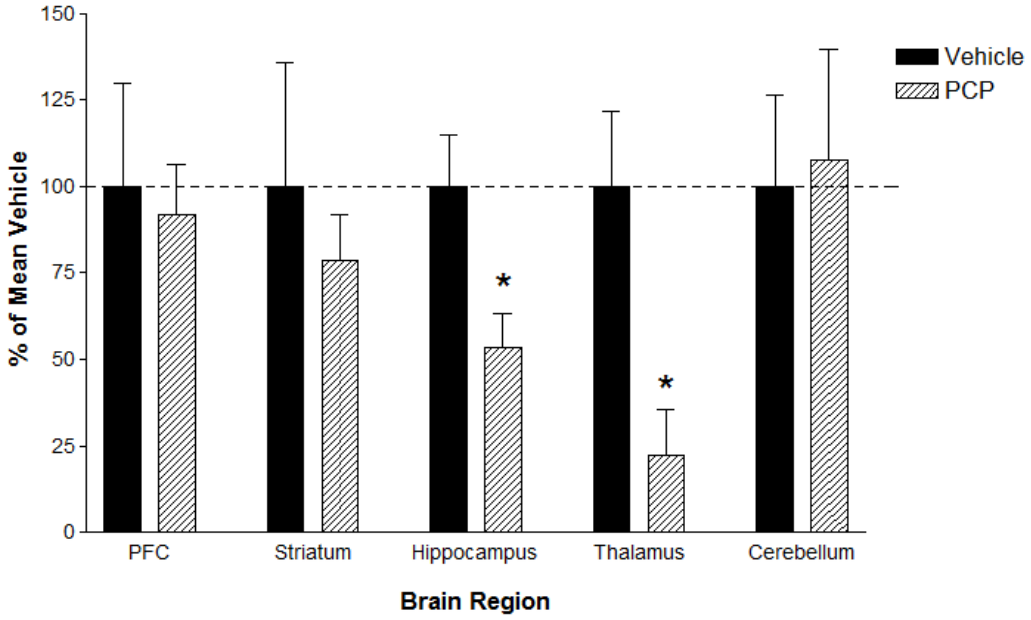

Figure 4.8. Thioredoxin reductase activity is decreased in hippocampi and thalami of mice treated with acute PCP. A significant decrease in thioredoxin reductase activity was observed in hippocampal (53.5 ± 9.7% of vehicle, p = .03) and thalamic (29.9 ± 12.0% of vehicle, p = .02) tissue homogenates in mice administered 5 mg.kg^{-1} PCP (n = 7) compared to vehicle treatment (n = 6). Data are presented as % of mean vehicle ± SEM, and were analysed using two-sample t-tests; *, p < .05 (t-test). Abbreviation: PFC, prefrontal cortex

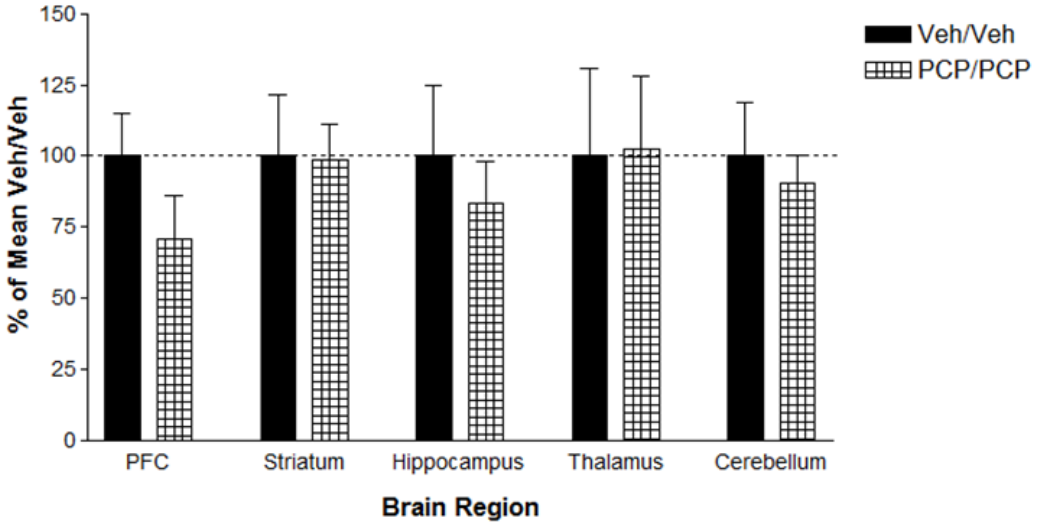

Figure 4.9. Thioredoxin reductase activity in brain regions of mice treated with subchronic PCP or vehicle. The activity of thioredoxin reductase was not significantly different in brain regions of mice following twice daily administrations of 5 $mg.kg^{-1}$ PCP (PCP/PCP; n = 8) or saline vehicle (Veh/Veh; n = 6) for 5 days. Data are presented as percent of mean Veh/Veh response, per brain region, and were analysed using two-sample t-tests. Abbreviation: PFC, prefrontal cortex

The activities of caspases 3, 8, and 9 were assessed in brain regions of mice with acute PCP treatment (n = 8) compared to vehicle treatment (n = 8). There was an overall significant influence of PCP treatment in brain regions on the activities of caspase 3 ($H_{(9)}$ = 47.4, p < .001), caspase 8 ($H_{(9)}$ = 51.9, p < .001), and caspase 9 ($H_{(9)}$ = 45.9, p < .001), as analysed by Kruskal-Wallis tests. No significant differences were detected between drug groups in brain regions using Dunn's multiple comparisons, or t-tests per region. **Figure 4.10a** shows the caspase 3 activities in brain regions between vehicle and PCP groups. AMC accumulation rates in each brain region samples were sensitive to the caspase 3 inhibitor, DMQD (20 μM). These were not compared statistically with experimental values due to insufficient data. Caspase activity data from mice administered acute vehicle and PCP are summarised in **Table 4.4**.

The activities of caspases 3, 8, and 9 were also assessed in brain regions of mice with subchronic PCP treatment (PCP/PCP, n = 7) compared to vehicle treatment (Veh/Veh, n = 6). **Figure 4.10b** shows how caspase 3 activities were significantly decreased ($t_{(6)}$ = 2.5, p = .048) in the hippocampi of the PCP/PCP group. Caspase 3 activities were unchanged between drug groups in the other regions sampled. There was a trend to overall significant effect of subchronic drug treatment ($F_{(1,12)}$ = 3.9, p = .056), and a highly significant influence of brain region ($F_{(4,12)}$ = 39.8, p < .001), as analysed by repeated measures ANOVA. There was no significant difference between AMC accumulation rates between samples with, and without the caspase 3 inhibitor, DMQD (20 μM) in the PFC, as determined by two-sample t-test. These data are summarised in **Table 4.5**.

Caspase 8 activity was influenced by an interaction of PCP treatment and brain region ($H_{(7)}$ = 25.8, p = .001), when analysed a Kruskal-Wallis test, but no significant difference between drug groups per brain region, as

determined by Dunn's multiple comparisons. There was a significant decrease (0.046 ± 0.006 µM AMC / min / mg total protein; $t_{(10)} = 3.6$, $p = .005$) in the activity of caspase 8 in the PFC of mice administered PCP/PCP compared to Veh/Veh treatment (0.071 ± 0.003 µM AMC / min / mg total protein). Caspase 8 activity in the cerebellum could not be detected in this experiment.

Caspase 9 activity varied significantly between brain regions ($F_{(3,12)} = 12.7$, $p < .001$). No differences between drug groups were detected in brain regions by Tukey's multiple comparisons or by individual brain region using two-sample t-tests. Caspase 9 activity in the hippocampus could not be detected in this experiment.

Table 4.4. Caspase activities in brain regions of mice administered acute PCP.

		Vehicle				PCP				t-test	Dunn's	DMQD	
		Median	Mean	SEM	*n*	Median	Mean	SEM	*n*	*p* value	*p* value	Average	*n*
Caspase 3	PFC	2.2	2.3	0.6	8	3.1	3.2	0.3	8	.204	.228	1.2	2
	Striatum	1.3	1.4	0.3	8	1.3	1.6	0.3	8	.669	.731	0.2	2
	Hippocampus	4.7	4.7	0.5	8	4.1	3.6	1.8	8	.211	.344	1.7	2
	Thalamus	2.0	2.2	0.3	8	2.2	2.8	0.7	8	.316	.355	2.6	2
	Cerebellum	0.4	0.4	0.1	8	0.3	0.5	0.4	8	.544	.699	0.5	2
Caspase 8	PFC	7.3	7.7	1.1	8	9.0	8.9	0.6	8	.321	.307		
	Striatum	5.5	6.6	1.2	8	5.6	5.5	0.9	8	.502	.707		
	Hippocampus	8.6	8.0	0.6	8	7.3	6.7	1.0	8	.379	.414		
	Thalamus	4.6	4.3	0.6	8	4.4	4.3	0.7	8	.982	.906		
	Cerebellum	0.7	0.7	0.3	8	0.7	0.8	0.2	8	.620	.940		
Caspase 9	PFC	1.2	1.3	2.6	8	1.7	1.6	0.4	8	.300	.606		
	Striatum	2.8	2.8	5.0	8	2.2	2.1	0.3	8	.289	.471		
	Hippocampus	2.7	2.6	0.3	8	2.6	2.2	1.0	8	.336	.540		
	Thalamus	1.1	1.4	0.2	8	4.3	1.5	0.3	8	.750	.805		
	Cerebellum	0.1	0.1	0	8	0.1	0.2	0.1	8	.737	.974		

The activities of caspases 3, 8, and 9 were determined in brain region homogenates of mice treated with acute vehicle or 5 $mg.kg^{-1}$ PCP. Data are presented as the median and mean of the rate of accumulation of cleaved product (nM AMC / min / mg Total Protein) from caspase selective substrates. Data were analysed using t-tests, and Kruskal-Wallis tests with Dunn's multiple comparisons. Sample replicate reactions were done in the presence of the caspase 3-selective inhibitor, DMQD.

Table 4.5 Caspase activities in brain regions of mice administered subchronic PCP.

		Veh/Veh				PCP/PCP				Tukey	t-test	Dunn's	DMQD		
		Median	**Mean**	**SEM**	***n***	**Median**	**Mean**	**SEM**	***n***	***p* value**	***p* value**	***p* value**	**Average**	**SEM**	***n***
Caspase 3	**PFC**	0.066	0.105	0.037	5	0.054	0.057	0.010	7	.935	.421		0.074	0.060	3
	Striatum	0.386	0.398	0.038	6	0.370	0.350	0.018	8	.999	.289		0.372		2
	Hippocampus	0.095	0.097	0.021	6	0.057	0.042	0.007	7	.177	**.048**		0.000		2
	Thalamus	0.153	0.200	0.057	6	0.117	0.159	0.027	8	.999	.890		0.104		2
	Cerebellum	0.106	0.101	0.015	6	0.130	0.125	0.014	8	.991	.263		0.053		2
Caspase 8	**PFC**	0.069	0.071	0.003	6	0.044	0.045	0.006	8		**.005**	.118			
	Striatum	0.059	0.062	0.010	6	0.067	0.061	0.006	8		.932	.904			
	Hippocampus	0.345	0.393	0.123	6	0.094	0.224	0.079	8		.174	.264			
	Thalamus	0.384	0.423	0.152	6	0.205	0.180	0.037	7		.386	.482			
	Cerebellum	**ND**				**ND**									
Caspase 9	**PFC**	0.023	0.045	0.023	5	0.023	0.024	0.002	4	.986	.972				
	Striatum	0.063	0.069	0.007	6	0.078	0.072	0.005	8	.999	.695				
	Hippocampus	**ND**				**ND**									
	Thalamus	0.043	0.047	0.016	6	0.037	0.047	0.009	8	.999	.789				
	Cerebellum	0.007	0.010	0.002	5	0.009	0.011	0.002	7	.999	.821				

The activities of caspases 3, 8, and 9 were determined in brain region homogenates of mice with twice daily administrations of vehicle (Veh/Veh) or 5 $mg.kg^{-1}$ PCP (PCP/PCP) for 5 days. Data are presented as the median and mean of the rate of accumulation of cleaved product (µM AMC / min / mg Total Protein) from caspase selective substrates. The activities of caspase 8 in the cerebellum, and caspase 9 in the hippocampus could not be detected (**ND**). Data were analysed using repeated measures ANOVA with Tukey's multiple comparisons, t-tests, and Kruskal-Wallis tests with Dunn's multiple comparisons, as appropriate. Sample replicate reactions were done in the presence of the caspase 3-selective inhibitor, DMQD.

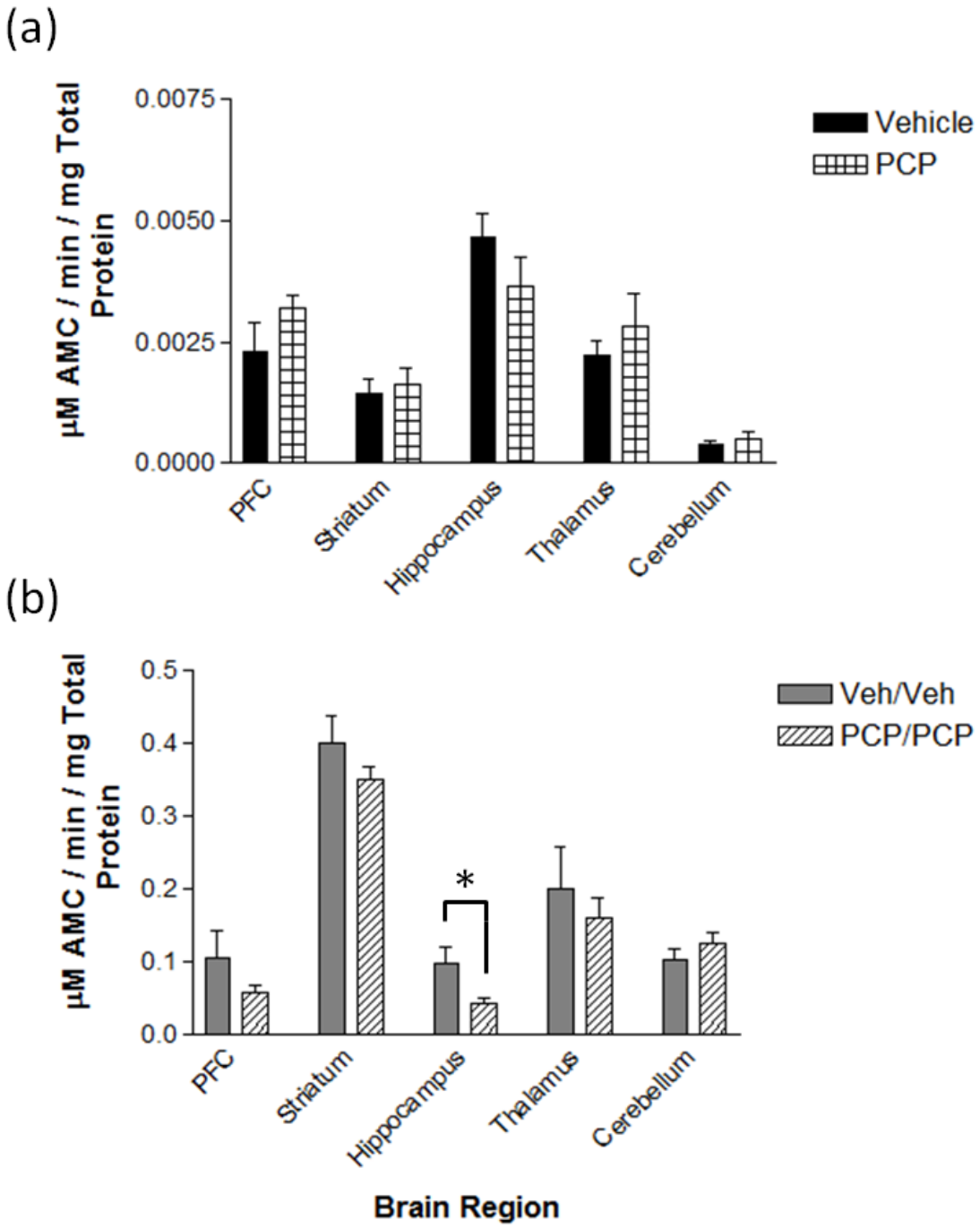

Figure 4.10. Caspase 3 activity is decreased in the hippocampus with subchronic PCP, but not acute PCP administration in mice. (**a**) The activities of caspase 3 were unchanged in brain regions of mice treated with acute 5 mg.kg^{-1} PCP (n = 8) or saline vehicle (n = 8). (**b**) A significant decrease (p = .048) in caspase 3 activity was detected in the hippocampi of mice following twice daily administrations of 5 mg.kg^{-1} PCP (PCP/PCP; n = 8), compared to those with saline vehicle (Veh/Veh; n = 6). Data were analysed by two-sample t-tests by brain region; *, p < .05 (t-test). Abbreviation: PFC, prefrontal cortex.

4.7 Locomotor activity and prepulse inhibition

4.7.1 Prepulse inhibition and startle reactivity with acute PCP

Prepulse inhibition (PPI) of acoustic startle was assessed in mice treated with 5 mg.kg^{-1} PCP or vehicle. **Figure 4.11a** illustrates how there was an overall decrease in PPI in mice administered PCP compared to the vehicle group. There was a clear prepulse-dependent increase in PPI as the prepulse intensity increased ($F_{(2,22)} = 19.9$, $p < .001$), and PPI overall was significantly decreased with PCP treatment ($F_{(1,22)} = 13.2$, $p < .001$), as analysed by repeated measures ANOVA. However, *post hoc* tests using Tukey's multiple comparisons did not detect significant differences between drug groups at any prepulse intensity.

The reactivity of mice to the startling stimulus was determined over the course of the PPI experiment. There was a habituation to the startling stimuli ($F_{(2,22)} = 16.1$, $p < .001$), but no influence of PCP treatment on startle reactivity, as determined by repeated measures ANOVA. Tukey's multiple comparisons revealed significant decreases in startle reactivity from the first stimulus to the second ($p = .003$) and third ($p < .001$) stimuli, but not between the latter two, as illustrated by **Figure 4.11b**.

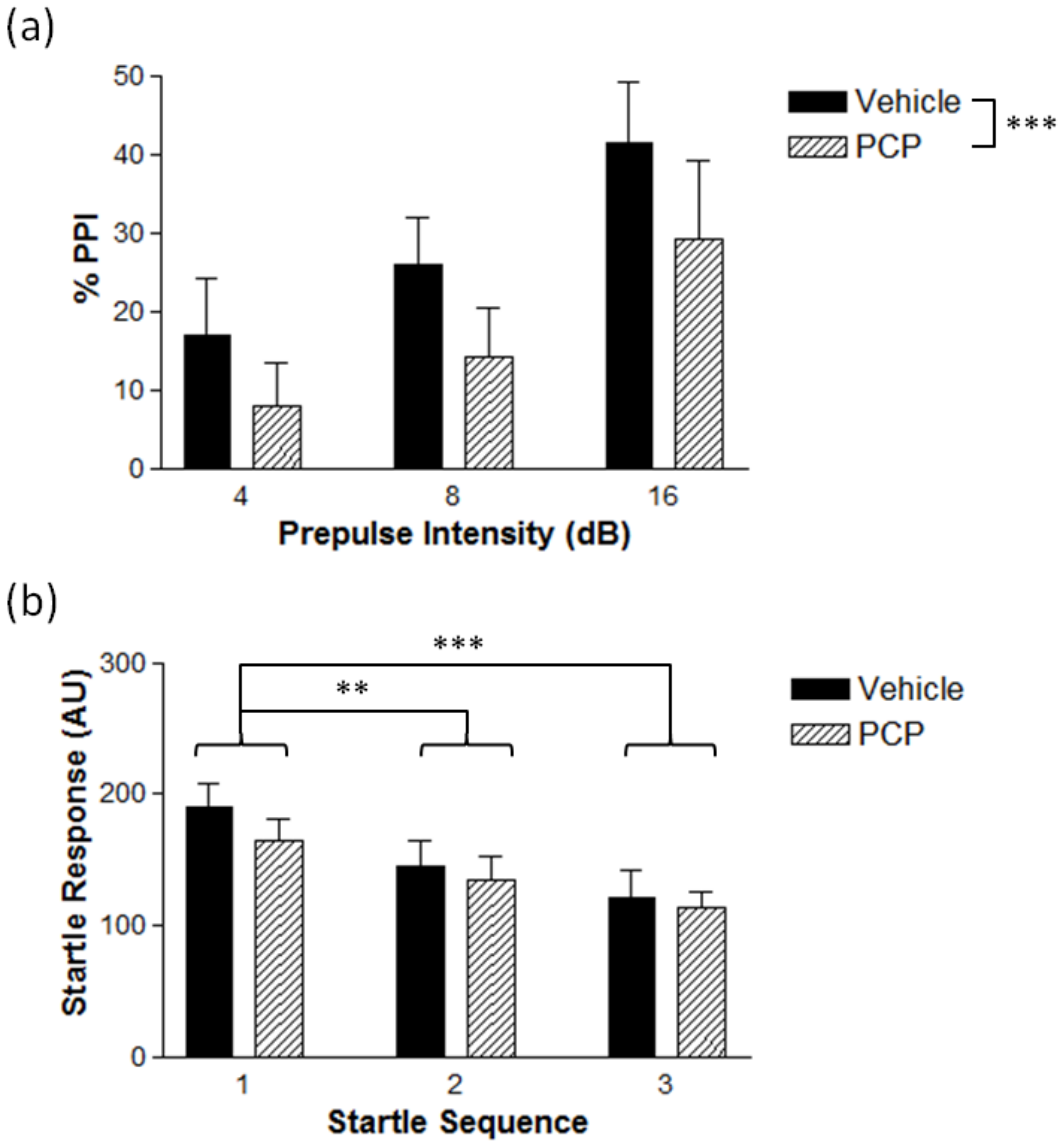

Figure 4.11. Prepulse inhibition and startle reactivity in mice administered acute PCP. Percent change in prepulse inhibition (PPI) of acoustic startle response of mice treated with 5 mg.kg^{-1} PCP (n = 12) or saline vehicle (n = 12). (**a**) A decreased PPI was present in mice treated with PCP ($F_{1,22}$ = 13.2, p < .001). (**b**) The startle response of mice decreased significantly from initial startle responses with subsequent presentations of 120 dB stimuli (2nd startle, p = .003; 3rd startle, p < 0.001 compared to 1st startle responses). **, p < .01; ***, p < .001 (ANOVA)

4.7.2 Prepulse inhibition and startle reactivity with subchronic PCP

Mice were administered twice daily injections of 5 $mg.kg^{-1}$ PCP or saline for 5 days. PPI was determined 72 hours following final drug administration. As was observed with acute drug treatment, PPI increased with increasing prepulse intensity ($F_{(2,12)} = 47.4$, $p < .001$), as determined by repeated measures ANOVA, and this was the case with multiple comparisons of the prepulse intensiisites individually (4 and 8, 4 and 16, 8 and 16 dB; $p < .001$) using *post hoc* Tukey's tests. No differences in PPI between drug groups at each prepulse intensity were detected, as illustrated by **Figure 4.12a**.

The startle reactivity of mice was determined over the course of the PPI experiment. There was an overall habituation to startle stimuli sequence ($F_{(2,12)} = 5.8$, $p = .009$), and startle reactivity was decreased overall with PCP treatment ($F_{(1,12)} = 11.6$, $p = .002$), as determined by repeated measures ANOVA. **Figure 4.12b** shows how startle reactivity was significantly decreased ($p = .007$) in both groups between the first and third presentation of the startle stimulus, as revealed by Tukey's multiple comparisons.

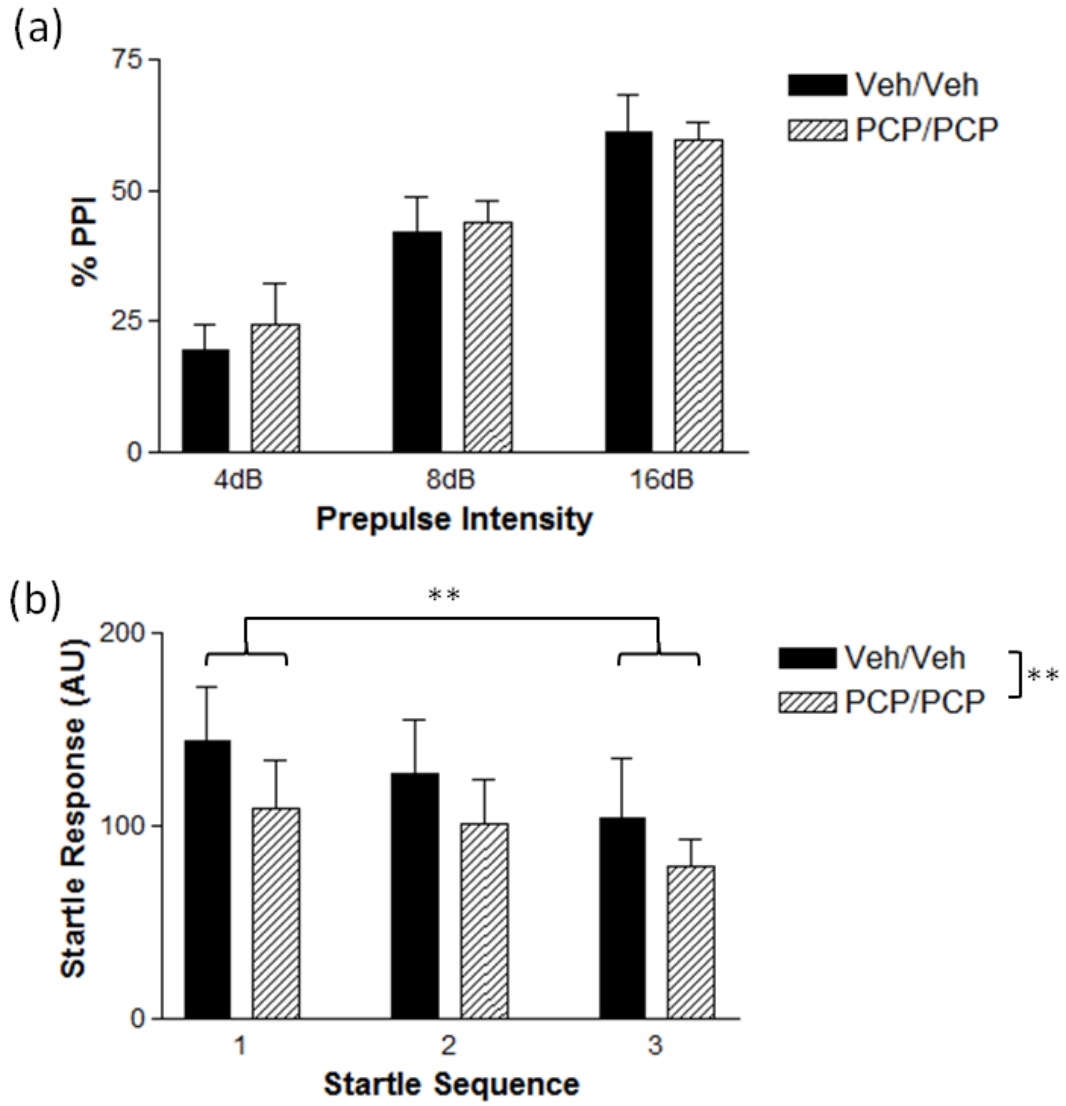

Figure 4.12. PPI deficits do not persist in mice with subchronic PCP administration. Prepulse inhibition (PPI) of acoustic startle response was determined in mice 72 hours following twice daily administrations of 5 mg.kg^{-1} PCP (PCP/PCP; n = 8) or saline vehicle (Veh/Veh; n = 6) for 5 days. (**a**) The percent decrease in startle response when presented with an antecedent less intense prepulse (4, 8, and 16 dB) as a function of startle response to 120 dB stimulus alone. (**b**) The startle response was significantly decreased in mice administered PCP/PCP ($F_{1,12}$ = 11.6, p = .002) compared to mice administered Veh/Veh. There was also a significant decrease in startle response of both groups related to the startle sequence (1st *vs.* 3rd startle, p = .007). Data were analysed by repeated measures ANOVA with Tukey's multiple comparisons tests; **, p < .01 (ANOVA).

4.7.3 Locomotor activity

4.7.4 Locomotor activity with acute PCP

Locomotor activity (LMA) was assessed for 1 hour to habituate mice to the open field arena, and for 30 mins following administration of 5 mg.kg^{-1} PCP (n = 8) or saline vehicle (n = 8). The mean distance travelled by mice within 10 min time bins is shown in **Figure 4.13a**. The velocity of mice was tested to establish whether PCP influences the distance travelled in the open field arenas. LMA significantly increased overall with PCP treatment ($F_{(1,14)}$ = 320.2, p < .001), and this varied significantly between drug groups, before and following drug administration ($F_{(1,14)}$ = 274.5, p < .001), as tested by repeated measures ANOVA. The velocity of mice was not significantly different between the vehicle group (5.0 ± 0.2 cm/s) and PCP group (5.3 ± 0.4 cm/s) during the habituation trial. There was a highly significant (p < .001) increase in velocity of mice following PCP administration (8.7 ± 0.8 cm/s) when compared to the vehicle group (3.0 ± 0.2 cm/s), as revealed by Tukey's multiple comparisons. These changes before and after drug administration were highly significant (p < .001 for both comparisons) in both PCP and vehicle groups.

The time spent in the inner half of the arena floor by mice was tested to determine if PCP influences anxiety-like behaviour. There were no significant differences in the percent time spent in the inner arena during habituation in vehicle- (15.9 ± 1.9 %) or PCP- (13.4 ± 1.7 %) treated mice, as shown in **Figure 4.13b**. No significant differences in time spent in the inner arena were detected following drug administration between vehicle (14.7 ± 4.4 %) or PCP (16.7 ± 2.2 %) groups. Data were analysed by repeated measures ANVOA with Tukey's multiple comparisons.

The average number of rotations made by mice was quantified to test whether the differences in LMA were due to circling behaviour in the PCP group. Rotational behaviour significantly increased in the PCP treated group ($F_{(1,14)} = 87.9$, $p < .001$), as tested by repeated measures ANOVA. *Post hoc* tests by Tukey's multiple comparison revealed that the mean number of rotations made by mice was not significantly different between the vehicle group (13.5 ± 1.0 rotations) and PCP group (14.0 ± 1.8) during the habituation trial. However, **Figure 4.13c** shows the highly significant ($p < .001$) increase in rotations of mice following PCP administration (42.8 ± 4.5 rotations) when compared to the vehicle group (5.9 ± 0.5 rotations). These changes before and after drug administration were highly significant ($p < .001$ for both comparisons) in both PCP and vehicle groups.

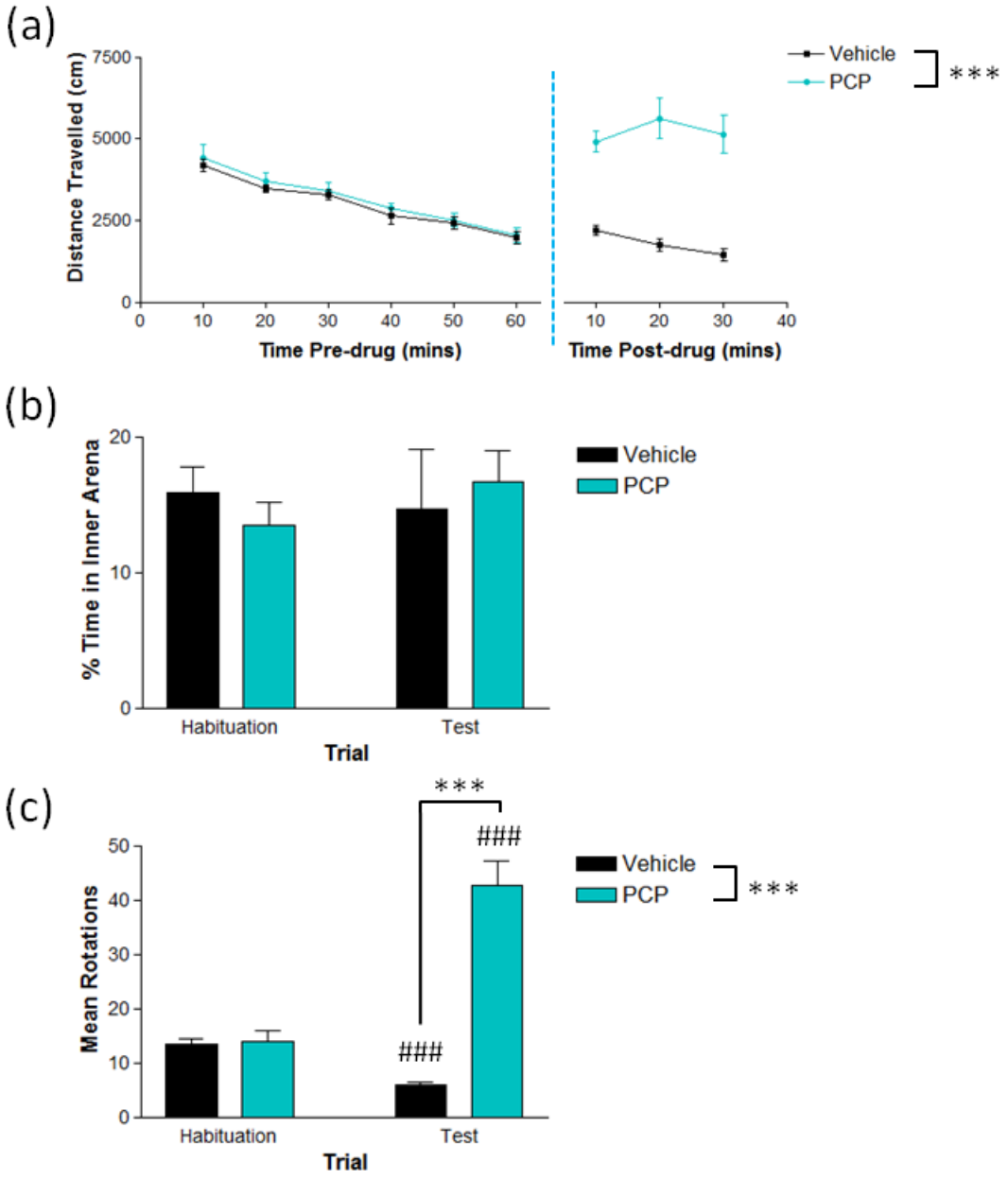

Figure 4.13. The influence of acute PCP administration on locomotor activity in mice. Locomotor activity was determined in mice for 60 mins habituation to the open field arena, and 30 mins following administration of saline vehicle (n = 6) or 5 mg.kg^{-1} PCP (n = 8). (**a**) There was a highly significant (p < .001) increase in the velocity of mice following drug administration in the PCP group when compared to the vehicle group. (**b**) No significant differences were detected between drug groups or between trials in the time spent in the inner 20 cm^2 of the open field arena. (**c**) A highly significant increase in the average rotations made by mice following PCP administration was detected when compared to the vehicle group (p < .001) and prior to drug administration (p < .001). There was a highly significant decrease in average rotations following vehicle administration (p < .001). Data were analysed by repeated measures ANOVA with Tukey's multiple comparisons tests; ***, p < .001; ###, p < .001 compared to the habituation trial in the same drug group.

4.7.5 Locomotor activity with subchronic PCP

Locomotor activity was assessed before, and immediately following the first injection of twice daily administrations of 5 $mg.kg^{-1}$ PCP (PCP/PCP) or saline vehicle (Veh/Veh) in mice for 5 days. Locomotor activity was also assessed 72 hours following the final injection (Day 8). Data were analysed as locomotor responses prior to drug administration, including Day 8 (off-drug), and following drug administration (on-drug).

Figure 4.14 shows the distance travelled of mice in the open field before and after daily doses of Veh/Veh or PCP/PCP. There was a significant overall variation in the mean velocity between drug groups per day prior to drug administration ($F_{(1,13)} = 5.9$, $p = .02$), and a highly significant overall variation of LMA over the course of the experiment (Days 1-8; $F_{(5,13)} = 23.0$, $p < .001$). There were significant decreases ($p < .001$, each day) in mouse velocity, before drug administration each day (off-drug), in the Veh/Veh group when comparing Day 1 with each subsequent day, except for 72 hours following final drug administration (Day 8; $p > .05$), as revealed by *post hoc* analyses using Tukey's multiple comparisons. A similar decline in velocity from the habituation response on the first day was observed in the PCP/PCP group (Day 1 – Day 2, $p = .001$; Day 1 – Day 2, 3, 4 or 5, $p < .001$; Day 1 – Day 8, $p = .01$). There were no significant differences between responses between Days 2 – 5 in either drug group, and no significant differences between drug groups per day, off-drug.

Following drug administration (on-drug), there was a highly significant overall increase in mouse velocity with PCP treatment ($F_{(1,13)} = 83.1$, $p < .001$), as analysed by repeated measures ANOVA. Tukey's multiple comparisons revealed that the responses to PCP/PCP were significantly increased to those from the Veh/Veh group each day but not on day 4 ($p =$

.002, < .001, = .007, = .129, = .008; Days 1- 5, sequentially). The responses of the PCP/PCP group and of the Veh/Veh group were not significantly different from each other by day. These data are summarised in **Error! Reference source not found.**.

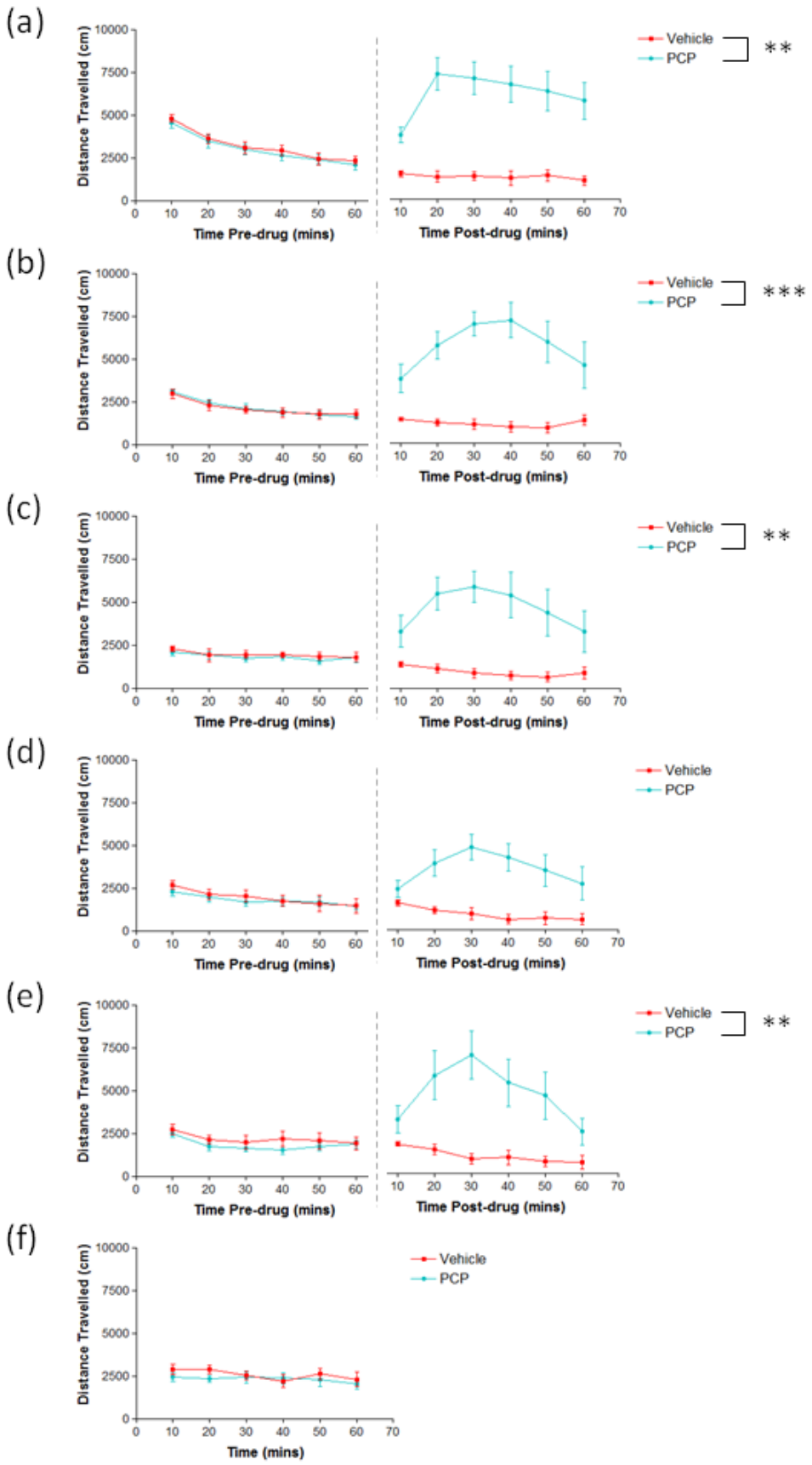
(a)
(b)
(c)
(d)
(e)
(f)
Distance Travelled (cm)
Time Pre-drug (mins)
Time Post-drug (mins)
Time (mins)
Vehicle
PCP
**
***
**
**

Figure 4.14. Mouse Locomotion During Repeated Administrations of PCP. The distance travelled by mice in open field arenas was assessed before (Pre-drug), and immediately following (Post-drug) the first injection of twice daily administrations of 5 $mg.kg^{-1}$ PCP (n = 8) or saline (n = 7) for 5 days (**a** – **e**, sequentially). (**f**) Locomotor activity was also assessed 72 hours following the final injection. The presented statistical comparisons are of mean velocity (cm/s) responses following drug administration (right side of graphs) as analysed by repeated measures ANOVA with Tukey's multiple comparisons tests; **, $p < .01$; ***, $p < .001$ (Tukey).

Figure 4.15a shows how the time spent in the inner 20 cm^2 of the open field arena by mice was influenced by subchronic administrations of Veh/Veh and PCP/PCP. Analysis by repeated measures ANOVA revealed that there was a significant overall effect of drug treatment ($F_{(1,13)} = 10.2$, $p = .002$) in the time spent in the inner arena when mice were assayed off-drug, and this behaviour was significantly variable over the course of the experiment ($F_{(5,13)} = 5.8$, $p < .001$). Conversely, there was no overall effect of drug treatment on this response when mice were on-drug. Though there was, again, a highly significant variability across the assay days ($F_{(5,13)} = 6.2$, $p < .001$). *Post hoc* analysis using Tukey's multiple comparisons revealed that time spent in the inner arena was significantly decreased ($p = .02$) 72 hours following final drug administration from responses before drug administration on day 1 in the PCP/PCP group, but not the Veh/Veh group. There was also a significant decrease ($p = .048$) in this response on the fifth day following PCP/PCP administration compared to the same condition on the first day.

The number of rotations made by mice while in the open field arena is summarised in **Figure 4.15b**. There was no overall effect of PCP treatment on this behaviour, off-drug, but a highly significant variability in rotational behaviours over the course of the experiment ($F_{(5,13)} = 23.7$, $p < .001$), as analysed by repeated measures ANOVA. Rotational behaviour was significantly diminished following the habituation trial (i.e. off-drug, day 1) in both Veh/Veh (day 1 – days 2, 3, 4, and 5, $p < .001$) and PCP/PCP (day1 – day 2, $p = .001$; day 1 – days 3, 4 and 5, $p < .001$) drug groups, as revealed using Tukey's multiple comparisons. Rotational behaviour was also significantly decreased ($p = .01$) 72 hours following final Veh/Veh injection from habituation (Day 1). This was not the case in the PCP/PCP group, and the number of rotations in this group were significantly increased ($p = .0495$) from their penultimate day of testing, off drug.

Conversely, there was a highly significant increase in overall rotational behaviour with drug treatment, on drug ($F_{(1,13)}$ = 173.1, p < .001), and no influence of the day assayed, as analysed by repeated measures ANOVA. Multiple comparisons using Tukey's *post hoc* tests revealed that rotational behaviour did not significantly differ between days in the Veh/Veh or the PCP/PCP groups, and that the number of rotations made by the PCP/PCP group were highly significantly increased (p < .001, per day) when compared to the Veh/Veh group per day.

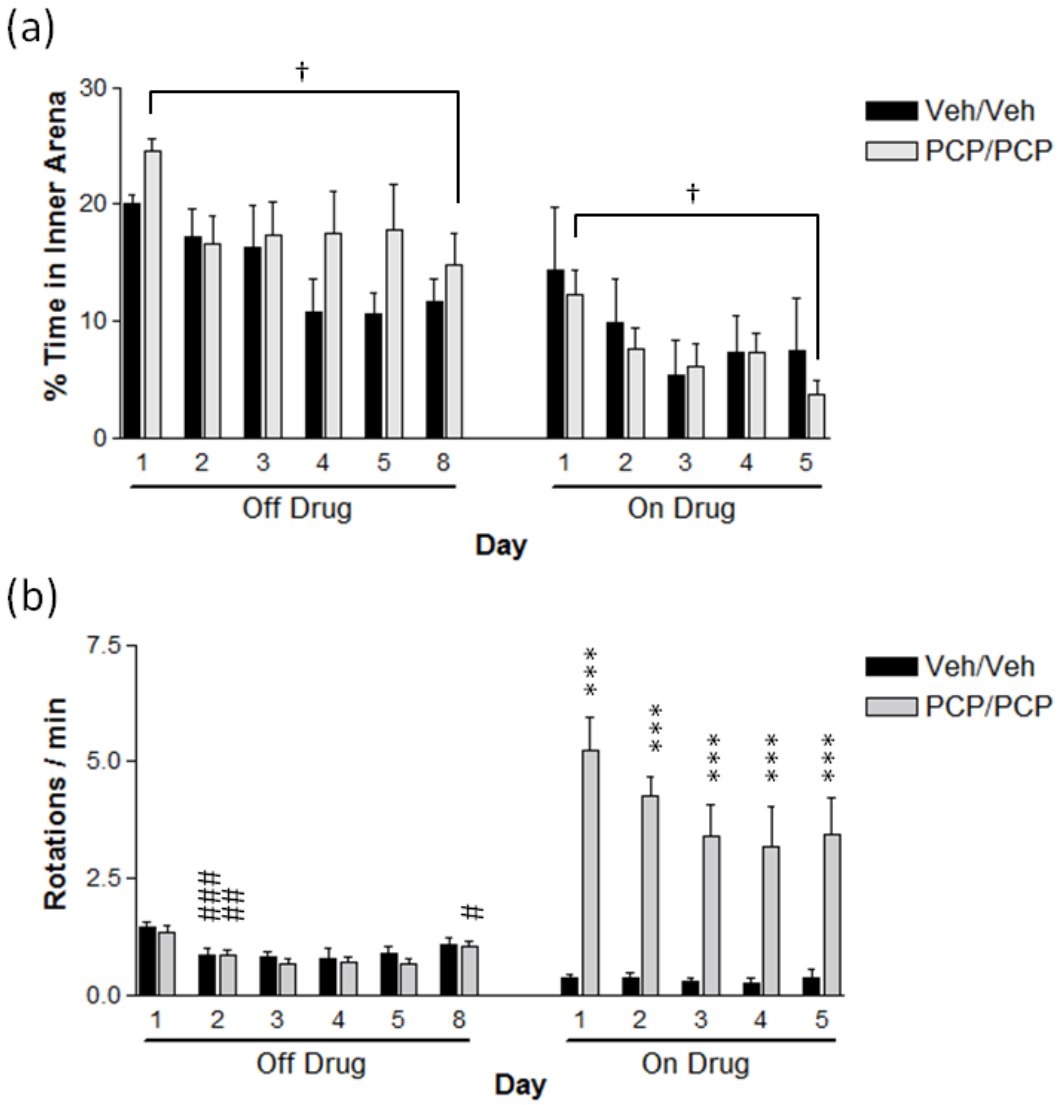

Figure 4.15. Time-dependent changes on locomotor activity with subchronic PCP in mice. Locomotor activity was assessed before (Off Drug), and immediately following (On Drug) the first injection of twice daily administrations of 5 mg.kg^{-1} PCP (PCP/PCP, n = 8) or saline vehicle (Veh/Veh, n = 7). (**a**) The time spent in the inner arena of open field boxes was significantly decreased in the PCP/PCP group (14.8 ± 2.7 %, p = .02, n = 8) 72 hours following final injection when compared to their drug-naive state (Off Drug, day 1; 24.5 ± 1.1 %). A significant decrease (3.7 ± 1.2 %, p = .048, n = 8) was also present in PCP/PCP mice on the fifth day when compared to the first day (12.3 ± 2.0 %, n = 6). (**b**) The total number of rotations by all mice, Off Drug, was significantly diminished on days 2, 3, 4 and 5 (all p < .01) when compared to the first day, and normalised in the PCP/PCP group on day 8 (61.3 ± 8.1 rotations, p = .0495, n = 8) compared to day 5 (39.8 ± 5.9 rotations), but not in the Veh/Veh group (Day 8, 64.0 ± 9.6 rotations, p = .01, n = 6, *vs*. Day 1, 86.7 ± 7.3 rotations, n = 7). Data are presented as mean ± SEM, and were analysed by repeated measures ANOVA with Tukey's multiple comparisons; †, p < .05. #, p < .05; ## p < .01; ###, p < .001 compared to the measurement by drug group on the previous day. *** p < .001 compared to Veh/Veh group.

4.8 Discussion

The main findings of this study are that NOS activity is increased in the hippocampus and, for the first time, that NOS activity is decreased in the reticular thalamus in mice administered acute PCP. NADPH-diaphorase activities were normalised in these regions in mice administered subchronic PCP, and decreased NOS activity in the PFC of these is shown for the first time. A novel finding, too, is that decreased TrxR activities coincide with the altered NADPH-diaphorase activities in the hippocampus and thalamus in mice with acute PCP, but were not altered with subchronic PCP administration. Acute PCP administration did not influence the activities of caspases, and decreased prefrontal caspase 8 and hippocampal caspase 3 are found with subchronic PCP. The significance in these caspase results is marginal and only seen with t-tests and not apparent by ANOVA. Further studies are needed to see if this is a reproducible effect. The main neurochemical findings of this study are summarised in **Table 4.6**. Deficits in PPI and LMA were found with both acute and subchronic PCP, but these deficits did not persist 72 hours following subchronic administration.

Table 4.6 Main neurochemical findings with acute and subchronic PCP.

	Acute PCP					Subchronic PCP				
	NOS	**TrxR**	**Caspase 3**	**Caspase 8**	**Caspase 9**	**NOS**	**TrxR**	**Caspase 3**	**Caspase 8**	**Caspase 9**
PFC	–	–	–	–	–	↓	–	–	↓	–
Striatum	–	–	–	–	–	–	–	–	–	–
Hippocampus	↑	↓	–	–	–	–	–	↓	–	ND
Thalamus	↓ (a)	↓	–	–	–	–	–	–	–	–
Cerebellum	–	–	–	–	–	–	–	–	ND	–

Summary table of the main effects observed with acute and subchronic PCP treatment on the activity of neurochemical measures; nitric oxide synthase (NOS), thioredoxin reductase (TrxR), and caspases. ↑ denotes an increase in activity, ↓ denotes a decrease in activity, and – denotes that no change was detected. **ND**, not determined; (**a**) change observed in the reticular thalamus.

4.8.1 NADPH-diaphorase staining is influenced by NOS inhibition

NADPH-diaphorase was used as a measure of NOS activity in histochemical sections (**Figure 4.4**) and in homogenates (**Figure 4.5**) of mouse brain regions following PCP or vehicle treatment *in vivo*. This assay has been shown to be indicative of both the presence (Bredt et al., 1991; Hope et al., 1991; Huang et al., 1993), and the level of activation of NOS at the point of fixation (Morris *et al.*, 1997). Using NADPH-diaphorase histochemistry, the activity of NOS in cells and in blood vessels could be discriminated (**Figure 4.3** and **Figure 4.4**), and produced staining as found by others (reviewed by:Blottner et al., 1995).

The influence of NOS inhibitors on the intensity of NADPH-diaphorase staining in the striatum of the rat brain was evaluated in section 4.4.1. **Figure 4.3** shows how incubation with 100 µM L-NNA and 1 mM L-NAME attenuated the ROD in replicate sections of the rat striatum. Therefore, at least 27% of NADPH-diaphorase reactivity is sensitive to NOS inhibition. The remaining signal may be non-specific. Alternatively, since tetrazolium salts bind to a different site on NOS than arginine and competitive inhibitors, it may be that this is the maximum level of inhibition attainable allosterically (Klatt *et al.*, 1992). Staining here was significantly higher in neurones than in blood vessels (73% of neuronal staining). This is also reflected in the mouse brain, as shown in Figure 4.3, Table 4.1 and Table 4.2. Therefore, the majority of the NADPH-diaphorase signal generated in brain region homogenates (**Figure 4.5** and **Figure 4.6**) may be accounted to that of a neuronal origin, as opposed to that of the vasculature.

Finally, these data show that NADPH-diaphorase activity may have been attenuated by NOS inhibitors that compete with arginine, both prior to (**Figure 4.3a**) and following fixation (**Figure 4.3b**). Considering that no NADPH-diaphorase activity was present when NADPH was omitted from

reactions (all findings in section 4.3), this indicates that enzymatic activity is present after fixation and is dependent on both the arginine substrate, and the NADPH cofactor. This also suggests that while NADPH-diaphorase activity is indicative of the level of activation at the point of fixation (Morris *et al.*, 1997), the enzyme activity (or at least, level of staining) may still be sensitive to modulation. Therefore, this may be a factor in the comparisons made between sample cohorts that may have be subject to different conditions prior to NADPH-diaphorase reactions. Experimental conditions were kept the same and all samples were processed together per experiment (unless otherwise stated) to minimise variability.

4.8.2 The influence of acute and subchronic PCP on NOS activity in the mouse brain

NADPH-diaphorase activity was assessed in mouse brain regions following acute PCP or vehicle treatment *in vivo*. No changes in NOS activity were detected in blood vessels in the brain regions investigated (**Figure 4.4ii**). Activity was significantly decreased in the reticular thalamus of mice treated with acute PCP, as shown in **Figure 4.4ci**. The thalamus is a highly connected brain region, and emerging evidence supports a role of its dysfunction in deficits found in schizophrenia (Pinault, 2011; Dauvermann et al., 2013; Parnaudeau et al., 2013), and particularly with the reticular thalamus in rodent models (Cochran et al., 2003; Dawson et al., 2011).

NOS activity in the hippocampus was increased (**Figure 4.5**) in mice administered acute PCP, as revealed in NADPH-diaphorase activity in tissue homogenates, but not in hippocampal subfields as assessed histochemically (**Figure 4.4bi**). Little or no NADPH-diaphorase staining was observed in the CA2 in histochemical sections, and so, was omitted from analysis. NADPH-diaphorase activity was increased in the dentate gyri, CA3 and CA1 of PCP-treated mice, but these failed to reach significance. This may be reflective of

a relative insensitivity of NADPH-diaphorase reactions histochemically, compared to those with tissue homogenates. The source of this may be in the tetrazolium salts used (i.e. NBT for histochemistry, XTT for homogenate reactions), or that the sum of nitrergic activity may be captured in homogenates of the whole hippocampi, and is not reflected in 20 µm samples of the hippocampus. The hippocampus is highly implicated in deficits found in schizophrenia (Tamminga *et al.*, 2010). As with the thalamus, the hippocampus is a highly connected brain structure, and its dysfunction may impact on multiple systems (Jones, 2010). The impact of dysfunction of the thalamus and hippocampus, and the relevance of altered NOS activity in these regions will be discussed in Chapter 7.

The ion channel of the NMDA receptor provides the source of calcium that drives nNOS activity, especially because of the physical tether between nNOS and the GluN2b subunit, as provided for by PSD-95 proteins (Christopherson et al., 1999; Sattler et al., 1999). Therefore, NMDA receptors directly link glutamate transmission with nitric oxide signalling (Bhardwaj et al., 1997a; Bhardwaj et al., 1997b). The blockade of NMDA receptor-mediated calcium influx by PCP is likely to explain the decrease in NOS activity in the reticular thalamus, especially considering the evidence for tonically-active NMDA receptors in this region (Zhang *et al.*, 2009b). The increased NOS activity in the hippocampus with acute PCP is less intuitive, however. One explanation for this may be the potentiation of glutamate transmission via the attenuation of GABAergic tone by PCP, as discussed in **Chapter 1.2.3**, and illustrated by **Figure 1.1**. The resultant excitatory drive may stimulate NOS activity. For it to be localised in the hippocampus, there may be a differential distribution of respondent calcium channels (or other source of intracellular calcium) in this region. Interestingly, nitric oxide has been shown to contribute to the increased glutamate concentration in the PFC with NMDA receptor blockade (Roenker *et al.*, 2012), and therefore may contribute to, and be influenced by (Fejgin *et al.*, 2009), GABAergic disinhibition.

Non-NMDA glutamate receptors may also contribute to NOS activity (Okada *et al.*, 2004). GluA2-lacking AMPA receptors may provide a source of calcium for NOS activation during NMDA receptor channel blockade (Frade *et al.*, 2009), and these may have an increased expression in hippocampal interneurones (Racca et al., 1996; González-Albo et al., 2001; Szabo et al., 2012), compared to the other brain regions investigated. AMPA has been shown to directly stimulate nitric oxide generation (Yamada and Nabeshima, 1997). AMPA receptors that colocalise with NOS show a decreased expression of GluA2 compared to those that do not (Catania *et al.*, 1995). Altered GluA2 subunit expression has been implicated in schizophrenia (Akbarian *et al.*, 1995). Nitric oxide signalling may alter the function of AMPA receptors (Dev and Morris, 1994), likely by the process of *S*-nitrosylation (Huang et al., 2005; Selvakumar et al., 2009), and therefore may serve as an adaptive process in response to NMDA receptor dysfunction mediated by nitric oxide (Rameau *et al.*, 2007).

Voltage-gated calcium channels (VGCCs) may also stimulate nitric oxide signalling (Oka *et al.*, 2003). Nitric oxide-mediated modulation of (NMDA receptor-independent) long-term potentiation in the hippocampus (Pigott and Garthwaite, 2012), and dopamine release in the striatum (Rocchitta *et al.*, 2005) have been shown to be sensitive to nifedipine. L-type calcium channels are also closely associated with NMDA receptors and nNOS, and may form functional microdomains at the cell membrane (Marques-da-Silva and Gutierrez-Merino, 2012). These suggest that VGCCs, and L-type channels in particular, may contribute to NOS activity in this region. VGCCs may be excited, and therefore supplement NOS with calcium during NMDA receptor blockade and the consequential increased glutamate transmission that may arise with GABAergic disinhibition.

The region-specific changes observed may be due to the altered eNOS activity in these regions. eNOS is predominantly expressed in endothelial

cells, and thus may confer an altered blood flow with its dysfunction. The histochemical data presented here do not support this, as illustrated in **Figure 4.4**. Here blood vessel NADPH-diaphorase activity is unchanged. Blood flow changes also appear not to be regionally specific with systemic NOS inhibition (Macrae *et al.*, 1993). However, blood vessels may respond to nitric oxide generated in proximal neurones (Rancillac et al., 2006; Attwell et al., 2010), and vice versa (Garthwaite et al., 2006; Hopper and Garthwaite, 2006). eNOS may also be expressed in neurones (Dinerman et al., 1994; Doyle and Slater, 1997) and astrocytes (Gabbott and Bacon, 1996), and its density may vary between brain regions (Kharazia *et al.*, 1994) and between species (Blackshaw *et al.*, 2003). The expression of eNOS may present a unique factor to give rise to the specific changes presented here. Keilhoff and colleagues (2004) revealed increased densities of NADPH-diaphorase positive neurones, but not nNOS immunoreactive neurones, in the hippocampi of rats administered subchronic ketamine, and may therefore be reflective of eNOS recruitment with NMDA receptor antagonism. The role of NOS isoforms in deficits found in mice with PCP are explored in Chapter 5.

Splice variants of nNOS may account for the variation shown here, as they have a differential expression between brain regions (Eliasson et al., 1997; Putzke et al., 2000). Genetic knock out of the predominant nNOSα, may give rise to upregulated expression of the splice variant, nNOSβ, but not nNOSγ (Putzke *et al.*, 2000). These variants lack the PDZ domains necessary for NMDA receptor interaction (Brenman *et al.*, 1997), and will therefore have a different subcellular localisation, and may not be activated with synaptic activity. nNOSβ, however, may still be functional (Eliasson *et al.*, 1997), but the mechanisms of its activity have yet to be elucidated.

Brains that were used for neurochemical assessment were collected 30 mins following acute PCP administration. From locomotor responses, illustrated by **Figure 4.13a** and **Figure 4.14**, it appears that PCP was imparting an effect

at that time point, and so therefore is a suitable point to assay for acute effects of the drug. The behavioural effects after subchronic PCP treatment were less pronounced (discussed in section 4.8.4), however. Subchronic PCP administration in mice resulted in differential activities of NOS in brain regions. The altered activities of NOS in the hippocampus and thalamus seen with acute PCP were normalised with subchronic PCP, as revealed by NADPH-diaphorase activities in tissue homogenates. However, NOS activity was decreased in the PFC of these mice compared to vehicle controls, as shown in **Figure 4.6**. Perhaps the discrepant behavioural outcomes between acute and subchronic PCP treatments may be accounted for by the differential neurochemical profiles present with these treatments. The relatedness of NOS and these behaviours are explored further in Chapter 5, and discussed in Chapter 7.

No differences in nitrite concentrations were detected in brain regions of mice treated with acute PCP, as shown in **Figure 4.7**. An increase in hippocampal nitrite concentration with acute ketamine, and then normalisation with repeated administrations, has been shown previously in Swiss albino mice (Chatterjee *et al.*, 2012). It should be noted that the dose of ketamine used in the aforementioned study was particularly high (100 $mg.kg^{-1}$), and that the chronic drug administration (100 $mg.kg^{-1}$ per day for 10 days) is not comparable with those used presented here (twice daily doses of vehicle or 5 $mg.kg^{-1}$ PCP for 5 days). This does not support the findings presented in Section 4.5, but does support those in Section 4.4.2. Nitrite concentrations were not assayed in brains with subchronic PCP as this assay appears insensitive to altered endogenous nitric oxide generation, as shown in Chapter 3.

NOS activity has been shown to be inhibited by NMDA antagonists in the cerebellum (Luo *et al.*, 1993) and whole brain (Desaiah *et al.*, 1999), as was seen in the thalamus with acute PCP (**Figure 4.5**), and the PFC with

subchronic PCP (**Figure 4.6**). This is the first characterisation of NOS activity in the reticular thalamus following acute PCP. Fejgin and colleagues (2008) revealed a nitric oxide-dependent increase in cGMP in the PFC of mice with acute PCP, and a more direct measure of this effect, using electrochemistry, has been shown in the rat PFC (Finnerty *et al.*, 2013). The increased NOS activity in the PFC with acute PCP, presented here (**Figure 4.4** and **Figure 4.5**), did not reach significance. Interestingly, NMDA receptor modulation has been shown not to alter NOS activity in the PFC as strongly as $GABA_A$ antagonism has (Pepicelli *et al.*, 2004). Presented here is the first evidence of decreased NOS activity in the PFC of mice following subchronic PCP administrations (PCP/PCP; **Figure 4.6**). Braun and colleagues (2007) found no increase in PFC NADPH-diaphorase density with subchronic MK-801 in rats. Increased NOS activity in the hippocampus with acute PCP administration has been found previously in rats (Klamer et al., 2005c), in support of the findings presented here (**Figure 4.5**), however the inverse has also been shown with MK801 (Bhardwaj et al., 1997a). Increased densities of NADPH-diaphorase expressing neurones in the hippocampus has been reported in rats with subchronic administration of ketamine (Keilhoff *et al.*, 2004), but not with MK801 (Braun *et al.*, 2007).

These changes observed following subchronic PCP compared to acute PCP may be explained by neuroadaptive processes in response to persistent NMDA receptor antagonism. Previous findings have shown that subchronic and chronic NMDA receptor antagonism produce long-lasting alterations in neurochemistry (Cochran et al., 2003; Keilhoff et al., 2004; Rujescu et al., 2006; Xiao et al., 2011), network dynamics (Zhang *et al.*, 2008), and behaviour (Egerton et al., 2008; Thomson et al., 2011). Altered NOS activity in neurones may also influence local blood flow (reviewed by: Garthwaite and Boulton, 1995). Especially interesting is the decreased NOS activity in the PFC seen with subchronic PCP, and that this may confer decreased PFC blood flow as seen in schizophrenia (Berman *et al.*, 1992).

The implications of altered NOS activity are wide and varied. The modulation of soluble guanylate cyclase (sGC) and thence cGMP signalling may influence many targets, as outlined in Chapter 1.4.1. There may also be alterations in protein function, by way of *S*-nitrosylation (Seth and Stamler, 2011). Of particular relevance to the findings presented here is that both NMDA receptor (Lei et al., 1992; Choi et al., 2000) and NOS activities (Qu *et al.*, 2012) may be inhibited by *S*-nitrosylation. The density of PSD-95 at synapses may also be influenced by this modification (Ho *et al.*, 2011), and so, may have implications on synaptic strength and plasticity (Nikonenko *et al.*, 2008). Finally, excess nitric oxide may be toxic (Brown, 2010). The acute toxic effects of nitric oxide appear to be dependent on the presence of superoxide to form peroxynitrite (Lipton *et al.*, 1993). However, persistent nitric oxide has been shown to be toxic independently of peroxynitrite formation (Meij et al., 2004; Fatokun et al., 2008). Nitric oxide-mediated stress and cell death are explored below.

4.8.3 The implications of acute and subchronic PCP on redox state and apoptosis in the mouse brain

TrxR activity was decreased in the hippocampi and thalami of mice administered acute PCP. The Trx/TrxR system has been shown to regulate nNOS activity (Qu *et al.*, 2012) and caspase activation (Tenneti et al., 1997; Benhar et al., 2008) by the process of denitrosylation. The neuroprotective actions of nitric oxide signalling have been accounted for by the upregulation of the Trx/TrxR system (Andoh *et al.*, 2003).

NOS activity was also altered in these regions with acute PCP treatment. The responses of these are not proportional in magnitude or by sign. NOS activity increased 34% (**Figure 4.5**), and TrxR activity decreased 46% (**Figure 4.8**) in the hippocampi of mice with acute PCP. NOS activity decreased 13%, and TrxR activity decreased 70% in the thalami of mice with acute PCP.

Interestingly, TrxR activity in the hippocampi and thalami normalised in mice with subchronic PCP (**Figure 4.9**), as occurred with NOS activity (**Figure 4.6**). A 29% decrease in TrxR activity in the PFC, although does not meet significance, does appear to follow with what occurs with NOS activity (42% decrease) with subchronic PCP. However, this does not appear to be the case in the thalamus. A larger sample size in both PCP and control groups may reduce the variance to further elucidate any concordance.

NMDA receptor inhibition may decrease Trx/TrxR activity via the suppression of synaptic activity (Papadia *et al.*, 2008). This appears to be the case in mice treated with acute PCP, as shown in **Figure 4.8**, but in a regionally-specific manner. TrxR may be stimulated by nitric oxide signalling (Forrester *et al.*, 2009). However, this does not appear to be the case in the hippocampi of mice with acute PCP (NOS, **Figure 4.5**; TrxR, **Figure 4.8**). Nitric oxide may exert its neuroprotective effects by the promotion of TrxR activity via PKG stimulation (Andoh *et al.*, 2003), suggestive that NOS activity influences TrxR via sGC/cGMP signalling. TrxR may denitrosylate, and therefore potentiate, nNOS activity via NMDA receptor signalling (Qu *et al.*, 2012). Together, these suggest that TrxR activity is functionally related to NMDA receptor and NOS signalling, and that the Trx/TrxR system has a reciprocal relationship with these. Finally, decreased TrxR activity has been shown to mediate apoptosis via caspase activation (Andoh *et al.*, 2002), and this effect may be exacerbated with high levels of nitric oxide (Ishikawa *et al.*, 1999). This relationship is explored further below.

No difference in caspase 3 activities was detected in mice with acute PCP or vehicle treatment. This was also the case with caspases 8 and 9. Significant decreases in hippocampal caspase 3 and prefrontal caspase 8 were detected in mice administered subchronic PCP (**Table 4.5**). The influence of nitric oxide signalling on the activation of caspases in the brain is well studied, Brown, 2010 especially in terms of initiating apoptosis (Brown, 2010;

Shahani and Sawa, 2011). What the functional relevance of a decrease in tone of these proteases may be is less well understood. A tonic activity of caspase 3 in the hippocampus has been shown previously, and may influence memory functioning (Dash et al., 2000; D'Amelio et al., 2011) and glutamate transmission (Li *et al.*, 2010).

Nitric oxide has been shown to inhibit caspase 8 via TrxR activity (Sengupta *et al.*, 2010), and nitric oxide-mediated caspase 3 inhibition via S-nitrosylation can be potentiated with TrxR inhibition (Sengupta *et al.*, 2009). TrxR-mediated caspase 3 activation appears to be mediated by caspase 9 (Andoh *et al.*, 2002). These relationships are not reflected in the results presented here. In the acute PCP-treated mice, no change in thalamic caspase activities was detected **Figure 4.10a**, and the increased NOS and decreased TrxR activities in the hippocampus did not confer any change in caspase activities either. In mice treated with subchronic PCP, the decreases in hippocampal caspase 3 and prefrontal caspase 8 (**Figure 4.10b**) do not coincide with altered TrxR activities (**Figure 4.9**), and NOS activity is decreased in the PFC (**Figure 4.6**). Therefore the observed caspase activities in the brains of these mice appear not to be related to NOS or TrxR activities.

Altered NMDA receptor signalling may also influence cell death independently of NOS (Anastasio *et al.*, 2009), and this may be via other signalling molecules than p38 (Li *et al.*, 2013), such as JNK (Soriano *et al.*, 2008). However, the activation of ASK-1 may be a common factor between NOS-dependent, and -independent activation of caspases (Liu *et al.*, 2013). Cellular loss, and particularly that of parvalbumin expressing interneurones, has been reported in schizophrenia (Nakazawa *et al.*, 2011), and in animals with prolonged NMDA receptor antagonism (Cochran et al., 2002; Keilhoff et al., 2004).

Caspase 3 activity was significantly different between brain regions of mice with acute drug administration (**Figure 4.10a**). This difference may be reflective of the cellular turnover, and possibly plasticity, in these regions. The regional activities of caspase 3 in mice with subchronic PCP (**Figure 4.10b**) do not mirror those as with acute PCP, however. This disparity may exist because of technical variation. However, both methods and reagents used were constant in both experiments. While caspase 3 activities in the acute drug samples were apparently sensitive to selective inhibition (**Table 4.4**), those in subchronic drug samples were not (**Table 4.5**), with the possible exception of hippocampal and cerebellar samples. The rates of AMC accumulation in subchronic treatment samples are approximately 20-100 times that seen in the acute group. These activities are likely nonspecific, because of their apparent insensitivity to inhibition by the caspase 3 inhibitor (although, inhibitor groups were n = 2). It is possible that stress associated with repeated injections may induce caspases. Further study would be required to explore these possibilities.

4.8.4 Behavioural deficits propagated by PCP

An overall significant decrease in PPI was observed in mice treated with acute PCP, as shown in **Figure 4.11a**. This provides evidence of a behavioural phenotype with this dose of PCP in c57bl6j mice; an important consideration given the variability in PPI response between substrains of these mice (Matsuo *et al.*, 2010). PPI deficits have been shown before in c57bl6j mice with 5 $mg.kg^{-1}$ PCP (Yee *et al.*, 2004), supporting the findings presented here. No difference in PPI was detected between drug groups 72 hours following subchronic drug administrations, as shown in **Figure 4.12a**. This is supported by findings in rats (Egerton *et al.*, 2008).

The startle responses of mice decreased with the sequence of stimulus presentation with both acute (**Figure 4.11b**) and subchronic (**Figure**

4.12b) drug treatments. These are suggestive of a habituation of response to the startling stimulus. Interestingly, there was an overall decrease in startle reactivity in mice treated with subchronic PCP compared to vehicle, but not with acute PCP. As PPI is calculated as a function of startle response, this measure may not impact upon PPI, *per se*. However, diminished startle reactivity may be indicative of deficits in dopaminergic D_2/D_3 signalling (Halberstadt and Geyer, 2009).

The neural correlates involved in PPI are widespread, and include brainstem, striatal, thalamic, cortical (Swerdlow *et al.*, 2001), and hippocampal structures (Swerdlow *et al.*, 2012). The transmitter systems that mediate PPI responses include cholinergic (Bosch and Schmid, 2008), dopaminergic, 5HTergic, and glutamatergic transmission (Geyer *et al.*, 2001). Together, the PPI and startle responses presented here suggest that acute PCP disrupts sensorimotor gating, as is found in people with schizophrenia (Braff *et al.*, 2001). This deficit does not persist 72 hours following repeated administrations of PCP, but a deficit in startle reactivity remains that may be related to altered dopamine transmission via NMDA receptor antagonism.

The LMA responses before and following drug administration are comparable between acute (**Figure 4.13**a) and the first day of subchronic (**Figure 4.14**) PCP experiments. The velocity of vehicle treated groups was 5.0 ± 0.2 cm/s (acute) and 5.3 ± 0.4 cm/s (subchronic) during habituation to the arena, and the velocity of PCP groups was 5.3 ± 0.4 cm/s (acute) and 5.0 ± 0.5 cm/s (subchronic). Similarly, following acute vehicle administration, the mean velocity of mice was 3.0 ± 0.2 cm/s, and in the PCP group was 8.7 ± 0.8 cm/s. Following the first drug administration in the subchronic groups, the mean velocity of mice was 2.1 ± 0.5 cm/s (Veh/Veh) and 10.2 ± 1.4 cm/s (PCP/PCP).

LMA responses over the course of 5 days of two daily injections of PCP do not support that neuroadaptive processes related to these behaviours are occurring. However, that locomotor and PPI deficits do not persist 72 hours following subchronic PCP administration, but NOS activity is decreased in the PFC, suggests that these changes may be independent. Therefore the behavioural measures used may not reflect that neuroadaptive changes that may occur, as discussed in Chapter 4.8.1.

Motor disturbances in people with schizophrenia may be present as both a function of the disorder itself, and due to chronic antagonism of dopamine transmission by antipsychotic drugs (Walther and Strik, 2012). Hyperlocomotion following subchronic PCP, but not chronic PCP has been shown in rats (Egerton *et al.*, 2008); the former does not support the findings presented here. The hyperlocomotor responses in mice treated with subchronic PCP appeared to diminish after peak between 20-40 mins following PCP administration, as shown in **Figure 4.14a-e** (Post-drug), and differences between groups did not persist the following morning (**Figure 4.14b-e**, Pre-drug; **Figure 4.15b**, Off Drug). Therefore, the clearance of PCP may be increased in these mouse compared to rats, owing to the lack of difference following drug withdrawal (**Figure 4.14f, Figure 4.15b**).

The time spent in the inner portion of open field arenas diminished in both groups by day, and significantly so in the PCP group, as shown in **Figure 4.15a**. This may be reflective of an increase in anxiety mediated by subchronic NMDA receptor antagonism, especially as this effect persists 72 hours following drug withdrawal. However, this effect is present in both groups and a better measure for anxiety, such as using the elevated plus maze, would be more appropriate to elucidate any influence of PCP treatment on anxiety behaviours. The hyperlocomotion that was predominantly rotational (**Figure 4.15b**) also appears purposeful. That is, the hyperlocomotor behaviours were preferentially spent close to the arena

walls, and therefore indicative of dithering or thigmotaxis, as opposed to non-purposeful movements regardless of surroundings.

The hyperlocomotion responses per day with subchronic PCP were suggestive of a desensitisation to PCP on day 4 (**Figure 4.14d**) compared to previous days (**Figure 4.14a-c**). However, PCP responses on the fifth day (**Figure 4.14e**) returned to a similar difference (and level of significance) in drug groups as on Days 1-3. Rotational behaviour in the PCP group also diminished on Days 1-4 (**Figure 4.15b**), but these were not significantly different from each other.

Dysregulated movements are common in people with schizophrenia, both unmedicated and with chronic dopamine antagonism via antipsychotic treatment (Honer *et al.*, 2005). PCP-induced hyperlocomotion can be reversed, and time spent in the inner zone of open field boxes decreased with $D_{2/3}$ antagonism (Sams-Dodd, 1998b). The persistent increase in anxiety-like behaviour may also involve multiple systems and transmitter interactions, including decreased GABAergic tone and dysfunctional 5HT transmission (Keshavan *et al.*, 2008), as found in schizophrenia (Muller *et al.*, 2004). The thalamic reticular nucleus and associated thalamocortical circuits may also be important in NMDA receptor antagonist-mediated hyperlocomotion (Lopez Hill and Scorza, 2012). Therefore, the locomotor deficits presented here are likely mediated by complex interactions between neurotransmitter systems that may involve decreased GABAergic tone and dopaminergic stimulation via NMDA receptor antagonism by PCP.

The influence of NOS on the behavioural deficits with acute PCP reported here is explored in Chapter 5.

4.9 Conclusions

Acute PCP administration in mice did not inhibit NOS globally, but did alter its activity in a regionally-specific manner. The data show an increase in NADPH-diaphorase activity in the hippocampus, and a decrease in the reticular thalamus. Subchronic PCP administrations did not exacerbate the effects found with acute PCP. With these drug treatments, hippocampal and thalamic NOS activities were normalised, and activity was decreased in the PFC.

TrxR activities were disrupted in the same brain regions where NADPH-diaphorase activity was altered. However, these were not proportional as increased hippocampal, and decreased thalamic NADPH-diaphorase activities, coincided with decreased TrxR activities in these regions. The changes observed with acute PCP were normalised in mice administered subchronic PCP, and therefore were not exacerbated. Altered NOS and TrxR activities did not confer changes in apoptotic state, as determined by caspase activities, with acute PCP. Decreased caspase 8 in the PFC, and a decrease caspase 3 activity in the hippocampus was found in mice with subchronic PCP treatment. The validity of these caspase findings is questionable, however, and replicates are needed to confirm this finding.

Acute PCP administration was sufficient to elicit an overall deficit in PPI, and increase in velocity and rotational behaviours of mice in the open field. Subchronic administrations of PCP gave rise to persistently increased LMA, but these deficits did not persist 72 hours following drug administrations and PPI was unchanged at this time-point. A cumulative increase in anxious-related behaviour was observed with subchronic PCP, and this persisted 72 hours after the final injection of PCP.

Together, these data implicate a dependency of NOS signalling upon NMDA receptor function. NOS and TrxR activities are altered in schizophrenia-related brain regions by NMDA receptor antagonism, and coincide with translational behavioural deficits. The changes observed are likely mediated by complex neurotransmitter, and brain region interactions, and merit further study.

5 The Influence of Nitric Oxide Synthase Isoforms on the Neurochemical and Behavioural Effects of Acute PCP

5.1 Introduction

In this chapter, the role of the constitutive isoforms of NOS in previously identified deficits found with acute PCP administration in mice will be explored. Acute PCP was shown to induce hyperlocomotion and a deficit in prepulse inhibition (PPI) in mice in Chapter 4. Acute PCP was also shown to increase hippocampal, and decrease reticular thalamic NADPH-diaphorase activity. NOS inhibitors will be used here to determine their influence on these behavioural deficits and on the activities of neuronal and vascular NADPH-diaphorase.

The most abundant selection of NOS inhibitors are those that compete with the arginine substrate. Used in this study is the non-selective arginine-based pro-drug, N^{ω}-nitro-L-arginine methyl ester (L-NAME); the ornithine derivative, and reportedly more selective eNOS inhibitor, N^{ω}-(1-iminoethyl)-L-ornithine (L-NIO) (Knowles et al., 1990; Rees et al., 1990); and the potent and selective arginine-based nNOS inhibitor, N^{ω}-propyl-L-arginine (L-NPA) (Zhang *et al.*, 1997). The selectivity of L-NIO (Babu and Griffith, 1998) and of L-NPA (Pigott *et al.*, 2013) has been brought in to question. These drugs were used in Chapter 3.4, and their IC_{50} values are given in Table 3.1. However, a comparison of these drugs has yet to be made *in vivo*, and here, the relative efficacy of these drugs to influence neuronal and vascular NOS activities will be compared.

Other means to inhibit NOS involve blocking cofactor activities or by sequestering the enzyme. Interruption of NOS cofactor binding using 7-nitroindazole has been shown to be effective to attenuate NMDA receptor antagonist-mediated behavioural deficits (Deutsch et al., 1996; Wiley, 1998).

Though commonly used as a selective nNOS inhibitor, this drug has been shown to be non-isoform-selective *in vitro* (Bland-Ward and Moore, 1995), and by itself may induce behavioural deficits such as working memory (Yamada *et al.*, 1996). Another means to selectively inhibit nNOS is to interrupt the association of nNOS with NMDA receptors via the PDZ interactions with PSD-95 (Doucet *et al.*, 2013), thereby mimicking the role of the endogenous nNOS sequestering protein, CAPON (Jaffrey *et al.*, 1998). There are also many drugs that modulate NOS outside of their main action (Moore and Handy, 1997), and the most relevant of these to schizophrenia research is the antibiotic drug, minocycline (Levkovitz *et al.*, 2010).

While the orthodox view is that only nNOS is expressed in neurones, the endothelial isoform has also been shown to be expressed in neurones (Dinerman *et al.*, 1994) and may therefore be functionally distinct (Kano *et al.*, 1998). However, the expression of eNOS in neurones is controversial, as some studies only find eNOS localised to endothelial cells (Blackshaw *et al.*, 2003). Cerebral blood flow is closely linked to neuronal function (Moore and Cao, 2008; Toda et al., 2009), and its disruption may influence even cognitive behaviours (de la Torre and Aliev, 2005). Therefore, a comparison of behaviours and of NOS activities in neurones and blood vessels with selective NOS inhibition may elucidate the role of NOS isoforms in the responses to PCP in mice.

5.2 Hypothesis and aims

PCP-mediated neurochemical and behavioural deficits will be improved by NOS inhibition. Selective inhibition of nNOS will improve deficits elicited by NMDA receptor antagonism because of the functional association between these.

The aim of this work is to evaluate the alterations in behaviours and nitric oxide signalling with selective and non-selective NOS inhibition, *in vivo* and

ex vivo. These drugs will be evaluated for their efficacy in altering acute PCP-induced behavioural deficits in mice. The brains of these mice will be used to assess NOS activities in brain regions that have been previously identified as being influenced by acute PCP.

5.3 Methods

Drugs administrations were given as described in Section 2.3.3, and behavioural and neurochemical assays were done as described in Chapters 2.9 and 2.5.1, respectively. Outlined in Figure 5.1. are these procedures.

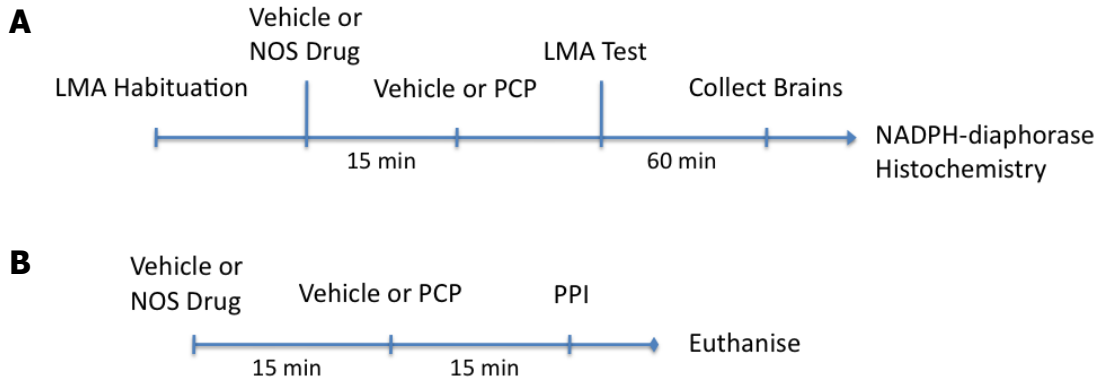

Figure 5.1. Experimental schemata for drug administrations, behavioural assays and histological sampling.

5.4 Behavioural deficits induced by PCP and the influence of NOS-modulating drugs

5.4.1 Prepulse inhibition

Prepulse inhibition (PPI) of acoustic startle was assessed in mice treated with acute PCP (5 mg.kg^{-1}) or vehicle, and pretreated with either vehicle or a NOS inhibitor; L-NAME (40 mg.kg^{-1}), L-NIO (20 mg.kg^{-1}), and L-NPA (20 mg.kg^{-1}) for 15mins. Figure 5.2 shows how PPI was significantly decreased in mice administered vehicle + PCP ($p < .001$) compared to vehicle + vehicle. This deficit was partially reversed with L-NIO pretreatment in mice ($p = .003$ *vs*. vehicle + PCP), but persisted in mice pretreated with L-NAME and L-NPA (both, $p < .001$ *vs*. vehicle + vehicle). There was an apparent prepulse facilitation in mice administered L-NAME, or L-NIO + vehicle, but these were not significantly different when compared to vehicle + vehicle. As expected, PPI increased with increasing prepulse intensity.

The reactivity of mice to the startling stimulus alone was determined at the beginning, middle and end of the PPI protocol. As shown in Figure 5.3, the startle response of mice declined sequentially. This trend was somewhat flattened in mice administered vehicle + PCP compared to vehicle + vehicle, and this was more apparent in mice administered L-NIO + vehicle. Startle reactivity was significantly increased in the L-NAME + PCP, and L-NPA + PCP groups compared to vehicle controls. Whereas, startle responses in mice administered L-NIO + vehicle were significantly decreased ($p < .001$) compared to the control group (vehicle + vehicle).

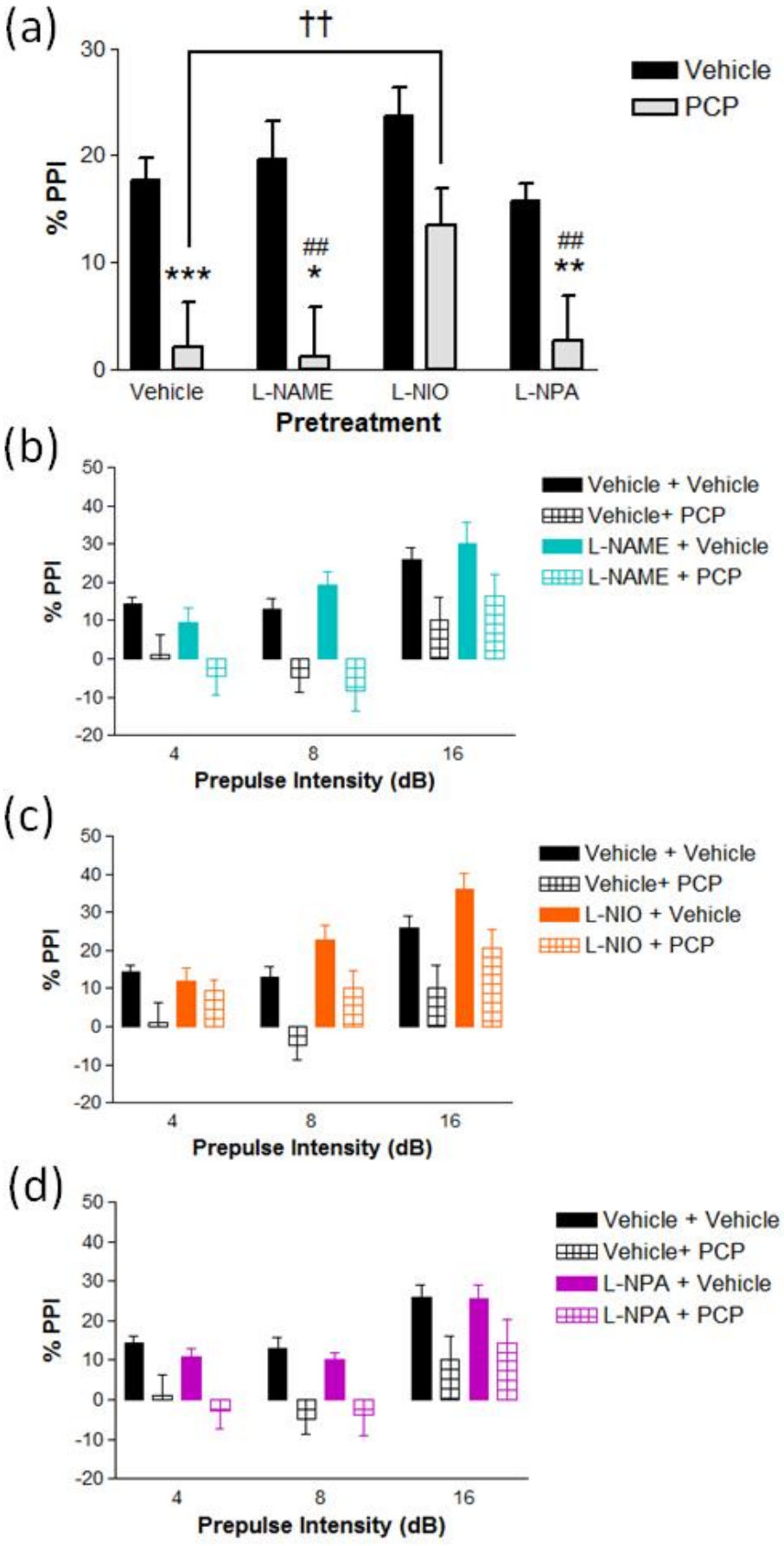
(a)
††
30
20
10
0
% PPI
***
##
*
##
**
Vehicle
PCP
Vehicle
L-NAME
L-NIO
L-NPA
Pretreatment
(b)
50
40
30
20
10
0
-10
-20
% PPI
Vehicle + Vehicle
Vehicle+ PCP
L-NAME + Vehicle
L-NAME + PCP
4
8
16
Prepulse Intensity (dB)
(c)
50
40
30
20
10
0
-10
-20
% PPI
Vehicle + Vehicle
Vehicle+ PCP
L-NIO + Vehicle
L-NIO + PCP
4
8
16
Prepulse Intensity (dB)
(d)
50
40
30
20
10
0
-10
-20
% PPI
Vehicle + Vehicle
Vehicle+ PCP
L-NPA + Vehicle
L-NPA + PCP
4
8
16
Prepulse Intensity (dB)

Figure 5.2. Influence of NOS-modulating drugs on prepulse inhibition deficits induced by PCP. Percent change in prepulse inhibition (PPI) of acoustic startle of mice treated with 40 $mg.kg^{-1}$ L-NAME, 20 $mg.kg^{-1}$ L-NIO, 20 $mg.kg^{-1}$ L-NPA for 15 mins and then either 5 $mg.kg^{-1}$ PCP or saline vehicle. There was an overall highly significant influence of PCP ($F_{1,281} = 135.6$, $p < .001$), NOS drug ($F_{3,281} = 12.6$, $p < .001$), and of prepulse intensity ($F_{2,281} = 72.0$, $p < .001$) on PPI response. (a) There was a significant decrease in PPI response when averaged across prepulse intensities in mice administered vehicle + PCP (2.1 ± 4.1 % PPI, $p < .001$), L-NAME + PCP (1.2 ± 4.6 % PPI, $p < .001$), and L-NPA + PCP (2.6 ± 4.3 % PPI, $p < .001$), compared to vehicle + vehicle treatment (17.7 ± 2.1 % PPI). Pretreatment with L-NIO reversed (13.5 ± 3.5 % PPI, $p < .003$) the deficit from vehicle in mice administered PCP. PPI responses at different prepulse intensities are given for (b) L-NAME, (c) L-NIO, and (d) L-NPA. Data are presented as mean ± SEM, and were analysed using a three-way ANOVA with Tukey's multiple comparisons, and presented statistical inferences are of PPI responses averaged across prepulse intensities. *, $p < .05$; **, $p < .01$; ***, $p < .001$ compared with corresponding vehicle control; ##, $p < .01$ compared with vehicle + vehicle; ††, $p < .01$ (Tukey). n = 12 per group, except L-NAME + vehicle and L-NIO + vehicle, n = 11.

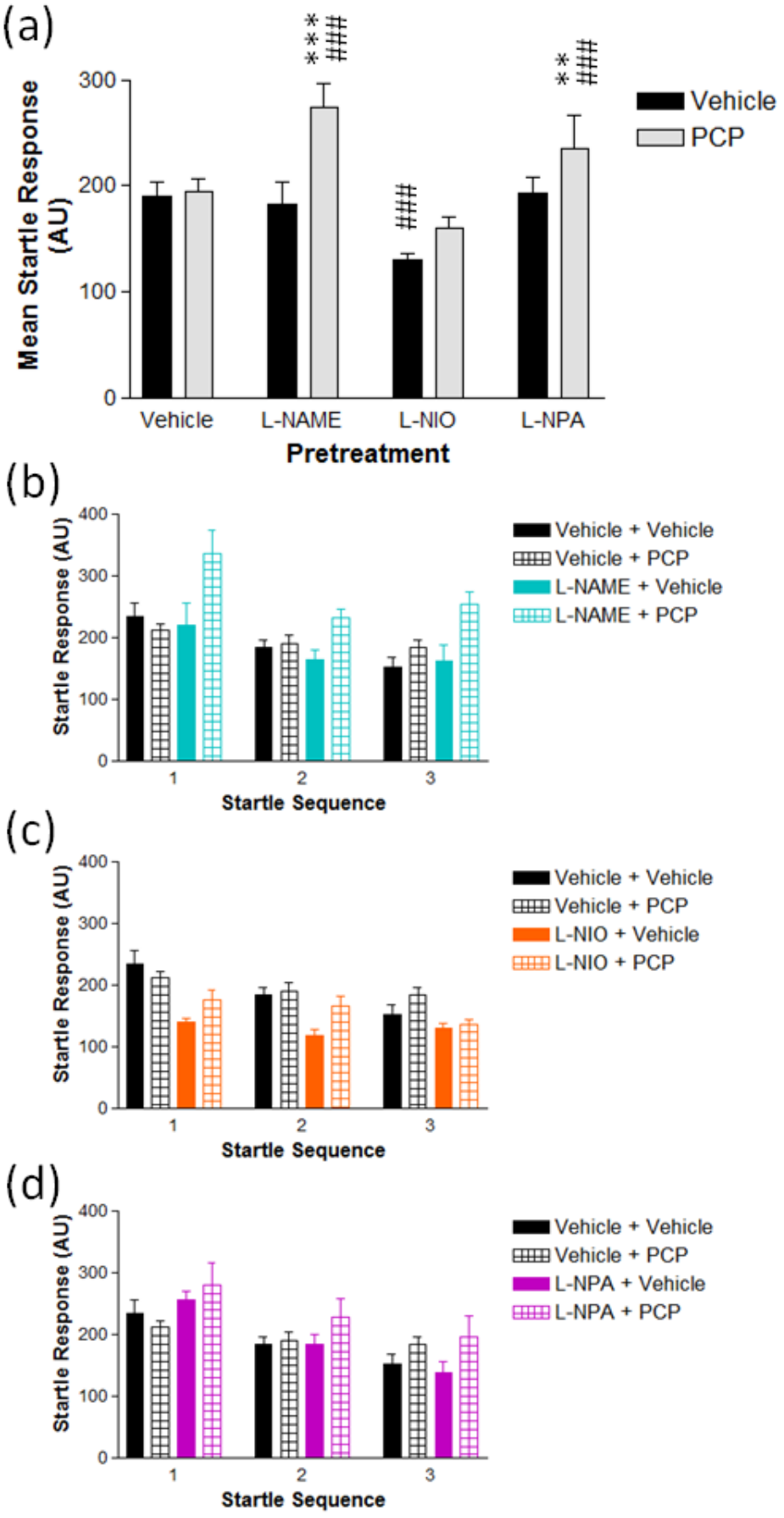
(a)
Mean Startle Response (AU)
300
200
100
0
Vehicle
L-NAME
L-NIO
L-NPA
Pretreatment
Vehicle
PCP
(b)
Startle Response (AU)
Startle Sequence
Vehicle + Vehicle
Vehicle + PCP
L-NAME + Vehicle
L-NAME + PCP
(c)
Startle Response (AU)
Startle Sequence
Vehicle + Vehicle
Vehicle + PCP
L-NIO + Vehicle
L-NIO + PCP
(d)
Startle Response (AU)
Startle Sequence
Vehicle + Vehicle
Vehicle + PCP
L-NPA + Vehicle
L-NPA + PCP

Figure 5.3. Mouse startle responses are altered with NOS inhibition with and without PCP. The startle responses of mice was assessed after administration of saline vehicle, 40 mg.kg^{-1} L-NAME, 20 mg.kg^{-1} L-NIO or 20 mg.kg^{-1} L-NPA for 15 mins, and vehicle or 5 mg.kg^{-1} PCP. Startle responses were significantly influenced by PCP ($F_{1,281} = 64.8$, $p < .001$), NOS inhibitor ($F_{3,281} = 48.5$, $p < .001$), and there was a significant interaction between these ($F_{3,281} = 11.8$, $p < .001$). There was also a significant influence of the sequence of startle presentation ($F_{2,281} = 52.5$, $p < .001$), and this interacted with NOS inhibition ($F_{6,281} = 4.6$, $p < .001$). (a) There was a highly significant increase in mean startle response in mice administered L-NAME + PCP (274.0 ± 22.7 AU, p < .001) compared to L-NAME + vehicle (183.1 ± 20.0 AU, $p < .001$), and vehicle + vehicle (190.3 ± 13.4 AU, $p < .001$). Mean startle responses were significantly decreased in mice administered L-NIO + vehicle (129.3 ± 7.2 AU, $p < .001$) compared to vehicle + vehicle. Mice administered L-NPA + PCP (235.0 ± 31.1 AU) had significantly increased startle responses compared to L-NPA + vehicle (193.4 ± 14.4 AU, $p = .002$), and vehicle + vehicle ($p < .001$). The habituation of startle responses over the course of the startle sequence are shown for (b) L-NAME, (c) L-NIO, and (d) L-NPA. Data are presented as mean ± SEM, and were analysed by three-way ANOVA with Tukey's multiple comparisons. **; $p < .01$; ***, $p < .001$ compared with corresponding vehicle control; ###, $p < .001$ compared with vehicle + vehicle. n = 12 per group, except L-NAME + vehicle and L-NIO + vehicle, n = 11.

5.4.2 Locomotor activity

The locomotor activity (LMA) of mice in an open field was quantified before and after drug administrations. **Figure 5.4** shows that mice habituated to the novel environment of the open field arena before drug administration, and how the distance travelled by mice was significantly increased with PCP treatment. This change in LMA was partially reversed with pretreatment with L-NAME, and with L-NIO, but not with L-NPA. All PCP-treated groups with NOS inhibition were significantly different from vehicle + vehicle. There was no significant difference between groups during the habituation trial, i.e. before drug administrations, and the distance travelled declined over time in all groups. This trend continued following administrations of vehicle + vehicle and with the NOS inhibitors + vehicle. The peak velocity in the vehicle + PCP group occurred at 30 mins following PCP in groups pretreated with vehicle and L-NIO. Whereas, velocities with L-NAME and L-NPA, + PCP, peaked at 20 mins. There was a highly significant overall influence of PCP treatment ($F_{1,191} = 829.9$, $p < .001$) and of the NOS inhibitors ($F_{3,191} = 94.5$, $p < .001$), and there was a significant interaction between these ($F_{3,191} = 101.6$, $p < .001$). Mouse velocity significantly altered between the 10 min time bins that were sampled ($F_{5,191} = 8.7$, $p < .001$), and this interacted with PCP treatment ($F_{5,191} = 14.4$, $p < .001$), but not with NOS inhibition, and there was a trend towards a significant interaction between time and both drug treatments ($F_{15,191} = 1.7$, $p = .07$).

A significant increase in the time spent in the inner arena of the open field box was observed in mice following vehicle + PCP administration compared to vehicle + vehicle, as shown in Figure 5.5a. No other drug combination altered this behaviour. Figure 5.5b shows how the number of rotations made by mice was highly significantly increased with PCP + vehicle. L-NAME pretreatment partially reversed this, but L-NIO, and L-NPA did not. The number of rotations of mice following administration of drugs was

significantly influenced by PCP ($F_{1,47}$ = 99.3, p < .001), and by NOS inhibitors ($F_{3,47}$ = 3.0, p = .04), and there was a significant interaction between these ($F_{3,47}$ = 5.6, p = .003).

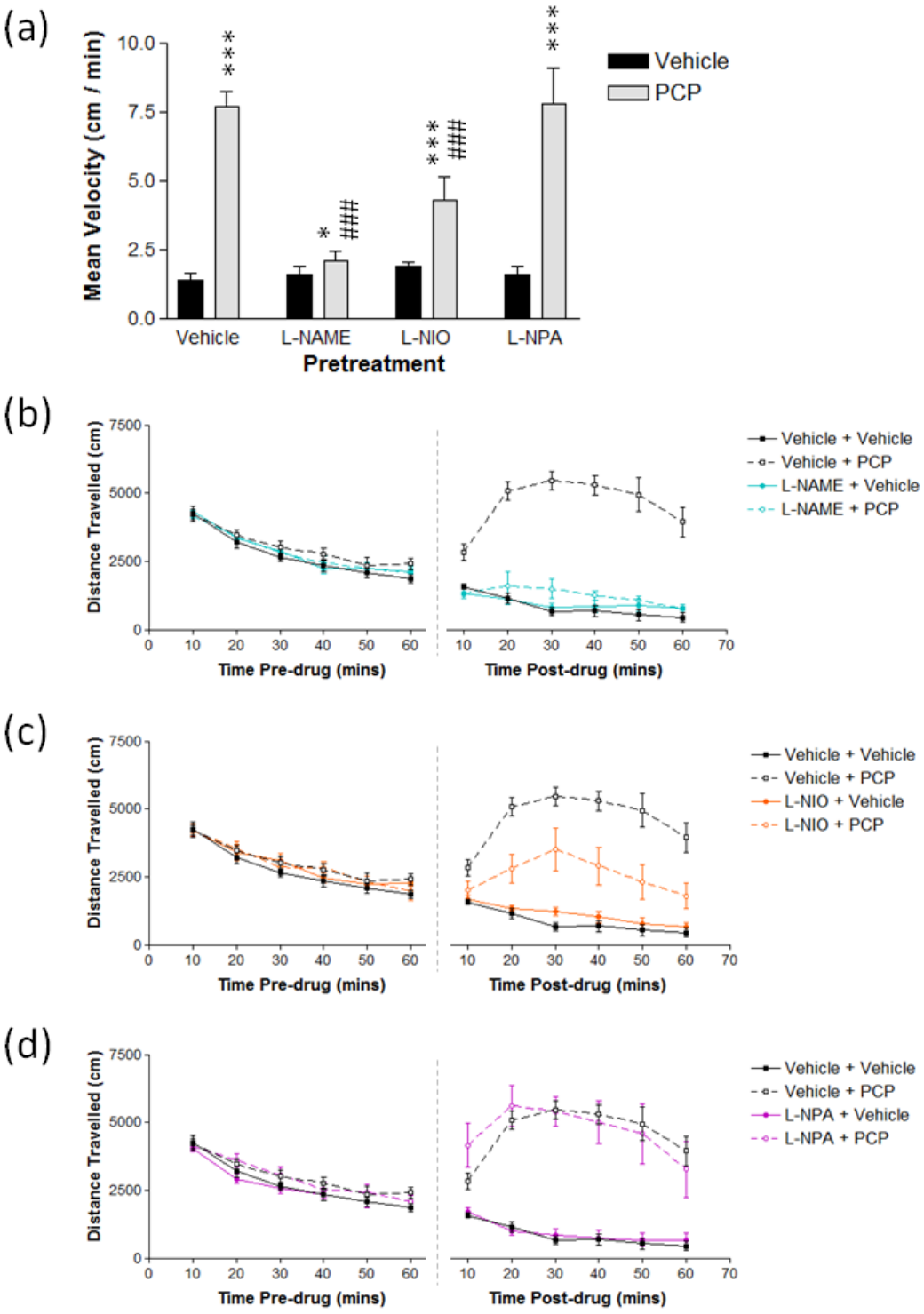
(a)
Mean Velocity (cm / min)
10.0
7.5
5.0
2.5
0.0
Vehicle
L-NAME
L-NIO
L-NPA
Pretreatment
Vehicle
PCP
(b)
Distance Travelled (cm)
Time Pre-drug (mins)
Time Post-drug (mins)
Vehicle + Vehicle
Vehicle + PCP
L-NAME + Vehicle
L-NAME + PCP
(c)
Distance Travelled (cm)
Time Pre-drug (mins)
Time Post-drug (mins)
Vehicle + Vehicle
Vehicle + PCP
L-NIO + Vehicle
L-NIO + PCP
(d)
Distance Travelled (cm)
Time Pre-drug (mins)
Time Post-drug (mins)
Vehicle + Vehicle
Vehicle + PCP
L-NPA + Vehicle
L-NPA + PCP

Figure 5.4. PCP-induced hyperlocomotion is reversed with NOS inhibition. The distance travelled by mice in an open field arena was quantified 60 mins before and after administration of saline vehicle, 40 $mg.kg^{-1}$ L-NAME, 20 $mg.kg^{-1}$ L-NIO or 20 $mg.kg^{-1}$ L-NPA for 15 mins, and vehicle or 5 $mg.kg^{-1}$ PCP. (a) There was a highly significant increase in the mean velocity of mice following administration of vehicle + PCP (8.2 ± 0.4 $cm.min^{-1}$, $p < .001$) compared to the vehicle + vehicle group (1.5 ± 0.2 $cm.min^{-1}$). In PCP-treated mice, velocity was significantly attenuated with L-NAME (2.4 ± 0.3 $cm.min^{-1}$, $p < .001$), L-NIO (4.5 ± 0.6 $cm.min^{-1}$, $p < .001$), but not by (c) L-NPA (8.0 ± 0.7 $cm.min^{-1}$), compared to vehicle + PCP. Each NOS drug + PCP gave velocities that were significantly different from vehicle + vehicle treatment (L-NAME, $p = .04$; L-NIO, $p < .001$; L-NPA, $p < .001$). There were no significant differences between groups before drug administrations, and the presented statistical values are from responses following drug administrations. The distances travelled over time are presented for (b) L-NAME, (c) L-NIO, and (d) L-NPA, and the vehicle + vehicle and vehixle + PCP groups are presented in all three graphs for comparison with the other groups. Data are presented as mean ± SEM, and were analysed using three-way ANOVAs with Tukey's multiple comparisons. *; $p < .05$; ***, $p < .001$ compared with vehicle + vehicle; ###, $p < .001$ compared with vehicle + PCP; n = 6 per group.

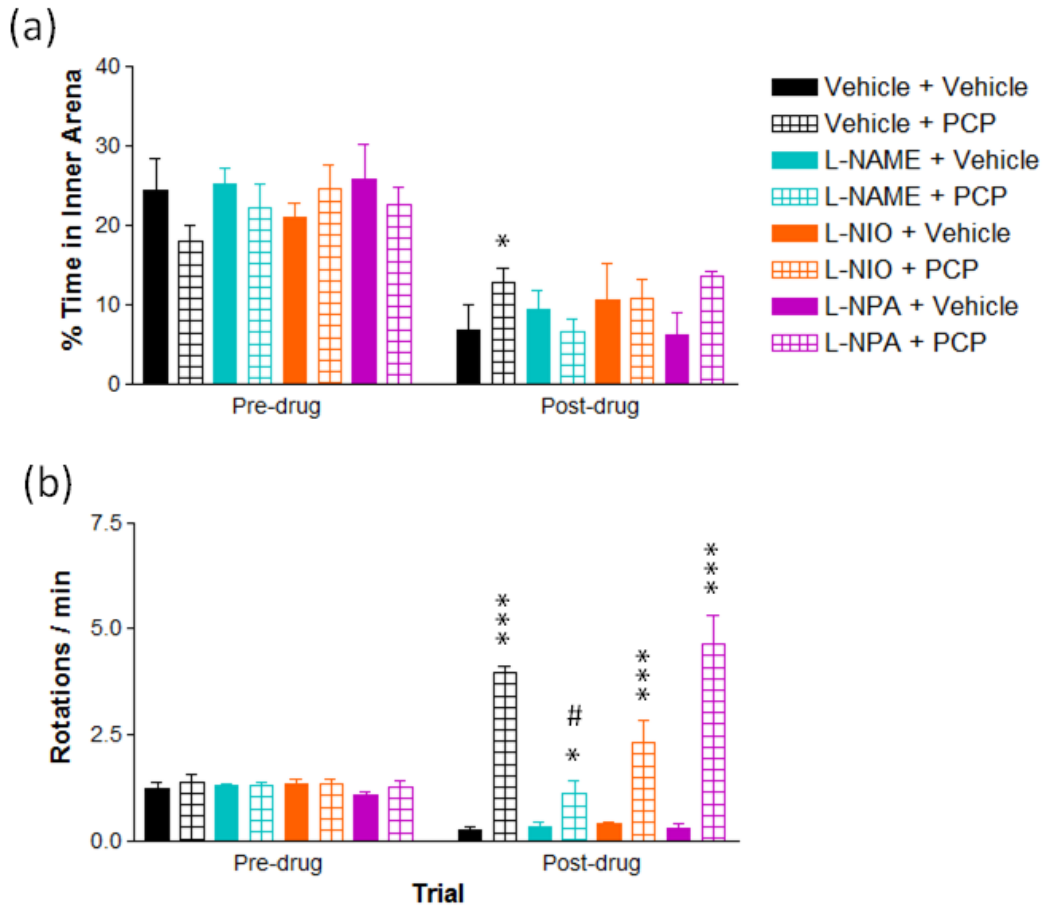

Figure 5.5. PCP alters locomotor activities: minimal influence of NOS inhibitiors. The locomotor activity of mice in an open field arena was quantified 60 mins before and after administration of saline vehicle, 40 mg.kg^{-1} L-NAME, 20 mg.kg^{-1} L-NIO or 20 mg.kg^{-1} L-NPA for 15 mins, and vehicle or 5 mg.kg^{-1} PCP. (a) The time spent in the inner arena of open field boxes was significantly increased in mice administered vehicle + PCP (12.7 ± 1.8 % of total time, median = 16.3 %, p = .045), and there was a trend towards a significant increase with L-NPA + PCP (13.5 ± 0.6 % of total time, median = 13.6 %, p = .053), compared to vehicle + vehicle (6.7 ± 3.2 % of total time, median = 2.3 %). There was a trend towards a significant decrease in time spent in the inner arena with L-NAME (6.6 ± 1.6 % of total time, median = 6.5 %, p = .053) compared to vehicle in the PCP group. No group was significantly different from the vehicle + vehicle group before drug administrations. These data were analysed using Kruskal-Wallis tests with Dunn's multiple comparisons. *, p < .05 compared to vehicle + vehicle (Dunn). (b) Rotating behaviour was significantly increased with vehicle + PCP (4.0 ± 0.16 rotations per min, p < .001), L-NAME + PCP (1.3 ± 0.05 rotations per min, p = .02), L-NIO + PCP (2.3 ± 0.54 rotations per min, p < .001), and by L-NPA + PCP (4.6 ± 0.68 rotations per min, p < .001), compared to vehicle + vehicle (0.2 ± 0.06 rotations per min). L-NAME significantly attenuated (p = .047) the rotating behaviour compared to vehicle treatment in the PCP group, as determined by two-way ANOVA with Tukey's multiple comparisons. There was no difference between groups tested before drug administrations. n = 6 per group. Data are presented as mean ± SEM. *, p < .05; ***, p < .001, compared to vehicle + vehicle. #, p < .05 compared to vehicle + PCP (Tukey).

5.5 NADPH-diaphorase activity in the hippocampus and reticular thalamus

Hippocampal NADPH-diaphorase activity was determined in neurones in the dentate gyrus (DG), CA1 and CA3. As illustrated by Figure 5.6, NADPH-diaphorase staining was most intense in the neuropil adjacent to the pyramidal cell layer of the CA1 and CA3 in the stratum oriens and stratum radiatum, and in the inner molecular layer of the dentate gyrus. Few NADPH-diaphorase positive cells were present in the CA2, and so this region was excluded from analysis. The mean intensity of neuronal NADPH-diaphorase staining in the DG, CA1 and CA3 are given in Table 5.1. Figure 5.7a shows how the general pattern of staining overall in the hippocampal results was a highly significantly increased staining with acute PCP, and this was reversed in groups pretreated with the NOS inhibitors (L-NAME, L-NIO, or L-NPA), as determined by two-way ANOVA. *Post hoc* analysis of hippocampal subfields revealed that L-NAME pretreatment significantly attenuated NADPH-diaphorase activity in the CA3 with PCP, as shown in Figure 5.6d, but not in the DG or CA1, as determined using Tukey's multiple comparisons. Changes in the DG, CA1 and CA3 were not detected with L-NIO or L-NPA pretreatment, and no NOS inhibitor significantly influenced NADPH-diaphorase activity in vehicle groups.

Hippocampal blood vessels were observed as discontinuous, ribbon like, and were generally less intensely stained than neurones, as illustrated in Figure 5.6e. Only vessels that were present in the longnitudinal, and not the transverse were sampled. The intensities of NADPH-diaphorase staining of blood vessels in the hippocampus are given in Table 5.2. Figure 5.7e shows how blood vessel NADPH-diaphorase staining was not influenced by drug treatments.

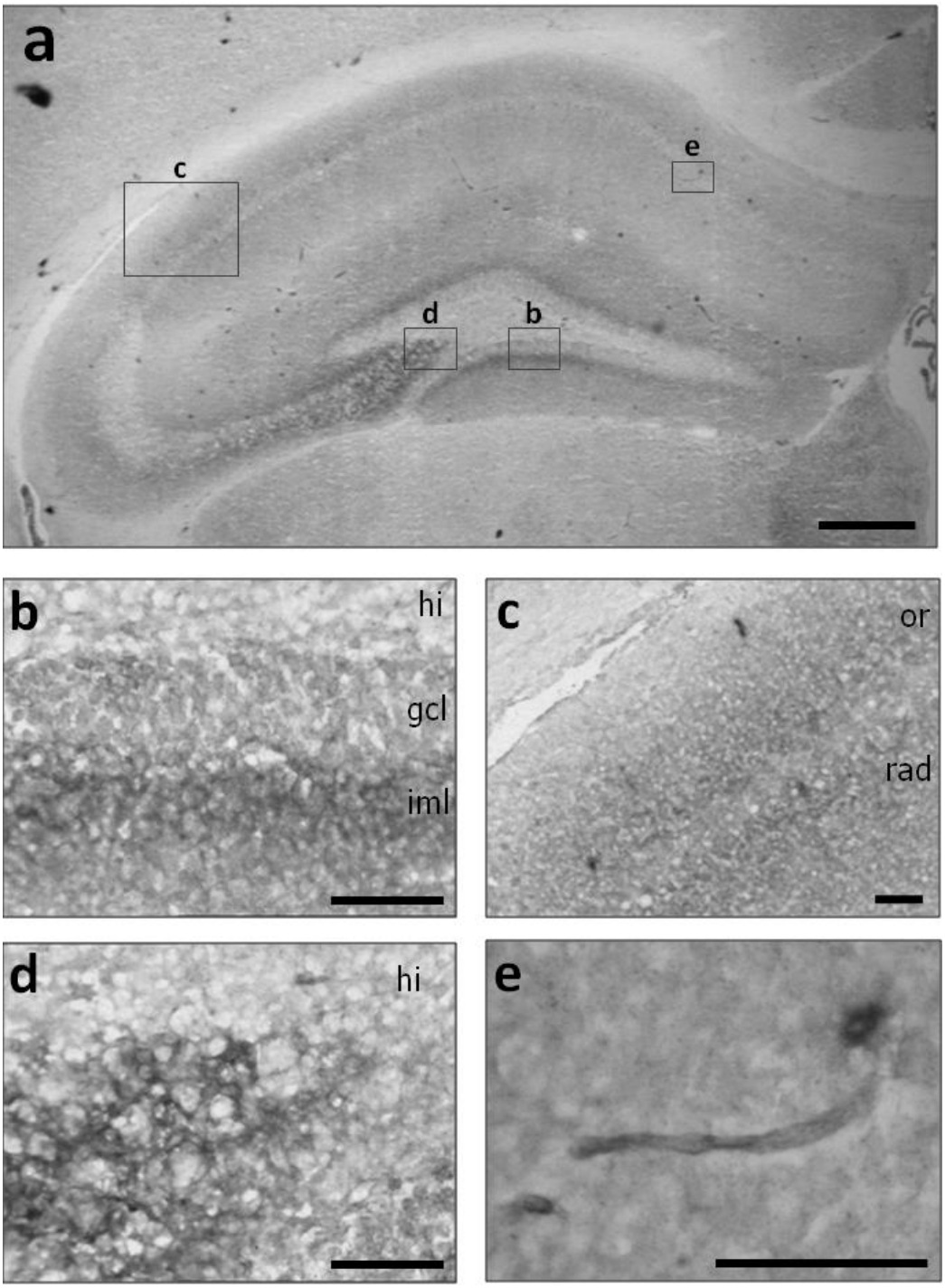

Figure 5.6. NADPH-diaphorase staining in the mouse hippocampus. (**a**) Cellular localisation of formazan product from NADPH-diaphorase histochemistry in the mouse hippocampus is prominent in the (**b**) inner molecular layer (iml), and less so in the graule cell layer (gcl) of the dentate gyrus, (**c**) neuropil of the stratum oriens (or) and radiatum (rad) in the CA1, and (**c**) in the CA3, especially where it invades the hilus (hi). (**e**) Blood vessels were discriminated from neurones by their ribbon-like morphology. Scale bars = (**a**) 300 µm, (**b**, **c**, **d** & **e**) 50 µm.

Table 5.1. Neuronal NADPH-diaphorase staining intensity in the hippocampus and thalamus.

Brain Region		Vehicle			L-NAME			L-NIO			L-NPA		
		ROD	**SEM**	***n***	**ROD**	**SEM**	***n***	**ROD**	**SEM**	***n***	**ROD**	**SEM**	***n***
DG	**Vehicle**	103.5	4.2	6	104.8	6.0	6	102.4	3.7	6	108.7	9.6	6
	PCP	112.1	6.4	6	101.2	6.3	6	108.9	5.4	6	99.9	7.5	6
CA1	**Vehicle**	84.2	5.3	6	82.6	4.7	6	85.6	3.7	6	88.4	8.9	6
	PCP	93.7	6.1	6	82.1	5.7	6	84.8	4.8	6	93.9	8.5	6
CA3	**Vehicle**	118.7	5.2	6	117.0	5.6	6	116.4	5.0	6	121.5	8.9	6
	PCP	128.1	7.3	6	114.3*	7.5	6	116.4	6.9	6	116.5	9.2	6
RtThal	**Vehicle**	49.2	3.5	6	50.8	2.0	6	49.4	1.8	6	51.6	4.9	6
	PCP	50.8	2.7	6	46.3	5.9	6	50.7	4.2	6	45.8	2.3	6

The mean relative optical density (ROD) of NADPH-diaphorase staining intensity in neurones in the hippocampus (dentate gyrus, DG; CA1 and CA3) and in the reticular thalamus (RtThal) of mice 90 mins following acute PCP (5 $mg.kg^{-1}$) or vehicle, and following 105 mins treatment with a nitric oxide synthase inhibitor (40 $mg.kg^{-1}$ L-NAME, 20 $mg.kg^{-1}$ L-NIO, or 20 $mg.kg^{-1}$ L-NPA). Overall hippocampal NADPH-diaphorase staining intensity was significantly increased with vehicle + PCP treatment ($p < .001$), and this was attenuated in mice pretreated with L-NAME ($p < .001$), L-NIO ($p < .01$) or L-NPA ($p < .001$), as determined by two-way ANOVA. Comparisons of drugs treatments in hippocampal subfields using Tukey's tests detected a significant attenuation of NADPH-diaphorase staining in the CA3 with L-NAME + PCP ($p = .04$, *****), compared to vehicle + PCP. *Post hoc* analyses revealed no other differences between drug treatments in the DG, CA1, or in the reticular thalamus.

Table 5.2. Blood vessel NADPH-diaphorase staining intensity in the hippocampus and thalamus

Brain Region		Vehicle			L-NAME			L-NIO			L-NPA		
		ROD	**SEM**	***n***	**ROD**	**SEM**	***n***	**ROD**	**SEM**	***n***	**ROD**	**SEM**	***n***
Hipp	**Vehicle**	83.6	5.0	6	81.4	4.4	6	82.9	5.7	6	84.9	2.3	6
	PCP	86.0	7.0	6	82.4	5.8	6	84.3	2.6	6	85.7	9.4	6
RtThal	**Vehicle**	44.6	3.6	6	39.8	2.8	6	41.0	2.9	6	42.8	5.2	6
	PCP	44.8	4.3	6	46.7	3.7	6	36.5	3.4	6	44.4	3.4	6

The mean relative optical density (ROD) of NADPH-diaphorase staining intensity in blood vessels in the hippocampus and in the reticular thalamus (RtThal) of mice 90 mins following acute PCP (5 mg.kg-1) or vehicle, and following 105 mins treatment with a nitric oxide synthase inhibitor (40 mg.kg-1 L-NAME, 20 mg.kg-1 L-NIO, or 20 mg.kg-1 L-NPA). No changes in NADPH-diaphorase staining intensity were detected between drug treatments in the hippocampus or reticular thalamus. Data were analysed by one-way ANOVAs with Tukey's multiple comparisons.

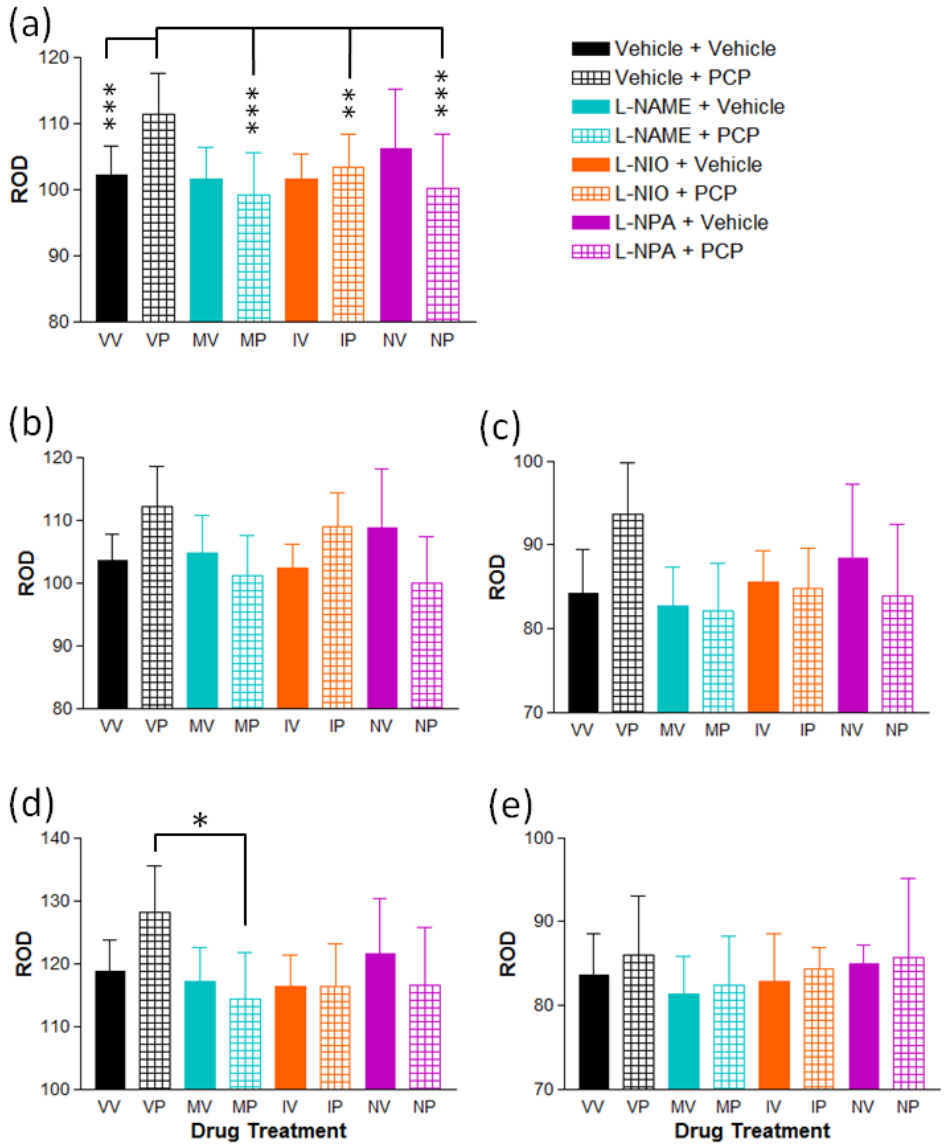

Figure 5.7. L-NAME attenuates PCP-induced increase in CA3 NADPH-diaphorase activity. The relative optical density (ROD) of hippocampal NADPH-diaphorase staining was significantly influenced by drug treatment ($F_{7,143}$ = 7.0, p < .001) and significantly different between hippocampal subfields ($F_{2,143}$ = 332.0, p < .001). (**a**) Overall hippocampal NADPH-diaphorase activity was significantly increased by 5 mg.kg^{-1} PCP (vehicle + PCP, p < .001), compared to vehicle + vehicle treatment, and this was reversed with pretreatment with L-NAME (40 mg.kg^{-1}; p < .001), L-NIO (20 mg.kg^{-1}; p = .007) and L-NPA (20 mg.kg^{-1}; p < .001). No significant diifferences between drug treatments was detected in the (**b**) dentate gyrus, or (**c**) the CA1 regions of the hippocampus. (**d**) A significant decrease in NADPH-diaphorase relative optical density (ROD) was observed in the CA3 in mice administered PCP with L-NAME pretreament (L-NAME + PCP; 114.3 ± 7.5 ROD, p = .04) compared to vehicle administration (vehicle + PCP; 128.1 ± 7.3 ROD), as determined by two-way ANOVA with Tukey's multiple comparisons. (**e**) No significant differences between drug treatments were detected in hippocampal blood vessels, as determined by one-way ANOVA with Tukey's multiple comparisons. Data are presented as mean ± SEM, n = 6 per group. Abbreviations: V, vehicle; P, PCP; M, L-NAME; I, L-NIO; N, L-NIO.

NADPH-diaphorase activity was determined in the reticular thalamus 105 mins following administration of a NOS inhibitor or vehicle, and 90mins following PCP or vehicle. The intensity of staining in the reticular thalamus was less intense than that found in the hippocampus, as summarised in Table 5.1. Figure 5.8a shows how NADPH-diaphorase activity with vehicle + vehicle (49.2 ± 3.5 ROD, n = 6) was unchanged in neurones by other drug treatments. The largest activity increase observed was found with L-NPA + vehicle (51.6 ± 4.9 ROD, n = 6), and the largest decrease was seen with L-NPA + vehicle (45.8 ± 2.3 ROD, n = 6). However, these changes were insufficient to meet significance. Figure 5.8b shows how NADPH-diaphorase activity was unchanged in blood vessels following drug treatments. The largest change from mean vehicle (44.6 ± 3.6 ROD, n = 6) was observed with L-NIO + PCP (36.5 ± 3.4 ROD, n = 6), but was not sufficient to meet significance, as determined by one-way ANOVA with Tukey's multiple comparisons. These data are summarised in Table 5.2.

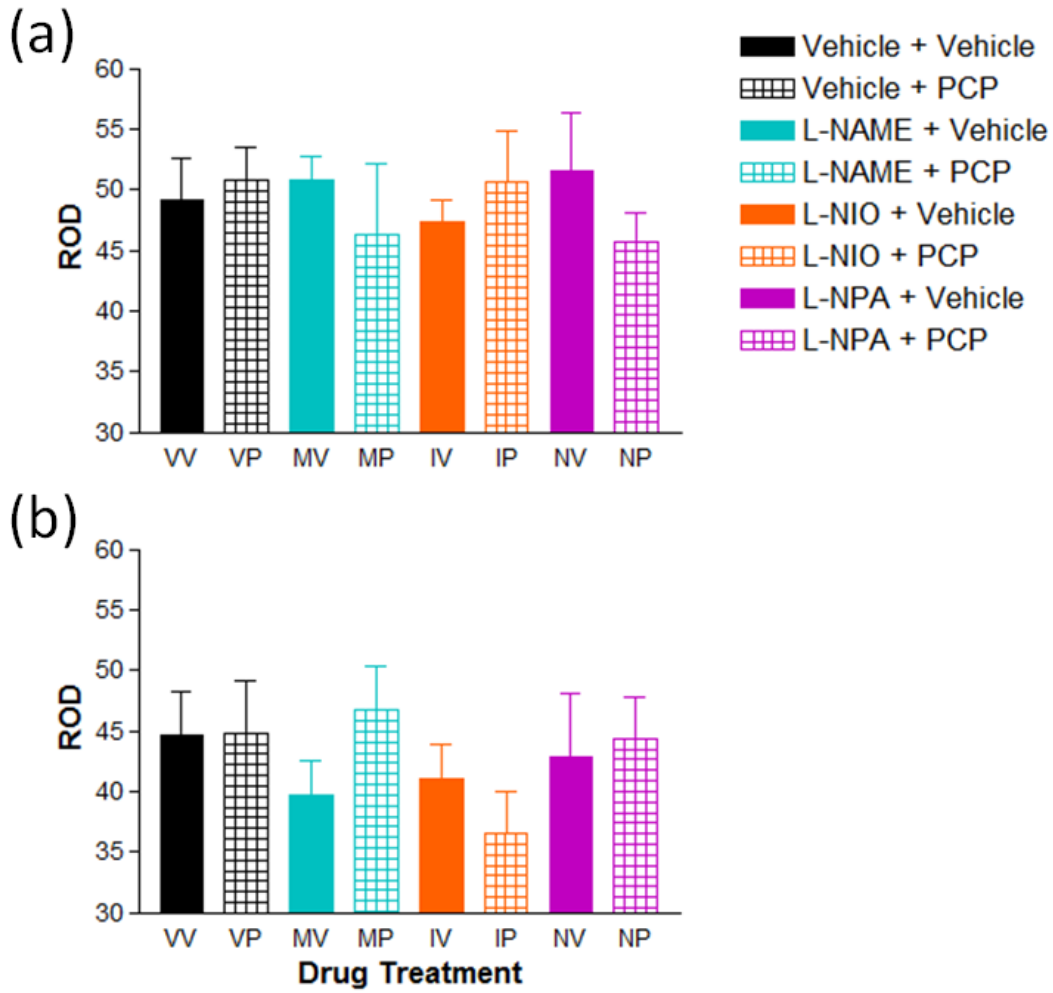

Figure 5.8. NADPH-diaphorase activity is unchanged in the reticular thalamus following antagonism of NMDA receptors and NOS. The relative optical density (ROD) of NADPH-diaphorase staining was determined in the reticular thalami of mice following administration of NOS inhibitors (40 mg.kg^{-1} L-NAME, 20 mg.kg^{-1} L-NIO, 20 mg.kg^{-1} L-NPA, or vehicle) and 5 mg.kg^{-1} PCP or vehicle. No significant differences between drug treatments were detected in (**a**) neurones, or (**b**) blood vessels, as determined by one-way ANOVAs with Tukey's multiple comparisons. Data are presented as mean ± SEM, n = 6 per group. Abbreviations: V, vehicle; P, PCP; M, L-NAME; I, L-NIO; N, L-NIO.

5.6 Discussion

The main findings presented here are that non-selective inhibition of NOS by L-NAME, and more-selective inhibition of eNOS by L-NIO was sufficient to partially reverse PCP-induced hyperlocomotion. L-NAME partially reversed the increased rotational locomotion observed in the presence of PCP, and only L-NIO was sufficient to reverse the PPI deficit elicited by PCP. Selective inhibition of nNOS by L-NPA did not influence these deficits. Startle reactivity was enhanced by L-NAME or L-NPA plus PCP, and L-NIO had the inverse effect. These suggest a differential role of NOS isoforms in PCP-mediated behaviours. The non-selective inhibition of NOS via L-NAME, but not the more selective inhibition of eNOS and nNOS (via L-NIO and L-NPA, respectively), was sufficient to reverse the PCP-induced stimulation of NOS and is suggestive that both constitutive isoforms of NOS contribute to this effect in the hippocampus.

5.6.1 Reversal of behavioural deficits with NOS inhibitors

PCP was found to induce deficits in PPI and LMA in mice in Chapter 4., and these findings were replicated here. These effects are also widely reported in rodent models of relevance to schizophrenia (reviewed by: Jones et al., 2011). Hyperlocomotion and a decrease in PPI was observed in mice administered acute PCP. Pretreatment with L-NAME or L-NIO partially reversed the hyperlocomotor activity elicited by PCP, and pretreatment with L-NIO reversed the PCP-induced deficit in PPI. Non-selective inhibition of NOS has been shown previously to reverse PCP-induced hyperlocomotion (Johansson, 1998; Klamer et al., 2004a) and PPI (Johansson *et al.*, 1997), and the inverse has also been shown (Bujas-Bobanovic *et al.*, 2000). In contrast to the findings presented here, Klamer and colleagues (2004b) have also shown that L-NPA may reverse PCP-induced deficits in LMA and PPI. Though, the dose of PCP used in this study (4 $mg.kg^{-1}$) was less than used here (5 $mg.kg^{-1}$); this was still sufficient to elicit behavioural deficits and so

the likely explanation for this contrast is in the strain of mice used (NMRI mice, while C57BL6J mice were used here). Differences in NOS expression have been shown between mouse strains (Blackshaw *et al.*, 2003), and behavioural responses can vary even between substrains of mice (Matsuo *et al.*, 2010).

The behavioural deficits observed here may be related to the interaction of nitric oxide with dopamine transmission (Sams-Dodd, 1998b; Geyer et al., 2001; Del Bel et al., 2005). Nitric oxide may modulate dopamine release in the cortex (Smith and Whitton, 2001), hippocampus (Segieth *et al.*, 2000) and striatum (Liang and Kaufman, 1998; Rocchitta et al., 2005). NMDA receptor-mediated dopamine release may be modulated by nitric oxide (West and Galloway, 1997), and the interactions of these neurotransmitters may also reciprocally influence NOS activity (Park and West, 2009). PCP-induced hyperlocomotion and deficits in PPI have been shown to be reversed with selective nNOS inhibition, but this is not the case with amphetamine (Johansson *et al.*, 1999). This is also the case with non-selective inhibition with L-NAME (Johansson, 1998). Complicating the matter, (non-selective) NOS inhibition may influence deficits induced by indirect (i.e. amphetamine) and by more direct (e.g. apomorphine) agonism of dopamine (Hong et al., 2005; Salum et al., 2006; Salum et al., 2011), and this is appears to be brain region-specific. Dopamine transmission may be modulated by nitric oxide, involving the *S*-nitrosylation of monoamine transporters (Kiss and Vizi, 2001; Eyerman and Yamamoto, 2007) and L-type calcium channels (Rocchitta *et al.*, 2005). NOS activity may also be differentially modulated by dopamine D1 and D2 receptor activities (Morris et al., 1997; Hoque et al., 2010), and nitric oxide may also modulate dopamine signalling (Liang and Kaufman, 1998). An aspect for further study would be to test the efficacy of the NOS inhibitors used here with amphetamine to further study the role of NOS isoforms in the modulation of dopamine-mediated behavioural deficits.

Nitric oxide interactions with other neurotransmitters may also contribute to the observed behavioural deficits. Glutamate and GABA release may also be modulated by nitric oxide signalling (Getting et al., 1996; Segovia and Mora, 1998), and NMDA receptor-stimulated acetylcholine release may be mediated by nNOS (Buchholzer and Klein, 2002). Glutamate receptors, including AMPA (Selvakumar *et al.*, 2009) and NMDA (Choi *et al.*, 2000) subtypes may be modulated by *S*-nitrosylation, as can nNOS itself (Qu *et al.*, 2012) and the scaffold protein that links it to NMDA receptors (Ho *et al.*, 2011). It should be noted that nitric oxide-mediated alterations in monoamine and choline transmitters are not found by all (Yamada et al., 1996; Kaye et al., 2000). PCP-induced hyperlocomotion is likely mediated by increased dopamine transmission (Sams-Dodd, 1998b), and the PPI deficits may be mediated by multiple neurotransmitters, including these discussed here (Geyer et al., 2001; Bosch and Schmid, 2008). Suffice it to say, NOS has multiple, and reciprocal interactions with neurotransmitter systems that may contribute to the behavioural deficits observed here.

Increased NOS activity coincident with NMDA receptor antagonism gives some indication of how NOS inhibitors may mitigate some of the deficits found with glutamatergic dysfunction, and that nitric oxide appears to have a role in these deficits. NOS inhibitors may displace PCP from its NMDA receptor binding site (Klamer et al., 2005b). Increased nitric oxide generation may also prevent the binding of PCP by arresting NMDA receptor activity via *S*-nitrosylation (Choi *et al.*, 2000), as the antagonist is use-dependent (Fagg, 1987).

An interesting finding was the differential startle reactivity of mice to the NOS inhibitors, as shown in Figure 5.3. Here, L-NAME and L-NPA with PCP increased startle responses, and L-NIO had the opposite effect. The functional relevance to the data presented in Figure 5.2 is negligible, as PPI is calculated as a function of the startle response of an individual. However,

the altered startle reactivity may be related to anxiety state, and if so, may imply a differential role of eNOS and nNOS as being anxiolytic and anxiogenic, respectively. No anxious-related behaviours were observed in the open field with the NOS inhibitors, such as time spent in the inner arena of boxes (Figure 5.5). It would be an interesting future course to study the effects of the NOS inhibitors in behavioural assays more relevant, such as elevated plus maze and social interaction/withdrawal.

NOS inhibitors have been shown to induce catalepsy (Del Bel et al., 2005; Iacopucci et al., 2012), and may explain the attenuation of PCP-induced hyperlocomotion with L-NAME and L-NIO shown in **Figure 5.4**, and may even contribute to the enhanced PPI responses with L-NAME and L-NIO shown in Figure 5.2a & b, and the decreased startle responses seen with L-NIO in Figure 5.3b. NOS inhibitor-induced catalepsy is unlikely in this case as the LMA of mice administered NOS inhibitors did not fall below that of vehicle controls, as shown in **Figure 5.4**. There is no evidence in the behavioural observations of mice that indicate that catalepsy was induced by the NOS inhibitors during experiments.

As illustrated in Table 3.1., L-NIO is not as strongly selective for eNOS as L-NPA is for nNOS. Therefore, inferences about this drug's effects being purely eNOS related are confounded by the possibility of its interactions with the other NOS isoforms. However, these inferences are strengthened by the reductive inference by the non-selective inhibition of NOS by L-NAME and the selective inhibition of nNOS by L-NPA. It should be noted that the selectivity of L-NPA has recently been brought to question (Pigott *et al.*, 2013). Another possible explanation for the findings observed with L-NAME and L-NIO are the inhibition of the inducible isoform of NOS. The use of a selective iNOS inhibitor such as aminoguanidine with PCP would address this, but was outside of the scope of this study as the focus was on the constitutive isoforms of NOS.

The lack of effects of L-NPA in the behavioural measures may be due to poor blood-brain barrier penetration of the drug, and therefore may not be present in sufficient levels to inhibit nNOS in the brain. However, (Klamer et al., 2004b) found L-NPA to reverse PCP-induced deficits in PPI and hyperlocomotion, and the overall influence of L-NPA with PCP in the hippocampal NADPH-diaphorase staining, presented in Figure 5.7, suggests otherwise.

Non-selective inhibition of NOS may affect cardiovascular function, and selective nNOS inhibition may not (Johansson *et al.*, 1999). The implications for the findings presented here are two-fold: altered cardiovascular function may influence the behavioural output of an animal, and the drugs identified as efficacious here may not be suitable therapeutically because of this unwanted effect. Targeting nNOS is attractive for its minimal influence on cardiovascular function (Moore et al., 1993; Johansson et al., 1999), but as shown in this report, this target is perhaps not suitable to reverse PCP-mediated deficits. As shown in Chapter 3.4, L-NAME and L-NPA appear only to be effective in inhibiting activated NOS, and therefore may lend to a state-dependent selectivity of these inhibitors. Non-selective inhibition of NOS did not alter blood vessel NADPH-diaphorase activity, as discussed below. However, the systemic effects of these were not a feature in these experiments, and are worthy of future study to elucidate any influences that systemic NOS inhibition has on the behavioural findings presented here.

5.6.2 Histochemical findings

The alterations in neuronal NADPH-diaphorase activity elicited by PCP in the hippocampus and reticular thalamus, as found in Chapter 4, were not replicated here. In Chapter 4, NADPH-diaphorase activity with acute PCP in mice was significantly increased in hippocampal homogenates, and significantly decreased in histochemical sections of the reticular thalamus. Overall, there was a highly significant influence of PCP in hippocampal

neurones, and not in blood vessels, as shown in Figure 5.7. No individual subfield met significance with the influence of vehicle + PCP. This was also the finding in previous histochemical findings (Figure 4.3b hipp diaph histo), and therefore may reflective of a general insensitivity of NADPH-diaphorase histochemistry to detect possible alterations in NOS activity. The effect of acute PCP was also lost in the reticular thalamus that was shown in (Figure 4.3c). A possible explanation for these discrepancies is that these samples were taken at a later time-point than those used in Chapter 4. These brains were collected 90 mins following PCP/vehicle administration, while those used in the previous chapter were collected 60 mins earlier. The locomotor activity of these mice is suggestive of a peak activity between 20 and 30 mins following drug administration, whereupon activity diminishes. The influences of these drugs on NADPH-diaphorase may have recovered from this peak activity, and therefore may not persist 90 mins after administration.

Figure 5.7 shows an overall significant influence of PCP on hippocampal neurones, and that this is reversed by each of the NOS inhibitors used. However, no change in NOS activity was detected in the absence of PCP with the NOS inhibitors. In Chapter 3, L-NAME reversed glutamate-stimulated nitric oxide generation, but not that of basal activity in cultured hippocampal neurones. In contrast, L-NPA inhibited both basal and glutamate-stimulated nitric oxide generation (Figure 3.7). Neither hippocampal nor thalamic NOS activity was altered in vehicle controls with the NOS inhibitors here, and may reflect a sensitivity of DAF-2DA imaging to detect changes over that with NADPH-diaphorase histochemistry. Alternatively, this may reflect an altered activity of the NOS inhibitors *in vivo* compared to that observed in neuronal cultures. This is possibly due to first-pass metabolism by using the intraperitoneal injection route in mice, and thus diminishing the availability of the NOS drugs. This may be tested by comparing different administration routes of NOS drugs (e.g. subcutaneous injection), and their influences on NADPH-diaphorase activity in the brain.

The targeted levels at which the hippocampus was sampled was -1.82 to -2.3 mm caudal to bregma, as determined using a mouse brain atlas (Paxinos and Franklin, 2001). As observed by Blackshaw and colleagues (2003), the expression of nNOS varies rostrocaudally. This has implications on the quantification of the density of NOS in this region. This has little impact on the data presented here as the cellular NADPH-diaphorase ROD was averaged per hippocampal region and no inferences were made about NOS-positive cellular densities. However, this study could be improved by using stereological methods to determine the full story of NOS activity within brain structures. However, given the labour involved in image analysis, such an approach would not be practical at this time.

A limitation of NADPH-diaphorase histochemistry is that cellular morphologies are not preserved. As illustrated by Figure 5.6, the staining in cells is localised to somata and proximal dendrites. However, the formazan dye accumulates within a cell, and may therefore alter the apparent cellular morphology and size. nNOS is expressed in a variety of hippocampal interneurones (Jinno and Kosaka, 2002; Liang et al., 2013), and a very interesting aspect for future study would be whether the influence of PCP is different between interneurone subtypes as this would provide more information on their possible functions in and outwith hippocampal circuits during NMDA receptor blockade.

5.7 Conclusions

The NOS inhibitors, L-NAME and L-NIO were found to reverse PCP-induced hyperlocomotion, and L-NIO also reversed the deficit in prepulse inhibition observed in PCP-treated mice. These behaviours were not altered with administration of L-NPA. Each drug reversed the overall increase in NOS activity in the hippocampi of mice treated with PCP, and L-NAME did so specifically in the CA3, but L-NIO and L-NPA did not.

The neurochemical findings with acute PCP and NOS inhibitor drugs presented here do not reflect what was found in prepulse inhibition and locomotor activity. This may be due to an inappropriate sample collection time or an insensitivity of NADPH-diaphorase histochemistry, for example. Further investigation is needed to explain these findings.

The results presented here reveal a differential influence of selective and non-selective NOS inhibition in PCP-treated mice. The neuronal isoform of NOS appears to not be involved in the behavioural and neurochemical deficits induced by PCP.

6 Tetrahydrobiopterin as a Target for the Modulation of Nitric Oxide Signalling

6.1 Introduction

Tetrahydrobiopterin (BH_4) is an essential cofactor for NOS activity, and has been implicated in promotion of dimerisation, NOS dimer stabilisation (Reif *et al.*, 1999), facilitating electron transfer (Alderton *et al.*, 2001). BH_4 is also a necessary for monoamine neurotransmitter synthesis as a cofactor for the aromatic amino acid hydroxylases phenylalanine hydroxylase, tyrosine hydroxylase, and tryptophan hydroxylase. BH_4 is synthesised, *de novo*, from guanosine triphosphate (GTP) in a chain reaction via GTP cyclohydrolase I (GTPCH), 6-pyruvoyltetrahydropterin synthase, and sepiapterin reductase. The efficacy of novel compounds that target BH_4 in the modulation of nitric oxide signalling will be explored in this chapter.

It is of interest to study novel compounds that modulate NOS to potentially discover therapeutic agents that may improve upon those currently available. It is also of interest to study compounds that modulate NOS by alternate targets as a means to elucidate mechanistic properties of NOS signalling. The most common inhibitors of NOS compete with arginine at the substrate binding site (reviewed by: Moore and Handy, 1997). However, arginine is essential for the metabolism of polyamines and glutamate, among others (reviewed by: Wu and Morris, 1998), and NOS inhibitors based on arginine competition may therefore have undesirable, nonselective effects. Unwanted effects may be reduced by using an alternative strategy to inhibit NOS activity. BH_4 and its precursor, sepiapterin, may promote NOS activity (reviewed by: Werner et al., 2003), and BH_4 has been shown to protect from superoxide ($O2^{-\bullet}$) damage (Kotsonis *et al.*, 2000). BH_4 is rapidly metabolised, and therefore, a more stable and longer-acting analogue may have more therapeutic potential.

NOS activity may be decreased by competitive BH_4 inhibitors (Pantke, *et al.*, 2001), and the GTPCH inhibitor, 2,4-diamino-6-hydroxypyrimidine (DAHP), has been shown to be an effective means to inhibit NOS (Wang *et al.*, 2008b). The efficacy of DAHP to modulate thioredoxin reductase and nitric oxide generation in neuronal cells will be compared to novel compounds that potentially inhibit NOS. 2-Amino-4-oxo-4,7-dihydro-3H-pyrrolo[2,3-*d*]pyrimidine-6-carboxylic acid ethyl ester (WSG2001) is an inhibitor of GTPCH (Gibson *et al.*, 2004). The influence of WSG2001 on NOS activity has yet to be determined. 2,6,7,7-Tetramethyl-7,8-dihydro-1-thia-3,3a,5,8,9-pentaazacyclopenta[*b*]naphthalen-4-one (WSG1023) is a novel, putative NOS inhibitor of unknown mechanism. The structures of these compounds are given in Figure 6.1.

6-acetyl-7,7-dimethyl-7,8-dihydropterin (ADDP; Figure 6.1b), is a BH_4 analogue that has been previously shown to activate NOS in macrophages and endothelial cells (Suckling *et al.*, 2008). The effectiveness of ADDP in the modulation of TrxR and NOS in neuronal cells is explored here.

6.2 Hypotheses and aim

It is hypothesised that NOS and TrxR activities in cerebellar granule cells will be altered in BH_4-deficient conditions and will normalise with the supplementation of a BH_4 analogue. The BH_4 analogue will not influence TrxR and NOS activities with unaltered BH_4 conditions. Inhibition of GTP cyclohydrolase I will inhibit NOS activity and thence stimulate TrxR activity via diminished BH_4 cofactor synthesis.

The aim of this work is to evaluate the novel BH_4-modulating drugs, ADDP and WSG2001, and the putative NOS inhibitor WSG1023 as a means to alter basal and calcium ionophore-stimulated nitric oxide signalling in neuronal cell cultures.

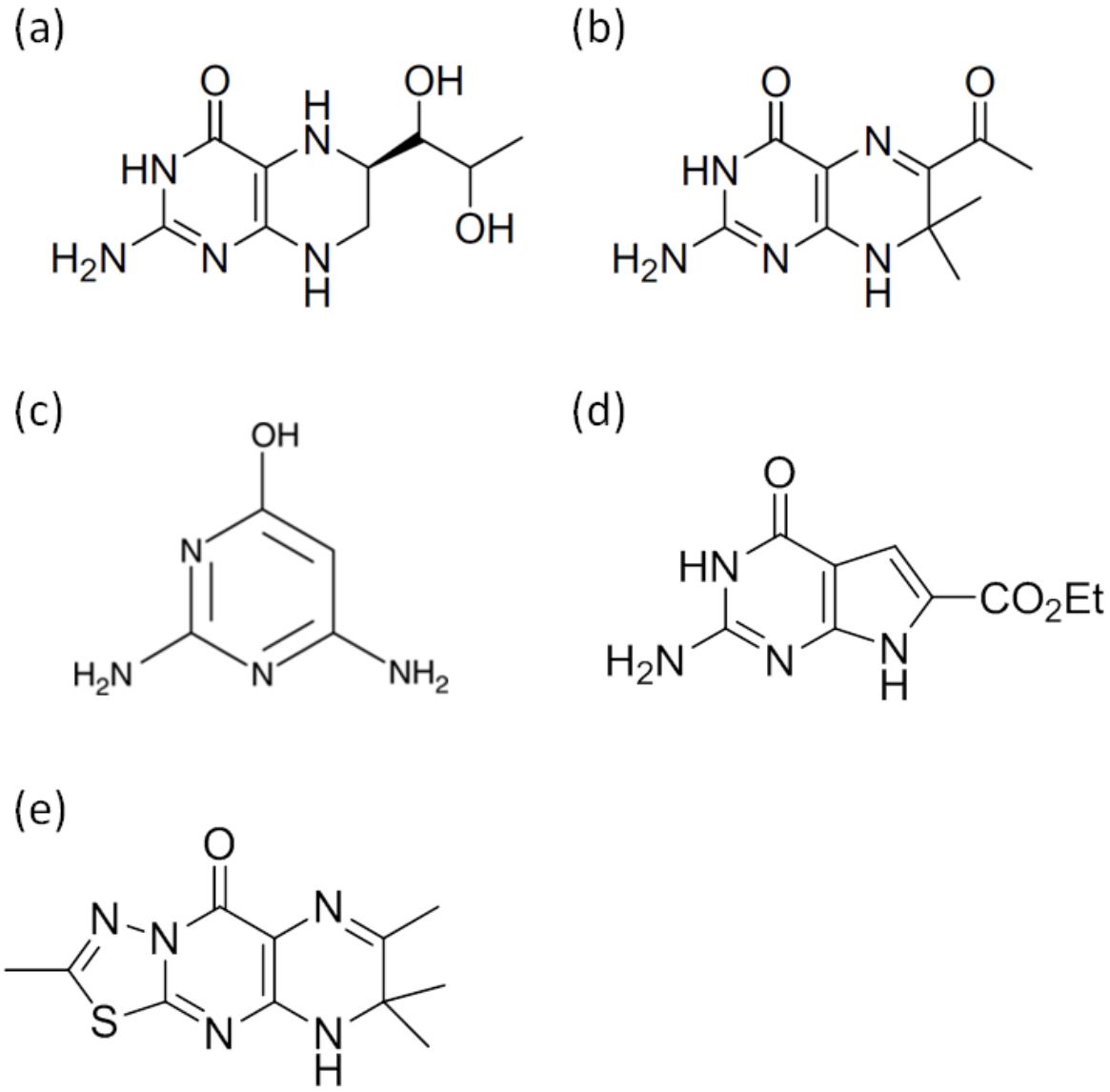

Figure 6.1. Chemical structures of NOS-modulating drugs. (**a**) Tetrahydrobiopterin (BH_4) is an essential cofactor for nitric oxide synthase (NOS) activity. (**b**) The structurally similar and chemically stable 6-acetyl-7,7-dimethyl-7,8-dihydropterin (ADDP), is a BH_4 analogue that may increase NOS activity. (**c**) 2,4-Diamino-6-hydroxypyrimidine (DAHP) is a GTP cyclohydrolase inhibitor that is commonly used to inhibit BH_4 synthesis. (**d**) 2-Amino-4-oxo-4,7-dihydro-3H-pyrrolo[2,3-*d*]pyrimidine-6-carboxylic acid ethyl ester (WSG2001) is a putative GTP cyclohydrolase inhibitor that may inhibit BH_4 synthesis. (**e**) 2,6,7,7-Tetramethyl-7,8-dihydro-1-thia-3,3a,5,8,9-pentaazacyclopenta[*b*]naphthalen-4-one (WSG1023) is a novel NOS inhibitor of unknown mechanism. DAHP, ADDP, WSG2001 and WSG1023 will be evaluated in efficacy to modulate NOS in neuronal cells.

6.3 Selective modulation of tetrahydrobiopterin

6.3.1 Activation of NOS using a BH_4 analogue

DAF-2T fluorescence was quantified in cerebellar granule cells (CGCs) following incubation with 4 mM DAHP or vehicle for 24 hours, 30 μM ADDP for 1 hour, and DAF-2DA for 30 mins. DAF-2T accumulated in the somata of neurones, as illustrated in Figure 6.2a. The relative fluorescence intensity (RFI) of DAF-2T in CGCs was 10.4 ± 1.1 RFI (n = 16) with vehicle, and 5.9 ± 0.7 RFI (n = 5) with DAHP pretreatment. **Figure 6.2**b shows how DAF-2T intensity was significantly increased in CGCs treated with ADDP, both with DAHP (18.7 ± 2.7 RFI, p = .002, n = 4), and without (23.5 ± 2.6 RFI, p = .001, n = 4), compared to their vehicle controls, as determined by two-way ANOVA with Tukey's multiple comparisons.

Thioredoxin reductase (TrxR) activity was determined in CGCs treated with a range of concentrations (1 – 100 μM) of ADDP for two hours. **Figure 6.2**c shows how there were no detectable changes in TrxR activity with ADDP. Parallel TrxR reactions of CGCs pretreated with 4 mM DAHP for 24 hours, similarly, did not respond to ADDP treatment. There was a trend towards a significant decrease in TrxR activity with 100 μM ADDP pretreated with DAHP (46.7 ± 16.6 % of vehicle, median = 56.4%, p = .068, n = 3), as determined by Kruskal-Wallis test with Dunn's multiple comparisons. 30 μM was the concentration of ADDP that gave rise to the largest difference between DAHP treatment (71.4 ± 17.7 % of vehicle) and without (148.8 ± 46.2 % of vehicle). This concentration was selected for DAF-2DA experiments in order to assess the influence of ADDP on nitric oxide generation in BH_4-depleted CGCs.

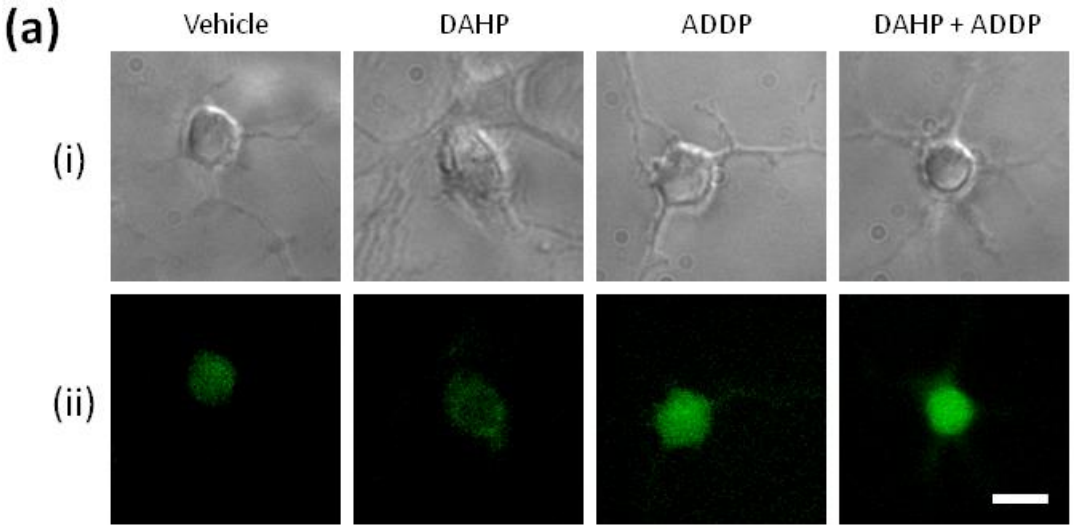
(a)
Vehicle
DAHP
ADDP
DAHP + ADDP
(i)
(ii)

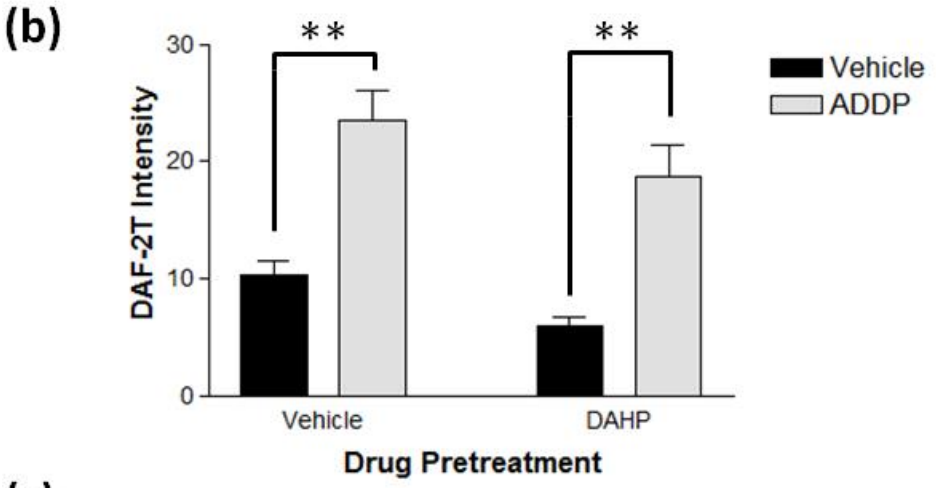
(b)
**
**
DAF-2T Intensity
30
20
10
0
Vehicle
DAHP
Drug Pretreatment
Vehicle
ADDP

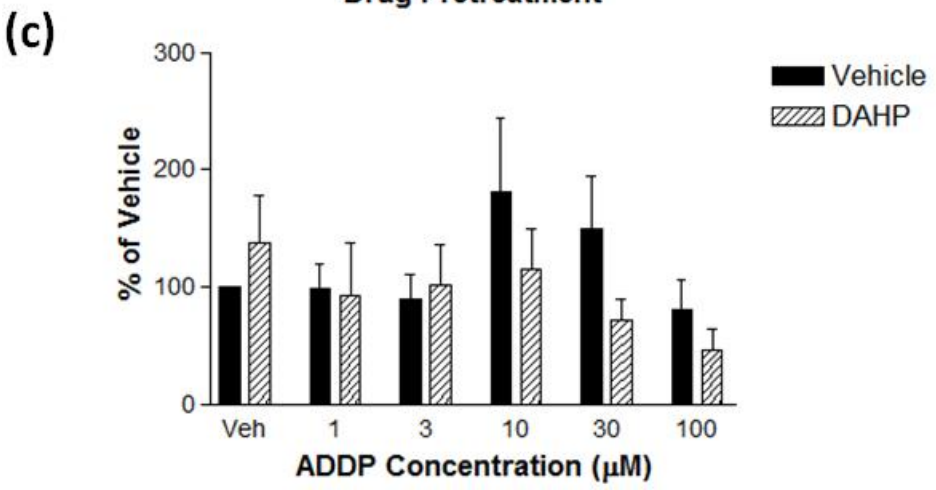
(c)
% of Vehicle
300
200
100
0
Veh
1
3
10
30
100
ADDP Concentration (μM)
Vehicle
DAHP

Figure 6.2. Neuronal nitric oxide production is stimulated with a BH_4 analogue while thioredoxin reductase activity is unaffected. (**a**) Illustrative bright field (**i**) and DAF-2T fluorescence (**ii**) micrographs of CGCs following 24 hour incubation with 4 mM DAHP or vehicle (0.07% DMSO), and the BH_4 analogue, ADDP for 1 hour. Scale bar = 10µm, and applies to all images. (**b**) There was an overall significant increase in relative fluorescence intensity (RFI) of DAF-2T in cells treated with 30 µM ADDP ($F_{1,28} = 35.2$, $p < .001$), and an overall significant decrease in RFI with BH_4 depletion (i.e. pretreatment with DAHP; $F_{1,28} = 6.0$, $p = .02$). DAF-2T intensity was significantly increased with ADDP (23.5 ± 2.6 RFI, $p = .001$, n = 4), compared to vehicle (10.4 ± 1.1 RFI, n = 16). DAF-2T was also significantly increased with ADDP (18.7 ± 2.7 RFI, $p = .002$, n = 4) in BH_4-depleted cells, compared to vehicle control (5.9 ± 0.7 RFI, n = 5). (**c**) Thioredoxin reductase (TrxR) activity was assessed in cerebellar granule cells that were incubated with 4 mM DAHP or vehicle for 24 hours, and with ADDP for 1 hour over a range of concentrations. TrxR data were analysed using Kruskal-Wallis tests with Dunn's multiple comparisons, and DAF-2T data were analysed using two-way ANOVA with Tukey's multiple comparisons. **, $p < .01$ (Tukey). Data are presented as mean ± SEM.

6.3.2 The influence of putative NOS inhibitors in neuronal nitric oxide signalling

DAF-2T fluorescence was quantified in CGCs following incubation with 4 mM DAHP, 30 µM WSG1023 or 30 µM WSG2001 for 24 hours and DAF-2DA for 30 mins. DAF-2T accumulated in the somata of neurones, as illustrated in **Figure 6.3**a. The fluorescence of DAF-2T in CGCs stimulated with A23187 was 15.1 ± 2.2 RFI (n = 4), and was significantly decreased in cells following 24 hour incubation with DAHP (4.2 ± 1.08 RFI, p = .003, n = 3), WSG2001 (5.2 ± 0.51 RFI, p = .032, n = 3), or WSG1023 (4.4 ± 1.05 RFI, p = .003, n = 3), as shown in **Figure 6.3**b. A23187-stimulated CGCs that were pretreated with DAHP (p = .026), and WSG1023 (p = .029) were also significantly decreased from vehicle controls lacking ionophore stimulation (10.4 ± 1.1 RFI, n = 16). No difference in DAF-2T intensities was detected between treatment groups lacking A23187 stimulation, as determined using one-way ANOVA with Tukey's multiple comparisons.

TrxR activity was determined in CGCs following 24 hour incubation with WSG1023 or WSG2001 over a range (3 – 300 µM) of concentrations. **Figure 6.3**c shows how TrxR activity was significantly increased (264 ± 118 % of vehicle, median = 158 %, p = .036, n = 5) in CGCs incubated with 30 µM WSG2001. There was also a trend towards a significant decrease (40.9 ± 10.2 % of vehicle, median = 30.9 %, p = .052, n = 3) in TrxR activity with 3 µM WSG1023, as determined by Kruskal-Wallis test with Dunn's multiple comparisons. 300 µM of either drug (n = 1 / group) was apparently toxic to cells and so further replicates were not acquired.

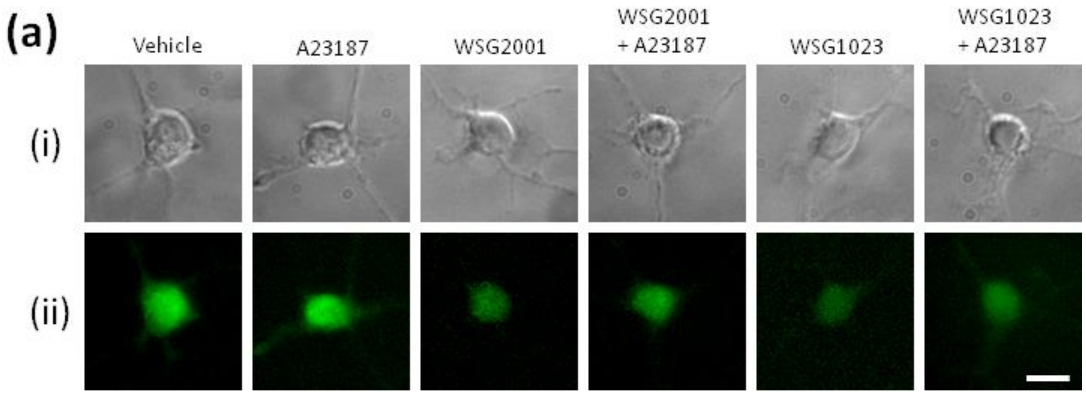
(a)
Vehicle
A23187
WSG2001
WSG2001 + A23187
WSG1023
WSG1023 + A23187
(i)
(ii)

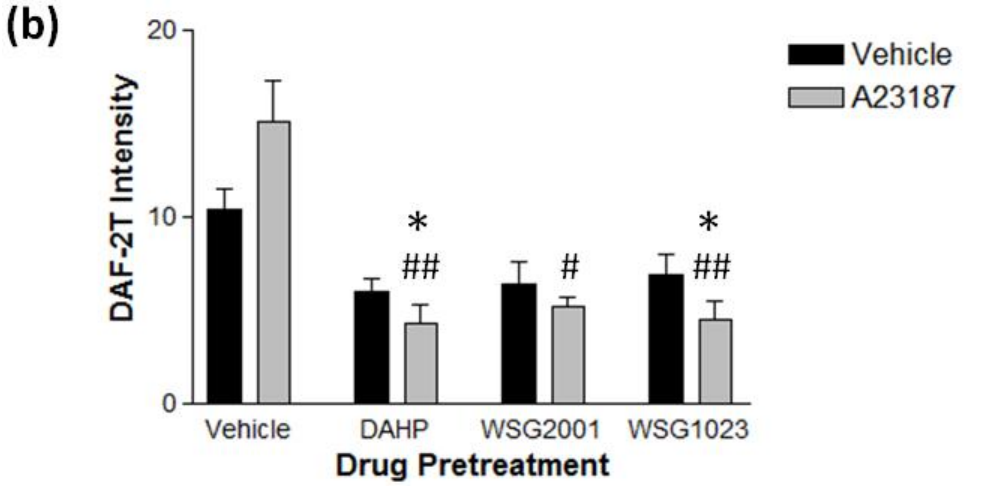
(b)
DAF-2T Intensity
20
10
0
*
##
#
*
##
Vehicle
DAHP
WSG2001
WSG1023
Drug Pretreatment
Vehicle
A23187

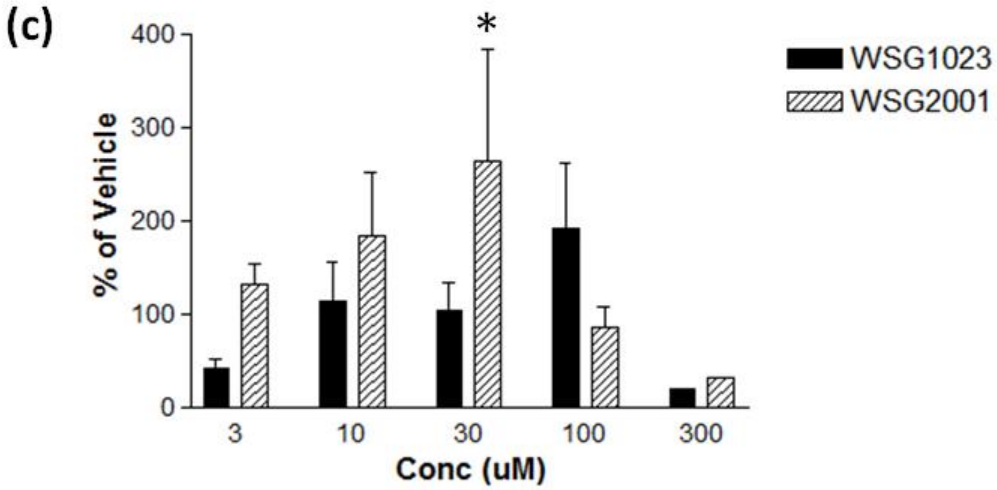
(c)
% of Vehicle
400
300
200
100
0
*
3
10
30
100
300
Conc (uM)
WSG1023
WSG2001

Figure 6.3. Neuronal TrxR and NOS activities are altered with GTP cyclohydrolase inhibition. (**a**) Illustrative bright field (**i**) and DAF-2T fluorescence (**ii**) micrographs of CGCs following incubation the calcium ionophore, A23187, or vehicle (0.07% DMSO) and the putative NOS inhibitors, WSG2001 or WSG1023. Scale bar = 10µm, and applies to all images. (**b**) The relative fluorescence intensity (RFI) of DAF-2T was significantly decreased in cells treated with 1 µM A23187 and pretreated with 4 mM DAHP (4.2 ± 1.08 RFI, p = .003, n = 3), or with 30 µM WSG2001 (5.2 ± 0.51 RFI, p = .032, n = 3) or WSG1023 (4.4 ± 1.05 RFI, p = .003, n = 3) for 24 hours. The A23187-stimulated cells that were pretreated with DAHP (p = .026), and WSG1023 (p = .029) were also significantly decreased from vehicle controls lacking ionophore stimulation. No difference was detected between groups in the absence of A23187. (**c**) Thioredoxin reductase (TrxR) activity was assessed in cerebellar granule cells that were incubated with WSG2001 or WSG1023 for 24 hours over a range of concentrations. TrxR activity was significantly increased with 30 µM WSG2001 (264 ± 118 % of vehicle, median = 158%, p = .036, n = 5), compared to vehicle controls. TrxR data were analysed using Kruskal-Wallis tests with Dunn's multiple comparisons, and DAF-2T data were analysed using one-way ANOVA with Tukey's multiple comparisons. *, p < .05 compared to vehicle. #, p < .05, and ##, p < .01 compared to controls administered A23187. Data are presented as mean ± SEM.

6.4 Discussion

The findings here show how novel drugs that target BH_4 function, either by changing its availability or its activity at NOS, are effective in the modulation of nitric oxide signalling in neurones. ADDP is shown here to be a powerful activator of NOS in CGCs in both basal and depleted BH_4 conditions. WSG2001 and WSG1023 inhibited nitric oxide generation in CGCs, and had varied effects on TrxR activity.

As shown in **Figure 6.2**, 30 μM ADDP increased CGC nitric oxide generation by 215% compared to vehicle in BH_4-depleted conditions (i.e. with 4 mM DAHP), and nitric oxide generation was increased 127% from vehicle in the absence of DAHP. ADDP has been previously shown to be an effective activator of iNOS and eNOS in macrophages and endothelial cells, respectively (Suckling *et al.*, 2008). Here, 30 μM ADDP gave rise to a 34% increase in nitrite production of BH_4-depleted endothelial cells, but a change was not detected in basal BH_4 conditions. Therefore, ADDP appears to be more potent in CGCs than in endothelial cells and may act in basal BH_4 conditions, unlike with endothelial cells.

Evidence of the role of BH_4 in schizophrenia has yet to be fully investigated. One group has reported that plasma BH_4 is decreased in people with schizophrenia and schizoaffective disorder (Richardson *et al.*, 2007). A preliminary, and anecdotal account from Choi and Tarazi (2010) suggests that mice deficient in the sepiapterin reductase gene (*spr* $^{-/-}$) display hyperlocomotion, and that this behavioural deficit is resistant to amphetamine and PCP treatments. These mice also show markedly decreased monoamine concentrations in brain regions (Yang *et al.*, 2006). It will be interesting to see what other phenotypes are present in *spr* $^{-/-}$ mice once they are characterised, especially to see how nitric oxide signalling is involved. An interesting avenue of research would be to see whether ADDP would reverse neurochemical and behavioural deficits in these mice, and how

ADDP acts *in vivo* comparing *spr* $^{-/-}$ to wildtype mice, i.e. if ADDP acts only in a BH_4-deficient state (Suckling et al., 2008; Kunuthur et al., 2011), or irrespective of this, as reported here.

Nitric oxide-stimulated dopamine release has been shown to be BH_4-dependent in the striatum (Liang and Kaufman, 1998). Nitric oxide itself may potentiate dopaminergic transmission via *S*-nitrosylation of monoamine transporters (reviewed by: Kiss and Vizi, 2001). Together, these indicate an excellent link of activities of BH_4 drugs that are appropriate in the context of schizophrenia. For example, GTPCH inhibition may inhibit enhanced neuronal NOS activity (the efficacy of NOS inhibition in reversing schizophrenia-related deficits is addressed in Chapter 1.5.4 and Chapter 5), and reduce dopamine transmission (i.e. by inhibiting monoamine synthesis and by enabling DAT activity).

The implications of the data presented here are that ADDP may serve as a means to stimulate nitric oxide generation in neurones without influencing cellular redox state. In combination with previous findings (Suckling et al., 2008; Kunuthur et al., 2011), ADDP appears to be a potent, and chemically stable, analogue of BH_4, that may stimulate nitric oxide generation from all NOS isoenzymes in a BH_4-depleted state, but may also increase neuronal nitric oxide generation independently of the state of this cofactor.

As shown in **Figure 6.3**b, both WSG1023 and WSG2001 acted as potent inhibitors of nitric oxide generation in CGCs, when compared to the typical GTPCH inhibitor, DAHP. These effects were detected in CGCs activated with A23187, but not without. These also had large, but very variable influences on TrxR activity. An interesting course for further study would be to see whether TrxR activity, as seen in **Figure 6.3**a, is further modulated by the WSG compounds with A23187 co-treatment.

Together, inhibition of activated NOS via WSG1023 and WSG2001, and direct stimulation of NOS using ADDP appears to have discrepant influences on TrxR activity. Inhibition with WSG1023 or WSG2001 gave variable, but generally increased TrxR activities, in support of findings with other NOS inhibitors in Figure 3.4. 30 μM WSG2001 stimulated TrxR activity, but WSG1023 did not in the concentration range used (**Figure 6.3**c). This may be due to the different targets of these compounds; WSG2001 inhibits GTPCH (Gibson *et al.*, 2004), whereas WSG1023 has an unknown mechanism. Despite this difference, both drugs were effective in inhibiting nitric oxide generation in the presence of A23187 (**Figure 6.3**b). Despite an established interaction between NOS signalling and TrxR activity (reviewed by: Shao et al., 2002; Sengupta and Holmgren, 2012), TrxR may also be influenced, for example, by changes in *Txnrd* gene expression in response to mitochondrial stress (Yoo *et al.*, 2003), and may also be directly influenced by dopamine and superoxide dismutase (Kim *et al.*, 1999).

Stimulation of NOS with ADDP did not influence TrxR in CGCs, as shown in Figure 6.2c. ADDP may mirror the action of BH_4 in the inhibition of superoxide generation by NOS, while stimulating nitric oxide synthesis (Vásquez-Vivar *et al.*, 1999). If so, then this has ramifications on findings in previous chapters where increased NOS activity was coincident with altered TrxR activity (e.g. Chapter 4.3.2 and 4.5). Specifically, that these together may indicate an increase in superoxide (and thus peroxynitrite) production and elicit oxidative stress, as opposed to nitric oxide and resultant change in redox maintenance by NOS and TrxR, respectively. Evaluation of superoxide dismutase activity in cells stimulated with A23187 compared to ADDP may elucidate any role for superoxide in these findings. The lack of TrxR response to ADDP may be due to the other activities, such as the inhibition of monoamine synthesis, or other unanticipated interactions.

Nitric oxide generation was stimulated in CGCs by ADDP in both BH_4 -depleted and unaltered conditions. TrxR activity was not influenced by ADDP or BH_4 concentrations. WSG1023 and WSG2001 decreased nitric oxide generation in CGCs stimulated with A23187 and did so with a >100 times potency compared to the typical GTPCH inhibitor, DAHP. TrxR activity was stimulated by WSG2001, but not by WSG1023. Together, these findings show that pharmacological manipulation of BH_4 via ADDP and WSG2001, and by WSG1023 is an effective means to modulate nitric oxide signalling in neuronal cells, and that further study is warranted to evaluate the effectiveness of these drugs in rodent models of relevance to schizophrenia.

7 General Discussion

The research presented here in this thesis is concerned with the role of nitric oxide signalling in mouse models with relevance to schizophrenia. Outlined in this chapter are the principle findings of this research, the technical considerations for these findings, and suggestions for possible future research to expand upon these results. Finally, this chapter will be concluded by addressing the general hypothesis and aims of this thesis that are stated in Chapter 1.6.

7.1 Key findings

Fluorescence imaging of nitric oxide generation using DAF-2DA revealed that NOS inhibition with L-NAME or L-NPA reversed the glutamate-mediated stimulation of nitric oxide generation in hippocampal neurones (Figure 3.7), and partially so in CGCs (Figure 3.5). L-NIO did not inhibit nitric oxide generation in either cell type, with or without stimulation. Glutamate-mediated stimulation of nitric oxide generation in CGCs was inhibited by the L-type calcium channel antagonist, nifedipine, whereas inhibition of NMDA receptors by MK801, or AMPA/kainate receptors by CNQX, did not. Conversely, all three inhibitors together were required to reverse glutamate stimulation of nitric oxide generation in hippocampal neurones. Together, these suggest that nNOS is the source of the majority of nitric oxide generation in neurones in the hippocampus and cerebellum and that NOS signalling has more complex interactions upstream than previously thought, with multiple receptors and channels that may contribute to NOS activity.

The work presented here shows that NOS activity is altered in brain regions of mouse models of NMDA receptor hypofunction. Increased NOS activity was found in the hippocampus, and decreased activity was found in the reticular thalamus with acute PCP in mice. Decreased TrxR activity was also

found in the regions, but caspase activities were unchanged, suggestive that dysfunctional NOS gives rise to a persistent nitrergic stress to cells in these regions that is not alleviated by apoptosis. With subchronic PCP, NOS activity was decreased in the PFC, and was normalised in the hippocampus and thalamus. TrxR activity was unchanged, and caspase 3 activity was decreased in the hippocampus with subchronic PCP treatment. Together, these results suggest that NMDA receptor dysfunction brings about regionally- and temporally- distinct changes in nitric oxide signalling, coincident with behavioural deficits in sensorimotor gating and locomotion.

This is the first study to compare the role of eNOS and nNOS in the behavioural and neurochemical deficits elicited by PCP. Behavioural deficits observed in mice treated with PCP were attenuated by NOS inhibition by L-NAME and L-NIO, but not by selective nNOS inhibition by L-NPA. Pretreatment with L-NIO was consistent in the reversal of PCP-elicited hyperlocomotion and PPI deficit. Though the selectivity of L-NIO for eNOS is not as great as L-NPA is for nNOS (Table 3.1), the lack of effect of the latter drug suggests that eNOS is involved in the modulation of the behavioural changes seen with PCP.

Modulation of nitric oxide signalling by novel drugs that target BH_4 was shown for the first time in neurones. WSG2001 attenuates BH_4 synthesis by the inhibition of GTPCH, and WSG1023 is a putative NOS inhibitor of unknown mechanism. These decreased nitric oxide generation in cerebellar neurones in the presence of A23187 (**Figure 6.3**). Treatment with the BH_4 analogue, ADDP, promoted nitric oxide generation in neurones both with and without endogenous BH_4 depletion. Together, these validate drugs that target BH_4 as an effective means to modulate nitric oxide signalling in neurones.

7.2 Technical considerations and future directions

7.2.1 On the suitability of methods for determining nitric oxide synthase activity

DAF-2DA imaging was sensitive enough to detect NMDA-mediated stimulation of NOS activity (Figure 3.3) and inhibition by L-NAME (Figure 3.5) in cerebellar granule cells. Inhibition of NOS by L-NPA was only detected in the presence of glutamate. This suggests that this inhibitor is only effective when NOS is stimulated, or that nitric oxide generation below that of basal activity is below the threshold of detection using DAF-2DA. Inhibition of nitric oxide generation with vehicle treatment was detected with L-NPA treatment in hippocampal neuronal cultures, and not by L-NAME or L-NIO (Figure 3.7). This discrepancy is likely due to variance between these groups, and further replicates are required to elucidate whether there is a true difference in response to selective NOS isoform inhibitors in hippocampal neurones.

A common finding in cerebellar and hippocampal neurones is that L-NAME and L-NPA were effective in inhibiting nitric oxide generation stimulated by glutamate, but L-NIO was not. The calcium ionophore, A23187, was used to determine whether NOS activities were altered from that with glutamate stimulation in hippocampal neurones. There appeared to be a stronger inhibition of nitric oxide generation by L-NIO with non-receptor-mediated NOS stimulation by A23187 than with glutamate stimulation, but these changes were not significant. It is likely that 1 μM A23187 was not sufficient to give rise to a significant increase on NOS activity and more replicates would be needed to explore this further. This may also be expanded on by investigating the contributions of selective agonists in the stimulation of NOS. As indicated by Figure 3.6 and Figure 3.8, multiple receptor/channel interactions may modulate NOS activity. Therefore, NOS may be stimulated

from multiple sources, eNOS in neurones may not be functionally linked to NMDA receptors as nNOS is, and these warrant further investigation.

Attempts were made to determine the rate of DAF-2T accumulation in live CGC and hippocampal cultures over time by fluorescence imaging, but yielded highly variable results (data not shown). Future directions to improve on this technique may be to optimise the conditions for live cell imaging so that repeated measures can be made, e.g. rate of nitric oxide generation before and after drug application. Unfortunately, DAF-2DA is unlikely to be suitable for use with *in vivo* microscopy because of the poor spread of the dye (Kasim *et al.*, 2001) and potential deleterious effects of DAF-2T accumulation (Shlosberg *et al.*, 2012). Another development to improve image analysis would be to use immunocytochemistry following DAF imaging to identify neuronal subtypes (such as calcium-binding proteins) or NOS isoform expression, which may give further detail as to the activity of neurones in a mixed population.

Microplate-based assays for NADPH-diaphorase activity and nitrite content via Griess assay were insensitive to changes in NOS activity with drug treatments (Figure 3.1and Figure 3.3). Changes in TrxR activity were also not detected in cultured cells (Figure 3.4). The likely explanation for this is that there is too little enzyme present at the cell culture density, and even cells cultured in 6-well microplates were insufficient. Culturing neuroblastoma cells in greater densities would be possible, but in the case of primary cultures would require the use of many more animals to enable the experimental comparisons that were done and this would be incongruent with current UK guidelines on the use of animals for experimentation: the Animals (Scientific Procedures) Act, 1986.

NADPH-diaphorase histochemistry allows discrimination of objects at a cellular resolution. This is especially relevant in the investigation of NOS activities to compare that of neurones and of blood vessels. The method also allows the distinction between brain region subfields and nuclei, as in the case of the reticular thalamus. In contrast, the assay for NADPH-diaphorase activity in brain region homogenates appeared to detect changes that the histochemical approach did not, i.e. in the hippocampus (**Figure 4.4** and **Figure 4.5**). This technique does not allow discrimination of objects and of regional subfields, but is perhaps more sensitive to detect changes in NOS activity in the whole region of interest. Electrochemistry appears to be sensitive enough to detect changes in nitric oxide release *in vivo* (Finnerty *et al.*, 2013). This technique also lacks the resolution to discriminate objects (i.e. neurones and blood vessels), but can provide an insight into nitric oxide generation in real-time. An advantage of assays for NADPH-diaphorase activity is that they allow multiple brain regions to be analysed. NADPH-diaphorase histochemistry also allows for multiple measures to be done in the same samples. For example, an improvement for the analysis of formazan staining in brain sections would be to use immunohistochemistry to label eNOS and nNOS –expressing neurones. Such an approach would enable discrimination of the possible differential responses of these neurones in response to PCP and NOS inhibitors. The use of immunohistochemistry may also improve analysis by the use of automated image analysis software such as CellProfiler (Lamprecht *et al.*, 2007). Attempts were made to automate image analysis using this software, but this gave unreliable results (data not shown) that were likely due to the heterogeneity of histological staining (e.g. Figure 5.6). Fluorescent labels of eNOS and nNOS –expressing neurones would provide a clear marker for the software to identify neurones, to sort the intensity of NADPH-diaphorase staining between these two subpopulations, and vastly speed-up the analysis of histological staining.

The influence of the NOS inhibitors used (i.e. L-NAME and L-NIO) on the behavioural deficits elicited by PCP was substantial (e.g. **Figure 5.4**) and yet their influence on NADPH-diaphorase staining was less marked in regions shown to be influenced by acute PCP (**Figure 4.4** and Figure 5.8, **Figure 4.5** and Figure 5.7). The likely explanation for this is that the drug-elicited changes in NOS activity seen in Chapter 4 (30 mins following PCP administration) did not persist long enough to be detected at 90 mins following PCP administration, as shown in Chapter 5. Other possible explanations may be that relatively small changes in NOS activity have dramatic effects on brain function and thence behavioural output, or that the technique is not sensitive enough to detect the true magnitude of changes in NOS activity.

Overall, the discrepancy of findings of NADPH-diaphorase activities between neuronal cultures and *ex vivo* brain samples is likely explained by the amount of sample available. Increasing the sample density of primary cultures would reduce the number of comparisons available to be made per brain (and thus increase variability) and would be impractical. DAF-2DA was determined to be sensitive enough to detect changes in nitric oxide generation at the cellular level (Chapter 3), but use of this probe is probably inappropriate for use *in vivo*. Cultured neurones are also dissociated from the complex interactions that they would possess *in vivo*, and so findings obtained *in vitro* may not fully account for what was found in the intact brain. Determining NADPH-diaphorase activities in brain sections and brain region homogenates are possibly best used together: to provide detail in histochemical sections, and the sensitivity to detect overall changes with tissue homogenates.

7.2.2 Neurochemical and behavioural changes with acute and subchronic PCP

The neurochemical findings from histological and homogenate samples of mouse brains revealed that NOS activity was increased in the hippocampus and decreased in the reticular thalamus with acute PCP. NOS activities in these regions were normalised 72 hours following subchronic PCP (PCP twice daily for 5 days), and NOS activity was decreased in the PFC in these mice.

It would be interesting to see how the activity of NOX corresponds to the altered NOS activities seen with PCP treatments. Subchronic ketamine is reported to stimulate NOX activity, and that this mediates the dysfunction and loss of PV interneurones in the cortex and hippocampus (Behrens *et al.*, 2007). Should both NOX and NOX activities be increased in the hippocampus, for example, then peroxynitrite may mediate the cell loss in these interneurones. Contradictory to this however, is that nitric oxide is thought to inhibit NOX activity (Selemidis *et al.*, 2007), and NOS is not commonly coincident with PV in neurones of the hippocampus (Jinno and Kosaka, 2002) and frontal cortex (Kubota *et al.*, 2011).

The changes in TrxR activity found in the hippocampus and thalamus with acute PCP (**Figure 4.8**) give some indication that changes in NOS activity may impact on redox state in those brain regions. The decrease in TrxR activity seen in the PFC with subchronic PCP did not meet significance, and further replicates would be needed to validate whether this activity corresponds with NOS activity, as seen with acute PCP. To date, the state of protein *S*-nitrosylation following NMDA receptor antagonism has not been reported. The changes in NOS and TrxR activities may confer altered protein function via this post-translational modification, and a proteomic approach using samples from brain regions of PCP-treated rodents may elucidate this.

Similarly, the nitrosylation state of proteins in the brains of people with schizophrenia has not been reported. Unfortunately, the transience of *S*-nitrosylation may mean that post mortem brain samples are unlikely to be suitable to investigate this. Such an investigation may be possible as technologies develop, and the most likely source to find evidence for altered nitrosylation state may be from induced pluripotent stem cells (i.e. re-differentiated to neurones) obtained from people with schizophrenia (Brennand *et al.*, 2011).

Hyperlocomotion was observed in mice immediately following administration of PCP and this persisted throughout the subchronic PCP dosing scheme. However, no residual effects of PCP were detected 72 hours following subchronic PCP in either locomotion (**Figure 4.14**) or PPI, though a slightly attenuated startle response was seen in the PCP group (**Figure 4.12**). Deficits in cognition are found in rodents with repeated administrations PCP, and less so with acute PCP (Thomson *et al.*, 2011). It would be interesting to test whether this was the case with these mice; to compare performances of mice treated with acute or subchronic PCP, and following withdrawal from subchronic PCP, in an attentional set-shifting task for assessment of cognitive flexibility, for example.

7.2.3 Selective NOS isoform inhibition

This is the first study that directly compares the role of constitutive isoforms of NOS in NMDA receptor antagonist-mediated deficits. Several nNOS-selective antagonist drugs are available (though, even their selectivity has come in to question: Pigott *et al.*, 2013), and there is a lack of selective eNOS drugs. Though L-NIO is selective for eNOS over other isoforms, its selectivity is not as strong as L-NPA is for nNOS (Table 3.1). L-NPA and L-NAME were effective in inhibiting glutamate-mediated nitric oxide generation

in hippocampal and cerebellar neurones in Chapter 3, and the responses to these drugs were not significantly different from each other. This suggests that nNOS is the major contributor to nitric oxide generation in these regions. The failure of L-NPA to ameliorate PCP-induced hyperlocomotion, and then of L-NAME in PPI deficits, suggests that eNOS may be involved in these behaviours downstream from NMDA receptor dysfunction. Alternatively, L-NPA may not be as selective for nNOS *in vivo* as it is *in vitro* (Zhang *et al.*, 1997). However, L-NPA has been shown to be efficacious *in vivo* previously (Klamer et al., 2004b). The lack of detectable changes with NADPH-diaphorase means that eNOS in neurones cannot be directly attributed to the effects seen with L-NIO. One cannot discount the involvement of glia (Bartus *et al.*, 2013) and blood vessels (Garthwaite *et al.*, 2006) in the modulation of neuronal activities.

The NOS inhibitors used in Chapter 5 may also impart effects on targets other than NOS, especially that these drugs are based on the amino acid and NOS substrate, arginine. Arginine is essential for the metabolism of urea, agmatine, polyamines and glutamate (reviewed by: Wu and Morris, 1998). Agmatine and polyamines such as spermine may modulate NMDA receptor activity (Yang and Reis, 1999). Arginine analogues, such as L-NAME, may interact with arginase and arginine decarboxylase, and thus modulate the synthesis of NMDA receptor interacting molecules such as agmatine. A possible future experiment would be to investigate the influence of arginine analogue drugs on the synthesis of NMDA receptor–interacting molecules derived from arginine, including that of glutamate.

Selective inhibition of nNOS using L-NPA did not improve the behavioural deficits observed with PCP treatment in Chapter 5. This drug was used at a dose and route (20 $mg.kg^{-1}$, i.p.) previously shown to be effective in reversing PCP-induced deficits in PPI and hyperlocomotion, albeit in a

different strain of mouse (Klamer et al., 2004b). The discrepancy between those findings and those presented in Chapter 5 may therefore be due to a differential behavioural profile between these mouse strains (Matsuo *et al.*, 2010). A topic for further study would be to see if the findings presented here are consistent across different mouse strains and substrains, and perhaps in stains of rat too.

Alternative strategies for the selective inhibition of NOS isoforms include RNA interference (RNAi). Such a method would allow both isoform selectivity and a regional selectivity (Mahairaki *et al.*, 2009). In the absence of a selective eNOS drug and considering potential unwanted cardiovascular effects, RNAi may be a useful therapeutic strategy to inhibit eNOS selectively in the brain that may improve deficits that potentially involve this NOS isoform.

It would be interesting to investigate the role of eNOS in other behaviours relevant to schizophrenia such as social withdrawal and working memory. Deficits in these are best reproduced with repeated administrations of an NMDA receptor antagonist (Wass et al., 2009; Smith et al., 2011), and such a dosing scheme is perhaps a better representation of schizophrenia-like symptoms than following acute administration (Egerton et al., 2008; Thomson et al., 2011). Decreased NOS activity was observed in the PFC of mice with subchronic PCP in Chapter 4, and so NOS inhibition is perhaps an inappropriate strategy to attempt to improve this deficit. Alternative strategies for the promotion of NOS may be the inhibition of endogenous NOS inhibitors, such as ADMA and CAPON; the latter being a strategy to selectively promote nNOS association with NMDA receptors. Experimentally, regional and temporal selectivity of activating neuronal subtypes may be achieved using optogenetics. As yet, there is no available means to promote eNOS activity selectively in neurones with a therapeutic potential.

From the evidence of a role for NOS in schizophrenia, it is inconclusive whether modulating NOS would be an effective treatment strategy. Clinical trials featuring drugs that possibly involve nitric oxide modulation are only recently taking place, and their findings are variable (Chapter 1.5.1). The genetic evidence outlined in Chapter 1.5.2 is compelling, but the work focuses on the association of the nNOS encoding gene and not of eNOS, and the outcomes of the possible dysfunction of these is yet to be elucidated. Finally, the evidence from biochemical findings is variable, and these may be explained by differences in stage of illness and by medication (Chapter 1.5.3), but is unclear from these whether inhibition or promotion of NOS would be beneficial for people with schizophrenia.

7.2.4 Targeting tetrahydrobiopterin as a means to modulate NOS activity

The BH_4 cofactor provides an interesting target with which to modulate NOS. The main effect of the GTPCH inhibitor, WSG2001 appears to be the inhibition of activated NOS, but not that of basally active NOS (Figure 6.3). This may be reflective of an insensitivity of the technique used, as previously discussed (Section 7.2.1), but may indicate a NOS-state-selectivity of these compounds. Should the latter be the case, GTPCH may be an effective drug target to inhibit overactive NOS but not that that is basally active. The influence of GTPCH on monoamine synthesis may also be beneficial in the context of schizophrenia. BH_4 is an essential cofactor for tyrosine hydroxylase-mediated dopamine synthesis (reviewed by: Ichinose et al., 2008), and nitric oxide may decrease dopamine reuptake (Salum *et al.*, 2008). Therefore, inhibition of GTPCH may both decrease dopamine synthesis and attenuate dopaminergic transmission. Possible future experiments would be to investigate both nitric oxide signalling and tyrosine hydroxylase activity with GTPCH inhibition to see if this is effective to reverse behaviours relevant to positive and negative symptoms.

There is evidence of a BH_4 deficit in people with schizophrenia (Richardson *et al.*, 2007). Should this be the case, then supplementation of BH_4 with ADDP may prove to be effective at reversing this deficit. BH_4 analogues may also be protective against superoxide (Kotsonis *et al.*, 2000), but, from the data presented in Figures 6.2 and 6.3, it appears that modulators of BH_4 do not influence TrxR activity, and therefore may not impact on redox state.

7.3 Concluding remarks

The aim to develop an *in vitro* assay for NOS activity was met by the use of fluorescence imaging in primary neuronal cultures using DAF-2T, which is indicative of intracellular nitric oxide generation. This assay was used successfully to characterise the influence of novel drugs that modulate BH_4 on nitric oxide generation in neuronal cultures. NOS activity in brain regions was determined in mice with acute and subchronic PCP administration, and a differential response was found with these administration schemes, both in regional NOS activities and in the possible downstream influences of these on TrxR and caspase activities. Behavioural deficits in sensorimotor gating and locomotion were ameliorated with non-selective NOS inhibition, but not by selective nNOS inhibition suggesting that the eNOS is involved in these deficits.

Together, the data presented here suggest a role of nitric oxide synthase in deficits observed in mouse models with relevance to schizophrenia, and that selectively targeting the endothelial isoform of NOS in the brain is a potential therapeutic avenue in NMDA receptor-mediated deficits found in schizophrenia.

8 References

Adams BW, Moghaddam B (2001) Effect of clozapine, haloperidol, or M100907 on phencyclidine-activated glutamate efflux in the prefrontal cortex. Biol Psychiatry 50:750-757.

Akbarian S, Smith MA, Jones EG (1995) Editing for an AMPA receptor subunit RNA in prefrontal cortex and striatum in Alzheimer's disease, Huntington's disease and schizophrenia. Brain Research 699:297-304.

Akbarian S, Viñuela A, Kim JJ, Potkin SG, Bunney WE, Jones EG (1993a) Distorted distribution of nicotinamide-adenine dinucleotide phosphate-diaphorase neurons in temporal lobe of schizophrenics implies anomalous cortical development. Arch Gen Psychiatry 50:178-187.

Akbarian S, Bunney WE, Potkin SG, Wigal SB, Hagman JO, Sandman CA, Jones EG (1993b) Altered distribution of nicotinamide-adenine dinucleotide phosphate-diaphorase cells in frontal lobe of schizophrenics implies disturbances of cortical development. Arch Gen Psychiatry 50:169-177.

Alderton WK, Cooper CE, Knowles RG (2001) Nitric oxide synthases: structure, function and inhibition. Biochem J 357:593-615.

Amann LC, Gandal MJ, Halene TB, Ehrlichman RS, White SL, McCarren HS, Siegel SJ (2010) Mouse behavioral endophenotypes for schizophrenia. Brain Research Bulletin.

Anastasio NC, Xia Y, O'Connor ZR, Johnson KM (2009) Differential role of N-methyl-D-aspartate receptor subunits 2A and 2B in mediating phencyclidine-induced perinatal neuronal apoptosis and behavioral deficits. Neuroscience 163:1181-1191.

Andoh T, Chock PB, Chiueh CC (2002) The roles of thioredoxin in protection against oxidative stress-induced apoptosis in SH-SY5Y cells. J Biol Chem 277:9655-9660.

Andoh T, Chiueh CC, Chock PB (2003) Cyclic GMP-dependent protein kinase regulates the expression of thioredoxin and thioredoxin peroxidase-1 during hormesis in response to oxidative stress-induced apoptosis. J Biol Chem 278:885-890.

Attwell D, Buchan AM, Charpak S, Lauritzen M, Macvicar BA, Newman EA (2010) Glial and neuronal control of brain blood flow. Nature 468:232-243.

Baba H, Suzuki T, Arai H, Emson PC (2004) Expression of nNOS and soluble guanylate cyclase in schizophrenic brain. Neuroreport 15:677-680.

Babu BR, Griffith OW (1998) N5-(1-Imino-3-butenyl)-L-ornithine. A neuronal isoform selective mechanism-based inactivator of nitric oxide synthase. J Biol Chem 273:8882-8889.

Balla A, Sershen H, Serra M, Koneru R, Javitt DC (2003) Subchronic continuous phencyclidine administration potentiates amphetamine-induced frontal cortex dopamine release. Neuropsychopharmacology 28:34-44.

Bartus K, Pigott B, Garthwaite J (2013) Cellular targets of nitric oxide in the hippocampus. PLoS ONE 8:e57292.

Bay-Richter C, O'Callaghan MJ, Mathur N, O'Tuathaigh CM, Heery DM, Fone KC, Waddington JL, Moran PM (2013) D-amphetamine and antipsychotic drug effects on latent inhibition in mice lacking dopamine D2 receptors. Neuropsychopharmacology 38:1512-1520.

Behrens MM, Sejnowski TJ (2009) Does schizophrenia arise from oxidative dysregulation of parvalbumin-interneurons in the developing cortex? Neuropharmacology 57:193-200.

Behrens MM, Ali SS, Dugan LL (2008) Interleukin-6 mediates the increase in NADPH-oxidase in the ketamine model of schizophrenia. J Neurosci 28:13957-13966.

Behrens MM, Ali SS, Dao DN, Lucero J, Shekhtman G, Quick KL, Dugan LL (2007) Ketamine-induced loss of phenotype of fast-spiking interneurons is mediated by NADPH-oxidase. Science 318:1645-1647.

Belforte JE, Zsiros V, Sklar ER, Jiang Z, Yu G, Li Y, Quinlan EM, Nakazawa K (2010) Postnatal NMDA receptor ablation in corticolimbic interneurons confers schizophrenia-like phenotypes. Nat Neurosci 13:76-83.

Benavides-Piccione R, DeFelipe J (2003) Different populations of tyrosine-hydroxylase-immunoreactive neurons defined by differential expression of nitric oxide synthase in the human temporal cortex. Cereb Cortex 13:297-307.

Benhar M, Forrester MT, Stamler JS (2009) Protein denitrosylation: enzymatic mechanisms and cellular functions. Nat Rev Mol Cell Biol 10:721-732.

Benhar M, Forrester MT, Hess DT, Stamler JS (2008) Regulated protein denitrosylation by cytosolic and mitochondrial thioredoxins. Science 320:1050-1054.

Benhar M, Thompson JW, Moseley MA, Stamler JS (2010) Identification of S-nitrosylated targets of thioredoxin using a quantitative proteomic approach. Biochemistry 49:6963-6969.

Benneyworth MA, Roseman AS, Basu AC, Coyle JT (2011) Failure of NMDA receptor hypofunction to induce a pathological reduction in PV-positive GABAergic cell markers. Neuroscience Letters 488:267-271.

Berman KF, Torrey EF, Daniel DG, Weinberger DR (1992) Regional cerebral blood flow in monozygotic twins discordant and concordant for schizophrenia. Arch Gen Psychiatry 49:927-934.

Bernstein H-G, Steiner J, Bogerts B (2009) Glial cells in schizophrenia: pathophysiological significance and possible consequences for therapy. Expert Rev Neurother 9:1059-1071.

Bernstein HG, Bogerts B, Keilhoff G (2005) The many faces of nitric oxide in schizophrenia. A review. Schizophrenia research 78:69-86.

Bhardwaj A, Northington FJ, Ichord RN, Hanley DF, Traystman RJ, Koehler RC (1997a) Characterization of ionotropic glutamate receptor-mediated nitric oxide production in vivo in rats. Stroke 28:850-856; discussion 856-857.

Bhardwaj A, Northington FJ, Martin LJ, Hanley DF, Traystman RJ, Koehler RC (1997b) Characterization of metabotropic glutamate receptor-mediated nitric oxide production in vivo. J Cereb Blood Flow Metab 17:153-160.

Bitanihirwe BKY, Woo T-UW (2011) Oxidative stress in schizophrenia: an integrated approach. Neurosci Biobehav Rev 35:878-893.

Black MD, Simmonds J, Senyah Y, Wettstein JG (2002) Neonatal nitric oxide synthase inhibition: social interaction deficits in adulthood and reversal by antipsychotic drugs. Neuropharmacology 42:414-420.

Black MD, Selk DE, Hitchcock JM, Wettstein JG, Sorensen SM (1999) On the effect of neonatal nitric oxide synthase inhibition in rats: a potential neurodevelopmental model of schizophrenia. Neuropharmacology 38:1299-1306.

Blackshaw S, Eliasson MJL, Sawa A, Watkins CC, Krug D, Gupta A, Arai T, Ferrante RJ, Snyder SH (2003) Species, strain and developmental variations in hippocampal neuronal and endothelial nitric oxide synthase clarify discrepancies in nitric oxide-dependent synaptic plasticity. Neuroscience 119:979-990.

Bland-Ward PA, Moore PK (1995) 7-Nitro indazole derivatives are potent inhibitors of brain, endothelium and inducible isoforms of nitric oxide synthase. Life sciences 57:PL131-135.

Blottner D, Grozdanovic Z, Gossrau R (1995) Histochemistry of nitric oxide synthase in the nervous system. Histochem J 27:785-811.

Blum-Degen D, Heinemann T, Lan J, Pedersen V, Leblhuber F, Paulus W, Riederer P, Gerlach M (1999) Characterization and regional distribution of nitric oxide synthase in the human brain during normal ageing. Brain Research 834:128-135.

Bosch D, Schmid S (2008) Cholinergic mechanism underlying prepulse inhibition of the startle response in rats. Neuroscience 155:326-335.

Bradford MM (1976) A rapid and sensitive method for the quantitation of microgram quantities of protein utilizing the principle of protein-dye binding. Anal Biochem 72:248-254.

Braff DL, Geyer MA, Swerdlow NR (2001) Human studies of prepulse inhibition of startle: normal subjects, patient groups, and pharmacological studies. Psychopharmacology (Berl) 156:234-258.

Braun I, Genius J, Grunze H, Bender A, Möller H-J, Rujescu D (2007) Alterations of hippocampal and prefrontal GABAergic interneurons in an animal model of psychosis induced by NMDA receptor antagonism. Schizophrenia Research 97:254-263.

Bredt DS, Glatt CE, Hwang PM, Fotuhi M, Dawson TM, Snyder SH (1991) Nitric oxide synthase protein and mRNA are discretely localized in neuronal populations of the mammalian CNS together with NADPH diaphorase. Neuron 7:615-624.

Brenman JE, Xia H, Chao DS, Black SM, Bredt DS (1997) Regulation of neuronal nitric oxide synthase through alternative transcripts. Dev Neurosci 19:224-231.

Brenman JE, Chao DS, Gee SH, McGee AW, Craven SE, Santillano DR, Wu Z, Huang F, Xia H, Peters MF, Froehner SC, Bredt DS (1996) Interaction of nitric oxide synthase with the postsynaptic density protein PSD-95 and alpha1-syntrophin mediated by PDZ domains. Cell 84:757-767.

Brennand KJ, Simone A, Jou J, Gelboin-Burkhart C, Tran N, Sangar S, Li Y, Mu Y, Chen G, Yu D, McCarthy S, Sebat J, Gage FH (2011) Modelling schizophrenia using human induced pluripotent stem cells. Nature 473:221-225.

Bringas ME, Morales-Medina JC, Flores-Vivaldo Y, Negrete-Diaz JV, Aguilar-Alonso P, León-Chávez BA, Lazcano-Ortiz Z, Monroy E, Rodríguez-Moreno A, Quirion R, Flores G (2011) Clozapine administration reverses behavioral, neuronal, and nitric oxide disturbances in the neonatal ventral hippocampus rat. Neuropharmacology 62:1848-1857.

Brown GC (2010) Nitric oxide and neuronal death. Nitric Oxide 23:153-165.

Brown LA, Key BJ, Lovick TA (1999) Bio-imaging of nitric oxide-producing neurones in slices of rat brain using 4,5-diaminofluorescein. J Neurosci Methods 92:101-110.

Brzozowski MJ, Alcantara SL, Iravani MM, Rose S, Jenner P (2011) The effect of nNOS inhibitors on toxin-induced cell death in dopaminergic cell lines depends on the extent of enzyme expression. Brain Research 1404:21-30.

Buchholzer M-L, Klein J (2002) NMDA-induced acetylcholine release in mouse striatum: role of NO synthase isoforms. J Neurochem 82:1558-1560.

Bujas-Bobanovic M, Robertson HA, Dursun SM (2000) Effects of nitric oxide synthase inhibitor N(G)-nitro-L-arginine methyl ester on phencyclidine-induced effects in rats. Eur J Pharmacol 409:57-65.

Catania MV, Tölle TR, Monyer H (1995) Differential expression of AMPA receptor subunits in NOS-positive neurons of cortex, striatum, and hippocampus. J Neurosci 15:7046-7061.

Chabrier PE, Demerle-Pallardy C, Auguet M (1999) Nitric oxide synthases: targets for therapeutic strategies in neurological diseases. Cellular and molecular life sciences : CMLS 55:1029-1035.

Chatterjee M, Verma R, Ganguly S, Palit G (2012) Neurochemical and molecular characterization of ketamine-induced experimental psychosis model in mice. Neuropharmacology 63:1161-1171.

Chaudhry IB, Hallak J, Husain N, Minhas F, Stirling J, Richardson P, Dursun S, Dunn G, Deakin B (2012) Minocycline benefits negative symptoms in early schizophrenia: a randomised double-blind placebo-controlled clinical trial in patients on standard treatment. J Psychopharmacol 26:1185-1193.

Chaves C, Marque CR, Trzesniak C, Machado de Sousa JP, Zuardi AW, Crippa JAS, Dursun SM, Hallak JE (2009) Glutamate-N-methyl-D-aspartate receptor modulation and minocycline for the treatment of patients with schizophrenia: an update. Braz J Med Biol Res 42:1002-1014.

Chittiprol S, Venkatasubramanian G, Neelakantachar N, Babu SVS, Reddy NA, Shetty KT, Gangadhar BN (2009) Oxidative stress and neopterin abnormalities in schizophrenia: A longitudinal study. J Psychiatr Res.

Choi YB, Tenneti L, Le DA, Ortiz J, Bai G, Chen HS, Lipton SA (2000) Molecular basis of NMDA receptor-coupled ion channel modulation by S-nitrosylation. Nat Neurosci 3:15-21.

Choi YK, Tarazi FI (2010) Alterations in dopamine and glutamate neurotransmission in tetrahydrobiopterin deficient spr-/- mice: relevance to schizophrenia. BMB reports 43:593-598.

Christopherson KS, Hillier BJ, Lim WA, Bredt DS (1999) PSD-95 assembles a ternary complex with the N-methyl-D-aspartic acid receptor and a bivalent neuronal NO synthase PDZ domain. J Biol Chem 274:27467-27473.

Cochran SM, Fujimura M, Morris BJ, Pratt JA (2002) Acute and delayed effects of phencyclidine upon mRNA levels of markers of glutamatergic and GABAergic neurotransmitter function in the rat brain. Synapse 46:206-214.

Cochran SM, Kennedy M, McKerchar CE, Steward LJ, Pratt JA, Morris BJ (2003) Induction of Metabolic Hypofunction and Neurochemical Deficits after Chronic Intermittent Exposure to Phencyclidine:

Differential Modulation by Antipsychotic Drugs. Neuropsychopharmacology 28:265-275.

D'Amelio M, Cavallucci V, Middei S, Marchetti C, Pacioni S, Ferri A, Diamantini A, De Zio D, Carrara P, Battistini L, Moreno S, Bacci A, Ammassari-Teule M, Marie H, Cecconi F (2011) Caspase-3 triggers early synaptic dysfunction in a mouse model of Alzheimer's disease. Nat Neurosci 14:69-76.

Das I, Khan NS, Puri BK, Hirsch SR (1996) Elevated endogenous nitric oxide synthase inhibitor in schizophrenic plasma may reflect abnormalities in brain nitric oxide production. Neuroscience letters 215:209-211.

Dash PK, Blum S, Moore AN (2000) Caspase activity plays an essential role in long-term memory. Neuroreport 11:2811-2816.

Dauvermann MR, Whalley HC, Romaniuk L, Valton V, Owens DG, Johnstone EC, Lawrie SM, Moorhead TW (2013) The application of nonlinear Dynamic Causal Modelling for fMRI in subjects at high genetic risk of schizophrenia. Neuroimage 73:16-29.

Dawson N, Morris BJ, Pratt JA (2011) Subanaesthetic Ketamine Treatment Alters Prefrontal Cortex Connectivity With Thalamus and Ascending Subcortical Systems. Schizophr Bull 39:366-377.

de la Torre JC, Aliev G (2005) Inhibition of vascular nitric oxide after rat chronic brain hypoperfusion: spatial memory and immunocytochemical changes. J Cereb Blood Flow Metab 25:663-672.

Dec AM, Kohlhaas KL, Nelson CL, Hoque KE, Leilabadi SN, Folk J, Wolf ME, West AR (2013) Impact of neonatal NOS-1 inhibitor exposure on neurobehavioural measures and prefrontal-temporolimbic integration in the rat nucleus accumbens. Int J Neuropsychopharmacol:1-13.

Del Bel EA, Guimarães FS, Bermúdez-Echeverry M, Gomes MZ, Schiaveto-de-souza A, Padovan-Neto FE, Tumas V, Barion-Cavalcanti AP, Lazzarini M, Nucci-da-Silva LP, de Paula-Souza D (2005) Role of nitric oxide on motor behavior. Cell Mol Neurobiol 25:371-392.

Delorme R, Betancur C, Scheid I, Anckarsäter H, Chaste P, Jamain S, Schuroff F, Nygren G, Herbrecht E, Dumaine A, Mouren MC, Råstam M, Leboyer M, Gillberg C, Bourgeron T (2010) Mutation screening of NOS1AP gene in a large sample of psychiatric patients and controls. BMC Med Genet 11.

Demjaha A, Egerton A, Murray RM, Kapur S, Howes OD, Stone JM, McGuire PK (2013) Antipsychotic Treatment Resistance in Schizophrenia Associated with Elevated Glutamate Levels but Normal Dopamine Function. Biol Psychiatry.

Desaiah D, Pande M, Vig PJS, Cameron JA, Ali SF (1999) In Vitro and In Vivo Inhibition of Rat Brain Nitric Oxide Synthase Activity by Phencyclidine. International Journal of Toxicology 18:245-250.

Deutsch SI, Rosse RB, Paul SM, Tomasino V, Koetzner L, Morn CB, Mastropaolo J (1996) 7-Nitroindazole and methylene blue, inhibitors of neuronal nitric oxide synthase and NO-stimulated guanylate cyclase, block MK-801-elicited behaviors in mice. Neuropsychopharmacology 15:37-43.

Dev KK, Morris BJ (1994) Modulation of alpha-amino-3-hydroxy-5-methylisoxazole-4-propionic acid (AMPA) binding sites by nitric oxide. J Neurochem 63:946-952.

Dinerman JL, Dawson TM, Schell MJ, Snowman A, Snyder SH (1994) Endothelial nitric oxide synthase localized to hippocampal pyramidal cells: implications for synaptic plasticity. Proc Natl Acad Sci USA 91:4214-4218.

Donohoe G, Walters J, Morris DW, Quinn EM, Judge R, Norton N, Giegling I, Hartmann AM, Möller H-J, Muglia P, Williams H, Moskvina V, Peel R, O'Donoghue T, Owen MJ, O'Donovan MC, Gill M, Rujescu D, Corvin A (2009) Influence of NOS1 on verbal intelligence and working memory in both patients with schizophrenia and healthy control subjects. Arch Gen Psychiatry 66:1045-1054.

Doucet MV, Levine H, Dev KK, Harkin A (2013) Small-molecule inhibitors at the PSD-95/nNOS interface have antidepressant-like properties in mice. Neuropsychopharmacology 38:1575-1584.

Doyle CA, Slater P (1997) Localization of neuronal and endothelial nitric oxide synthase isoforms in human hippocampus. Neuroscience 76:387-395.

Duchemin S, Boily M, Sadekova N, Girouard H (2012) The complex contribution of NOS interneurons in the physiology of cerebrovascular regulation. Front Neural Circuits 6:51.

Echeverry MB, Salgado ML, Ferreira FR, da-Silva CA, Del Bel EA (2007) Intracerebroventricular administration of nitric oxide-sensitive guanylyl cyclase inhibitors induces catalepsy in mice. Psychopharmacology 194:271-278.

Egberongbe YI, Gentleman SM, Falkai P, Bogerts B, Polak JM, Roberts GW (1994) The distribution of nitric oxide synthase immunoreactivity in the human brain. Neuroscience 59:561-578.

Egerton A, Reid L, McKerchar CE, Morris BJ, Pratt JA (2005) Impairment in perceptual attentional set-shifting following PCP administration: a rodent model of set-shifting deficits in schizophrenia. Psychopharmacology 179:77-84.

Egerton A, Reid L, McGregor S, Cochran SM, Morris BJ, Pratt JA (2008) Subchronic and chronic PCP treatment produces temporally distinct deficits in attentional set shifting and prepulse inhibition in rats. Psychopharmacology 198:37-49.

Eliasson MJ, Blackshaw S, Schell MJ, Snyder SH (1997) Neuronal nitric oxide synthase alternatively spliced forms: prominent functional localizations in the brain. Proc Natl Acad Sci USA 94:3396-3401.

Eyerman DJ, Yamamoto BK (2007) A rapid oxidation and persistent decrease in the vesicular monoamine transporter 2 after methamphetamine. J Neurochem 103:1219-1227.

Ezeoke A, Mellor A, Buckley P, Miller B (in press) A systematic, quantitative review of blood autoantibodies in schizophrenia. Schizophrenia Research Advance online publication DOI: 101016/jschres201307029.

Fagg GE (1987) Phencyclidine and related drugs bind to the activated N-methyl-D-aspartate receptor-channel complex in rat brain membranes. Neurosci Lett 76:221-227.

Fallin MD, Lasseter VK, Avramopoulos D, Nicodemus KK, Wolyniec PS, McGrath JA, Steel G, Nestadt G, Liang K-Y, Huganir RL, Valle D, Pulver AE (2005) Bipolar I disorder and schizophrenia: a 440-single-nucleotide polymorphism screen of 64 candidate genes among Ashkenazi Jewish case-parent trios. Am J Hum Genet 77:918-936.

Fang J, Silverman RB (2009) A cellular model for screening neuronal nitric oxide synthase inhibitors. Anal Biochem 390:74-78.

Fatokun AA, Stone TW, Smith RA (2008) Prolonged exposures of cerebellar granule neurons to S-nitroso-N-acetylpenicillamine (SNAP) induce neuronal damage independently of peroxynitrite. Brain Research 1230:265-272.

Featherstone RE, Kapur S, Fletcher PJ (2007) The amphetamine-induced sensitized state as a model of schizophrenia. Prog Neuropsychopharmacol Biol Psychiatry 31:1556-1571.

Featherstone RE, Rizos Z, Kapur S, Fletcher PJ (2008) A sensitizing regimen of amphetamine that disrupts attentional set-shifting does not disrupt working or long-term memory. Behav Brain Res 189:170-179.

Featherstone RE, Liang Y, Saunders JA, Tatard-Leitman VM, Ehrlichman RS, Siegel SJ (2012) Subchronic ketamine treatment leads to permanent changes in EEG, cognition and the astrocytic glutamate transporter EAAT2 in mice. Neurobiol Dis 47:338-346.

Fejgin K, Pålsson E, Wass C, Svensson L, Klamer D (2008) Nitric oxide signaling in the medial prefrontal cortex is involved in the biochemical and behavioral effects of phencyclidine. Neuropsychopharmacology 33:1874-1883.

Fejgin K, Pålsson E, Wass C, Finnerty N, Lowry J, Klamer D (2009) Prefrontal GABAB Receptor Activation Attenuates Phencyclidine-Induced Impairments of Prepulse Inhibition: Involvement of Nitric Oxide. Neuropsychopharmacology 34:1673-1684.

Finnerty NJ, O'Riordan SL, Palsson E, Lowry JP (2012) Brain nitric oxide: regional characterisation of a real-time microelectrochemical sensor. J Neurosci Methods 209:13-21.

Finnerty NJ, Bolger FB, Pålsson E, Lowry JP (2013) An investigation of hypofrontality in an animal model of schizophrenia using real-time microelectrochemical sensors for glucose, oxygen and nitric oxide. ACS Chem Neurosci 4:825-831.

Fletcher PJ, Tenn CC, Rizos Z, Lovic V, Kapur S (2005) Sensitization to amphetamine, but not PCP, impairs attentional set shifting: reversal by a D1 receptor agonist injected into the medial prefrontal cortex. Psychopharmacology (Berl) 183:190-200.

Fletcher PJ, Tenn CC, Sinyard J, Rizos Z, Kapur S (2007) A sensitizing regimen of amphetamine impairs visual attention in the 5-choice serial reaction time test: reversal by a D1 receptor agonist injected into the medial prefrontal cortex. Neuropsychopharmacology 32:1122-1132.

Fone KC, Porkess MV (2008) Behavioural and neurochemical effects of post-weaning social isolation in rodents-relevance to developmental neuropsychiatric disorders. Neurosci Biobehav Rev 32:1087-1102.

Forrester MT, Seth D, Hausladen A, Eyler CE, Foster MW, Matsumoto A, Benhar M, Marshall HE, Stamler JS (2009) Thioredoxin-interacting protein (Txnip) is a feedback regulator of S-nitrosylation. J Biol Chem 284:36160-36166.

Frade JG, Barbosa RM, Laranjinha J (2009) Stimulation of NMDA and AMPA glutamate receptors elicits distinct concentration dynamics of nitric oxide in rat hippocampal slices. Hippocampus 19:603-611.

Fritzen S, Lauer M, Schmitt A, Töpner T, Strobel A, Lesch KP, Reif A (2007) NO synthase-positive striatal interneurons are decreased in schizophrenia. European Neuropsychopharmacology 17:595-599.

Gabbott PLA, Bacon SJ (1996) Localisation of NADPH diaphorase activity and NOS immunoreactivity in astroglia in normal adult rat brain. Brain Research 714:135-144.

Garthwaite G, Bartus K, Malcolm D, Goodwin D, Kollb-Sielecka M, Dooldeniya C, Garthwaite J (2006) Signaling from blood vessels to CNS axons through nitric oxide. The Journal of neuroscience : the official journal of the Society for Neuroscience 26:7730-7740.

Garthwaite J (2005) Dynamics of cellular NO-cGMP signaling. Frontiers in bioscience : a journal and virtual library 10:1868-1880.

Garthwaite J, Boulton CL (1995) Nitric oxide signaling in the central nervous system. Annu Rev Physiol 57:683-706.

Garthwaite J, Charles SL, Chess-Williams R (1988) Endothelium-derived relaxing factor release on activation of NMDA receptors suggests role as intercellular messenger in the brain. Nature 336:385-388.

Genius J, Geiger J, Dolzer AL, Benninghoff J, Giegling I, Hartmann AM, Moller HJ, Rujescu D (2013) Glutamatergic Dysbalance and Oxidative Stress in In Vivo and In Vitro Models of Psychosis Based on Chronic NMDA Receptor Antagonism. PLoS ONE 8:e59395.

Georgiadou G, Pitsikas N (2011) Repeated administration of the nitric oxide synthase inhibitor l-NAME differentially affects rats' recognition memory. Behavioural Brain Research 224:140-144.

Getting SJ, Segieth J, Ahmad S, Biggs CS, Whitton PS (1996) Biphasic modulation of GABA release by nitric oxide in the hippocampus of freely moving rats in vivo. Brain research 717:196-199.

Geyer MA, Krebs-Thomson K, Braff DL, Swerdlow NR (2001) Pharmacological studies of prepulse inhibition models of sensorimotor gating deficits in schizophrenia: a decade in review. Psychopharmacology (Berl) 156:117-154.

Gibson CL, La Rosa S, Ohta K, Boyle PH, Leurquin F, Lemaçon A, Suckling CJ (2004) The synthesis of 7-deazaguanines as potential inhibitors of guanosine triphosphate cyclohydrolase I. Tetrahedron 60:943-959.

Giegling I, Genius J, Benninghoff J, Rujescu D (2010) Genetic findings in schizophrenia patients related to alterations in the intracellular Ca-homeostasis. Prog Neuropsychopharmacol Biol Psychiatry 34:1375-1380.

Goff DC, Cather C, Freudenreich O, Henderson DC, Evins AE, Culhane MA, Walsh JP (2008) A placebo-controlled study of sildenafil effects on cognition in schizophrenia. Psychopharmacology 202:411-417.

González-Albo MC, Elston GN, DeFelipe J (2001) The human temporal cortex: characterization of neurons expressing nitric oxide synthase, neuropeptides and calcium-binding proteins, and their glutamate receptor subunit profiles. Cereb Cortex 11:1170-1181.

Gotti S, Sica M, Viglietti-Panzica C, Panzica G (2005) Distribution of nitric oxide synthase immunoreactivity in the mouse brain. Microsc Res Tech 68:13-35.

Grant MKO, Cuadra AE, El-Fakahany EE (2002) Endogenous expression of nNOS protein in several neuronal cell lines. Life Sciences 71:813-817.

Halberstadt AL, Geyer MA (2009) Habituation and sensitization of acoustic startle: opposite influences of dopamine D1 and D2-family receptors. Neurobiology of learning and memory 92:243-248.

Hall CN, Garthwaite J (2009) What is the real physiological NO concentration in vivo? Nitric Oxide 21:92-103.

Hallak JEC, Maia-de-Oliveira JP, Abrao J, Evora P, Zuardi AWaldo, Crippa JAS, Belmonte-de-Abreu P, Baker GB, Dursun SM (2013) Rapid Improvement of Acute Schizophrenia Symptoms After Intravenous Sodium Nitroprusside A Randomized, Double-blind, Placebo-Controlled Trial. JAMA Psychiatry.

Hara H, Waeber C, Huang PL, Fujii M, Fishman MC, Moskowitz MA (1996) Brain distribution of nitric oxide synthase in neuronal or endothelial nitric oxide synthase mutant mice using [3H]L-NG-nitro-arginine autoradiography. Neuroscience 75:881-890.

Harrison PJ, Weinberger DR (2005) Schizophrenia genes, gene expression, and neuropathology: on the matter of their convergence. Mol Psychiatry 10:40-68.

Ho GPH, Selvakumar B, Mukai J, Hester LD, Wang Y, Gogos JA, Snyder SH (2011) S-nitrosylation and S-palmitoylation reciprocally regulate synaptic targeting of PSD-95. Neuron 71:131-141.

Honer WG, Kopala LC, Rabinowitz J (2005) Extrapyramidal symptoms and signs in first-episode, antipsychotic exposed and non-exposed patients with schizophrenia or related psychotic illness. J Psychopharmacol 19:277-285.

Hong J-T, Kim H-C, Kim H-S, Lee Y-M, Oh K-W (2005) The role of nitric oxide on glutaminergic modulation of dopaminergic activation. Pharmacol Res 52:298-301.

Hope BT, Vincent SR (1989) Histochemical characterization of neuronal NADPH-diaphorase. J Histochem Cytochem 37:653-661.

Hope BT, Michael GJ, Knigge KM, Vincent SR (1991) Neuronal NADPH diaphorase is a nitric oxide synthase. Proceedings of the National Academy of Sciences 88:2811-2814.

Hopper R, Lancaster B, Garthwaite J (2004) On the regulation of NMDA receptors by nitric oxide. The European journal of neuroscience 19:1675-1682.

Hopper RA, Garthwaite J (2006) Tonic and phasic nitric oxide signals in hippocampal long-term potentiation. J Neurosci 26:11513-11521.

Hoque KE, Indorkar RP, Sammut S, West AR (2010) Impact of dopamine-glutamate interactions on striatal neuronal nitric oxide synthase activity. Psychopharmacology 207:571-581.

Howes OD, Kambeitz J, Kim E, Stahl D, Slifstein M, Abi-Dargham A, Kapur S (2012) The nature of dopamine dysfunction in schizophrenia and what this means for treatment. Arch Gen Psychiatry 69:776-786.

Huang PL, Dawson TM, Bredt DS, Snyder SH, Fishman MC (1993) Targeted disruption of the neuronal nitric oxide synthase gene. Cell 75:1273-1286.

Huang Y, Man H-Y, Sekine-Aizawa Y, Han Y, Juluri K, Luo H, Cheah J, Lowenstein C, Huganir RL, Snyder SH (2005) S-nitrosylation of N-ethylmaleimide sensitive factor mediates surface expression of AMPA receptors. Neuron 46:533-540.

Iacopucci AP, Mello RO, Barbosa-Silva R, Melo-Thomas L (2012) L-NOARG-induced catalepsy can be influenced by glutamatergic neurotransmission mediated by NMDA receptors in the inferior colliculus. Behavioural brain research 234:149-154.

Ichinose H, Nomura T, Sumi-Ichinose C (2008) Metabolism of tetrahydrobiopterin: its relevance in monoaminergic neurons and neurological disorders. Chem Rec 8:378-385.

Incontro S, Ramirez-Franco J, Sanchez-Prieto J, Torres M (2011) Membrane depolarization regulates AMPA receptor subunit expression in cerebellar granule cells in culture. Biochim Biophys Acta 1813:14-26.

Ishii H, Shibuya K, Ohta Y, Mukai H, Uchino S, Takata N, Rose JA, Kawato S (2006) Enhancement of nitric oxide production by association of nitric oxide synthase with N-methyl-D-aspartate receptors via postsynaptic density 95 in genetically engineered Chinese hamster ovary cells: real-time fluorescence imaging using nitric oxide sensitive dye. J Neurochem 96:1531-1539.

Ishikawa A, Kubota Y, Murayama T, Nomura Y (1999) Cell death by 1-chloro-2,4-dinitrobenzene, an inhibitor of thioredoxin reductase and its dual regulation by nitric oxide in rats. Neuroscience Letters 277:99-102.

Issy AC, Lazzarini M, Szawka RE, Carolino ROG, Anselmo-Franci JA, Bel EAD (2010) Nitric oxide synthase inhibitors improve prepulse inhibition responses of Wistar rats. Behavioural Brain Research 217:416-423.

Jaaro-Peled H (2009) Gene models of schizophrenia: DISC1 mouse models. Prog Brain Res 179:75-86.

Jaffrey S, Snowman A, Eliasson M, Cohen N, Snyder S (1998) CAPON: A Protein Associated with Neuronal Nitric Oxide Synthase that Regulates Its Interactions with PSD95. Neuron 20:115-124.

Janowsky DS, Risch C (1979) Amphetamine psychosis and psychotic symptoms. Psychopharmacology (Berl) 65:73-77.

Javitt DC, Zukin SR, Heresco-Levy U, Umbricht D (2012) Has an angel shown the way? Etiological and therapeutic implications of the PCP/NMDA model of schizophrenia. Schizophr Bull 38:958-966.

Javitt DC, Spencer KM, Thaker GK, Winterer G, Hajós M (2008) Neurophysiological biomarkers for drug development in schizophrenia. Nat Rev Drug Discov 7:68-83.

Jentsch JD, Roth RH (1999) The neuropsychopharmacology of phencyclidine: from NMDA receptor hypofunction to the dopamine hypothesis of schizophrenia. Neuropsychopharmacology 20:201-225.

Jentsch JD, Taylor JR, Roth RH (1998a) Subchronic phencyclidine administration increases mesolimbic dopaminergic system responsivity and augments stress- and psychostimulant-induced hyperlocomotion. Neuropsychopharmacology 19:105-113.

Jentsch JD, Tran A, Taylor JR, Roth RH (1998b) Prefrontal cortical involvement in phencyclidine-induced activation of the mesolimbic dopamine system: behavioral and neurochemical evidence. Psychopharmacology 138:89-95.

Jinno S, Kosaka T (2002) Patterns of expression of calcium binding proteins and neuronal nitric oxide synthase in different populations of hippocampal GABAergic neurons in mice. J Comp Neurol 449:1-25.

Johansson C (1998) The nitric oxide synthase inhibitor. L-NAME, blocks certain phencyclidine-induced but not amphetamine-induced effects on behaviour and brain biochemistry in the rat. Progress in Neuro-Psychopharmacology and Biological Psychiatry 22:1341-1360.

Johansson C, Jackson DM, Svensson L (1997) Nitric oxide synthase inhibition blocks phencyclidine-induced behavioural effects on prepulse inhibition and locomotor activity in the rat. Psychopharmacology 131:167-173.

Johansson C, Deveney AM, Reif D, Jackson DM (1999) The neuronal selective nitric oxide inhibitor AR-R 17477, blocks some effects of phencyclidine, while having no observable behavioural effects when given alone. Pharmacol Toxicol 84:226-233.

Jones C, Watson D, Fone K (2011) Animal models of schizophrenia. British Journal of Pharmacology 164:1162-1194.

Jones MW (2010) Errant ensembles: dysfunctional neuronal network dynamics in schizophrenia. Biochem Soc Trans 38:516-521.

Kano T, Shimizu-Sasamata M, Huang PL, Moskowitz MA, Lo EH (1998) Effects of nitric oxide synthase gene knockout on neurotransmitter release in vivo. Neuroscience 86:695-699.

Kasim N, Branton RL, Clarke DJ (2001) Neuronal nitric oxide synthase immunohistochemistry and 4,5-diaminofluorescein diacetate: tools for nitric oxide research. J Neurosci Methods 112:1-8.

Kaye DM, Gruskin S, Smith AI, Esler MD (2000) Nitric oxide mediated modulation of norepinephrine transport: identification of a potential target for S-nitrosylation. Br J Pharmacol 130:1060-1064.

Keilhoff G, Becker A, Grecksch G, Wolf G, Bernstein HG (2004) Repeated application of ketamine to rats induces changes in the hippocampal expression of parvalbumin, neuronal nitric oxide synthase and cFOS similar to those found in human schizophrenia. Neuroscience 126:591-598.

Keshavan M, Tandon R, Boutros N, Nasrallah H (2008) Schizophrenia, "just the facts": What we know in 2008Part 3: Neurobiology. Schizophrenia Research 106:89-107.

Kharazia VN, Schmidt HH, Weinberg RJ (1994) Type I nitric oxide synthase fully accounts for NADPH-diaphorase in rat striatum, but not cortex. Neuroscience 62:983-987.

Kiedrowski L, Costa E, Wroblewski JT (1992) Glutamate receptor agonists stimulate nitric oxide synthase in primary cultures of cerebellar granule cells. J Neurochem 58:335-341.

Kim KJ, Jang YY, Han ES, Lee CS (1999) Modulation of brain mitochondrial membrane permeability and synaptosomal Ca2+ transport by dopamine oxidation. Molecular and cellular biochemistry 201:89-98.

King M, Gildemeister O, Gaston B, Mannick JB (2005) Assessment of S-nitrosothiols on diaminofluorescein gels. Anal Biochem 346:69-76.

Kirchner L, Weitzdoerfer R, Hoeger H, Url A, Schmidt P, Engelmann M, Villar S, Fountoulakis M, Lubec G, Lubec B (2004) Impaired cognitive performance in neuronal nitric oxide synthase knockout mice is associated with hippocampal protein derangements. Nitric Oxide 11:316-330.

Kiss JP, Vizi ES (2001) Nitric oxide: a novel link between synaptic and nonsynaptic transmission. Trends in Neurosciences 24:211-215.

Klamer D, Engel JA, Svensson L (2004a) Phencyclidine-induced behaviour in mice prevented by methylene blue. Basic Clin Pharmacol Toxicol 94:65-72.

Klamer D, Engel JA, Svensson L (2004b) The neuronal selective nitric oxide synthase inhibitor, Nomega-propyl-L-arginine, blocks the effects of phencyclidine on prepulse inhibition and locomotor activity in mice. Eur J Pharmacol 503:103-107.

Klamer D, Engel JA, Svensson L (2005a) Effects of phencyclidine on acoustic startle and prepulse inhibition in neuronal nitric oxide synthase deficient mice. Eur Neuropsychopharmacol 15:587-590.

Klamer D, Zhang J, Engel JA, Svensson L (2005b) Selective interaction of nitric oxide synthase inhibition with phencyclidine: behavioural and NMDA receptor binding studies in the rat. Behavioural brain research 159:95-103.

Klamer D, Pålsson E, Fejgin K, Zhang J, Engel JA, Svensson L (2005c) Activation of a nitric-oxide-sensitive cAMP pathway with phencyclidine: elevated hippocampal cAMP levels are temporally associated with deficits in prepulse inhibition. Psychopharmacology 179:479-488.

Klatt P, Heinzel B, John M, Kastner M, Bohme E, Mayer B (1992) Ca2+/calmodulin-dependent cytochrome c reductase activity of brain nitric oxide synthase. J Biol Chem 267:11374-11378.

Kleppisch T, Feil R (2009) cGMP signalling in the mammalian brain: role in synaptic plasticity and behaviour. Handb Exp Pharmacol:549-579.

Knowles RG, Palacios M, Palmer RM, Moncada S (1990) Kinetic characteristics of nitric oxide synthase from rat brain. The Biochemical journal 269:207-210.

Kojima H, Nakatsubo N, Kikuchi K, Urano Y, Higuchi T, Tanaka J, Kudo Y, Nagano T (1998) Direct evidence of NO production in rat hippocampus and cortex using a new fluorescent indicator: DAF-2 DA. Neuroreport 9:3345-3348.

Komsuoglu-Celikyurt I, Gocmez SS, Mutlu O, Gacar N, Aricioglu F, Utkan T (2011) Evidence for the involvement of neuronal nitric oxide synthase and soluble guanylate cyclase on cognitive functions in rats. Life Sciences 89:905-910.

Konradi C, Yang CK, Zimmerman EI, Lohmann KM, Gresch P, Pantazopoulos H, Berretta S, Heckers S (2011) Hippocampal interneurons are abnormal in schizophrenia. Schizophrenia Research 131:165-173.

Kopf J, Schecklmann M, Hahn T, Dresler T, Dieler AC, Herrmann MJ, Fallgatter AJ, Reif A (2011) NOS1 ex1f-VNTR polymorphism influences prefrontal brain oxygenation during a working memory task. NeuroImage.

Kotsonis P, Fröhlich LG, Shutenko ZV, Horejsi R, Pfleiderer W, Schmidt HH (2000) Allosteric regulation of neuronal nitric oxide synthase by tetrahydrobiopterin and suppression of auto-damaging superoxide. Biochem J 346 Pt 3:767-776.

Kremeyer B, García J, Kymäläinen H, Wratten N, Restrepo G, Palacio C, Miranda AL, López C, Restrepo M, Bedoya G, Brzustowicz LM, Ospina-Duque J, Arbeláez MP, Ruiz-Linares A (2009) Evidence for a role of the NOS1AP (CAPON) gene in schizophrenia and its clinical dimensions: an association study in a South American population isolate. Hum Hered 67:163-173.

Kubota Y, Shigematsu N, Karube F, Sekigawa A, Kato S, Yamaguchi N, Hirai Y, Morishima M, Kawaguchi Y (2011) Selective Coexpression of Multiple Chemical Markers Defines Discrete Populations of Neocortical GABAergic Neurons. Cereb Cortex 21:1803-1817.

Kulikov AV, Rzhaninova AA, Goldshtein DV, Boldyrev AA (2007) Expression of NMDA receptors in multipotent stromal cells of human adipose tissue under conditions of retinoic acid-induced differentiation. Bulletin of experimental biology and medicine 144:626-629.

Kunuthur SP, Milliken PH, Gibson CL, Suckling CJ, Wadsworth RM (2011) Tetrahydrobiopterin analogues with NO-dependent pulmonary vasodilator properties. Eur J Pharmacol 650:371-377.

Lahti AC, Weiler MA, Tamara Michaelidis BA, Parwani A, Tamminga CA (2001) Effects of ketamine in normal and schizophrenic volunteers. Neuropsychopharmacology 25:455-467.

Lamprecht MR, Sabatini DM, Carpenter AE (2007) CellProfiler: free, versatile software for automated biological image analysis. BioTechniques 42:71-75.

Lapray D, Lasztoczi B, Lagler M, Viney TJ, Katona L, Valenti O, Hartwich K, Borhegyi Z, Somogyi P, Klausberger T (2012) Behavior-dependent specialization of identified hippocampal interneurons. Nat Neurosci.

Large CH (2007) Do NMDA receptor antagonist models of schizophrenia predict the clinical efficacy of antipsychotic drugs? J Psychopharmacol (Oxford) 21:283-301.

Lauer M, Johannes S, Fritzen S, Senitz D, Riederer P, Reif A (2005) Morphological Abnormalities in Nitric-Oxide-Synthase-Positive Striatal Interneurons of Schizophrenic Patients. Neuropsychobiology 52:111-117.

Lee B-H, Kim Y-K (2008) Reduced plasma nitric oxide metabolites before and after antipsychotic treatment in patients with schizophrenia compared to controls. Schizophrenia Research 104:36-43.

Lei SZ, Pan ZH, Aggarwal SK, Chen HS, Hartman J, Sucher NJ, Lipton SA (1992) Effect of nitric oxide production on the redox modulatory site of the NMDA receptor-channel complex. Neuron 8:1087-1099.

Leikert JF, Räthel TR, Müller C, Vollmar AM, Dirsch VM (2001) Reliable in vitro measurement of nitric oxide released from endothelial cells using low concentrations of the fluorescent probe 4,5-diaminofluorescein. FEBS Lett 506:131-134.

Levkovitz Y, Mendlovich S, Riwkes S, Braw Y, Levkovitch-Verbin H, Gal G, Fennig S, Treves I, Kron S (2010) A double-blind, randomized study of minocycline for the treatment of negative and cognitive symptoms in early-phase schizophrenia. J Clin Psychiatry 71:138-149.

Lewis DA, Hashimoto T, Volk DW (2005) Cortical inhibitory neurons and schizophrenia. Nat Rev Neurosci 6:312-324.

Li L-L, Ginet V, Liu X, Vergun O, Tuittila M, Mathieu M, Bonny C, Puyal J, Truttmann AC, Courtney MJ (2013) The nNOS-p38MAPK Pathway Is

Mediated by NOS1AP during Neuronal Death. J Neurosci 33:8185-8201.

Li Z, Jo J, Jia JM, Lo SC, Whitcomb DJ, Jiao S, Cho K, Sheng M (2010) Caspase-3 activation via mitochondria is required for long-term depression and AMPA receptor internalization. Cell 141:859-871.

Liang LP, Kaufman S (1998) The regulation of dopamine release from striatum slices by tetrahydrobiopterin and L-arginine-derived nitric oxide. Brain Research 800:181-186.

Liang Z, Zhang L, Wang X, Gao F, Wang X, Zhou S, Yu S, Zhan R-Z (2013) Distribution and Neurochemical Features of Neuronal Nitric Oxide Synthase-Expressing Interneurons in the Rat Dentate Gyrus. Brain research.

Lipton SA, Choi YB, Pan ZH, Lei SZ, Chen HS, Sucher NJ, Loscalzo J, Singel DJ, Stamler JS (1993) A redox-based mechanism for the neuroprotective and neurodestructive effects of nitric oxide and related nitroso-compounds. Nature 364:626-632.

Liu DH, Yuan FG, Hu SQ, Diao F, Wu YP, Zong YY, Song T, Li C, Zhang GY (2013) Endogenous nitric oxide induces activation of apoptosis signal-regulating kinase 1 via S-nitrosylation in rat hippocampus during cerebral ischemia-reperfusion. Neuroscience 229:36-48.

Lodge DJ, Grace AA (2009) Gestational methylazoxymethanol acetate administration: a developmental disruption model of schizophrenia. Behav Brain Res 204:306-312.

Lopez Hill X, Scorza MC (2012) Role of the anterior thalamic nucleus in the motor hyperactivity induced by systemic MK-801 administration in rats. Neuropharmacology 62:2440-2446.

Lu J, Papp LV, Fang J, Rodriguez-Nieto S, Zhivotovsky B, Holmgren A (2006) Inhibition of Mammalian thioredoxin reductase by some flavonoids: implications for myricetin and quercetin anticancer activity. Cancer Res 66:4410-4418.

Lu J, Katano T, Okuda-Ashitaka E, Oishi Y, Urade Y, Ito S (2009) Involvement of S-nitrosylation of actin in inhibition of neurotransmitter release by nitric oxide. Mol Pain 5.

Lu YF, Kandel ER, Hawkins RD (1999) Nitric oxide signaling contributes to late-phase LTP and CREB phosphorylation in the hippocampus. Journal of Neuroscience 19:10250-10261.

Luby ED, Cohen BD, Rosenbaum G, Gottlieb JS, Kelley R (1959) Study of a new schizophrenomimetic drug; sernyl. AMA Arch Neurol Psychiatry 81:363-369.

Luo D, Knezevich S, Vincent SR (1993) N-methyl-D-aspartate-induced nitric oxide release: an in vivo microdialysis study. Neuroscience 57:897-900.

Macrae IM, Dawson DA, Norrie JD, McCulloch J (1993) Inhibition of nitric oxide synthesis: effects on cerebral blood flow and glucose utilisation in the rat. J Cereb Blood Flow Metab 13:985-992.

Mahairaki V, Xu L, Farah MH, Hatfield G, Kizana E, Marbán E, Koliatsos VE (2009) Targeted knock-down of neuronal nitric oxide synthase expression in basal forebrain with RNA interference. J Neurosci Methods 179:292-299.

Maia-de-Oliveira JP, Trzesniak C, Oliveira IR, Kempton MJ, Rezende TMNd, Iego S, Baker GB, Dursun SM, Machado-de-Sousa JP, Hallak JEC (2012) Nitric oxide plasma/serum levels in patients with schizophrenia: a systematic review and meta-analysis. Rev Bras Psiquiatr 34 Suppl 2:s149-155.

Marques-da-Silva D, Gutierrez-Merino C (2012) L-type voltage-operated calcium channels, N-methyl-D-aspartate receptors and neuronal nitric-oxide synthase form a calcium/redox nano-transducer within lipid rafts. Biochem Biophys Res Commun 420:257-262.

Marsman A, van den Heuvel MP, Klomp DW, Kahn RS, Luijten PR, Hulshoff Pol HE (2013) Glutamate in schizophrenia: a focused review and meta-analysis of (1)H-MRS studies. Schizophr Bull 39:120-129.

Martínez-Ruiz A, Cadenas S, Lamas S (2011) Nitric oxide signaling: Classical, less classical, and nonclassical mechanisms. Free Radic Biol Med 51:17-29.

Martinez V, Sarter M (2008) Detection of the moderately beneficial cognitive effects of low-dose treatment with haloperidol or clozapine in an animal model of the attentional impairments of schizophrenia. Neuropsychopharmacology 33:2635-2647.

Matsuo N, Takao K, Nakanishi K, Yamasaki N, Tanda K, Miyakawa T (2010) Behavioral profiles of three C57BL/6 substrains. Front Behav Neurosci 4.

McDonald C, Murray RM (2000) Early and late environmental risk factors for schizophrenia. Brain Res Brain Res Rev 31:130-137.

Meffert MK, Premack BA, Schulman H (1994) Nitric oxide stimulates Ca(2+)-independent synaptic vesicle release. Neuron 12:1235-1244.

Meij JTA, Haselton CL, Hillman KL, Muralikrishnan D, Ebadi M, Yu L (2004) Differential mechanisms of nitric oxide- and peroxynitrite-induced cell death. Mol Pharmacol 66:1043-1053.

Meyer U (2013) Prenatal Poly(I:C) Exposure and Other Developmental Immune Activation Models in Rodent Systems. Biol Psychiatry.

Miyamoto S, Miyake N, Jarskog LF, Fleischhacker WW, Lieberman JA (2012) Pharmacological treatment of schizophrenia: a critical review of the pharmacology and clinical effects of current and future therapeutic agents. Mol Psychiatry 17:1206-1227.

Miyaoka T, Yasukawa R, Yasuda H, Hayashida M, Inagaki T, Horiguchi J (2008) Minocycline as adjunctive therapy for schizophrenia: an open-label study. Clin Neuropharmacol 31:287-292.

Moghaddam B, Adams B, Verma A, Daly D (1997) Activation of glutamatergic neurotransmission by ketamine: a novel step in the pathway from NMDA receptor blockade to dopaminergic and cognitive disruptions associated with the prefrontal cortex. J Neurosci 17:2921-2927.

Moore CI, Cao R (2008) The hemo-neural hypothesis: on the role of blood flow in information processing. J Neurophysiol 99:2035-2047.

Moore PK, Handy RLC (1997) Selective inhibitors of neuronal nitric oxide synthase–is no NOS really good NOS for the nervous system? Trends in Pharmacological Sciences 18:204-211.

Moore PK, Wallace P, Gaffen Z, Hart SL, Babbedge RC (1993) Characterization of the novel nitric oxide synthase inhibitor 7-nitro indazole and related indazoles: antinociceptive and cardiovascular effects. British Journal of Pharmacology 110:219-224.

Moore WM, Webber RK, Fok KF, Jerome GM, Kornmeier CM, Tjoeng FS, Currie MG (1996) Inhibitors of human nitric oxide synthase isoforms with the carbamidine moiety as a common structural element. Bioorganic & medicinal chemistry 4:1559-1564.

Morales-Medina JC, Mejorada A, Romero-Curiel A, Aguilar-Alonso P, Leon-Chavez BA, Gamboa C, Quirion R, Flores G (2008) Neonatal administration of N-omega-nitro-L-arginine induces permanent decrease in NO levels and hyperresponsiveness to locomotor activity by D-amphetamine in postpubertal rats. Neuropharmacology 55:1313-1320.

Morris BJ (1995) Stimulation of immediate early gene expression in striatal neurons by nitric oxide. J Biol Chem 270:24740-24744.

Morris BJ, Simpson CS, Mundell S, Maceachern K, Johnston HM, Nolan AM (1997) Dynamic changes in NADPH-diaphorase staining reflect activity of nitric oxide synthase: evidence for a dopaminergic regulation of striatal nitric oxide release. Neuropharmacology 36:1589-1599.

Müller D, Greenland KJ, Speth RC, Middendorff R (2010) Neuronal differentiation of NG108-15 cells has impact on nitric oxide- and membrane (natriuretic peptide receptor-A) cyclic GMP-generating proteins. Mol Cell Endocrinol 320:118-127.

Muller JE, Koen L, Soraya S, Emsley RA, Stein DJ (2004) Anxiety disorders and schizophrenia. Current psychiatry reports 6:255-261.

Mullinger KJ, Mayhew SD, Bagshaw AP, Bowtell R, Francis ST (2013) Poststimulus undershoots in cerebral blood flow and BOLD fMRI responses are modulated by poststimulus neuronal activity. Proc Natl Acad Sci U S A 110:13636-13641.

Nakatani-Pawlak A, Yamaguchi K, Tatsumi Y, Mizoguchi H, Yoneda Y (2009) Neonatal phencyclidine treatment in mice induces behavioral, histological and neurochemical abnormalities in adulthood. Biol Pharm Bull 32:1576-1583.

Nakazawa K, Zsiros V, Jiang Z, Nakao K, Kolata S, Zhang S, Belforte JE (2011) GABAergic interneuron origin of schizophrenia pathophysiology. Neuropharmacology 62:1574-1583.

Negrete-Díaz JV, Baltazar-Gaytán E, Bringas ME, Vazquez-Roque RA, Newton S, Aguilar-Alonso P, León-Chávez BA, Flores G (2010) Neonatal ventral hippocampus lesion induces increase in NO levels which is attenuated by subchronic haloperidol treatment. Synapse 64:941-947.

Nelson CA, 3rd, Zeanah CH, Fox NA, Marshall PJ, Smyke AT, Guthrie D (2007) Cognitive recovery in socially deprived young children: the Bucharest Early Intervention Project. Science 318:1937-1940.

Nicodemus KK, Law AJ, Radulescu E, Luna A, Kolachana B, Vakkalanka R, Rujescu D, Giegling I, Straub RE, McGee K, Gold B, Dean M, Muglia P, Callicott JH, Tan H-Y, Weinberger DR (2010) Biological validation of increased schizophrenia risk with NRG1, ERBB4, and AKT1 epistasis via functional neuroimaging in healthy controls. Arch Gen Psychiatry 67:991-1001.

Nikonenko I, Boda B, Steen S, Knott G, Welker E, Muller D (2008) PSD-95 promotes synaptogenesis and multiinnervated spine formation through nitric oxide signaling. J Cell Biol 183:1115-1127.

Nomura K, Lee M, Banks C, Lee G, Morris BJ (2013) An ASK1-p38 signalling pathway mediates hydrogen peroxide-induced toxicity in NG108-15 neuronal cells. Neuroscience Letters 549:163-167.

O'Donoghue T, Morris DW, Fahey C, Costa AD, Foxe JJ, Hoerold D, Tropea D, Gill M, Corvin A, Donohoe G (2011) A NOS1 variant implicated in cognitive performance influences evoked neural responses during a high density EEG study of early visual perception. Hum Brain Mapp 33:1202-1211.

O'Donovan MC et al. (2008) Identification of loci associated with schizophrenia by genome-wide association and follow-up. Nat Genet 40:1053-1055.

Ogren SO, Goldstein M (1994) Phencyclidine- and dizocilpine-induced hyperlocomotion are differentially mediated. Neuropsychopharmacology 11:167-177.

Ohkuma S, Katsura M, Chen DZ, Chen SH, Kuriyama K (1994) Presence of N-methyl-D-aspartate (NMDA) receptors in neuroblastoma x glioma hybrid NG108-15 cells-analysis using [45Ca2+]influx and [3H]MK-801 binding as functional measures. Brain Res Mol Brain Res 22:166-172.

Oka M, Itoh Y, Wada M, Yamamoto A, Fujita T (2003) Gabapentin blocks L-type and P/Q-type Ca2+ channels involved in depolarization-stimulated nitric oxide synthase activity in primary cultures of neurons from mouse cerebral cortex. Pharm Res 20:897-899.

Okada D, Yap CC, Kojima H, Kikuchi K, Nagano T (2004) Distinct glutamate receptors govern differential levels of nitric oxide production in a layer-specific manner in the rat cerebellar cortex. Neuroscience 125:461-472.

Okumura T, Okochi T, Kishi T, Ikeda M, Kitajima T, Yamanouchi Y, Kinoshita Y, Kawashima K, Tsunoka T, Ujike H, Inada T, Ozaki N, Iwata N (2009) No association between polymorphisms of neuronal oxide synthase 1 gene (NOS1) and schizophrenia in a Japanese population. Neuromolecular Med 11:123-127.

Owen MJ (2012) Implications of genetic findings for understanding schizophrenia. Schizophr Bull 38:904-907.

Owen MJ, Craddock N, O'Donovan MC (2010) Suggestion of roles for both common and rare risk variants in genome-wide studies of schizophrenia. Arch Gen Psychiatry 67:667-673.

Pålsson E, Lowry J, Klamer D (2010) Information processing deficits and nitric oxide signalling in the phencyclidine model of schizophrenia. Psychopharmacology.

Papadia S, Soriano FX, Léveillé F, Martel M-A, Dakin KA, Hansen HH, Kaindl A, Sifringer M, Fowler J, Stefovska V, McKenzie G, Craigon M, Corriveau R, Ghazal P, Horsburgh K, Yankner BA, Wyllie DJA, Ikonomidou C, Hardingham GE (2008) Synaptic NMDA receptor activity boosts intrinsic antioxidant defenses. Nat Neurosci 11:476-487.

Papaleo F, Lipska BK, Weinberger DR (2012) Mouse models of genetic effects on cognition: relevance to schizophrenia. Neuropharmacology 62:1204-1220.

Park DJ, West AR (2009) Regulation of striatal nitric oxide synthesis by local dopamine and glutamate interactions. J Neurochem 111:1457-1465.

Parnaudeau S, O'Neill P-K, Bolkan SS, Ward RD, Abbas AI, Roth BL, Balsam PD, Gordon JA, Kellendonk C (2013) Inhibition of mediodorsal

thalamus disrupts thalamofrontal connectivity and cognition. Neuron 77:1151-1162.

Paxinos G, Franklin KBJ (2001) The mouse brain in stereotaxic coordinates, 2nd Edition. San Diego: Academic Press.

Pepicelli O, Brescia A, Gherzi E, Raiteri M, Fedele E (2004) GABA(A), but not NMDA, receptors modulate in vivo NO-mediated cGMP synthesis in the rat cerebral cortex. Neuropharmacology 46:480-489.

Pettersson-Yeo W, Allen P, Benetti S, McGuire P, Mechelli A (2011) Dysconnectivity in schizophrenia: Where are we now? Neurosci Biobehav Rev 35:1110-1124.

Pigott B, Garthwaite J (2012) Involvement of NO in NMDA receptor-independent long-term potentiation. Nitric Oxide 27:S19.

Pigott B, Bartus K, Garthwaite J (2013) On the selectivity of neuronal NOS inhibitors. Br J Pharmacol 168:1255-1265.

Pinault D (2011) Dysfunctional thalamus-related networks in schizophrenia. Schizophr Bull 37:238-243.

Porteous DJ, Millar JK, Brandon NJ, Sawa A (2011) DISC1 at 10: connecting psychiatric genetics and neuroscience. Trends in molecular medicine 17:699-706.

Prabakaran S, Swatton JE, Ryan MM, Huffaker SJ, Huang JTJ, Griffin JL, Wayland M, Freeman T, Dudbridge F, Lilley KS, Karp NA, Hester S, Tkachev D, Mimmack ML, Yolken RH, Webster MJ, Torrey EF, Bahn S (2004) Mitochondrial dysfunction in schizophrenia: evidence for compromised brain metabolism and oxidative stress. Mol Psychiatry 9:684-697, 643.

Prast H, Philippu A (2001) Nitric oxide as modulator of neuronal function. Progress in Neurobiology 64:51-68.

Pratt J, Winchester C, Dawson N, Morris B (2012) Advancing schizophrenia drug discovery: optimizing rodent models to bridge the translational gap. Nature reviews Drug discovery 11:560-579.

Pratt JA, Winchester C, Egerton A, Cochran SM, Morris BJ (2008) Modelling prefrontal cortex deficits in schizophrenia: implications for treatment. British Journal of Pharmacology 153:S465-S470.

Putzke J, Seidel B, Huang PL, Wolf G (2000) Differential expression of alternatively spliced isoforms of neuronal nitric oxide synthase (nNOS) and N-methyl-D-aspartate receptors (NMDAR) in knockout mice deficient in nNOS alpha (nNOS alpha(Delta/Delta) mice). Brain Res Mol Brain Res 85:13-23.

Qu Z-W, Miao W-Y, Hu S-Q, Li C, Zhuo X-L, Zong Y-Y, Wu Y-P, Zhang G-Y (2012) N-methyl-d-aspartate receptor-dependent denitrosylation of

neuronal nitric oxide synthase increase the enzyme activity. PLoS ONE 7.

Racca C, Catania MV, Monyer H, Sakmann B (1996) Expression of AMPA-glutamate receptor B subunit in rat hippocampal GABAergic neurons. Eur J Neurosci 8:1580-1590.

Rameau GA, Tukey DS, Garcin-Hosfield ED, Titcombe RF, Misra C, Khatri L, Getzoff ED, Ziff EB (2007) Biphasic coupling of neuronal nitric oxide synthase phosphorylation to the NMDA receptor regulates AMPA receptor trafficking and neuronal cell death. J Neurosci 27:3445-3455.

Rancillac A, Rossier J, Guille M, Tong X-K, Geoffroy H, Amatore C, Arbault S, Hamel E, Cauli B (2006) Glutamatergic Control of Microvascular Tone by Distinct GABA Neurons in the Cerebellum. J Neurosci 26:6997-7006.

Rees DD, Palmer RM, Schulz R, Hodson HF, Moncada S (1990) Characterization of three inhibitors of endothelial nitric oxide synthase in vitro and in vivo. British journal of pharmacology 101:746-752.

Reif A, Fröhlich LG, Kotsonis P, Frey A, Bömmel HM, Wink DA, Pfleiderer W, Schmidt HH (1999) Tetrahydrobiopterin inhibits monomerization and is consumed during catalysis in neuronal NO synthase. J Biol Chem 274:24921-24929.

Reif A, Schecklmann M, Eirich E, Jacob CP, Jarczok TA, Kittel-Schneider S, Lesch KP, Fallgatter AJ, Ehlis AC (2011) A functional promoter polymorphism of neuronal nitric oxide synthase moderates prefrontal functioning in schizophrenia. Int J Neuropsychopharmacol 14:887-897.

Reif A, Herterich S, Strobel A, Ehlis AC, Saur D, Jacob CP, Wienker T, Töpner T, Fritzen S, Walter U, Schmitt A, Fallgatter AJ, Lesch KP (2006) A neuronal nitric oxide synthase (NOS-I) haplotype associated with schizophrenia modifies prefrontal cortex function. Mol Psychiatry 11:286-300.

Richardson MA, Read LL, Reilly MA, Clelland JD, Clelland CLT (2007) Analysis of plasma biopterin levels in psychiatric disorders suggests a common BH4 deficit in schizophrenia and schizoaffective disorder. Neurochem Res 32:107-113.

Riley B, Thiselton D, Maher BS, Bigdeli T, Wormley B, McMichael GO, Fanous AH, Vladimirov V, O'Neill FA, Walsh D, Kendler KS (2009) Replication of association between schizophrenia and ZNF804A in the Irish Case–Control Study of Schizophrenia sample. Mol Psychiatry 15:29-37.

Rocchitta G, Migheli R, Mura MP, Grella G, Esposito G, Marchetti B, Miele E, Desole MS, Miele M, Serra PA (2005) Signaling pathways in the nitric oxide and iron-induced dopamine release in the striatum of freely moving rats: role of extracellular Ca2+ and L-type Ca2+ channels. Brain research 1047:18-29.

Rodefer JS, Saland SK, Eckrich SJ (2012) Selective phosphodiesterase inhibitors improve performance on the ED/ID cognitive task in rats. Neuropharmacology 62:1182-1190.

Rodriguez J, Specian V, Maloney R, Jourd'heuil D, Feelisch M (2005) Performance of diamino fluorophores for the localization of sources and targets of nitric oxide. Free Radic Biol Med 38:356-368.

Roenker NL, Gudelsky GA, Ahlbrand R, Horn PS, Richtand NM (2012) Evidence for involvement of nitric oxide and GABA(B) receptors in MK-801- stimulated release of glutamate in rat prefrontal cortex. Neuropharmacology.

Rojas JC, Bruchey AK, Gonzalez-Lima F (2012) Neurometabolic mechanisms for memory enhancement and neuroprotection of methylene blue. Progress in Neurobiology 96:32-45.

Rose EJ, Greene C, Kelly S, Morris DW, Robertson IH, Fahey C, Jacobson S, O'Doherty J, Newell FN, McGrath J, Bokde A, Garavan H, Frodl T, Gill M, Corvin AP, Donohoe G (2012) The NOS1 variant rs6490121 is associated with variation in prefrontal function and grey matter density in healthy individuals. Neuroimage 60:614-622.

Rujescu D, Bender A, Keck M, Hartmann AM, Ohl F, Raeder H, Giegling I, Genius J, McCarley RW, Möller H-J, Grunze H (2006) A pharmacological model for psychosis based on N-methyl-D-aspartate receptor hypofunction: molecular, cellular, functional and behavioral abnormalities. Biol Psychiatry 59:721-729.

Salum C, Guimarães FS, Brandão ML, Del Bel EA (2006) Dopamine and nitric oxide interaction on the modulation of prepulse inhibition of the acoustic startle response in the Wistar rat. Psychopharmacology 185:133-141.

Salum C, Issy AC, Brandão ML, Guimarães FS, Bel EAD (2011) Nitric oxide modulates dopaminergic regulation of prepulse inhibition in the basolateral amygdala. J Psychopharmacol (Oxford) 25:1639-1648.

Salum C, Raisman-Vozari R, Michel PP, Gomes MZ, Mitkovski M, Ferrario JE, Ginestet L, Del Bel EA (2008) Modulation of dopamine uptake by nitric oxide in cultured mesencephalic neurons. Brain Research 1198:27-33.

Sammut S, Threlfell S, West AR (2010) Nitric oxide-soluble guanylyl cyclase signaling regulates corticostriatal transmission and short-term synaptic plasticity of striatal projection neurons recorded in vivo. Neuropharmacology 58:624-631.

Sams-Dodd F (1995) Distinct effects of d-amphetamine and phencyclidine on the social behaviour of rats. Behav Pharmacol 6:55-65.

Sams-Dodd F (1996) Phencyclidine-induced stereotyped behaviour and social isolation in rats: a possible animal model of schizophrenia. Behav Pharmacol 7:3-23.

Sams-Dodd F (1998a) Effects of continuous D-amphetamine and phencyclidine administration on social behaviour, stereotyped behaviour, and locomotor activity in rats. Neuropsychopharmacology 19:18-25.

Sams-Dodd F (1998b) Effects of dopamine agonists and antagonists on PCP-induced stereotyped behaviour and social isolation in the rat social interaction test. Psychopharmacology (Berl) 135:182-193.

Sato M (2006) Renaming schizophrenia: a Japanese perspective. World psychiatry : official journal of the World Psychiatric Association 5:53-55.

Sattler R, Xiong Z, Lu WY, Hafner M, MacDonald JF, Tymianski M (1999) Specific coupling of NMDA receptor activation to nitric oxide neurotoxicity by PSD-95 protein. Science 284:1845-1848.

Schiavone S, Sorce S, Dubois-Dauphin M, Jaquet V, Colaianna M, Zotti M, Cuomo V, Trabace L, Krause KH (2009) Involvement of NOX2 in the Development of Behavioral and Pathologic Alterations in Isolated Rats. Biol Psychiatry 66:384-392.

Schindelin J, Arganda-Carreras I, Frise E, Kaynig V, Longair M, Pietzsch T, Preibisch S, Rueden C, Saalfeld S, Schmid B, Tinevez J-Y, White DJ, Hartenstein V, Eliceiri K, Tomancak P, Cardona A (2012) Fiji: an open-source platform for biological-image analysis. Nat Methods 9:676-682.

Segieth J, Fowler L, Whitton P, Pearce B (2000) Nitric oxide-mediated regulation of dopamine release in the hippocampus in vivo. Neuropharmacology 39:571-577.

Segovia G, Mora F (1998) Role of nitric oxide in modulating the release of dopamine, glutamate, and GABA in striatum of the freely moving rat. Brain research bulletin 45:275-279.

Selemidis S, Dusting GJ, Peshavariya H, Kemp-Harper BK, Drummond GR (2007) Nitric oxide suppresses NADPH oxidase-dependent superoxide production by S-nitrosylation in human endothelial cells. Cardiovasc Res 75:349-358.

Selvakumar B, Huganir RL, Snyder SH (2009) S-nitrosylation of stargazin regulates surface expression of AMPA-glutamate neurotransmitter receptors. Proc Natl Acad Sci USA 106:16440-16445.

Sengupta R, Holmgren A (2012) The role of thioredoxin in the regulation of cellular processes by S-nitrosylation. Biochimica Et Biophysica Acta 1820:689-700.

Sengupta R, Billiar TR, Kagan VE, Stoyanovsky DA (2010) Nitric oxide and thioredoxin type 1 modulate the activity of caspase 8 in HepG2 cells. Biochem Biophys Res Commun 391:1127-1130.

Sengupta R, Billiar TR, Atkins JL, Kagan VE, Stoyanovsky DA (2009) Nitric oxide and dihydrolipoic acid modulate the activity of caspase 3 in HepG2 cells. FEBS Lett 583:3525-3530.

Seshadri S, Zeledon M, Sawa A (2013) Synapse-specific contributions in the cortical pathology of schizophrenia. Neurobiol Dis 53:26-35.

Seth D, Stamler JS (2011) The SNO-proteome: causation and classifications. Curr Opin Chem Biol 15:129-136.

Shahani N, Sawa A (2011) Protein S-nitrosylation: Role for nitric oxide signaling in neuronal death. Biochimica Et Biophysica Acta 1820:736-742.

Shao L-E, Tanaka T, Gribi R, Yu J (2002) Thioredoxin-related regulation of NO/NOS activities. Ann N Y Acad Sci 962:140-150.

Shinkai T, Ohmori O, Hori H, Nakamura J (2002) Allelic association of the neuronal nitric oxide synthase (NOS1) gene with schizophrenia. Mol Psychiatry 7:560-563.

Shlosberg D, Buskila Y, Abu-Ghanem Y, Amitai Y (2012) Spatiotemporal alterations of cortical network activity by selective loss of NOS-expressing interneurons. Front Neural Circuits 6.

Silberberg G, Ben-Shachar D, Navon R (2010) Genetic analysis of nitric oxide synthase 1 variants in schizophrenia and bipolar disorder. Am J Med Genet B Neuropsychiatr Genet 153B:1318-1328.

Smith J, Whitton P (2001) The regulation of NMDA-evoked dopamine release by nitric oxide in the frontal cortex and raphe nuclei of the freely moving rat. Brain Research 889:57-62.

Smith JW, Gastambide F, Gilmour G, Dix S, Foss J, Lloyd K, Malik N, Tricklebank M (2011) A comparison of the effects of ketamine and phencyclidine with other antagonists of the NMDA receptor in rodent assays of attention and working memory. Psychopharmacology 217:255-269.

Smoller JW, Craddock N, Kendler K, Lee PH, Neale BM, Nurnberger JI, Ripke S, Santangelo S, Sullivan PF, Consortium PG (2013) Identification of risk loci with shared effects on five major psychiatric disorders: a genome-wide analysis. Lancet 381:1371-1379.

Sohal VS, Zhang F, Yizhar O, Deisseroth K (2009) Parvalbumin neurons and gamma rhythms enhance cortical circuit performance. Nature 459:698-702.

Soriano FX, Martel M-A, Papadia S, Vaslin A, Baxter P, Rickman C, Forder J, Tymianski M, Duncan R, Aarts M, Clarke P, Wyllie DJA, Hardingham

GE (2008) Specific targeting of pro-death NMDA receptor signals with differing reliance on the NR2B PDZ ligand. J Neurosci 28:10696-10710.

St Clair D, Blackwood D, Muir W, Carothers A, Walker M, Spowart G, Gosden C, Evans HJ (1990) Association within a family of a balanced autosomal translocation with major mental illness. Lancet 336:13-16.

Stojkovic T, Colin C, Le Saux F, Jacque C (1998) Specific pattern of nitric oxide synthase expression in glial cells after hippocampal injury. Glia 22:329-337.

Stricker S, Manahan-Vaughan D (2009) Regulation of long-term depression by increases in [guanosine 3',5'-cyclic monophosphate] in the hippocampal CA1 region of freely behaving rats. Neuroscience 158:159-166.

Suckling CJ, Gibson CL, Huggan JK, Morthala RR, Clarke B, Kununthur S, Wadsworth RM, Daff S, Papale D (2008) 6-Acetyl-7, 7-dimethyl-5, 6, 7, 8-tetrahydropterin is an activator of nitric oxide synthases. Bioorganic & Medicinal Chemistry Letters.

Sun ZW, Zhang L, Zhu SJ, Chen WC, Mei B (2010) Excitotoxicity effects of glutamate on human neuroblastoma SH-SY5Y cells via oxidative damage. Neurosci Bull 26:8-16.

Swerdlow NR, Geyer MA, Braff DL (2001) Neural circuit regulation of prepulse inhibition of startle in the rat: current knowledge and future challenges. Psychopharmacology (Berl) 156:194-215.

Swerdlow NR, Light GA, Breier MR, Shoemaker JM, Saint Marie RL, Neary AC, Geyer MA, Stevens KE, Powell SB (2012) Sensory and sensorimotor gating deficits after neonatal ventral hippocampal lesions in rats. Developmental neuroscience 34:240-249.

Szabo A, Somogyi J, Cauli B, Lambolez B, Somogyi P, Lamsa KP (2012) Calcium-permeable AMPA receptors provide a common mechanism for LTP in glutamatergic synapses of distinct hippocampal interneuron types. J Neurosci 32:6511-6516.

Tamminga CA, Stan AD, Wagner AD (2010) The hippocampal formation in schizophrenia. Am J Psychiatry 167:1178-1193.

Tanda K, Nishi A, Matsuo N, Nakanishi K, Yamasaki N, Sugimoto T, Toyama K, Takao K, Miyakawa T (2009) Abnormal social behavior, hyperactivity, impaired remote spatial memory, and increased D1-mediated dopaminergic signaling in neuronal nitric oxide synthase knockout mice. Molecular Brain 2.

Tandon R, Keshavan MS, Nasrallah HA (2008) Schizophrenia, "Just the Facts" What we know in 2008. 2. Epidemiology and etiology. Schizophrenia Research 102:1-18.

Tandon R, Nasrallah HA, Keshavan MS (2009) Schizophrenia, "just the facts" 4. Clinical features and conceptualization. Schizophr Res 110:1-23.

Tang W, Huang K, Tang R, Zhou G, Fang C, Zhang J, Du L, Feng G, He L, Shi Y (2008) Evidence for association between the 5' flank of the NOS1 gene and schizophrenia in the Chinese population. Int J Neuropsychopharmacol 11:1063-1071.

Tenn CC, Kapur S, Fletcher PJ (2005) Sensitization to amphetamine, but not phencyclidine, disrupts prepulse inhibition and latent inhibition. Psychopharmacology (Berl) 180:366-376.

Tenneti L, D'Emilia DM, Lipton SA (1997) Suppression of neuronal apoptosis by S-nitrosylation of caspases. Neuroscience Letters 236:139-142.

Terpolilli NA, Moskowitz MA, Plesnila N (2012) Nitric oxide: considerations for the treatment of ischemic stroke. Journal of cerebral blood flow and metabolism : official journal of the International Society of Cerebral Blood Flow and Metabolism 32:1332-1346.

The Schizophrenia Commission (2012) The abandoned illness: a report from the Schizophrenia Commission. London: Rethink Mental Illness.

Thomson DM, McVie A, Morris BJ, Pratt JA (2011) Dissociation of acute and chronic intermittent phencyclidine-induced performance deficits in the 5-choice serial reaction time task: influence of clozapine. Psychopharmacology 213:681-695.

Toda N, Ayajiki K, Okamura T (2009) Cerebral blood flow regulation by nitric oxide in neurological disorders. Can J Physiol Pharmacol 87:581-594.

Tricoire L, Vitalis T (2012) Neuronal nitric oxide synthase expressing neurons: a journey from birth to neuronal circuits. Front Neural Circuits 6.

Tsai G, Passani LA, Slusher BS, Carter R, Baer L, Kleinman JE, Coyle JT (1995) Abnormal excitatory neurotransmitter metabolism in schizophrenic brains. Arch Gen Psychiatry 52:829-836.

Tseng KY, Chambers RA, Lipska BK (2009) The neonatal ventral hippocampal lesion as a heuristic neurodevelopmental model of schizophrenia. Behav Brain Res 204:295-305.

Tseng KY, Lewis BL, Hashimoto T, Sesack SR, Kloc M, Lewis DA, O'Donnell P (2008) A neonatal ventral hippocampal lesion causes functional deficits in adult prefrontal cortical interneurons. The Journal of neuroscience : the official journal of the Society for Neuroscience 28:12691-12699.

Uhlhaas PJ, Singer W (2010) Abnormal neural oscillations and synchrony in schizophrenia. Nat Rev Neurosci 11:100-113.

Utkan T, Gocmez SS, Ozer C, Gacar N, Aricioglu F (2012) Selective and nonselective neuronal NOS inhibitors impair cognitive function in the

three panel runway and passive avoidance tasks in rats. Pharmacol Biochem Behav 101:515-519.

Vallance P, Leone A, Calver A, Collier J, Moncada S (1992) Accumulation of an endogenous inhibitor of nitric oxide synthesis in chronic renal failure. Lancet 339:572-575.

Vásquez-Vivar J, Hogg N, Martásek P, Karoui H, Pritchard KA, Kalyanaraman B (1999) Tetrahydrobiopterin-dependent inhibition of superoxide generation from neuronal nitric oxide synthase. J Biol Chem 274:26736-26742.

Walther S, Strik W (2012) Motor symptoms and schizophrenia. Neuropsychobiology 66:77-92.

Wang CZ, Yang SF, Xia Y, Johnson KM (2008a) Postnatal phencyclidine administration selectively reduces adult cortical parvalbumin-containing interneurons. Neuropsychopharmacology 33:2442-2455.

Wang S, Paton JFR, Kasparov S (2006) The challenge of real-time measurements of nitric oxide release in the brain. Auton Neurosci 126-127:59-67.

Wang S, Xu J, Song P, Wu Y, Zhang J, Chul Choi H, Zou MH (2008b) Acute inhibition of guanosine triphosphate cyclohydrolase 1 uncouples endothelial nitric oxide synthase and elevates blood pressure. Hypertension 52:484-490.

Wass C, Klamer D, Fejgin K, Pålsson E (2009) The importance of nitric oxide in social dysfunction. Behavioural Brain Research 200:113-116.

Wass C, Svensson L, Fejgin K, Pålsson E, Archer T, Engel JA, Klamer D (2008) Nitric oxide synthase inhibition attenuates phencyclidine-induced disruption of cognitive flexibility. Pharmacology, Biochemistry and Behavior 89:352-359.

Wass C, Archer T, Pålsson E, Fejgin K, Alexandersson A, Klamer D, Engel J, Svensson L (2006) Phencyclidine affects memory in a nitric oxide-dependent manner: Working and reference memory. Behavioural Brain Research 174:49-55.

Werner ER, Gorren ACF, Heller R, Werner-Felmayer G, Mayer B (2003) Tetrahydrobiopterin and nitric oxide: mechanistic and pharmacological aspects. Exp Biol Med (Maywood) 228:1291-1302.

West AR, Galloway MP (1997) Endogenous nitric oxide facilitates striatal dopamine and glutamate efflux in vivo: role of ionotropic glutamate receptor-dependent mechanisms. Neuropharmacology 36:1571-1581.

Wiley JL (1998) Nitric oxide synthase inhibitors attenuate phencyclidine-induced disruption of prepulse inhibition. Neuropsychopharmacology 19:86-94.

Wittchen HU, Jacobi F, Rehm J, Gustavsson A, Svensson M, Jonsson B, Olesen J, Allgulander C, Alonso J, Faravelli C, Fratiglioni L, Jennum P, Lieb R, Maercker A, van Os J, Preisig M, Salvador-Carulla L, Simon R, Steinhausen HC (2011) The size and burden of mental disorders and other disorders of the brain in Europe 2010. Eur Neuropsychopharmacol 21:655-679.

Wood KC, Batchelor AM, Bartus K, Harris KL, Garthwaite G, Vernon J, Garthwaite J (2011) Picomolar nitric oxide signals from central neurons recorded using ultrasensitive detector cells. J Biol Chem 286:43172-43181.

Wright IC, Rabe-Hesketh S, Woodruff PW, David AS, Murray RM, Bullmore ET (2000) Meta-analysis of regional brain volumes in schizophrenia. Am J Psychiatry 157:16-25.

Wu C, Parrott AM, Fu C, Liu T, Marino SM, Gladyshev VN, Jain MR, Baykal AT, Li Q, Oka S, Sadoshima J, Beuve A, Simmons WJ, Li H (2011) Thioredoxin 1-mediated post-translational modifications: reduction, transnitrosylation, denitrosylation, and related proteomics methodologies. Antioxid Redox Signal 15:2565-2604.

Wu G, Morris SM, Jr. (1998) Arginine metabolism: nitric oxide and beyond. The Biochemical journal 336 (Pt 1):1-17.

Wu J, Kikuchi T, Wang Y, Sato K, Okumura F (2000) NOx- concentrations in the rat hippocampus and striatum have no direct relationship to anaesthesia induced by ketamine. Br J Anaesth 84:183-189.

Wu Z, Zhang XY, Wang H, Tang W, Xia Y, Zhang F, Liu J, Fu Y, Hu J, Chen Y, Liu L, Chen DC, Xiu MH, Kosten TR, He J (2012) Elevated plasma superoxide dismutase in first-episode and drug naive patients with schizophrenia: Inverse association with positive symptoms. Prog Neuropsychopharmacol Biol Psychiatry 36:34-38.

Wultsch T, Chourbaji S, Fritzen S, Kittel S, Grünblatt E, Gerlach M, Gutknecht L, Chizat F, Golfier G, Schmitt A, Gass P, Lesch KP, Reif A (2007) Behavioural and expressional phenotyping of nitric oxide synthase-I knockdown animals. J Neural Transm Suppl:69-85.

Xiao X, Dawson N, Macintyre L, Morris BJ, Pratt JA, Watson DG, Higham DJ (2011) Exploring metabolic pathway disruption in the subchronic phencyclidine model of schizophrenia with the Generalized Singular Value Decomposition. BMC Syst Biol 5.

Xie H-r, Hu L-s, Li G-y (2010) SH-SY5Y human neuroblastoma cell line: in vitro cell model of dopaminergic neurons in Parkinson's disease. Chin Med J 123:1086-1092.

Xing G, Chavko M, Zhang LX, Yang S, Post RM (2002) Decreased calcium-dependent constitutive nitric oxide synthase (cNOS) activity in

prefrontal cortex in schizophrenia and depression. Schizophr Res 58:21-30.

Xu B, Wratten N, Charych EI, Buyske S, Firestein BL, Brzustowicz LM (2005) Increased Expression in Dorsolateral Prefrontal Cortex of CAPON in Schizophrenia and Bipolar Disorder. Plos Med 2.

Xue J-G, Masuoka T, Gong X-D, Chen K-S, Yanagawa Y, Law SKA, Konishi S (2011) NMDA receptor activation enhances inhibitory GABAergic transmission onto hippocampal pyramidal neurons via presynaptic and postsynaptic mechanisms. J Neurophysiol 105:2897-2906.

Yamada K, Nabeshima T (1997) Two pathways of nitric oxide production through glutamate receptors in the rat cerebellum in vivo. Neurosci Res 28:93-102.

Yamada K, Hiramatsu M, Noda Y, Mamiya T, Murai M, Kameyama T, Komori Y, Nikai T, Sugihara H, Nabeshima T (1996) Role of nitric oxide and cyclic GMP in the dizocilpine-induced impairment of spontaneous alternation behavior in mice. Neuroscience 74:365-374.

Yang S, Lee YJ, Kim JM, Park S, Peris J, Laipis P, Park YS, Chung JH, Oh SP (2006) A murine model for human sepiapterin-reductase deficiency. Am J Hum Genet 78:575-587.

Yang XC, Reis DJ (1999) Agmatine selectively blocks the N-methyl-D-aspartate subclass of glutamate receptor channels in rat hippocampal neurons. The Journal of pharmacology and experimental therapeutics 288:544-549.

Yao JK, Leonard S, Reddy RD (2004) Increased nitric oxide radicals in postmortem brain from patients with schizophrenia. Schizophr Bull 30:923-934.

Ye X, Kim W-S, Rubakhin SS, Sweedler JV (2004) Measurement of nitric oxide by 4,5-diaminofluorescein without interferences. Analyst 129:1200-1205.

Yee BK, Chang DLT, Feldon J (2004) The Effects of dizocilpine and phencyclidine on prepulse inhibition of the acoustic startle reflex and on prepulse-elicited reactivity in C57BL6 mice. Neuropsychopharmacology 29:1865-1877.

Yilmaz N, Herken H, Cicek H, uuml, lya K, Celik A, uuml, rekli M, Akyol, Ouml, mer (2007) Increased Levels of Nitric Oxide, Cortisol and Adrenomedullin in Patients with Chronic Schizophrenia. Med Princ Pract 16:137-141.

Yoo MS, Chun HS, Son JJ, DeGiorgio LA, Kim DJ, Peng C, Son JH (2003) Oxidative stress regulated genes in nigral dopaminergic neuronal cells: correlation with the known pathology in Parkinson's disease. Brain Res Mol Brain Res 110:76-84.

Zhang HQ, Fast W, Marletta MA, Martasek P, Silverman RB (1997) Potent and selective inhibition of neuronal nitric oxide synthase by N omega-propyl-L-arginine. J Med Chem 40:3869-3870.

Zhang XY, Chen DC, Xiu MH, Yang FD, Tan YL, He S, Kosten TA, Kosten TR (2012a) Thioredoxin, a novel oxidative stress marker and cognitive performance in chronic and medicated schizophrenia versus healthy controls. Schizophrenia research.

Zhang XY, Zhou DF, Shen YC, Zhang PY, Zhang WF, Liang J, Chen DC, Xiu MH, Kosten TA, Kosten TR (2012b) Effects of risperidone and haloperidol on superoxide dismutase and nitric oxide in schizophrenia. Neuropharmacology 62:1928-1934.

Zhang XY, Chen DC, Xiu MH, Wang F, Qi LY, Sun HQ, Chen S, He SC, Wu GY, Haile CN, Kosten TA, Lu L, Kosten TR (2009a) The novel oxidative stress marker thioredoxin is increased in first-episode schizophrenic patients. Schizophrenia Research 113:151-157.

Zhang Y, Behrens MM, Lisman JE (2008) Prolonged exposure to NMDAR antagonist suppresses inhibitory synaptic transmission in prefrontal cortex. J Neurophysiol 100:959-965.

Zhang Y, Llinas RR, Lisman JE (2009b) Inhibition of NMDARs in the Nucleus Reticularis of the Thalamus Produces Delta Frequency Bursting. Front Neural Circuits 3:20.

Zoubovsky SP, Pogorelov VM, Taniguchi Y, Kim S-H, Yoon P, Nwulia E, Sawa A, Pletnikov MV, Kamiya A (2011) Working memory deficits in neuronal nitric oxide synthase knockout mice: Potential impairments in prefrontal cortex mediated cognitive function. Biochem Biophys Res Commun.